The role of low-density lipoprotein modified by myeloperoxidase-derived oxidants on vascular dysfunction in atherosclerosis

Adrian Abdo

BMedSci (Hon)

Sydney Medical School

The University of Sydney

Australia

2018

This thesis is submitted in fulfillment of the requirements for the award of the degree of

Doctor of Philosophy (PhD)

Declaration

The intellectual content in this thesis is the original work conducted by Adrian Abdo at the Heart Research Institute, Sydney. It has not been submitted to any other institution for a higher degree. Any assistance received in the writing of this thesis has been sincerely acknowledged and all materials previously published or written by another person have been acknowledged

This thesis contains material published in [1]. This is Sections 5.3, the results associated with Figures 5.4 to 5.6, 5.8, 5.10, 5.12 and 5.14. I designed the study, performed the experiments, analysed the data and wrote the drafts of the manuscript.

Adrian Issa Abdo

Acknowledgements

Having completed my PhD has been one of the most difficult and satisfying times of my life. The Heart Research Institute was such a supportive and nurturing environment for growth as a professional researcher and a person. The foremost people I wish to thank are my supervisors, Prof. Clare Hawkins, Dr. Benjamin Rayner and Dr. David van Reyk, for their valuable advice and teaching through the development of my project and publication. I wish to give them my biggest gratitude for this opportunity.

I would like to express my gratitude to the other scientists who took their valuable time to help me in my work. My thanks to Dr. Bronwyn Brown, Dr. Fahd Ismael and Diba Sheipouri at the Heart Research Institute for their technical assistance, helpful discussion and friendly understanding. I would also like to thank Dr. Matthew Padula and Iain Berry from the UTS Proteomics Core Facility for their assistance with mass spectrometry and data analysis for apoB-100 fragmentation studies in Chapter 3.

The Heart Research Institute was also a place where I made some life-long friends. Thank you Kelly Gardiner and Pam Vanichkitrungruang for being such happy, little, laughing, singing, geeky friends for whom I am not worthy. Your mastery of Mexican food and shared giggling fits over literally nothing will always stick with me. Thank you also to Vickie Tang, Leila Reyes and Carmen Zhang for always being willing to hear my rants and ravings.

The rest of the Heart Research Institute, particularly the Inflammation Group and Free Radical Group. Thank you for your efforts and advice, and for the great science over the last 4.5 years since I started my Honours.

Lastly, to my parents Elias and Rose Abdo, my sister Mariana Abdo, and my girlfriend Mariah Williams, thank you for your emotional support and sacrifice for me through my PhD experience. I would not have gotten this far without your love.

Table of Contents

Abstract

Atherosclerosis is the most common cause of cardiovascular disease (CVD), which is the leading cause of death in the world. Atherosclerosis is characterised by aberrant lipid transport and metabolism that leads to the deposition of low-density lipoproteins (LDL) in the artery wall. The deposited LDL is then susceptible to modification, principally by oxidation, and is ingested by macrophages to form "foam cells". Modified LDL can also be taken up by endothelial cells, which can lead to impairment of endothelium-dependent vasorelaxation, termed 'endothelial dysfunction'. This dysfunction causes the arterial stiffening that is characteristic of atherosclerosis.

There are several potential sources of LDL modification that have been implicated *in vivo*, including lipoxygenases, glucose, reactive oxygen and nitrogen species and the haem enzyme myeloperoxidase (MPO). However, the type(s) that are most relevant to atherosclerosis are still a subject of controversy. There is strong evidence for the role of MPO, an enzyme released by neutrophils upon inflammation, in causing oxidative damage to host tissue and biomolecules, including LDL, that leads to vascular cell damage in atherosclerosis. MPO produces oxidants hypochlorous acid (HOCl) and hypothiocyanous acid (HOSCN), by catalysing the reaction of hydrogen peroxide (H_2O_2) with the respective (pseudo)halides, Cl^- and SCN^-. While it is well established that HOCl causes extensive LDL modification, which is present in atherosclerotic lesions, less is known regarding the impact of the other major MPO-derived oxidant, HOSCN in atherosclerosis. Generation of HOSCN may be of relevance to smokers, whom have significantly elevated plasma SCN^- levels, which can shift the ratio of MPO oxidants to favour HOSCN formation. Elevated HOSCN formation and consequent modifications of important biomolecules such as LDL may therefore be a contributing factor to the deleterious effects of smoking in the development of CVD.

Chapter 3 examines alterations in the pattern of modification of LDL by HOSCN compared to HOCl. Exposure of LDL to HOCl led to extensive aggregation and non-specific fragmentation of apoB-100, whereas HOSCN was shown to selectively cleave apoB-100 at two sites. Peptide mass mapping experiments revealed the formation of two similarly sized apoB-100 fragments, resulting from cleavage near the N- and C-termini. This selective fragmentation was significantly ablated by the free radical scavenger, butylated hydroxytoluene, consistent with a radical-mediated fragmentation pathway. However, further work is required to characterise the mechanism involved and the specific peptide cleavage sites.

Chapter 4 examines the effect of LDL modified by HOCl or HOSCN on endothelial dysfunction using human coronary artery endothelial cells (HCAEC) as a model. Exposure of HCAEC to LDL modified by HOCl or HOSCN did not result in altered scavenger receptor expression or significant lipid uptake. Similarly, there was no discernible effect on the expression of adhesion molecules or cytokines, or neutrophil adhesion, indicating that HCAEC did not promote an inflammatory response to HOSCN- or HOCl-modified LDL. Similarly, HOCl- and HOSCN-modified LDL did not induce endoplasmic reticulum stress and related signalling cascades in the unfolded protein response. However, each type of modified LDL was able to perturb nitric oxide (NO) production in the cells, which is described in Chapter 5.

Exposure of HCAEC to HOSCN-modified LDL in particular, resulted in a significant decrease in endothelial nitric oxide synthase (eNOS) activity, which was linked to eNOS uncoupling. This decreased NO production, consistent with endothelial dysfunction, was supported by the observation that exposure of rat aortic segments to HOSCN- (and HOCl-) modified LDL *ex vivo* resulted in a decrease in endothelium-dependent vasorelaxation. An upregulation of eNOS mRNA expression in HCAEC was apparent after exposure to HOSCN-modified LDL, but not HOCl-modified LDL, indicating that there are some differences in the HCAEC response to each type of modified LDL.

Vascular smooth muscle cells (VSMC) also play a crucial role in the development of atherosclerosis, as these cells can transdifferentiate from a contractile phenotype, which modulates vessel relaxation, to a synthetic phenotype, which aids in vascular remodelling in atherosclerosis. VSMC can also undergo calcification, which is common in complex atherosclerotic lesions, and has been shown to be caused by other types of modified LDL. Chapter 6 uses human coronary artery smooth muscle cells (HCASMC) as a model to assess the effect of exposure to HOSCN- and HOCl-modified LDL on the expression of the synthetic, contractile and calcification VSMC phenotype markers. The gene expression of contractile markers, α-smooth muscle actin and calponin were stunted, and the expression of the synthetic marker osteopontin was elevated by exposure to HOSCN- or HOCl-modified LDL compared to the non-treated control cells. This response was not due to lipid accumulation by the uptake of modified LDL, which can lead to VSMC-derived foam cell formation. These preliminary data are consistent with a potential role for LDL modified by MPO-derived oxidants HOSCN or HOCl to promote a synthetic phenotype in VSMC.

Overall, the data from this study support a potential role for the MPO-derived oxidant HOSCN to promote vascular dysfunction by the modification of LDL, which is an important mechanism that promotes the development of atherosclerosis. That HOSCN-modified LDL induces endothelial dysfunction and promotes a synthetic VSMC phenotype is consistent with a role for SCN^- to exacerbate atherosclerosis. This complements previous studies showing that elevated plasma SCN^- levels correlate with increased LDL deposition in the arteries of young smokers. However, further work is needed to assess the role of HOSCN-modified LDL on the development of atherosclerosis *in vivo*, particularly as the role of SCN^-, both as a circulating antioxidant and a substrate for MPO, in cell signalling pathways that maintain health and promote disease still need to be elucidated.

Abbreviations

$(SCN)_2$	Thiocyanogen
2-OH-E^+	2-hydroxyethidium
3,5-diClTyr	3,5-dichlorotyrosine
3-Br-Tyr	3-bromotyrosine
3-Cl-Tyr	3-chlorotyrosine
3-nitroTyr	3-nitrotyrosine
4-HNE	4-hydroxynonenal
5-BrU	5-bromouracil
5-ClU	5-chlorouracil
9-HODE	9-Hydroxyoctadecadienoic acid
ABAH	4-aminobenzoic acid hydrazide
ACh	Acetylcholine
ACS	Acute coronary syndrome
AGE	Advanced glycation end-products
AP-1	Activator protein-1
apoA-1	Apolipoprotein A-1
apoB-100	Apolipoprotein B-100
apoE-4	Apolipoprotein E-4
ARE	Antioxidant Response Element
ATF4	Activating transcription protein-4
ATF6	Activating transcription protein-6
BH_4	Tetrahydrobiopterin
BHA	Benzohydroxamic acid
BHT	Butylated hydroxytoluene
CAD	Coronary artery disease
CaM	Calmodulin
cav-1	Caveolin-1
CFTR	Cystic fibrosis transmembrane conductance regulator
CHD	Coronary heart disease
CHOP	C/EBP homologous protein
CKD	Chronic kidney disease

CRP	C-reactive protein
Cu^{2+}	Copper(II) ion
CVD	Cardiovascular disease
Cx43	Connexin 43
DTT	Dithiothreitol
DFO	Desferrioxamine
DHE	Dihydroethidium
ECM	Extracellular matrix
eIF2α	Eukaryotic translation initiation factor 2 alpha subunit
eNOS	Endothelial nitric oxide synthase
EPO	Eosinophil peroxidase
EPR	Electron paramagnetic resonance
ER	Endoplasmic reticulum
ERK1/2	Extracellular signalling-related kinase 1/2
FAD	Flavin adenine dinucleotide
fMLFK	Formyl-Met-Leu-Phe-Lys
FMN	Flavin mononucleotide
Gclc	Glutamate-cysteine ligase catalytic subunit
Gclm	Glutamate-cysteine ligase modifier subunit
GMP	Guanidine monophosphate
GR	Glutathione reductase
GRP78	78 kDa glucose-regulating protein
Grx	Glutathione reductase
GS	Glutathione synthetase
GSH	Glutathione
GSSG	Glutathione disulfide
H_2O_2	Hydrogen peroxide
HAEC	Human aortic endothelial cells
HCAEC	Human coronary artery endothelial cells
HDL	High-density lipoprotein
$HO^{\bullet}$	Hydroxyl radical
HO-1	Haem oxygenase 1

HOBr	Hypobromous acid
$HOCl/OCl^-$	Hypochlorous acid/hypochlorite
HOI	Hypoiodous acid
$HOSCN/OSCN^-$	Hypothiocyanous acid/ hypothiocyanite
HUVEC	Human umbilical vein endothelial cells
ICAM-1	Intracellular adhesion molecule-1
IL-1β	Interleukin-1 beta
IL-6	Interleukin-6
IL-8	Interleukin-8
IRE1	Inositol requiring kinase-1
LDL	Low-density lipoprotein
LDLR	LDL receptor
L-NIO	N^5-(1-iminoethyl)-L-ornithine
LOX-1	Lectin-like oxidised LDL receptor-1
LPO	Lactoperoxidase
MAPK	Mitogen-activated protein kinase
MCP-1	Monocyte chemoattractant protein-1
MGD	N-methyl-D-glucamine dithiocarbamate
MI	Myocardial infarction
MMP	Matrix metalloproteinase
MPO	Myeloperoxidase
Msr	Methionine sulfoxide reductase
NADH	Nicotinamide adenine dinucleotide
NE	Norepinephrine
NF-κB	Nuclear factor-kappa B
NO	Nitric oxide
NOX	NADPH Oxidase
Nrf2	Nuclear factor (erythroid-derived 2)-like 2
$O_2^{\bullet-}$	Superoxide anion radical
OCN^-	Cyanate
Olfml3	Olfactomedin-like 3
$ONOO^-$	Peroxynitrite
OPN	Osteopontin

PDGF	Platelet-derived growth factor
PERK	Protein kinase-like ER kinase
pHBAH	p-hydroxy benzoic acid hydrazide
PI3K	Phosphoinositide 3-kinase
PKC	Protein kinase C
PKG	Protein kinase G
PPARγ	Peroxisome proliferator-activated receptor gamma
PTP	Protein Tyrosine Phosphatases
R-NH_2	Amine
R-NHBr	Bromamine
R-NHCl	Chloramine
R-NH-SCN	Amino thiocyanate
$RO^{\bullet}$	Alkoxyl radical
$ROO^{\bullet}$	Peroxyl radical
ROS	Reactive oxygen species
$R\text{-}S^{\bullet}$	Thiyl radical
R-SCl	Sulfenyl chloride
R-SeH	Selenol
R-Se-SCN	Selenothiocyanate
R-SeSe-R	Diselenide
R-SH	Thiol
R-SSCN	Sulfenyl thiocyanate
R-SS-R	Disulfide
Runx2	Runt-related transcription factor 2
S100A4	S100 calcium-binding protein A4
SCN^{-}	Thiocyanate
SERCA	Sarco/endoplasmic reticulum Ca^{2+}-ATPase
SHA	Salicylhydroxamic acid
SNP	Sodium nitroprusside
SNPC	Substantia nigra pars compacta
SOD	Superoxide dismutase
SP-1	Specificity protein-1
SR-A1	Scavenger receptor class A1

SR-A2	Scavenger receptor class A2
SR-B1	Scavenger receptor class B1
SR-B2	Scavenger receptor class B2
SREC-1	Scavenger receptor expressed by endothelial cell 1
STEMI	ST-elevated myocardial infarction
sXBP1	Spliced X-box binding protein
TF	Tissue factor
TM	Tunicamycin
TNF-α	Tumor necrosis factor-alpha
TPO	Thyroid peroxidase
Trx	Thioredoxin
TrxR	Thioredoxin reductase
UPR	Unfolded protein response
VCAM-1	Vascular cell adhesion molecule-1
VLDL	Very low-density lipoprotein
VPO	Vascular peroxidase
VSMC	Vascular smooth muscle cell
α-SMA	Alpha smooth muscle actin
β2M	Beta-2 microglobulin

List of Figures

List of Tables

Chapter 1. Introduction

1.1. Inflammation in Atherosclerosis

In Australia, atherosclerosis-dependent cardiovascular disease (CVD) is the leading cause of hospitalisations and deaths [2]. Atherosclerosis is characterised by the accumulation of macrophage lipid-laden "foam" cell formation, leading, initially, to fatty-lesion formation and eventually a large lipid-laden and necrotic core of complex chemical composition and morphology in the intimal artery walls [3, 4]. This progressive, chronic inflammatory disorder of the arteries leads to a progressive narrowing of the lumen and a significant or total occlusion of blood flow. This may lead to ischaemia (inadequate supply of blood) of the tissue downstream of the artery. Prolonged ischaemia can result in infarction; i.e. tissue death and subsequent scarring. Alternatively, an unstable lesion can rupture to release a plethora of pro-inflammatory material that can cause thrombosis (formation of a blood clot, termed a 'thrombus', within the blood vessel which causes partial or total occlusion of blood flow) which in the coronary artery, can cause sudden cardiac death [5]. Coronary heart disease (CHD), also known as ischaemic heart disease, occurs when there is a blockage of the coronary artery impeding blood flow, resulting in cardiac muscle damage and subsequent scarring. CHD and its *sequelae* are the most common cause of death in Australia [6]. While thrombotic occlusion of vessels serving the brain can lead to stroke [7].

There are many risk factors involved in the initiation and progression of atherosclerosis. Some are deemed non-modifiable risk factors (gender [8], family history [9], age), while others are modifiable, or "lifestyle" risk factors (low fruit/vegetable diet [10, 11], replaced with a diet of high trans-fatty acids [12], smoking [13], lack of exercise, obesity and hypertension [14, 15]), and both groups undoubtedly contribute to a person's risk of developing CVD. In addition to measures of lipid metabolism and those of cardiovascular function, clinical measurements of CVD risk include increases in circulating levels of inflammatory markers and markers of

tissue damage (C-reactive protein, troponin T, serum amyloid-A, fibrinogen, reviewed [16]) as it is well established that inflammation is a driving force responsible for the development of atherosclerosis [3, 17].

The role of inflammation in the initiation, progression and destabilisation of atherosclerosis has been extensively reviewed [3, 17-20]. The peroxidase enzyme, myeloperoxidase (MPO; EC 1.11.1.7) is released during inflammation and is found in atherosclerotic plaques at multiple stages of the disease process [21]. MPO is a key peroxidase enzyme in the innate immune system that destroys pathogens by catalysing the production of reactive oxidants collectively called the hypohalous acids, namely; hypochlorous acid (HOCl), hypothiocyanous acid (HOSCN), hypobromous acid (HOBr) and hypoiodous acid (HOI) [22]. However, there is also evidence for host tissue damage caused by these oxidants, implicating MPO as having a role as a key effector of chronic inflammatory diseases including atherosclerosis [23, 24]. Whilst other peroxidase enzymes play a role in the immune system, including lactoperoxidase (LPO) [25], eosinophil peroxidase (EPO) [26], vascular peroxidase (VPO) [27] and thyroid peroxidase (TPO) [28]; MPO has been the most implicated in the pathogenesis of atherosclerosis (described in Section 1.6.6).

1.2. Myeloperoxidase

1.2.1. Role of MPO in innate immunity

Upon the invocation of inflammation, either by injury or an ingress of a pathogen, neutrophils (also called polymorphonuclear leukocytes) are the first recruited immune cells to the site of inflammation [29]. When activated, neutrophils undergo a "respiratory burst," in which oxygen consumption is increased many fold compared to basal levels *via* NADPH-oxidase (NOX), which catalyses production of the superoxide anion radical ($O_2^{\bullet-}$; Figure 1.1) [30]. $O_2^{\bullet-}$ either spontaneously, or via the action of superoxide dismutase (SOD) [31],

dismutates to hydrogen peroxide (H_2O_2). Concomitantly, neutrophils will degranulate, causing the extracellular release of the contents of azurophilic granules (including MPO) at the site of inflammation [29]. MPO utilises H_2O_2 to convert halides, or the pseudohalide SCN^-, to produce hypohalous acids (refer to Figure 1.1).

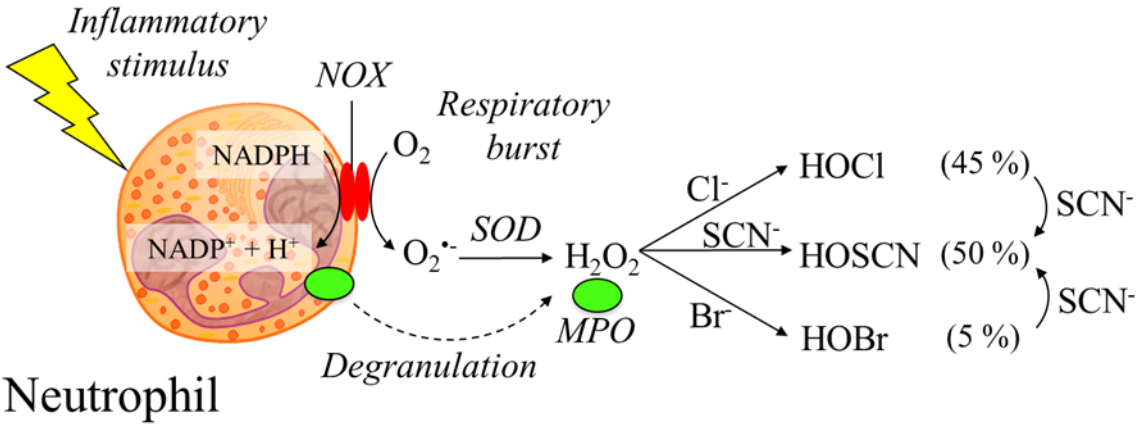

Figure 1.1. Neutrophil activation and the production of hypohalous acids. *Activation of neutrophils promotes oxygen consumption by NADPH oxidase-2 to produce $O_2^{\bullet-}$, which dismutates to H_2O_2. Concurrently, MPO is released to catalyse the halogenation of H_2O_2 to the hypohalous acids HOCl, HOSCN and HOBr by the respective (pseudo)halides (Cl^-, SCN^- and Br^-). At high concentrations of SCN^-, HOCl and HOBr can be effectively scavenged to produce more HOSCN.*

1.2.2. The Catalytic cycle of MPO

MPO is a cationic, homodimeric haem-peroxidase enzyme approximately 146 kDa in mass, with each monomer consisting of a heavy and light chain [32, 33]. MPO utilises H_2O_2 to convert halides (Cl^-, Br^- and I^-) and the pseudohalide thiocyanate (SCN^-) to their respective hypohalous acids (HOX, where X = Cl^-, Br^-, I^- and SCN^-; Figure 1.1). Collectively this combination is referred to as the MPO-H_2O_2-X^- system, with hypohalous acid formation occurring *via* the halogenation cycle (Figure 1.2). The haem group is the catalytic site for hypohalous acid production, however MPO has a complex catalytic cycle. The native MPO-Fe^{3+} haem group is enzymatically inactive, but reacts with H_2O_2 rapidly ($k \sim 1.4 \times 10^7$ $M^{-1}{\cdot}s^{-1}$) to form compound

I, the highly active MPO-Fe^{4+}-oxo-porphyrin radical species [34]. Compound I then catalyses the production of HOCl, HOBr, HOI and HOSCN from Cl^-, Br^-, I^- and SCN^- ions, respectively (Reaction 1), by a two-electron redox reaction whilst reducing MPO back to the native state [35].

$$H_2O_2 + X^- \longrightarrow HOX + H_2O \qquad (1) \qquad (X = Cl, Br, I, SCN)$$

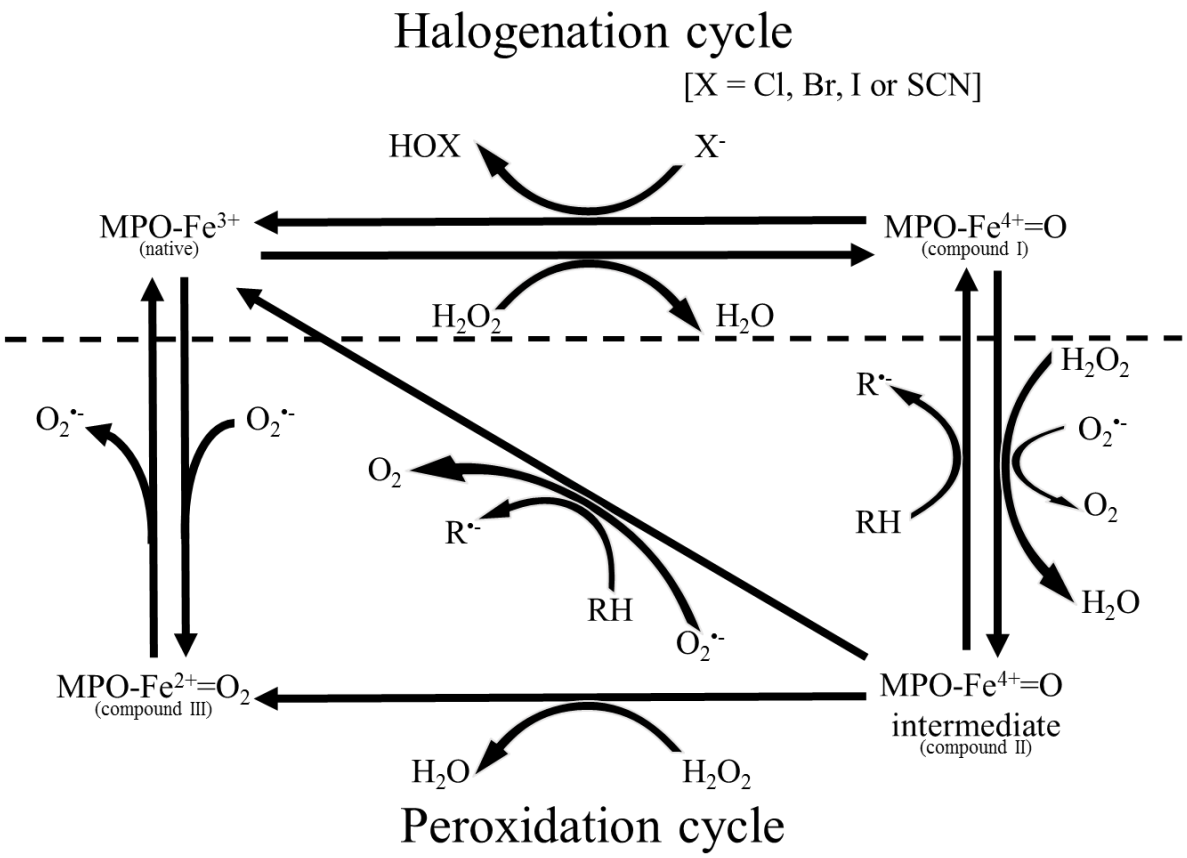

Figure 1.2. The enzymatic cycle of MPO (adapted from [33]). *Native MPO is oxidised by H_2O_2 to form compound I (MPO-Fe^{4+}=O). Hypohalous acids HOCl, HOBr, HOI and HOSCN are produced by a two-electron oxidation of the respective (pseudo)halides Cl-, Br-, I- or SCN^- and restoring MPO to the native state (halogenation cycle). Alternatively, native MPO can be restored by one-electron oxidation of compound I to a compound II intermediate by reaction with H_2O_2 or $O_2^{\bullet-}$, followed by reaction with $O_2^{\bullet-}$ or a number of organic or inorganic substrates (RH) (peroxidation cycle). H_2O_2 can also convert compound II to compound III (MPO-Fe^{2+}=O_2), which is an inactive state of MPO. RH can also restore compound I from compound II. $O_2^{\bullet-}$ can also cycle MPO between native form and compound III.*

Alternatively, MPO can conform to the MPO-Fe^{4+}-oxy ferryl intermediate radical (compound II) before reducing back to the native enzyme involving two subsequent one-electron reductions, *via* a peroxidase cycle [33]. The peroxidase cycle generates radicals from organic and inorganic substrates, including tyrosine, tryptophan, thiols, ascorbate, steroidal `compounds, urate and many drug compounds, which inhibit MPO halogenation activity [33]. MPO also has a reduced, enzymatically inactive MPO-Fe^{2+}=O_2/$O^{\bullet-}$ species (compound III), which is formed by the reduction of compound II by H_2O_2 or native MPO by $O_2^{\bullet-}$ [36]. MPO has been reported to be oxidised in the presence of high levels of H_2O_2, from the compound I and III state, causing the destruction of the haem group and the release of iron [36]. Although iron release has prospects of being a secondary source of oxidative stress in cells [37], in the experiments reported [36], purified MPO was exposed to supra-physiological concentrations (1.5 mM) of H_2O_2, which presents an unlikely scenario *in vivo*, although these conditions may be relevant inside the phagosome under conditions of depleted (pseudo)halides.

Although physiological concentrations of Cl^- are orders of magnitude higher than SCN^- and Br^- in the plasma (*cf.* 100 – 140 mM Cl^-, 20 – 120 µM SCN^- and 20 – 100 µM Br^-), approximately the same quantity of H_2O_2 is converted to HOCl and HOSCN, whilst comparatively low levels of HOBr are formed [38]. This is due to the high selectivity of MPO for SCN^- compared to Br^- and Cl^- (specificity constants are 730:60:1, respectively [39]). As a result, SCN^- is converted to HOSCN rapidly by MPO compared to the production of HOCl and HOBr (*c.f.* rate constants in $M^{-1}.s^{-1}$; k_{HOSCN} = 9.6 × 10^6, k_{HOBr} = 1.1 × 10^6 and k_{HOCl} 2.5 × 10^4, respectively [35]). In addition, HOCl and HOBr are rapidly reduced by SCN^- ions to HOSCN ($k \sim 2 \times 10^7$ $M^{-1}.s^{-1}$ and 2.3 × 10^9 $M^{-1}.s^{-1}$, respectively [40, 41]) with the calculated physiological half-life of HOCl in the plasma reported to be 400 µs before reduction by SCN^- [40]. This conversion is likely to have considerable consequences for cigarette smokers, for whom SCN^- is significantly elevated in the plasma [42, 43], reaching above 250 µM in some cases [43]

(described further in Section 1.6.6.1). The pK_a values of HOCl, HOBr and HOSCN are 7.59, 8.7 and 5.3, respectively [44, 45], resulting in a mixture of neutral and ionic HOX/OX^- species being present at physiological pH (7.4). Therefore, approximately equal quantities of HOCl/OCl^- are present, while HOBr predominates over OBr^- and $OSCN^-$ is almost completely predominant (>99%) over HOSCN under physiological conditions. This is important in understanding the reactivity of these oxidants with cells, as the charged conjugate bases $OSCN^-$ and OCl^- can differ markedly in their reactivity compared to the parent acid [46].

1.3. Reactions of hypohalous acids with biomolecules

MPO-derived hypohalous acids have a range of biological targets. HOCl and HOBr are very potent oxidants that indiscriminately react with a range of different biomolecules. Modifications of proteins, lipids, nucleotides and carbohydrates by HOCl have been extensively characterised, while biological damage wrought by HOSCN is more selective, in particular targeting thiols. HOCl and HOBr have both been implicated in many diseases, owing to the presence of specific chlorinated and brominated biomarkers *in vivo* [47-51]. The contribution of HOSCN to disease is less clear as there is no known biomarker for its reactivity and that the thiol oxidation can usually be repaired (reviewed in [33, 46, 52, 53]). Indeed, for this reason, it has been postulated that SCN^- has a protective role as it reduces the formation of HOCl and HOBr by MPO and scavenges the oxidants directly [41, 54-56]. This section will overview the current knowledge of the biological reactivities of the MPO-derived oxidants HOCl, HOBr and HOSCN.

1.3.1. Proteins

Proteins and amino acids are an important target for oxidation by MPO-derived hypohalous acids and, with regard to these targets, there are significant differences in the comparative reactivities of HOCl and HOBr compared to HOSCN (Reviewed [52]). HOCl and HOBr are

potent oxidants that react with a range of amino acid side-chains, due to their large standard reduction potentials (1.28 V and 1.13 V at pH 7, respectively [57]) while HOSCN is regarded as a mild, thiol (R-SH)-selective oxidant (0.56 V at pH 7 [57]) (Table 1). What follows is a summary of the reaction products in approximate order of reactivity, particularly with regards to HOCl and HOBr.

Table 1.1. Summary of the rate constants of HOCl, HOBr and HOSCN with amino acids.

	k_2 ($M^{-1}.s^{-1}$)		
	HOCl[a]	HOBr[d]	HOSCN[e]
Methionine (Met)	3.4×10^{7} [b]	3.6×10^{6}	-
Cysteine (Cys)	3.6×10^{8} [b]	1.2×10^{7}	7.8×10^{4}
Histidine (His)	1.0×10^{5}	3.0×10^{6}	-
Tryptophan (Trp)	1.1×10^{4}	3.7×10^{6}	ND
Lysine (Lys)	5.0×10^{3}	2.9×10^{5}	-
Tyrosine (Tyr)	23[c]	2.3×10^{5}	-
Arginine (Arg)	26	1.8×10^{3}	-
Glutamine (Gln)	0.03	1.9	-
Asparagine (Asn)	0.03	1.9	-
Selenocysteine (Sec)	ND	ND	1.24×10^{6}
Selenomethionine (SeMet) [f]	3.2×10^{8}	1.4×10^{7}	2.8×10^{3}

[a] Rate constants for the reactivity of HOCl from Pattison *et al* [58]; [b] Revised rate constants for the reactivity of HOCl with Met and Cys [59]; [c] revised rate constant for HOCl with Tyr [60]; [d] kinetics of HOBr with peptidyl residues [61]. All reactions with HOCl and HOBr were measured at pH 7.4 and 22 °C; [e] Reactivity of peptidyl residues with HOSCN are only apparent with Cys [62], selenocysteine (Sec) [63] and Trp [64], however no kinetic data are available for Trp. No significant reactions are found with HOSCN and other peptidyl residues (-); [f] rate constants for SeMet with HOCl, HOBr and HOSCN [65]. ND = not determined.

1.3.1.1. Methionine, cysteine and glutathione

Both HOCl and HOBr oxidise the thioether moiety (R-S-CH_3) of methionine (Met) to produce methionine sulfoxide (MetSO) [66-69], whereas no reaction occurs with HOSCN [64]. However, MetSO is not considered a reliable biomarker for these specific mechanisms of protein oxidation, as it is produced by oxidation of Met by a variety of oxidants and is enzymatically reversibly reduced back to Met [70]. Additionally, under conditions of high oxidant concentrations, MetSO can be further oxidised irreversibly to methionine sulfone ($MetSO_2$) [71] as shown in Figure 1.3. There is strong support for the role of Met oxidation in protecting protein functionality as an oxidant scavenger that prevents the oxidation of other peptidyl residues essential to protein function, given the Met residues are not generally integral to the microenvironment of active sites [70, 72, 73]. When Met is in the catalytic domain and oxidation does lead to the inactivation of an enzyme, e.g. α_1-antitrypsin [74-76], then Met oxidation may act as a switch for protein function [73]. In these cases, reduction of MetSO back to Met, catalysed by MetSO reductases (Msr) A and B [70, 77], can lead to reactivation of the enzyme. However, in a chronic inflammatory state, this switch mechanism could fail due to MetSO oxidation to $MetSO_2$ [78], which may result in inactivation and catabolism of proteins.

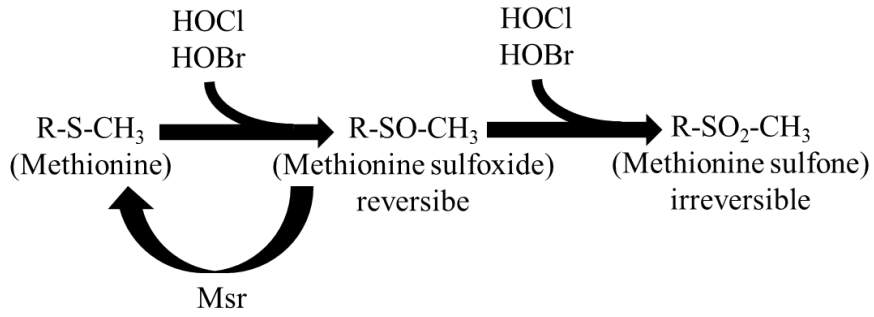

Figure 1.3. Reaction scheme of HOCl and HOBr with Met. *Met oxidation by HOCl or HOBr forms MetSO, which can be reversed back to Met by MetSO reductase (Msr). Alternatively, further oxidation of MetSO by HOCl or HOBr can form Met sulfone, which is irreversible.*

Two independent, simultaneous studies have also shown that N-terminal Met can be cyclised to dehydromethionine by HOCl and HOBr, which may be a potential biomarker for hypohalous acid-induced oxidative stress [67, 79]. Recently, exposure of calprotectin (isolated from human neutrophils) to HOCl resulted in *N*-Met oxidation and formation of dehydromethionine as well as MetSO [80]. However, the use of dehydromethionine as an *in vivo* biomarker has not been properly evaluated and requires further investigation.

Recently, Ronsein *et al* [66] found that HOBr and bromamines (R-NHBr), and to a lesser extent, HOCl and chloramines (R-NHCl) induced sulfilimine cross-linking (>S=N-) of Met with the nucleophilic nitrogen-centre of the Lys ε-amino group in the model peptide formyl-Met-Leu-Phe-Lys (fMLFK) for which they proposed independent mechanisms for intramolecular and intermolecular cross-links involving these peptidyl species. However, the biological significance of this cross-link species produced by hypohalous acid attack is yet to be determined with proteins *in vivo*.

The thiol group (R-SH) of cysteine (Cys) residues is a major target of oxidation from HOCl, HOBr and HOSCN. Although HOCl and HOBr react with Cys at three orders of magnitude faster than HOSCN (*cf.* in $M^{-1}.s^{-1}$; $k_{HOCl} = 3.6 \times 10^8$ [59], $k_{HOBr} = 1.2 \times 10^7$ [61] and $k_{HOSCN} = 7.8 \times 10^4$ [62]), HOCl and HOBr undergo a number of competing reactions with other residues in competition with thiols, while HOSCN exhibits very limited reactivity with other biological substrates. Thus, in being thiol selective, increased production of HOSCN can consequently lead to increased cellular damage by targeted oxidation of thiols, such as cysteine residues, which are commonly biologically active functional groups [81]. Initially, the thiol is halogenated to produce sulfenyl halide intermediates (R-SX; X = Cl, Br and SCN) [62, 68, 69, 82]. Sulfenyl chloride (R-SCl) then undergoes hydrolysis to produce sulfenic (R-SOH), sulfinic ($R\text{-}SO_2H$); and ultimately and irreversibly, sulfonic acid ($R\text{-}SO_3H$; Figure 1.4) [68, 69]. The sulfenyl thiocyanate (R-SSCN) derivative can also be formed by reaction of HOSCN with

thiols, which was shown to be more stable than the analogous R-SCl product [83]. However, at high molar ratios of HOSCN, further irreversible oxidation to sulfonic acid derivatives can also occur [83].

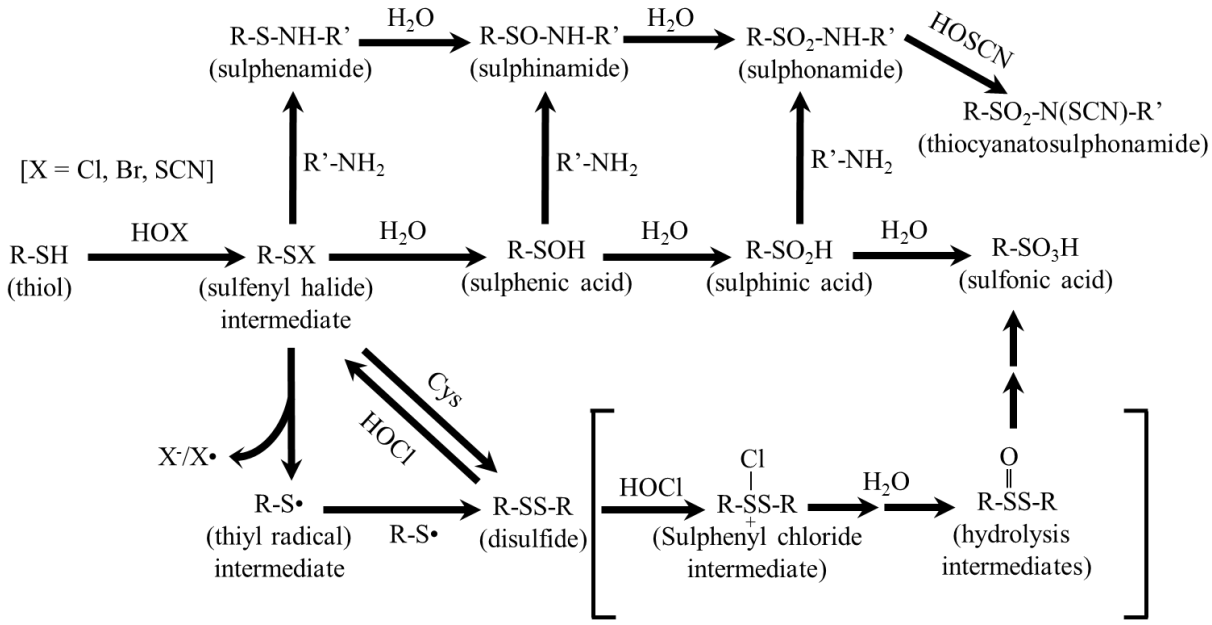

Figure 1.4. Reactions of hypohalous acids with Cys/thiols. *Scheme summarises the reactions of thiols with hypohalous acids described in Section 1.3.1.1. Sources cited in the main text.*

Alternatively, sulfenyl chloride and sulfenic/sulfinic acid intermediates can react with non-backbone amines (e.g. Lys or Arg) to form intra- and intermolecular sulfenamide, sulfinamide and sulfonamide cross-links [84-86] (Figure 1.4). There is currently no evidence for these cross-links being formed by sulfenyl bromides. Interestingly, HOSCN has been shown to react with sulfonamides to form a thiocyanatosulfonamide [87]. Unlike the R-SSCN, R-SCl is unstable and readily decomposes to a thiyl radical (R-S$^{\bullet}$) [88]. R-SCl, R-S$^{\bullet}$ and R-SSCN can all oxidise other thiols to form disulfides (R-SS-R') [89-91]. Most commonly, these disulfides will form between two Cys residues to produce cystine. Cystine can be oxidised by HOCl cleaving the disulfide bond (possibly *via* a sulfenyl chloride intermediate) and undergoing a series of intermediary hydrolysis reactions to form the sulfonic acid derivative, cysteic acid [68].

Glutathione (GSH), a tripeptide of γ-Glu-Cys-Gly and a ubiquitous cellular antioxidant, is highly reactive towards HOCl, HOBr and HOSCN [85]. However, the products of GSH-derived products differ between each oxidant. HOCl reacts with GSH to predominantly form GSH sulfonamide and some dehydroglutathione. HOBr preferentially forms the sulfinic acid and dehydroglutathione with minor amounts of sulfonamide. Only the glutathione disulfide (GSSG) is produced with HOSCN [85]. GSH can also react with the cysteinyl halide (R-SX) to form a mixed disulfide, also referred to as glutathionylation, which is an important regulatory signalling mechanism in cells [92].

1.3.1.2. Tryptophan

HOCl and HOBr readily react with Trp (*cf.* 1.1×10^4 $M^{-1}.s^{-1}$ [58] and 3.7×10^6 $M^{-1}.s^{-1}$ [61], respectively). These hypohalous acids cause hydroxylation of the indole group to produce 2-hydroxytryptophan (oxindoylalanine) and dioxindoylalanine [93, 94] (Figure 1.5). When a Gly residue is adjacent to Trp, Trp can be chlorinated to form the chloroindole derivative chlorotryptophan [94, 95]. This is due to the lack of steric hindrance by Gly and it is likely that chlorinated Trp becomes increasingly minor as the adjacent residue is larger. These Trp modifications by hypohalous acids have been implicated in protein dysfunction. MPO-derived oxidation of apolipoprotein-A1 (apoA-1), the apolipoprotein of high density lipoprotein (HDL), leads to the impaired capacity of the protein to mediate cholesterol efflux from cholesterol-(over)loaded macrophages [96]. This largely attributed to the oxidation of Trp forming mono- and dihydroxytryptophan [97, 98].

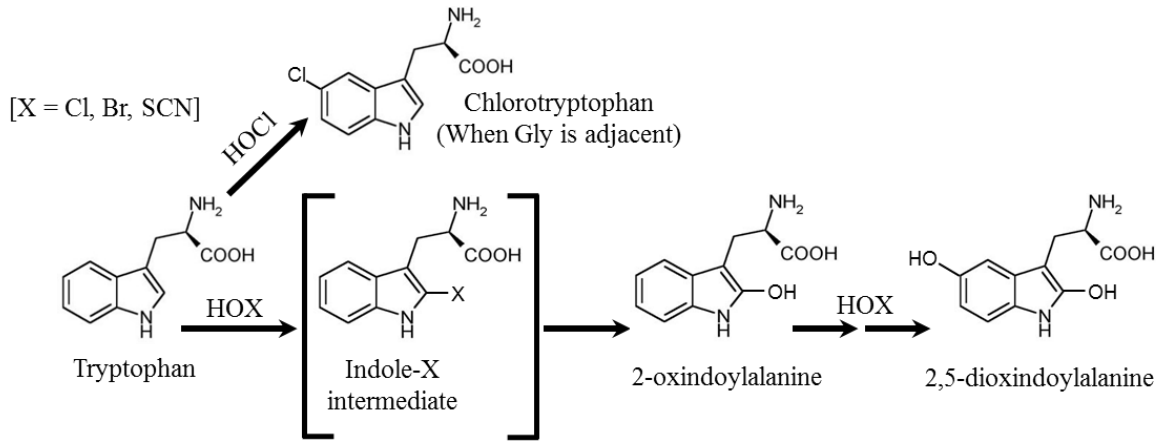

Figure 1.5. Trp oxidation by hypohalous acids. *Tryptophan can be oxidised by HOCl, HOBr or HOSCN to form the 2-oxindoylalanine, which can be further oxidised again to 2,5-dioxindoylalanine.*

Evidence for the reactivity of HOSCN and Trp is available [64]. Under conditions of localised thiol depletion or in the absence of thiols, Trp may become a viable target of HOSCN. HOSCN was shown to exhibit reactivity towards Trp residues of apolipoprotein A-I, which lacks Cys residues, resulting in the formation of mono- and dioxyindoylalanine which affected the ability of this protein to efflux cholesterol from cells [99]. In a related study, HOSCN was proposed to produce the oxindoylalanine species of Trp oxidation *via* hydrolysis of indole-SCN intermediates [100]. However, a subsequent study has shown that HOSCN-mediated Trp oxidation is only significant under highly acidic conditions (pH 2) which may facilitate thiocyanogen ($(SCN)_2$) reactivity [101]. Therefore, the physiological relevance of HOSCN-derived oxidation of Trp remains to be established.

1.3.1.3. Lysine and Histidine

HOCl and HOBr are highly reactive with α-amino and side-chain nitrogen moieties of Lys and His forming reactive halamines [61, 102, 103]. HOCl and HOBr halogenate the secondary amine of the imidazolic ring of His, which can undergo halogen transfer reactions to other peptidyl groups, acting as an important intermediate oxidant [102]. Lys residues are halogenated at the α- and ε-amino groups (Reaction 3 and 4) [104]. These halamine species

also retain some oxidative properties of their parent oxidant (reviewed [105]), thus acting as secondary oxidants potentially causing additional oxidative damage [102]. Indeed, chloramines can be more efficient at oxidising thiols (leading to the formation of disulfides (Reaction 5 and 6)) due to their higher specificity compared to HOCl [106, 107]. This may be applicable to analogous bromamines, but this has not been experimentally verified.

$$R\text{-}NH_2 + HOCl \longrightarrow R\text{-}NHCl \qquad (3)$$

$$R\text{-}NH_2 + HOBr \longrightarrow R\text{-}NHBr \qquad (4)$$

$$R\text{-}NHCl + R\text{-}SH \longrightarrow R\text{-}NH_2 + R\text{-}SCl \qquad (5)$$

$$R\text{-}SCl + R\text{-}SH \longrightarrow R\text{-}SS\text{-}R + H^+ + Cl^- \qquad (6)$$

The decomposition of side-chain chloramines and bromamines (e.g. Lys ε-amino group) on low-molecular mass amino acid derivatives, peptides and proteins can produce nitrogen-centred radicals (ε-aminyl radicals; R-N(H)$^\bullet$) [108-110]. Nitrogen-centred radicals can rearrange to produce carbon-centred radicals *via* multiple radical intermediates leading to protein fragmentation [108, 109]. The decomposition of protein-derived chloramines has also been implicated in the propagation of damage to other targets. Lys chloramines formed on exposure of low-density lipoprotein (LDL) to HOCl are implicated in the induction of lipid peroxidation in the same particles [111]. Other studies present evidence for chlorination of Lys-rich histones to form chloramines that break down to free-radicals, mediating cross-linking and fragmentation of DNA and nucleosides [112, 113]. DNA fragmentation and cross-linking could have implications for MPO activity in cell apoptosis in inflammatory diseases like atherosclerosis, and in carcinogenesis, but further investigation into the relevance of this chloramine activity *in vivo* is still required.

Evidence suggests that HOSCN can react with imidazole (as in His) to form thiocyanatimines (R-N(SCN)-R'), which retain the oxidising capacity of HOSCN [87].

Similarly, a poly-Lys model has shown amino thiocyanate (R-NH-SCN) species can form on the ε-amine of Lys [64] (Reaction 7). However, R-NH-SCN is unstable and is readily reversible by hydrolysis [87]. Thus, it is uncertain that amino thiocyanate formation is relevant in biological systems. Regardless, R-NH-SCN would not be as detrimental compared to chloramine species which can undergo auto-degradation to form nitrogen-centred radicals.

$$R\text{-}NH_2 + HOSCN \rightleftharpoons R\text{-}NH\text{-}SCN + H_2O \qquad (7)$$

1.3.1.4. Tyrosine

The reaction of HOCl and HOBr with Tyr residues involves the electrophilic halogenation substitution reaction with a hydrogen atom in the phenol group to produce the stable halogenated products 3-chlorotyrosine (3-Cl-Tyr) and 3-bromotyrosine (3-Br-Tyr; Reaction 8), as well as 3,5-dichlorotyrosine and 3,5-dibromotyrosine, respectively [61, 114-116].

$$RR'CH + HOX \longrightarrow RR'CX + H_2O \qquad (8) \qquad [X = Cl, Br]$$

Notably, ring halogenation occurs ~10 000-fold faster with HOBr to form 3-Br-Tyr compared with HOCl to form 3-Cl-Tyr [61]. Tyr chlorination by secondary chloramines, such as lysine chloramine, is shown to increase the formation of 3-Cl-Tyr in biological systems [117]. Despite the relatively slow reactivity of HOCl with tyrosyl residues (k = 23 $M^{-1}{\bullet}s^{-1}$ [60]), 3-Cl-Tyr is a well-established biomarker of MPO activity and systemic inflammation [118]. Although 3-Cl-Tyr is an established biomarker, it was found to be unreliable as a quantitative measure of MPO activity, as it is oxidised further in the presence of high concentrations of HOCl and $ONOO^-$ [60, 119]. Another confounding factor is that elevated circulating SCN^- levels perturb 3-Cl-Tyr formation, which was shown to be reduced in smokers with elevated plasma SCN^- [120]. Even though 3-Cl-Tyr is a valid signature of MPO activity, it cannot be reliably used to quantify oxidation. Other biomarkers need to be assessed for this purpose. No appreciable reaction is believed to occur directly between HOSCN and Tyr at physiological

pH. However, Tyr-SCN adducts are observed upon following the exposure of proteins to thiocyanogen $(SCN)_2$ or the LPO-H_2O_2-SCN^- system [82].

Tyr is also a substrate of MPO. MPO compound I catalyses the formation of tyrosyl radicals *via* 1 electron oxidation while transforming to compound II *via* the peroxidation cycle [121]. Tyr radicals can cause lipid damage by the generation of lipid hydroperoxides [122]. Alternatively, Tyr radicals can dimerise to form the major conformational product o,o'-dityrosine (Figure 1.6) [123, 124]. Intra- and inter-molecular cross-linking can form between proteins *via* these dityrosine adducts, altering or inactivating proteins. Tyr was shown to be competitive to Cl^- as a substrate of MPO, where supraphysiological Cl^- concentrations (600 mM) only halved the Tyr oxidation [121]. However, the greater specificity of SCN^- compared to Cl^- to MPO may effectively compete with Tyr oxidation by compound I, although inhibition of Tyr oxidation by SCN^- supplementation has not been empirically tested.

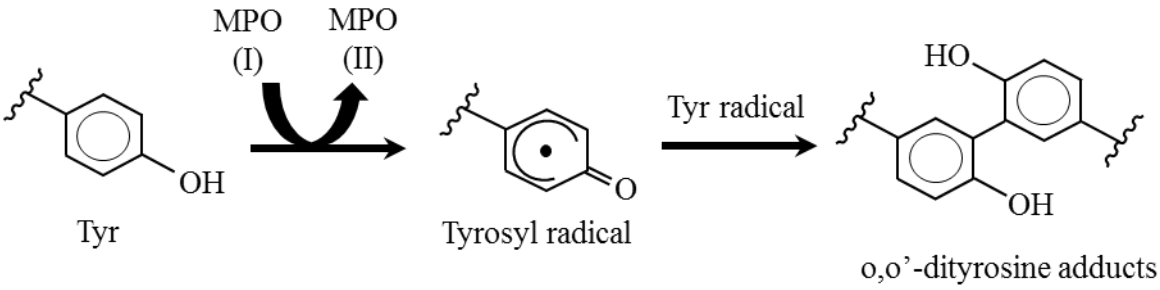

Figure 1.6. Dityrosine formation by MPO. *Tyr residues can be oxidised by MPO compound I to produce a Tyr radical species and MPO compound II. Further reaction with another Tyr radical forms the o'o-dityrosine adduct.*

1.3.1.5. Selenium-containing amino acids

Selenocysteine (Sec) is unique as the only selenium-containing amino acid that is genetically coded into proteins, albeit exclusively those of the cellular antioxidant defences, which will be summarised in Section 1.4.3. HOCl and HOBr reactivity towards Sec is too rapid to kinetically measure, while HOSCN has been measured to have high reactivity to Sec (k_{HOSCN}

= 1.24 × 10^6 M^{-1}•s^{-1} [63]). The reaction of the selenol group (R-SeH) of Sec with HOSCN is similar with thiols, with the initial formation of a selenothiocyanate (R-Se-SCN) intermediate (Reaction 9). The R-Se-SCN species can react with another selenol to form a diselenide (R-SeSe-R') or thiols to form a mixed R-SSe-R bridge (Reaction 10 and 11) [63]. The higher reactivity of Sec as a selenium-based thiol analogue to hypohalous acids makes Sec an attractive exogenous antioxidant, in addition to bolstering the selenoenzyme antioxidative capacity of the thioredoxin and glutaredoxin (Section 1.4.3).

$$\text{R-SeH} + \text{HOSCN} \longrightarrow \text{R-Se-SCN} + \text{H}_2\text{O} \qquad (9)$$

$$\text{R-Se-SCN} + \text{R'-SeH} \longrightarrow \text{R-SeSe-R'} + \text{SCN}^- + \text{H}^- \qquad (10)$$

$$\text{R-Se-SCN} + \text{R'-SH} \longrightarrow \text{R-SeS-R'} + \text{SCN}^- + \text{H}^- \qquad (11)$$

Notably, all three hypohalous acids show high reactivity towards selenomethionine (SeMet; *cf.* k_{HOSCN} = 2.8 × 10^3 M^{-1}•s^{-1} [63], k_{HOCl} = 3.2 × 10^8 M^{-1}•s^{-1} [65] and k_{HOBr} = 1.4 × 10^7 M^{-1}•s^{-1} [65]), the selenium analogue of Met. Although there is no codon for SeMet, SeMet can substitute for Met into proteins as the tRNA for Met cannot discriminate between the two species [125]. Analogous to sulfoxides formed with the reaction of HOCl or HOBr to Met, this reaction with SeMet results in the formation of selenoxides (MetSeO; R-SeO-CH_3) [63, 126]. A major difference between MetSO and MetSeO is that MetSeO formation is readily reversible by thiols and ascorbate [127, 128]. This has implications to bolstering the antioxidative capability of cells by the cycling between free SeMet and MetSeO, or protect SeMet-incorporated proteins from oxidation-induced inactivation. Based on this, dietetic and pharmacological studies into selenium supplementation in preventative measures of cardiovascular disease may be performed in the future to investigate their efficacy.

1.3.1.6. Reactions with other amino acids

HOCl and HOBr show relatively marginal activity towards arginine (Arg) [58, 61]. Products derived from Arg halogenation have not been extensively studied, but current evidence supports guanidine chlorination [129]. HOBr reacts approximately 70-fold faster with Arg than HOCl (see Table 1.1) and could form analogous bromamides, however no characterisation of this reaction has been performed. Gln and Asn react very slowly (k_{HOCl} = 0.03 M^{-1}•s^{-1} [58] and k_{HOBr} = 1.9 M^{-1}•s^{-1} [61]), therefore the halamides derived from these residues are unlikely to be relevant *in vivo*. As individual amino acids, alanine (Ala), valine (Val), proline (Pro), leucine (Leu), isoleucine (Ile), phenylalanine (Phe), aspartic acid (Asp) and glutamic acid (Glu) have reactive α-amino groups that form halamines when reacted with HOCl and HOBr [105], but show poor reactivity in proteins due to the low reactivity of amide linkages and aliphatic functional groups [53, 61].

1.3.2. Lipids

MPO-derived hypohalous acids are capable of oxidising lipids. HOCl and HOBr react with the double bonds of unsaturated fatty acids, phospholipids, and cholesterol to form halohydrins [130, 131] (Figure 1.7). Halohydrins are characteristic markers of hypohalous-derived lipid oxidation. Halohydrin-incorporated oleic acid micelles caused haemolysis [132], were cytotoxic to human umbilical vein endothelial cells (HUVEC) [133], and were shown to deplete adenosine triphosphate (ATP) levels in U937 cells and enhance leukocyte adhesion to arterial segments isolated from mice [134].

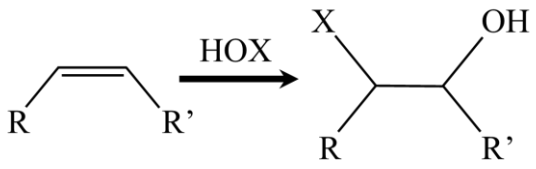

Figure 1.7. Halohydrin formation by HOCl and HOBr on unsaturated lipids.

HOCl and HOBr exert significantly lower reactivity to most lipids compared to sulfydryl or amino groups of proteins, but phosphatidylserine and phosphatidylethanolamine also react with HOCl and HOBr at rates competitive with hypohalous acid modification of amino acids (*ca.* $k_{HOCl} \sim 10^5$ $M^{-1}.s^{-1}$ [135] and $k_{HOBr} \sim 10^6$ $M^{-1}.s^{-1}$ [136]) and could be competitive reactants *in vivo*. As a result, stable chloramines are produced on the amine head group [131, 135]. The corresponding bromamines generated are unstable and could likely decompose to form radicals that propagate secondary oxidation reactions [136], however this remains unconfirmed. Plasmalogens are also a major lipid component of the plasma, lipid pools of cells and in LDL, and are reactive with the MPO-H_2O_2-Cl^- system at the ester linkage to form 2-chloro-fatty aldehyde derivatives and lysophosphatidylcholine [137-139], the latter of which can further react with HOCl to form chlorohydrins [130, 140]. Notably, 2-chloro-fatty aldehyde products have been detected in elevated levels in human aortic lesions compared to the normal aorta [141] and may have clinical relevance to atherosclerosis in myocardial ischaemia (reviewed [142]).

The addition of SCN^- to an MPO system has been shown to promote oxidation of plasma lipids [143]. Further, a study by Exner *et al* demonstrated the formation of lipid hydroperoxides and conjugated dienes when LDL was incubated with a MPO-H_2O_2-SCN^-system [144]. However, the mechanism of oxidation in a MPO-H_2O_2-SCN^- system is not well defined. It is postulated to involve the formation of $SCN^{\bullet}$, $SCN^{\bullet-}$ or $(SCN)_2^{\bullet-}$ species in the MPO system [144, 145], though LDL lipid oxidation is also seen with isolated HOSCN [146]. In contrast, Spalteholz *et al* showed no apparent reactivity of HOSCN with the double bonds of the lipid, 1-palmitoyl-2-oleoyl-sw-glycero-3-phosphocholine (POPC) [147]. Therefore, it is likely that HOSCN reacts selectively with cholesteryl linoleate and arachidonate species [146]. LDL-lipid modification by HOSCN and SCN^- in enzymatic systems will be further discussed in Section 1.6.2.1.c.

1.3.3. Nucleic acids

HOCl and HOBr are strong oxidants of DNA and RNA molecules forming stable and unstable halogenated species. HOCl and HOBr react with heterocyclic (ring-NH groups) and exocyclic (NH_2 groups of guanosine, adenosine and cytidine) amino groups to form a variety of *N*-chlorinated and *N*-brominated derivatives, respectively. These are unstable intermediates that can lead to the formation of stable, carbon-bound halogenated products, 8-chloro-(2'-dioxy)adenosine (8-Cl(d)A), 8-chloro-(2'-dioxy)guanosine (8-Cl(d)G), 5-chloro-(2'-deoxy)cytidine (5-Cl(d)C) and 5-chlorouracil (5-ClU) [148-152]; while HOBr and bromamines can form the brominated equivalents [48, 50, 153-156]. Chlorinated nucleoside products are formed in various inflammatory conditions, including 5-ClU in human atherosclerotic tissue [49]. 5-ClU and 5-BrU have also been found in "neutrophil-rich human inflammatory tissue" [48]. However, brominated nucleosides may be more relevant in diseases involving eosinophil peroxidase (EPO) activity (e.g. Asthma, [157, 158]), known to be highly specific for HOBr production. Contrastingly, HOSCN does not seem to react with nucleosides or DNA [159, 160].

1.3.4. Carbohydrates

Carbohydrates, particularly glycosaminoglycans such as hyaluronan and chondroitin sulfate, also react readily with MPO-derived hypohalous acids [161]. Glycosaminoglycans, which are heteropolysaccharides consisting of repeating amino and uronic sugar-based disaccharides [162], are an integral component of the extracellular matrix (ECM) [162]. The modification of these ECM structures by HOCl and HOBr, by targeting the amine groups present, leads to the formation halamines, dihalamines, halamides and halosulfonamide species [161, 163, 164]. Like other amine modifications mentioned previously, this involves the decomposition to free radical species, which may potentiate damage, leading to altered cell adhesion, growth and signalling [164]. Modification of ECM proteins by MPO-derived

oxidants is likely to play a key role in the development of atherosclerosis, as epitopes of HOCl-induced damage have been colocalised with ECM proteins in diseased tissue [165]. HOCl displays very slow reactivity towards deoxyribose and ribose [166, 167]. Therefore, the reactivity of nitrogenous bases to hypohalous acids rather than the attached sugars is likely to be more significant when considering oxidation of nucleic acids. Unlike HOCl and HOBr, HOSCN has not exhibited any reactivity with carbohydrates [168].

1.4. Exposure of mammalian cells to hypohalous acids

Due to the diverse reactivities of hypohalous acids with biomolecules, there is the potential for cellular dysfunction, damage or death arising from exposure of cells to these oxidants, which can in turn exacerbate existing inflammation. HOCl exposure to mammalian cells has been studied extensively, while the actions of HOBr and HOSCN upon cells are comparatively less well characterised. Comparisons of the effects of these MPO-derived oxidants on cells has recently been reviewed [24]. This section will briefly summarise the effects of HOCl, HOBr and HOSCN on mammalian cells.

1.4.1. Haemolysis

The most extensively studied model of HOCl-induced cellular damage is exposure of human red blood cells, which are haemolysed by HOCl in a dose-dependent manner [169-172]. This was considered likely to result from membrane and cytoskeletal protein modifications leading to destabilisation and lysis [170]. HOBr has been shown to invoke more haemolysis at lower concentrations than by HOCl due to the former's higher reactivity with membrane lipids and proteins [170, 173]. Notably, eosinophils were also shown to be more efficient at haemolysis than neutrophils [174], most likely due to EPO-dependent HOBr production. The haemolytic action of HOSCN has not been demonstrated conclusively. HOSCN has displayed haemolytic

properties, but this was only significant under acidic conditions (pH 6.0) [175], where the low pK_a of HOSCN (pK_a 5.3 [45]) favours the protonated form which can pass through the plasma membrane. More broadly, haemolysis is not proven to contribute significantly to vascular pathology, due to the large number of red blood cells in circulation and high erythrocyte turnover rate, but it is still used as a model of cellular damage consequential to direct hypohalous acid exposure.

1.4.2. Vascular cell apoptosis

In atherosclerosis, endothelial and macrophage death in the arterial wall contributes to the development of a necrotic core linked with destabilisation of atherosclerotic plaques which can lead to rupturing of the fibrous cap and releasing a plethora of thrombogenic material [176]. Exposure of vascular cells to HOCl, HOBr and HOSCN results in extensive cellular dysfunction, enzyme inactivation and cell death (reviewed [24]). Direct HOCl exposure (≤ 500 μM) causes apoptosis of vascular cells, including endothelial cells [23, 177], macrophages [81, 178, 179], and vascular smooth muscle cells (VSMC) [180] *in vitro*. Similarly, HOBr induces apoptosis in endothelial cells [181], monocytes and macrophages [81]. The action upon VSMC has not been reported, although HOBr has been shown to degrade the ECM synthesised by VSMC, which can impair cellular function [164]. With regard to relative impacts, it was reported that HOBr induced apoptosis to a lesser extent than HOCl in HL-60 (human promyelocytic leukaemic) cells, but resulted in greater necrosis than HOCl [182].

Interestingly, HOSCN was shown to be more potent than HOCl and HOBr in inducing apoptosis in HCAEC and macrophages [23, 81]. This is explicable given that HOSCN induced a greater endoplasmic reticular-Ca^{+} efflux into the cytosol of HCAEC than HOCl [183]. The mechanism of Ca^{2+} efflux was shown to occur through the sarco/endoplasmic reticulum Ca^{2+}-ATPase (SERCA) Ca^{2+} pump [183]. SERCA has a high Cys content critical to its ATPase

activity, and HOSCN was shown to more effectively oxidise these thiols compared to HOCl [183]. This could lead to inactivation of SERCA and increased cytosolic Ca^{2+}, posing a plausible mechanism for the difference in potency, with regarding to inducing apoptosis/necrosis, between the three oxidants. However, in this study the apoptosis induced by HOCl may have been underestimated, as apoptosis was determined by the degree that annexin V-binding the ligand of which is the plasma membrane phospholipid, phosphatidylserine. Consideration needs to be made given that phosphatidylserine is a target of HOCl and HOBr [135, 136]. In contrast, Bozonet *et al* [184] observed that HOSCN initially inhibited apoptosis in HUVEC by disrupting the caspase-dependent apoptotic signalling pathway, and suggested HOSCN could play a role in inappropriate survival of damaged cells, which could lead to later necrosis. This was in contrast to later findings in HCAEC, which observed time- and concentration-dependent apoptosis induced by exposure to HOSCN [23]. This discrepancy may be related to phenotypic differences between umbilical vein and adult aortic endothelial cells, which have been shown to responded differently to other inflammatory stimuli; such examples have been demonstrated between human iliac vein and artery endothelial cells [185], as well as HUVEC and HCAEC [186].

Reactive halamines can also cause secondary damage to cells. The range of cellular targets of reactive chloramines is diverse and includes: halogenation of nucleosides and nucleotides [187] and subsequently inhibiting DNA repair [188]; chemical and structural modification of proteins leading to inactivation of cellular enzymes [107, 189] and eventually activating cell apoptosis [190]. Data on the activity of bromamines is limited, but given the similar chemical properties to chloramines, bromamines may have similar effects upon cellular function. Although HOBr induced apoptosis in HL-60 cells, amine-free media negated HOBr induced apoptosis [182], implicating that bromamines and not HOBr are the main cause of apoptosis.

1.4.3. Inflammatory pathway signalling

In conjunction with, or prior to HOCl inducing apoptosis, HOCl has also been shown to activate pro-inflammatory pathways in several mammalian cell types. The extracellular signalling-related kinase 1/2 (ERK1/2) and p38 branches of the mitogen-activated protein kinase (MAPK) signalling pathway—which are crucial to regulation of cell differentiation, proliferation and cell death [191]—were activated in HUVEC and fibroblasts incubated with HOCl [192]. The authors also showed that maximum activation in endothelial cells occurred rapidly and at sub-lethal concentrations, specifically; 20 μM HOCl for 2 min for maximal ERK1/2 stimulation and 15 min for p38 stimulation [192]. Furthermore, inhibition of MAPK/ERK1/2 partially prevented HOCl-induced necrosis (but not apoptosis) of HUVEC [192], implicating an important role of MAPK activation in regulating appropriate management of cell death.

In J774A.1 macrophages, incubation with 50 μM HOSCN significantly inhibited protein tyrosine phosphatases (PTP) together with elevated phosphorylation of MAPK p38 and to a lesser extent, ERK1/2 [193]. In the case of PTP1B, this was linked to the selective oxidation by HOSCN of the Cys in the active site [193]. HOCl also significantly reduced PTP activity [193], which could, at least in part, contribute to the stimulation of p38 and ERK1/2 [192]. HOSCN also induced the expression of tissue factor (TF), via activation of NF-κB and phosphorylated ERK1/2 MAPK in HUVEC to far greater extent than HOCl or HOBr [194]. This was concomitant with an upregulation of endothelial cell adhesion molecules (E-selectin, ICAM-1 and VCAM-1) and increased neutrophil adhesion in HUVEC incubated with ≥ 150 μM HOSCN [195]. This data supports a pro-inflammatory role of HOSCN through promoting neutrophil adhesion and extravasation to sites of inflammation. However, this would be better modelled on a more relevant cell lineage, such as HCAEC.

1.4.4. Cellular antioxidant systems for scavenging hypohalous acids

Although there is strong evidence for cellular damage induced by MPO-derived oxidants, evidence is also mounting for hypohalous acids activating cellular antioxidant defence systems. As mentioned previously, thiols are major targets for HOCl, HOBr and HOSCN [61, 62, 196]. GSH acts as a ubiquitous antioxidant, maintaining redox homeostasis in cells by scavenging free radicals and active oxidants. The oxidation of GSH by HOCl, HOBr and HOSCN leads to formation of their respective sulfenyl halides and further oxidation of thiols to form GSSG [89, 196]. Disulfide bonds can also form with GSH and protein-bound Cys residues (R-SSG), referred to as *S*-gluathionylation.

Over the last two decades, reversible *S*-glutathionylation has been increasingly recognised as a protective mechanism of cellular signalling homeostasis (reviewed [92, 197]). *S*-glutathionylation may be protective of further, irreversible Cys oxidation (e.g. sulfonic acid) [92] as *S*-glutathionylation can be reversed by the Sec-containing thioredoxin (Trx) or glutaredoxin (Grx) system to form GSSG and the reduced Cys, thus restoring protein function (reviewed [56, 198-200]; Figure 1.8). Subsequently, GSSG can be reduced back to GSH by the NADPH-dependent glutathione reductase (GR) system to restore GSH levels and thus redox homeostasis [201]. Notably, under oxidative stress elements such as GSH depletion by hypohalous acids, enzymes involved in GSH synthesis, including GSH synthetase (GS), GR, glutamate-cysteine ligase modifier subunit (Gclm) and catalytic subunit (Gclc) are upregulated [24]. However, this was demonstrated *in vitro* and has not been confirmed in the vasculature under oxidative stress or atherosclerosis *in vivo*.

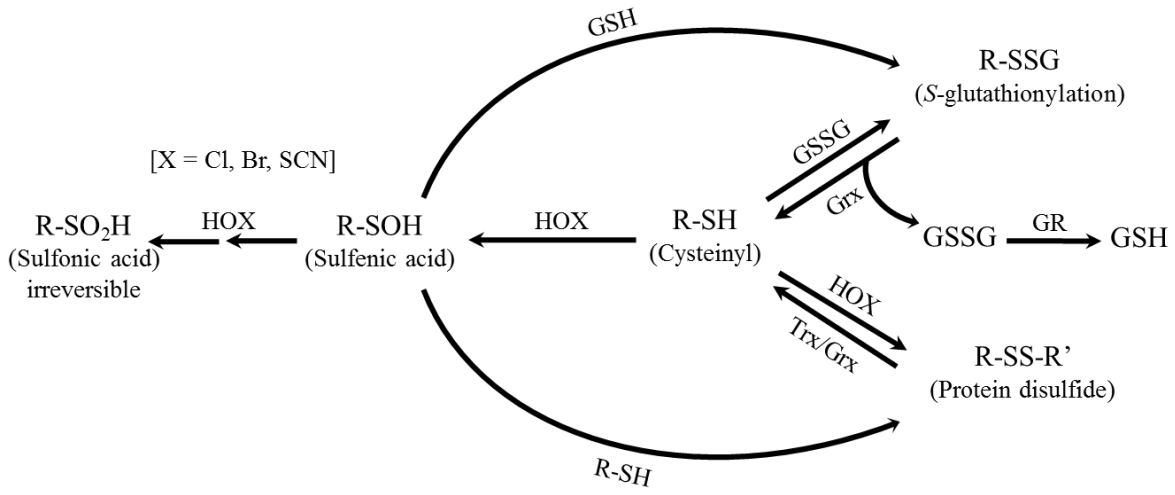

Figure 1.8. Antioxidant protection of proteins by GSH, and the glutaredoxin and thioredoxin system. *Scheme summarises the mechanism of Trx and Grx activity on restoring thiols following oxidation by hypohalous acid described in Section 1.4.4. Sources cited in the main text.*

Trx and Trx reductase (TrxR) activity are also pertinent to the detoxification of HOSCN (reviewed [56]). TrxR is a selenocysteine-containing enzyme responsible for the redox cycling of Trx, but can also reduce HOSCN to SCN^- [202]. HOSCN can also be scavenged by GR, however this is seven-fold slower than the turnover rate with TrxR [202]. Supplementation of Sec to mammalian cells—in addition to its antioxidant properties—also improved the scavenging of HOCl, HOBr and HOSCN by bolstering the resistance of TrxR to oxidation [203]. As well as scavenging of HOSCN produced by peroxidases, this activity by TrxR forms an antioxidant defence mechanism for scavenging of HOX by SCN^-, independent of MPO-dependent production of HOSCN (Figure 1.9).

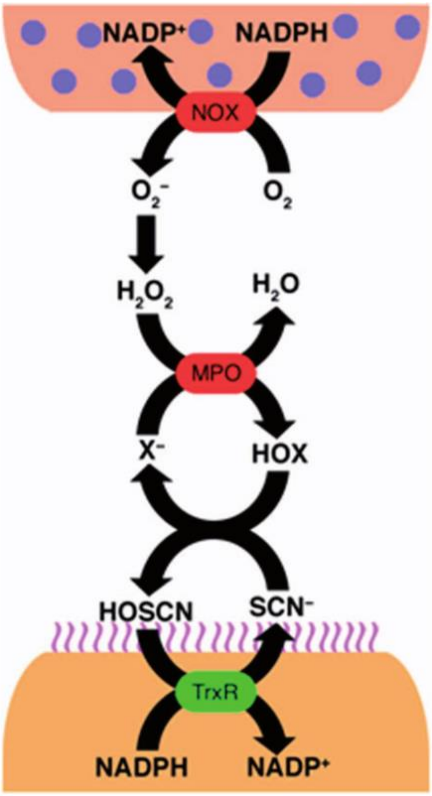

Figure 1.9. HOSCN, SCN- and TrxR as an antioxidant defense mechanism (adapted from [56]). *Respiratory burster by NOX at the cost of NADPH produces $O_2^{\bullet-}$, wihch dismutates to H_2O_2 for utilisation by MPO to produce HOX. HOX is scavenged by SCN^- to produce HOSCN, which is cycled back to SCN^- by TrxR at an additional cost of NADPH.*

1.5. Role of MPO in health and disease

1.5.1. Beneficial role of MPO in the immune system

The MPO-H_2O_2-halide system has shown potent antimicrobial activity that contributes to host-defence against microbial pathogens, especially in the early phases of infection [29, 204-206]. Pilot studies by Klebanoff showed that I^-, Br^- and Cl^- ions added to purified MPO and H_2O_2 effectively killed *Escherichia coli* and *Lactobacillus acidophilus in vitro*, which was prevented with endogenous MPO inhibitors to accentuate the importance of the MPO halogenation cycle [22, 207]. *Actinobacillius actinomycetemcomitans* were also killed with MPO-H_2O_2-Cl^- and I^- systems, but remained viable in a MPO-H_2O_2-SCN^- system [208], while

Helicobacter pylori were actually bacteriostatic at early time points and recovery was prolonged in a similar LPO-H_2O_2-SCN^- system [209]. HOCl has been shown to target multiple chemical groups to impede bacterial viability, such as iron-sulfur, thioether, haem and unsaturated fatty acid groups (reviewed in [118]). In addition to MPO released by degranulation, HOCl was also generated in the phagosome to kill ingested bacteria, which was demonstrated *in vitro* with *Staphylococcus aureus* [210].

In contrast to HOCl, HOSCN is bacteriostatic. HOSCN is likely a major product in the oral cavity, as SCN^- levels are very high (0.5 – 3 mM [211]) and LPO, present in high amounts in the oral cavity, has a high affinity for SCN^- [212]. HOSCN completely inhibited the sugar-synthesising enzyme, hexokinase, and partially inhibited glucose 6-phosphate dehydrogenase [213]. This was supported by Clem and Klebanoff, who demonstrated that HOSCN, though not cytotoxic, inhibited glutamic acid uptake into *L. acidophilus* [214]. LPO activity and SCN^- concentrations are also relatively high in the airway and lung epithelia [215-217], which would protect the airway in similar fashion to the oral cavity. This is made even more apparent in the cases of cystic fibrosis patients who have high susceptibility to lung infections and impaired SCN^- transport [218, 219].

1.5.1.1. MPO deficiency in animal models and the clinic

The contribution of MPO to immune function is underscored in mouse models of MPO deficiency, where the mice are healthy under pathogen-free conditions, but exhibit severely impaired immune function in eliminating infections. Homozygous mutant MPO deficient-mice systemically infected with *Candida albicans* had significantly higher presence (> 100-fold) of *C. albicans* [220], *C. tropicalis*, *Trichosporon asahii*, *Pseudomonas aeruginosa* [221] and *Klebsiella pneumoniae* [222] compared to their respective wild-type, demonstrating a lack of host antibacterial activity in the absence of active MPO. Infection of the lungs with non-viable

C. albicans also increased the number of infiltrating neutrophils in $MPO^{-/-}$ mice compared to the wild-type, indicating the lack of MPO hindered resolution of the inflammatory response [223]. However, *S. aureus*, *Streptococcus pneumoniae, C. glabrate* or *Cryptococcus neoformans* infections in MPO-deficient mice were of similar severity to the wild-type [221], suggesting that some microbial strains are (i) adapted to MPO activity, and/or are (ii) sensitive to MPO-independent immunity. A mechanism independent of MPO halogenating activity has been proposed by way of NADPH oxidase activity promoting electron transport into the vacuole to form $O_2^{\bullet-}$, increasing the pH and depolarising the vacuolar membrane of the neutrophil, leading to K^+ and proton pumping, the latter resulting in activation of neutral proteases to digest the pathogen (reviewed [224]).

Genetic MPO deficiency occurs in between 1:2000 – 1: 4000 people in European and US populations [225], and as low as 1:57000 in Japan [226]. Based on the numerous *in vitro* and animal data, MPO deficiency should result in severe impediment to host defence and could result in recurrent and frequent infections as described above, however this was not the case in humans. A study of 100 people with partial or total MPO deficiency did find higher severity of infections compared to a control population, but not higher susceptibility to the onset of infection [227]. This is contrasting to chronic granulomatous disease, an immunodeficiency disease caused by NOX dysfunction resulting in frequent, severe and sometimes deadly infections [228], which strongly supports the role of NOX over MPO in neutrophil-mediated microbial killing proposed by Segal *et al* [224]. Therefore, the author has proposed that MPO can actually act as a catalase, by reacting with H_2O_2 to form compound I then cycling back to native MPO through the peroxidase cycle, to protect digestive enzymes inside the vacuolar-space during microbial killing, but may act as an antimicrobial, halogenating enzyme when released into the extracellular space [224]. As studies into the role of MPO in the progression of atherosclerosis usually focus on the MPO halogenating activity, this reasoning justifies

further investigation into MPO peroxidation activity in atherosclerosis, which is far less characterised *in vivo*.

1.5.2. MPO, atherosclerosis and cardiovascular disease

Evidence supporting the role of MPO in atherosclerosis is extensive (reviewed [229, 230]). Activated MPO is present through all stages of human atherosclerotic lesion development [21]. Staining of MPO appeared adjacent to cholesterol deposits in advanced lesions and was particularly concentrated near the shoulder region of the atherosclerotic lesions [21]. This is significant as MPO-derived HOCl can activate MMPs [231] and deactivate MMP inhibitors [232] to promote fibrous cap degradation and destabilise plaques, which often occurs at the shoulder regions [4]. Increased MPO activity was supported by the detection of elevated 3-Cl-Tyr levels in LDL and HDL isolated from atherosclerotic tissue compared to normal aortic intima [96, 233]. In agreement with this, HOCl-damaged proteins, as detected using an antibody specific for HOCl-modified protein, colocalised with intimal thickening in atherosclerotic plaques, together with increased apolipoprotein content [234].

Blood and lesion MPO levels are a promising predictive biomarker of CVD and in CVD-related risk stratification. Zhang *et al* [235] pioneered one of the first studies supporting blood and leukocyte MPO levels as an inflammatory marker of atherosclerosis and a risk factor for CAD. The EPIC-Norfolk study [236] of 1 138 CAD patients with 2 237 age- and gender-matched controls supported MPO as a powerful predictor of CAD amongst healthy individuals independent of other classic risk markers (smoking, total cholesterol, HDL, hypertension and leukocyte count). However, blood MPO levels were not predictive of CVD-related mortality [237]. Patients with unstable CAD, characterised by frequent, sporadic symptoms, which can occur at rest, had blood MPO levels significantly higher than those of stable CAD patients, whose symptoms express at predictable times, e.g. after meals or exercise [238]. CAD patients

with elevated MPO levels also had higher risk of developing non-ST segmented-elevated MI (patients presenting a MI with ST-segment depression on an electrocardiogram) and other major adverse cardiac events [239-241]. MPO has not provided risk-stratification in peripheral artery diseases [242], probably as peripheral artery disease has lesser risk of mortality compared to CAD except in cases of carotid and cerebral artery diseases, which can lead to stroke.

High levels of MPO are also implicated in acute coronary syndrome (ACS); a spectrum of cardiovascular symptoms associated with myocardial ischaemia and a high risk of CHD and recurring MI [243, 244]. As stated previously, MPO is not an independent predictor of mortality in stable CAD [237], however it may be predictive following non-fatal ST-elevated MI (STEMI; patients presenting with ST-segment elevation on an electrocardiogram), as well as being predictive of recurring MI [245, 246]. Plasma MPO levels were observed to increase significantly soon after MI, followed by depression within 24 h post-MI [245]. This aligns with findings of increased neutrophil infiltration at to the onset of MI [247].

Considering these studies together, the independent predictive capacity of MPO is limited. Also, MPO has very low specificity for distinguishing categories of CVD independent of other classic markers [248, 249]. Instead, MPO is a useful predictive end-point marker of pre-diagnosed CVD, but not useful for diagnosis independent of other established markers. Furthermore, whether elevated circulating MPO is correlated to increased MPO activity contributing to worse outcomes in these studies, or whether the circulating MPO spectates and is only an indicator of cardiovascular condition needs to be confirmed.

Existing clinical studies do have significant limitations. This is due primarily to the fact that there is no established normal range of plasma MPO, instead a wide range of MPO plasma concentrations have been determined drawing from different patient pools. In addition, heparin,

which is used in anti-coagulation therapy in the clinic, is known to liberate MPO from the endothelium to circulation [250], consequently elevating plasma MPO levels. Some studies declared the use of heparins prior to taking blood samples [244, 248], while others declared heparin was not administered [237, 239, 240], but many others did not disclose heparin administration information [236, 238, 241, 242, 245, 246, 249, 251]. Therefore, standardised protocol to measure plasma MPO levels in the clinic should be devised to allow cross-reference between studies and to establish normal ranges of circulating MPO. However, it remains that the current clinical evidence supports a role of MPO in the development and progression of atherosclerosis and several cardiovascular complications.

1.5.2.1. Role of SCN^- in atherosclerosis

As described earlier, there is substantial evidence for MPO-derived HOCl in the development and progression of CVD. This is less clear for HOSCN. For example, there is still debate on the beneficial vs. the detrimental effects of SCN^- in atherosclerosis. As previously mentioned, smoking is a major risk factor for the early progression of atherosclerosis [13]. A prospective study of 34 439 British doctors and their smoking habits over 50 years found that life-long smokers had a three-fold increase in mortality risk, which halved upon smoking cessation at age 50, and almost completely ameliorated risk upon cessation at age 30 [252]. The thoracic and abdominal aorta of male smokers aged 30-34 had evidence of greater macrophage infiltration and foam cell formation, which correlated with higher plasma SCN^- levels although there was no attempt to relate this to another key component of the disease: modified (i.e. oxidised) LDL [253]. Whereas, in a similar study by Scanlon *et al* showed the abdominal aortas of young people who smoked had elevated levels of malondialdehyde- and 4-hydroxynonenal (4-HNE)-modified Lys (markers of lipid peroxidation) in LDL from atherosclerotic plaques in people with high serum SCN^- versus low serum SCN^- concentrations [254]. This suggested that elevated levels of SCN^-, possibly as a substrate for MPO, promoted

LDL oxidation leading to plaque development, although the authors did not observe an increase in LDL deposition or plaque area [254].

Thiol loss was shown to be greater in the plasma from smokers (with approximately three-fold greater plasma SCN^- levels on average) compared to non-smokers when plasma samples were incubated with MPO and H_2O_2, while plasma thiol levels between smokers and non-smokers were unchanged [42, 55]. This finding supported the hypothesis that elevated SCN^- levels drive MPO-derived production of HOSCN in the plasma, resulting in loss of thiols.

OCN^- and its conjugate acid (isocyanic acid; OCNH) can readily react with amino and sulfhydryl groups, with the reaction with Lys ε-amines resulting in the formation of homocitrulline; a marker of protein carbamylation in renal disease ([255]; Figure 1.10). Protein carbamylation can cause alteration of protein function and is a marker linking renal diseases to atherosclerosis and MPO [256, 257]. In addition to observing a link between conversion of SCN^- to OCN^- by MPO, to uraemia (pathological elevation of circulating levels of urea) and protein (including LDL) carbamylation in renal disease, Wang *et al* [255] also found protein-bound homocitrulline levels were a predictive risk factor for CAD, MI, stroke and death [255]. HDL isolated from five atherosclerotic lesions were found to be heavily carbamylated, but not chlorinated, and in the same study the researchers showed that addition of SCN^- to an MPO-H_2O_2-Cl^- system promoted apoA-1 carbamylation over chlorination *in vitro* and that HOCl was able to convert urea to OCN^- and thus further promote carbamylation [258]. The latter finding has adverse implications for patients with uraemia, regardless of receiving haemodialysis, particularly as in another study plasma MPO levels were shown to be increased—correlative with oxidised LDL—in patients undergoing haemodialysis [259]. CKD and renal failure are associated with elevated protein carbamylation. In patients with chronic renal failure, OCN^- levels in the plasma have been detected at three-fold greater concentration than the control group [260]. However, in the context of renal disease without elevated levels of SCN^-, uraemia

is likely the primary cause of protein carbamylation, due to the equilibrium with OCN^- leading to a rise in OCN^- levels by Le Chatelier principle. SCN^- has also been linked to elevated LDL carbamylation induced by the MPO-H_2O_2-SCN^- system in smokers compared to non-smokers [255], linking the long-established association between inflammation, smoking and atherosclerosis (Figure 1.10).

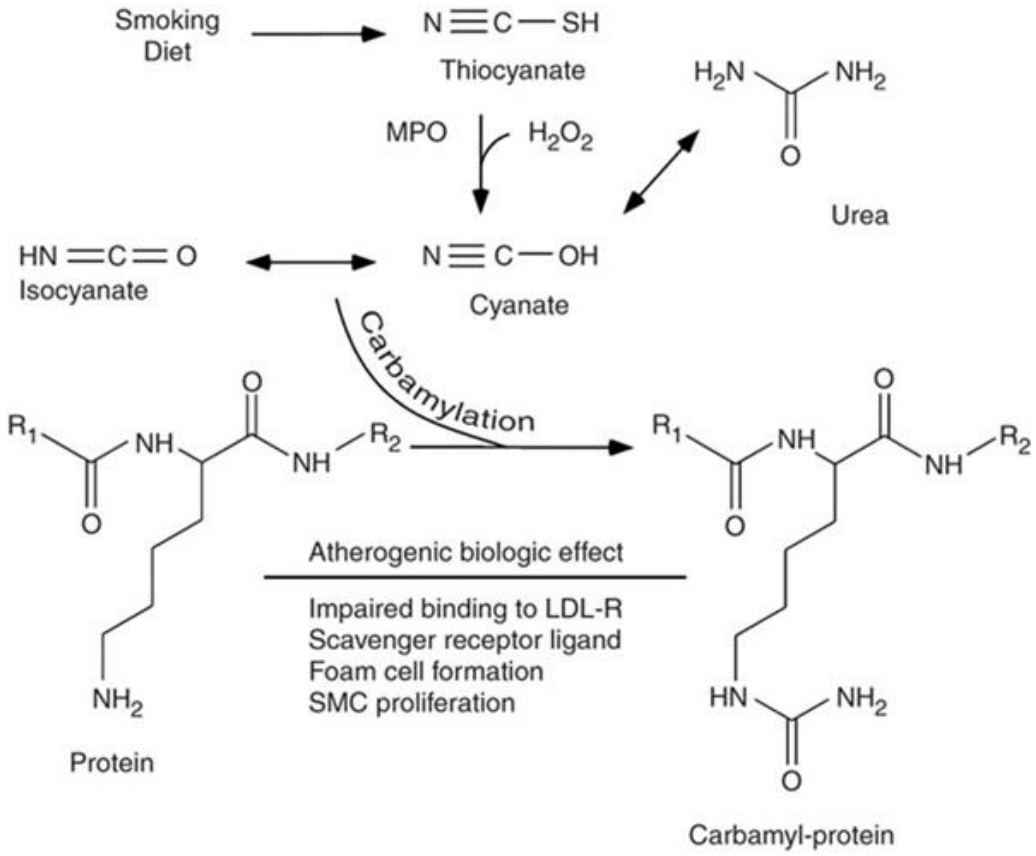

Figure 1.10. Scheme of MPO-mediated conversion of SCN- to OCN- promoting protein carbamylation linked to atherosclerosis (adapted from [255]). *Smoking elevates SCN^- levels in the plasma. MPO utilises H_2O_2 and SCN^- to OCN^- as a minor product besides HOSCN. OCN^- and OCNH promote protein carbamylation at inflammatory sites.*

While the previous studies support the role of SCN^- in CVD and renal disease, there is also evidence to support a beneficial role of elevated SCN^- in the blood. Human MPO transgenic $LDLR^{-/-}$ mice supplemented with SCN^- in drinking water for 12 weeks had plaque area reduced by 26 % [261]. Although plasma SCN^- levels increased three-fold in the plasma compared to

the control (and at concentrations similar to human smokers [42]), there was no change in circulating cholesterol, thiol, MPO or triglyceride levels [261], implicating a local beneficial effect on plaques despite no change to systemic improvement. In addition, a study measuring the mortality of post-MI patients (amongst whom were smokers, non-smokers and past smokers) found that elevated plasma SCN^- levels (categorised as below- and above-median levels in the plasma) were beneficial to survival [55]. Post-MI patients with elevated SCN^- levels had increased survival independent of whether patients had below- or above-median MPO levels, compared to the equivalent cohort with below-median SCN^- levels [55]. These findings were independent of age within each patient group. This was rationalised by the proposition that low MPO with high SCN^- concentrations shifted the MPO-derived production of HOCl to HOSCN [55], limiting the production of HOCl which reacts with a variety of targets compared to HOSCN which reacts mainly with thiols [52]. This is supported by the finding that smokers had significantly reduced levels of 3-Cl-Tyr, which inversely correlated with elevated SCN^- concentration in the plasma [120]. However, further work is required to see if this is related to alterations in MPO-derived oxidant formation.

1.6. Role of LDL in atherosclerosis

1.6.1. Native LDL

High circulating cholesterol is one of the most well-established predictors of atherosclerosis, with LDL-derived lipid accumulation in the artery walls recognised as a hallmark of this disease [262-264]. LDL ($1.019 < \rho < 1.063$ $kg{\cdot}L^{-1}$) is synthesised endogenously by the hydrolysis of very low-density lipoprotein (VLDL; $\rho < 1.019$ $kg{\cdot}L^{-1}$) in the liver [265, 266]. Highlighted by its broad density range, LDL (Figure 1.11) is a complex molecule composed of ~ 3000 lipid molecules (~ 1 600 cholesterol esters (CE), 600 cholesterol, 700 phospholipids and 170 triglycerides [266]), antioxidants (α-tocopherol, Q-tocopherol, carotenoids,

oxycaratenoids and ubiquinol-10 [266]), and a single, large 4536 amino acid, approximately 515 kDa apolipoprotein-B100 (apoB-100; [267]) that binds to the LDL receptor (LDLR). The binding of the C-terminal region of apoB-100 to the LDLR facilitates clearance of LDL from circulation into cells by endocytosis of the LDL-LDLR complex [268-270]. The main function of LDL is to transport cholesterol to cells in the body, to be incorporated into plasma membranes and to provide substrate for steroid hormone production, which is essential to the viability of cells and cell division [271, 272].

1.6.2. Oxidised LDL

LDL can be modified *via* different chemical reactions, including oxidation [263], glycation [273], carbamylation [274] and acetylation [275]. These modified forms of LDL are no longer recognised by the LDLR, but by the scavenger receptors of immune and vascular cells. Oxidised LDL binding to the scavenger receptors present on endothelial, mononuclear leukocytes and smooth muscle cells is believed to lead to the increased deposition of lipids in the vessel wall and inflammation which together drive atherogenesis (reviewed [19, 276, 277]).

Oxidised LDL has been extensively studied in atherosclerosis. Currently, it is generally assumed that the oxidation occurs mostly within the arterial wall, where LDL is sequestered from circulating antioxidants [278, 279]. However, as direct identification of the nature of LDL modification *in vivo* is still elusive, there is controversy regarding the source(s) of LDL oxidation that are relevant *in vivo*. LDL modified by different mechanisms generally have distinct products that induce different responses in cells (extensively reviewed [280]) and will be briefly discussed in this section.

1.6.2.1. MPO-derived oxidation of LDL

There has been extensive research into the modification of LDL, particularly the apoB-100 moiety, by MPO and HOCl [53]. There is robust evidence for an association between LDL,

MPO and atherosclerosis with related adverse cardiac events. HOCl-modified LDL are demonstrable in atherosclerotic lesions [281], contribute to lesion development [282] and can predict the occurrence of CHD [283]. Moreover, MPO and HOCl-modified LDL epitopes are colocalised in advanced atherosclerotic lesions [284]. The modification of LDL by MPO and HOCl results in a particle with pro-atherogenic properties, including promoting foam cell formation and endothelial dysfunction (reviewed [285]). The extent and nature of pro-atherogenic behaviour is related to the extent of modification observed.

1.6.2.1.a. MPO binding to LDL

MPO has a strong binding affinity for LDL, most likely due to the ionic interaction of the cationic MPO (pI > 10 [286]) with the anionic apoB-100 (pI ~ 5.4 [287]). Recently, apoB-100 binding was demonstrated to modulate MPO activity. Delporte *et al* showed that the presence of LDL promoted both halogenation and peroxidation activity of MPO [288], while both activities were partially attenuated when MPO was bound to HOCl-modified LDL [288]. Sokolov *et al* tested a number of small oligopeptides matching sequences of apoB-100 containing anionic residues (*i.e.* Asp (D) and Glu (E)) to find potential binding sites for MPO on LDL [289]. The authors tested peptides ^{1}EEEMLEN^{7}, ^{53}VELEVPQ^{59} and found that only the latter peptide competitively prevented MPO binding to LDL, thus indirectly identifying a possible MPO binding domain on LDL. Soon after, Sokolov *et al* observed that ^{445}EQIQDDCTGDED^{456} peptide added to a MPO-H_2O_2-halide-bound LDL system significantly prevented cholesterol accumulation after both 12 and 72 h incubation with monocytes/macrophages [290]. This study also found that SCN^- added to a MPO-H_2O_2-halide-bound LDL system almost completely prevented cholesterol accumulation [290], suggesting that a MPO-H_2O_2-SCN^- system preserves native LDL (at least when MPO is bound to LDL). These studies support investigations into a small peptide-based pharmacological approach to inhibit MPO activity localised to modifying LDL molecules *in vivo*.

1.6.2.1.b. Apolipoprotein B-100 modification by MPO

LDL modified by HOCl and the MPO-H_2O_2-Cl^- system has been meticulously characterised (reviewed [53]). However, it should be noted that differences in LDL modification may arise between a HOCl reagent and MPO enzymatic system [291]. In agreement with reaction kinetics (Table 1.1), the order of depletion of apoB-100 residues was Cys >> Lys > Trp when LDL was treated with HOCl at 300-fold molar excess [111, 292]. Yang *et al* identified Met, Cys, Lys, Trp and Tyr as targets of HOCl and the MPO-H_2O_2-Cl^- system [291]. Extensive Met oxidation (31 residues), multiple Trp oxidation sites (8 oxidised Trp and 3 di-oxidised Trp), and 3 chlorinated Tyr residues have recently been detected by rapid resolution LC-MS/MS in LDL modified with up to 100 µM HOCl (50:1 HOCl/LDL ratio) [288]. However, this did not match an equivalent (up to 100 µM H_2O_2) MPO-H_2O_2-Cl^- system, which failed to oxidise 19 Met, 2 Tyr and all the Trp residues that were able to be oxidised by reagent HOCl [288]. Much greater H_2O_2 concentrations were required (1 250 µM) to reach a similar extent of oxidation as 100 µM reagent HOCl, showing that the binding of MPO caused targeted oxidation of LDL residues [288]. Recently, a more comprehensive analysis has measured the relative reactivities of residues in apoB-100 to HOCl in the order of Met ≈ Cys > Lys ≈ Tyr > His ≈ Arg [53]. Trp may be elusive targets of an MPO-H_2O_2-Cl^- system due to their scarcity (only 32 Trp residues in the entire 4 536 residue apoB-100 [266]), and possibly because of the hydrophobic indole group preferentially burying into the lipid structure of LDL.

Similarly to Trp, Met is a hydrophobic amino acid and is relatively scant in apoB-100 (78 residues of 4 536 [266]), yet Met is the prime target of MPO-derived oxidation of apoB-100 [53, 288]. It has been suggested that Met oxidation could pose a protective mechanism against oxidative damage for some proteins [72], especially since MetSO can be repaired by Msr [77]. Although MPO binding to LDL increases MPO activity, it may also reduce the capability of

MPO to target key residues [288]. Hence, it cannot yet be disregarded that MPO-LDL binding may be a mechanism limiting the oxidation of residues that are key to the protein's function.

The chlorination products 3-Cl-Tyr and 3,5-diClTyr have been observed in apoB-100 when LDL was exposed to HOCl (100-1000 μM) [116] and are present in LDL isolated from human atherosclerotic lesions [233, 281]. Unlike 3-Cl-Tyr, 3-Br-Tyr has not been established as a biomarker of apoB-100 modification [61, 93]. This is likely due to the low abundance of Br^- ions in circulation (20 – 100 μM) [38].

Oxidised amino acid species of LDL can form inter- and intramolecular peptidyl cross-links (adducts), leading to changes in secondary to quaternary structure [293]. A characteristic mechanism of LDL oxidation is caused by dityrosine formation *via* tyrosyl radical formation mediated by the peroxidation cycle of MPO [121, 122]. LDL isolated from atherosclerotic lesions contained up to 100-fold higher concentrations of dityrosine [294]. However, the amount of dityrosine generated did not account for the total cross-links formed. Inter- and intramolecular sulfenamide, sulfinamide and sulfonamide cross-links have been indicated to form between thiols and Lys or Arg residues of HOCl-modified LDL and could contribute to further cross-linking [84]. Additionally, HOCl can cause cross-linking of Lys with other ε-amino groups *via* Schiff base (-N=C-) formation [293, 295].

There are less data regarding HOSCN-modified apoB-100, as there are no specific biomarkers of HOSCN activity *in vivo*. Regardless, more extensive deposits of oxidised LDL and macrophage foam cells have been found in young smokers who have elevated SCN^- levels [253, 254]. Therefore, increased SCN^- levels, coupled with increased activation of neutrophils in smokers [296, 297], could exacerbate the atherogenic process in smokers. Ismael *et al* [146] have recently found that only 5 μM of HOSCN (1:2.5 ratio of protein: oxidant) was needed for complete oxidation of thiol-accessible Cys residues in the apoB-100. Significant oxidation of

Trp at higher concentrations of HOSCN (≥250 μM) was also observed [146], though the hydrolysis conditions incorporated to measure Trp oxidation result in low pH (≤2) which could lead to artefactual oxidation of Trp residues [100]. Additionally, Trp oxidation was not different between 30 min and 24 h incubation with HOSCN and was also seen on incubation of LDL for 24 h with no oxidant [146]. Other residues of LDL (Met, Lys and Tyr) did not react with up to 750 μM HOSCN [146]. This seems in contradiction to Sokolov *et al* who observed near complete prevention of LDL modification with a MPO-H_2O_2-SCN^- [290]. However, MPO binding to LDL in that study would sequester activity near the binding site (^{445}EQIQDDCTGDED^{456}) [290] which is not the case with reagent HOSCN.

1.6.2.1.c. Lipid modification by MPO

The lipid moieties of LDL are also targets of MPO-derived oxidants, though LDL lipid oxidation may be a secondary process mediated by apoB-100-derived chloramines [293]. Cholesterol oxidation by HOCl and HOBr yields oxysterols, namely 7-ketocholesterol, as well as their corresponding halohydrins and hydroperoxides [93, 298]. Unsaturated phospholipids present in LDL (linoleoyl and arachidonoyl fatty acid phosphatidylcholines) form chlorohydrins [299]. Jerlich *et al* [299] also found that these chlorohydrins were formed in LDL with the absence of peroxides, hence chlorohydrins rather than peroxides may be the major products of LDL phospholipid oxidation by HOCl or the MPO-H_2O_2-Cl^- system. Halohydrins can degrade to yield epoxides [293], however cholesterol chlorohydrins are susceptible to epoxidation during gas chromatography-mass spectrometry (GC-MS) analysis, and notably, electron spray-mass spectrometry (ES-MS) analysis showed epoxides are not a significant secondary product of chlorohydrins [300]. Therefore, the epoxides detected are likely an artefact to the methods for analysing the chlorohydrins.

HOCl and HOBr, also react with amine groups of phospholipids, particularly with phosphatidylethanolamine and phosphatidylserine present in LDL [131]. The reactions of HOCl with phosphatidylethanolamine and phosphatidylserine ($k \sim 10^5$ $M^{-1}{\cdot}s^{-1}$ [135]) are comparable to those of HOCl with many peptidyl side chains. However, reaction rates of HOCl with the major phospholipids in LDL, those of phosphatidylcholine and sphingomyelin, are slow ($k \leq 10$ $M^{-1}{\cdot}s^{-1}$ [135]). It has been proposed that phospholipid chloramines may mediate lipid peroxidation via nitrogen-centred radical intermediary reactions [301]. HOCl produces predominantly chloramines and only chlorohydrins when phospholipid amines were completely chlorinated, while HOBr produced both bromamines and bromohydrins independently [131]. Given that chlorohydrins are less favoured products than chloramines on phospholipids, the presence of chlorohydrins could indicate the severity of MPO-induced phospholipid oxidation *in vivo*.

HOSCN and the MPO-H_2O_2-SCN^- system oxidise LDL lipids to produce conjugated dienes and lipid hydroperoxides *in vitro* [144]. The mechanism was suggested to involve reactions of SCN^- derived radicals ($OSCN^{\bullet-}$ or $(SCN)_2^{\bullet-}$) formed by MPO utilising SCN^- as a peroxidase substrate [33, 168]. However, this is thermodynamically unfavourable and evidence has emerged displaying a loss of cholesterol and cholesteryl esters (linoleate and arachidonate species) in LDL exposed to HOSCN (100 – 750 µM) and an MPO-H_2O_2-SCN^- system (50 – 200 µM SCN^-) [146]. In addition to lipid hydroperoxides, specific products of linoleate and arachidonate oxidation, that being 9-hydroxy-10,12-octadecadienoic acid (9-HODE) and F_2-isoprostanes respectively, were also generated both by HOSCN and the MPO-H_2O_2-SCN^- system [146]. This was mitigated by the addition of butylated hydroxytoluene (BHT) [146], consistent with a radical-mediated pathway of cholesterol modification, however this still warrants verification.

1.6.2.2. Other sources of LDL modification

1.6.2.2.a. Transition metal ions

Transition metal ion (Cu^{2+} and Fe^{2+})-mediated oxidation of LDL has been extensively utilised in experiments to contribute to our understanding of LDL oxidation in atherosclerosis. Esterbauer *et al* [302] established a method of Cu^{2+}-mediated oxidation of LDL, to simulate biological responses to oxidised LDL *in vitro*. This method leads to extensive lipid oxidation through free radical generation, causing the reduction or depletion of free cholesterol, unsaturated fatty acid cholesterol esters and α-tocopherol, the formation of cholesterol ester hydroperoxides [303, 304]. This has been shown to induce several proatherogenic effects; including uptake by macrophages to produce foam cells leading to caspase-dependent apoptosis [305], promotion of ROS production in vascular smooth muscle cells [306], enhanced monocyte and leukocyte adhesion to endothelial cells [307, 308]; and reduced endothelial nitric oxide synthase (eNOS) expression and NO production in endothelial cells [309]. Cu^{2+}-oxidised LDL is also known to induce activation of proinflammatory transcription factors in vascular cells; such as nuclear factor-kappa B (NF-κB) [306, 310, 311], activator protein-1 (AP-1) [312, 313], hypoxia-inducible factor-1 (HIF-1) [314] and nuclear factor of activated T cells (NFAT) [315, 316].

There is controversy as to whether the modification of LDL by Cu^{2+} ions could contribute to atherosclerosis *in vivo*. Wilson disease; a rare hereditary disorder causing Cu^{2+} ion accumulation in vital organs, has not been linked to atherosclerosis in the literature, and cardiac events linked to Wilson's disease are rare [317]. Ceruloplasmin, which binds 95 % of Cu^{2+} ions in a healthy adult [304], has been shown to contribute to LDL modification [318]. A single ceruloplasmin can bind to up to seven Cu^{2+} ions, however the loss of just a single Cu^{2+} prevents ceruloplasmin-derived LDL modification [318]. Furthermore, LDL levels were actually

decreased and LDL oxidisability was not significantly different between Wilsons disease patients and the control group [319]. Therefore, the relevance of transition metal ions to LDL oxidation and atherosclerosis faces considerable doubt.

Tissue homogenates from atherosclerotic plaques contain elevated amounts of transition metal ions [320], however the process of homogenisation itself can artificially generate catalytically active ions [321]. This was addressed in a study by Stadler *et al*, where elevated levels of Cu^{2+} and iron in advanced human carotid arterial plaque samples (both calcified and complex lesions) were measured by EPR and in acid-digested tissues by inductively coupled plasma mass spectrometry, which was also correlated to cholesterol accumulation [322]. However, the metal ion levels reported (approximately 0.5 nmol Fe and 0.01 nmol Cu per 1 mg of tissue from advanced atherosclerotic lesions [322]) found in advanced lesions might be helpful to indicate range of concentrations seen and how this relates to conditions used to oxidise LDL *in vitro*. Pioneering investigations found epidemiological evidence demonstrating a correlation between iron status and atherosclerosis, particularly in males [37, 323, 324]. A correlation was found between serum oxidised-LDL/LDL ratio and serum ferritin (an indicator or iron levels), but only in males [325]. Despite this, results from a considerable number of clinical and animal studies examining iron overload and haemochromatosis genotype in atherogenesis do not support iron as an independent risk factor of atherosclerosis and CVD [326-332], with a possible exception to the homozygous haemochromatosis genotype H63D [330]. Thus, there is not enough evidence to support a role of transition metal ions in driving *in vivo* LDL oxidation during the initial stages of atherosclerosis or development of CVD.

1.6.2.2.b. Lipoxygenase

The lipoxygenase class proteins are (non-haem) iron-containing enzymes that catalyse the oxidation of polyunsaturated fatty acids [333]. Elevated lipoxygenase activity has been

implicated in a variety of diseases including atherosclerosis, carcinogenesis, diabetes, metabolic syndrome, neurodegeneration, stroke and various infectious disease (reviewed [334]). Of interest to LDL modification in atherosclerosis is the activity of 12- and 15-lipoxygenase. Both Lipoxygenase-12 and -15 were observed to oxidise linoleic acid, arachidonic acid and the arachidonate- and linoleate-esterised cholesterol moieties of LDL to form hydroxy fatty acids and carbonyl derivatives which alter the electronegativity of apoB-100 [335, 336]. The mRNA and protein of 15-lipoxygenase and its derived epitope of oxidised LDL has been colocalised in human atherosclerotic lesions, supporting a proatherogenic role of lipoxygenase-mediated lipid oxidation [337]. It should be noted that 12- and 15-lipoxygenase are both encoded by the *ALOX15* gene, the specificity of each isoform is determined by various single amino acid substitutions at crucial binding sites [338, 339]. Evidence shows that 12-lipoxygenase contributes to cholesterol accumulation and fatty acid oxidation in macrophages, while 15-lipoxygenase activity in endothelial cells mediates fatty acid oxidation in LDL [340, 341]. While this could aid in cholesterol clearance from circulation mediated by endothelial cells, it also led to foam cell formation in macrophages if LDL deposition into the vessel wall was left unchecked. One study showed that inhibiting 15-lipoxygenase with 5,8,11,14-eicosatetraynoic acid (EYTA) in endothelial and macrophage cells did not inhibit LDL oxidation *in vitro* [342], but the LDL was incubated in Ham's F10 media contains transition metals at levels that can oxidise LDL [343]. The knowledge of the biological relevance of 12- and 15-lipoxygenase in atherosclerosis is still limited and not fully evaluated [334].

1.6.2.2.c. Glucose

It has been proposed that hyperglycaemia in people with diabetes mellitus (DM) may promote metal ion-mediated glycation of LDL to yield advanced glycation end-products (AGE) [344, 345] and there is evidence for increased formation of AGE adducts on plasma proteins

(including apoB-100) from people with DM [346, 347]. However, the role for AGE-modified LDL in atherosclerosis is not well established. One study found that LDL isolated from DM patients was more susceptible to oxidation than from the control group, but LDL was not glycated [348]. Interestingly, α-tocopherol levels were not reduced in LDL from DM patients compared control groups [348], which further implicated transition metal ions were not involved. Intracellular cholesterol levels in macrophages, endothelial and smooth muscle cells were not significantly altered when treated with glucose-treated LDL, but accumulation was seen in macrophages treated with methylglyoxal- and glycolaldehyde-treated LDL [349], which react more rapidly than glucose [350]. This implies a DM-related mechanism of LDL modification leading to foam cell formation dependent on hyperglycaemia and inflammation, but the relevance of this to the elevated risk of cardiovascular morbidities in DM patients remains unclear.

1.6.2.2.d. Nitrogen species

NO derived from nitric oxide synthases (NOS), and $O_2^{\bullet-}$ can react together to form a potent oxidant peroxynitrite ($ONOO^-$). The high reactivity of $ONOO^-$ can potentiate nitration, nitrosylation and nitroxidation of biomolecules [351-353], such as nitration of Tyr residues to form 3-nitrotyrosine (3-nitroTyr) on apoB-100 [354]. 3-nitroTyr has also been detected in human atherosclerotic lesions but not in plasma, implying a role in plaque progression [354, 355]. $ONOO^-$ can also oxidise the lipid fraction of LDL to produce lipid hydroperoxides and increase LDL uptake by macrophages [356-358]. Interestingly, MPO can utilise nitrite (NO_2^-) to form inflammatory oxidants $NO_2^{\bullet}$ and NO_2Cl, which also nitrate Tyr residues [359]. Additionally, an MPO-H_2O_2-NO_2^- system can induce LDL lipid peroxidation, which converts LDL into an high-uptake atherogenic form [360, 361] and produce 7α- and 7β-hydroxycholesterol, which were cytotoxic to HUVEC [362].

1.6.2.3. Prevention of LDL modification

1.6.2.3.a. α-tocopherol and ascorbate

Ascorbate (Vitamin C) and α-tocopherol (Vitamin E) have been shown to prevent LDL cholesterol oxidation under exposure to atmospheric oxygen [363]. Ascorbate is also sacrificially oxidised to preserve LDL-sourced α-tocopherol levels [363], making it an attractive anti-atherogenic pharmacological antioxidant. Also, ascorbate can react quite rapidly with MPO compound I (1.1×10^6 $M^{-1}.s^{-1}$) and compound II (1.1×10^4 $M^{-1}.s^{-1}$) by the peroxidation cycle [364], which has been shown to prevent MPO-mediated consumption of NO [365], forming the ascorbate radical which can be recycled, while preventing hypohalous acid production. Alpha-tocopherol reacts with HOCl (1.3×10^3 $M^{-1}.s^{-1}$), but supplementation with α-tocopherol did not prevent apoB-100 oxidation [366].

In addition to these *in vitro* studies, lipid oxidation products are detected in LDL associated with reduced antioxidants ascorbate and α-tocopherol in atherosclerotic lesions [367-369] (reviewed [370]). Based on this evidence, high interest was garnered on the efficacy of lipid-antioxidant supplementation on the outcome of atherosclerosis. A large body of epidemiological evidence showed that supplementation with α-tocopherol, but not ascorbate was linked to significant risk reduction in adverse cardiovascular outcomes (reviewed [371]). Unfortunately, overall on comparison of multiple studies, supplementation with antioxidants, such as α-tocopherol, ascorbate, or beta-carotene did not prove successful in reducing atherosclerosis and CVD in clinical trials. A large study of 29 133 Finnish male smokers aged 50 – 69 found that supplementation with α-tocopherol, β-carotene or both did not reduce cardiovascular mortality [372]. This was later supported by randomised, controlled and blinded studies, involving collaboration between the Primary Prevention Project and the Vitamin E

Atherosclerosis Prevention Study (VEAPS), that found no reduction in cardiovascular mortality with α-tocopherol within a 4-year follow-up [373, 374].

1.6.2.3.b. Flavonoids/Phenolic compounds

Other dietary antioxidants have also been trialled in preventing CVD associated morbidity/mortality. Hydroxyl ($OH^{\bullet}$), alkoxyl ($RO^{\bullet}$) and peroxyl ($ROO^{\bullet}$) radicals are formed by transition metal ions reacting with H_2O_2 and other peroxide compounds present on LDL, including lipids and α-tocopherol [375-377]. Flavonoids are effective scavengers of potent oxidants of $OH^{\bullet}$, $RO^{\bullet}$ and $ROO^{\bullet}$ radicals (reviewed [378]), as well as NO and $ONOO^-$ [379]. Wine-derived phenolics were more effective than α-tocopherol in inhibiting conjugated diene formation in LDL [376]. Similarly, isolated catechins, which are enriched in green tea, accumulated in LDL and protected it from oxidation in the plasma in a small study of 19 healthy subjects given green tea extract [380]. Therefore, flavonoids may be beneficial sacrificial antioxidants.

Epidemiological evidence showed that flavonoids and corresponding phenolic compounds are beneficial to preventing CHD (reviewed [381]). Increasing dietary intake of catechin-rich green tea was correlated with reduced aortic atherosclerosis [382]. Similarly, red wine which is rich in flavonoids may exert the same benefit [383]. Caution is required however, given the previously described elevation of MPO levels in people at risk of CVD. The reason being that MPO can catalyse the formation of highly reactive phenolic species which can react with proteins [384]. MPO compound I can redox cycle phenolic compounds, which lead to phenoyl radical formation and severe reduction in available thiols in HL-60 cells [385]. This was also observed in HL-60 cells with apigenin, accompanied by elevated apoptosis and necrosis [386]. Therefore, flavonoids and phenolic compounds act as MPO inhibitors by diverting MPO activity from halogenation to peroxidation, but conversely a high presence of active

peroxidases may cycle the production of phenoxyl radicals which propagate oxidative stress in inflammatory situations, despite the flavonoid antioxidant properties.

1.6.2.4. MPO halogenation activity inhibitors

1.6.2.4.a. Azide and aryl hydroxamic acids

The prevention of MPO-mediated damage by administering MPO inhibitors may be an effective means of pharmacological intervention in atherosclerosis and significant effort has been placed on the development of agents to inhibit MPO *in vivo* (reviewed [33]). Cyanide is able to inhibit MPO *in vitro* [387], but along with its high toxicity, cyanide undergoes rapid endogenous detoxification by mitochondrial rhodanase enzymes to form SCN^- [388] and together these considerations don't support its therapeutic use. Two early studies demonstrated that two aryl hydroxamic acids, salicylhydroxamic acid (SHA) and benzohydroxamic acid (BHA), significantly inhibited MPO compound II formation by competing with the haem-H_2O_2 binding domain with inhibition of MPO by SHA occurred at three orders of magnitude lower concentration than BHA [389, 390]. Further, SHA, BHA, azide and p-hydroxy benzoic acid hydrazide (pHBAH) inhibited oxidation of apoB-100 by the MPO-H_2O_2-Cl^- system *in vitro*, as assessed by the loss of Trp residues [391]. This same study showed that pHBAH most effectively inhibited MPO-mediated damage of LDL Trp residues compared to azide, BHA and SHA [391]. 4-aminobenzoic acid hydrazide (ABAH) also competes with halogenation substrates and irreversibly inhibit MPO [392]. These studies provide a class of compounds with high efficacy for inhibiting MPO, however a lack of pharmacokinetic data has hindered investigating their effectiveness in preventing MPO-mediated damage *in vivo*.

1.6.2.4.b. Paracetamol

Paracetamol is a common over-the-counter analgaesic/antipyretic drug [393] that was also shown to inhibit MPO halogenation activity [394]. Although not strictly an inhibitor, paracetamol acts as a substrate for compound I to form compound II, then reacts with compound II to reform the native MPO [394], allowing MPO to react with more H_2O_2 to reform compound I. This infers that paracetamol can convert the MPO catalytic cycle into a more catalase-like form without halogenation activity. This was supported by studies showing paracetamol competes with Cl^- and Br^- for reactivity with compound I to reduce the corresponding hypohalous acid production at therapeutic concentrations [395-397]. Paracetamol has been shown to inhibit MPO-H_2O_2-nitrite-mediated damage of LDL [398] and partially inhibited lipid peroxidation in LDL from hypercholesterolaemic rabbits [399]. However, this is contraindicated by the finding that phenoxyl radicals formed by MPO catalyse lipid oxidation of LDL [400]. The formation of acetaminophen free radicals by MPO [394], which can rapidly polymerise and lose their function as an MPO substrate [401], and the hepatotoxicity of long-term paracetamol administration [402] likely makes paracetamol inefficacious in ablating MPO-mediated damage *in vivo*.

1.6.2.4.c. Nitroxides

Nitroxides (TEMPOL-derived compounds), which can oxidise to form stable nitroxide radical groups, have been shown to exhibit oxidant-scavenging properties in inflammation models in animals (reviewed [403]). More recently, TEMPOL was shown to inhibit MPO-dependent Tyr nitration by reacting with compound I and II at favourable rates (3.5×10^5 $M^{-1}{\cdot}s^{-1}$ and 2.1×10^4 $M^{-1}{\cdot}s^{-1}$, respectively [404]) to promote peroxidation cycling [404, 405]. H_2O_2 consumption by MPO and HOCl production by the MPO-H_2O_2-Cl^- system was also inhibited with a range of nitroxide compounds, 4-aminoTEMPO being the most potent [406]. Thus

nitroxide compounds may act as safe and efficacious pharmacological inhibitors of MPO, but the beneficial effects of nitroxides may likely be due to antioxidant activity *in vivo* [403], while inhibiting halogenation activity of MPO may be a minor pleiotropic benefit.

1.7. Vascular dysfunction and oxidised LDL in atherosclerosis

LDL exposed to MPO and its oxidants affects the different tissues of the vasculature in variety of ways that promote inflammation and propagate atherosclerosis. HOCl-modified LDL epitopes are found in atherosclerotic lesions [281, 284], linking to multiple cellular disruptions. While the most characterised pathological process of atherosclerosis is the formation of foam cells [407, 408], endothelial dysfunction is also an important atherogenic process which promotes localised inflammation at the site of lesions [407]. Vascular smooth muscle cell (VSMC) functions are also significantly altered which can manifest in physical alterations such as arterial wall thickening and calcification, leading to the formation of complex lesions [409, 410]. These processes will be described in this section.

1.7.1. Macrophage "foam cell" formation

One of the earliest hallmarks of atherosclerosis is the deposition of lipids within the arterial wall. Macrophages are present in few numbers in normal arterial intima [411]. However, lipoproteins that embed in the vascular wall are prone to modification into high-uptake forms that are recognised by scavenger receptors, leading, and amongst other things, to the accumulation of lipids in these macrophages to form "foam cells" [275]. The scavenger receptors: class A (SR-A1 and 2), class B (SR-B1 and SR-B2, otherwise known as CD36) and lectin-like oxidised LDL receptor-1 (LOX-1): are the most characterised scavenger receptors responsible for unregulated uptake of oxidised LDL in macrophages (reviewed [412]). Scavenger receptor recognition of oxidised LDL leads to multiple proinflammatory signalling

processes, including PKC, NF-κB and MAPK activation, in turn leading to cytokine production [412]. The release of cytokines, such as monocyte chemoattractant protein-1 (MCP-1) and tumour necrosis factor-alpha (TNF-α) leads to activation and chemotaxis of circulating monocytes/macrophages to inflamed vessel walls, which take up oxidised LDL and apoptotic bodies to form foam cells [413, 414].

Uptake of LDL modified by HOCl in macrophages is greater than that for native LDL *in vitro*, leading to intracellular accumulation of cholesterol/cholesteryl esters [292]. MPO-modified LDL induced caspase-dependent apoptosis in THP-1 monocytes and TNF-α production [415], however when differentiated to macrophages, these cells were resistant to apoptosis [305]. HOSCN-modified LDL did induce foam cell formation in macrophages, but not to the same extent as HOCl-modified LDL [146]. However, HOSCN-modified LDL contains significant levels of 9-HODE [146] (as a result of HOSCN-derived modification of cholesteryl esters present in LDL), an endogenous stimulus of peroxisome proliferator-activated receptor gamma (PPARγ). This suggests HOSCN-modified LDL could have other effects on lipid metabolism as PPARγ regulates cellular lipid uptake and upregulated the expression of scavenger receptors on macrophages [416, 417]. Oxidised LDL-induced activation of PPARγ also resulted in C-C chemokine receptor type 2 (CCR2) downregulation to reduce response to MCP-1-mediated chemotaxis [418]. These effects are capable of prolonging macrophage survival and enhancing oxidised LDL uptake with the effect of enhancing atherogenesis.

1.7.2. Endothelial dysfunction

Endothelial cells regulate vascular relaxation *via* NO signalling. However more recently endothelial cells have been acknowledged as playing key regulatory roles in vascular inflammation. Damage to vascular endothelial cells by proinflammatory stimuli is commonly

termed “endothelial dysfunction.” Endothelial dysfunction refers to the reduced endothelium-derived vasodilation and enhanced leukocyte adhesion to facilitate leukocyte infiltration into the arterial wall; a hallmark characteristic of atherosclerotic lesions [247]. Scavenger receptors SR-B1, SR-B2 and LOX-1 are expressed by endothelial cells providing a possible mode of the pro-atherogenic activity of oxidised LDL [419-421].

1.7.2.1. Leukocyte adhesion cascade

During inflammation, endothelial cells residing in inflamed regions will upregulate the expression of adhesion molecules (ICAM-1; intercellular adhesion molecule-1, VCAM-1; vascular cell adhesion molecule 1, and E-selectin) to mediate the attachment and extravasation of leukocytes to the damage site [422]. This process is typically simplified to a three-step leukocyte adhesion cascade; (1) rolling, (2) adhesion, and (3) diapedesis [423]. E-selectin binds to leukocytes expressing P-selectin glycoprotein ligand-1 (PSGL-1) to facilitate leukocyte rolling [424, 425] to extend transit time across the inflamed tissue. VCAM-1 and ICAM-1 on endothelial cells then bind to very late antigen-4 (VLA-4) and lymphocyte function-associated antigen-1 (LFA-1) on neutrophils, respectively, to both facilitate slower rolling along and subsequent arrest onto the endothelium, and ICAM-1 also facilitates diapedesis [426-431].

Thus, in inflammatory disorders like atherosclerosis, adhesion molecule expression sequesters MPO-rich leukocytes to the inflamed vessel, making them strong candidates in contributing to atherosclerosis and perpetuating vascular damage. Uptake of unmodified LDL by HCAEC can increase VCAM-1 and E-selectin *via* an LDLR-related pathway [432], but this only reached approximately 14 % of the magnitude of TNF-α stimulated HCAEC. Cu^{2+}-oxidised LDL has been shown to upregulate ICAM-1, VCAM-1 and in some cases, E-selectin in endothelial cells to promote adhesion of neutrophils [307, 433-435]. Cu^{2+}-oxidised LDL also promotes the release of MCP-1 from endothelial cells to promote chemotaxis and adhesion of

monocytes [436]. One study had observed VCAM-1 mRNA expression in proximal tube endothelial cells was induced in response to LDL heavily modified by HOCl (400:1 molar ratio of HOCl to apoB-100) [437]. However, prospective changes to the expressions of ICAM-1 and E-selectin is currently lacking and requires investigation. HOCl-modified LDL incubated with endothelial cells lead to enhanced adhesion of RAW 264.7 murine macrophages *in vitro*, which was prevented by a CD36 antibody [438]. The effects of HOSCN-modified LDL in endothelial dysfunction has not yet been characterised. Additionally, reactive oxygen species generation, degranulation and adhesion to HUVEC was stimulated in neutrophils incubated with HOCl-modified LDL, but not native LDL or Cu^{2+}-modified LDL [439].

1.7.2.2. Endothelial nitric oxide synthase function and dysfunction

Under physiological conditions, endothelial cells produce NO using the homodimeric eNOS enzyme. NO is a potent messenger molecule, which ligates to guanylyl cyclases, a lyase enzyme that converts guanidine monophosphate (GMP) to cyclic GMP (cGMP), activating the protein kinase G (PKG) signal cascade leading to the upregulation of transcription factors, cytosolic calcium ion efflux and smooth muscle cell relaxation, and consequently vasodilation. NADPH is oxidised to $NADP^+$ in the reductase domain of eNOS to donate an electron, which is transported via calmodulin-regulated flavin adenine dinucleotide (FAD) and flavin mononucleotide (FMN) reduction chain to reduce ferric (Fe^{3+}) haem to ferrous (Fe^{2+}) haem, allowing oxygen binding to the haem (Figure 1.12) [440, 441]. Fe^{2+}-haem binds to cofactor 5,6,7,8-tetrahydrobiopterin (BH_4, or alternatively THB) and L-Arg. BH_4 and a zinc ion bound tetrahedrally to a CXXXXC motif from each eNOS monomer (referred to as a zinc-sulfur (Zn-S) cluster) is needed to stabilise the homodimeric structure of eNOS [442, 443]. L-Arg is then catabolised to form NO in the oxygenase domain of the opposite monomer, releasing L-citrulline (L-Cit) as a by-product.

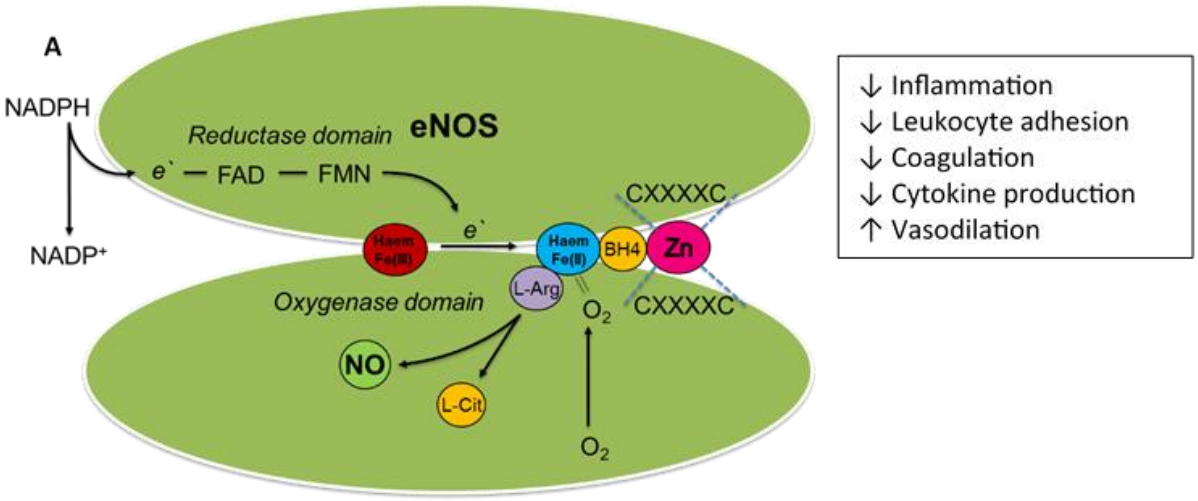

Figure 1.11. Catalytic scheme of NO production by eNOS dimer. *NADPH donates an electron which is shuttled through the reductase domain by FAD and FMN and reduces the Fe(III)-haem to Fe(II)-haem. O_2 binds to haem and BH_4 facilitates catalysis of L-Arg to L-Cit in the oxygenase domain of the opposite monomer of the eNOS dimer, liberating NO. The zinc-sulfur cluster ($Zn(CXXXXC)_2$) stabilises the eNOS dimer. Sources cited in the accompanying text.*

Endothelial dysfunction is defined by reduced NO bioavailability, leading to the promotion of coagulation and reduced arterial distensibility [407]. This occurs by altered function of eNOS switching from NO to $O_2^{\bullet-}$ production, conventionally referred to as uncoupling [441, 444]. Briefly, uncoupled eNOS is no longer stabilised by the Zn-S cluster, so cannot bind haem or BH_4 and functions as a monomer [445]. Under these circumstances, electron transport through the reductase domain cannot transfer electrons to haem, but rather to O_2 directly to form $O_2^{\bullet-}$ (Figure 1.13B). $O_2^{\bullet-}$ and NO can combine to produce the potent oxidant peroxynitrite ($ONOO^-$) which can cause cell stress by nitration, nitrosylation and nitroxidation of biomolecules as well as potentiating further reducing NO bioavailability. This will manifest as the impairment of endothelium-mediated vessel dilation characteristic of atherosclerosis [351].

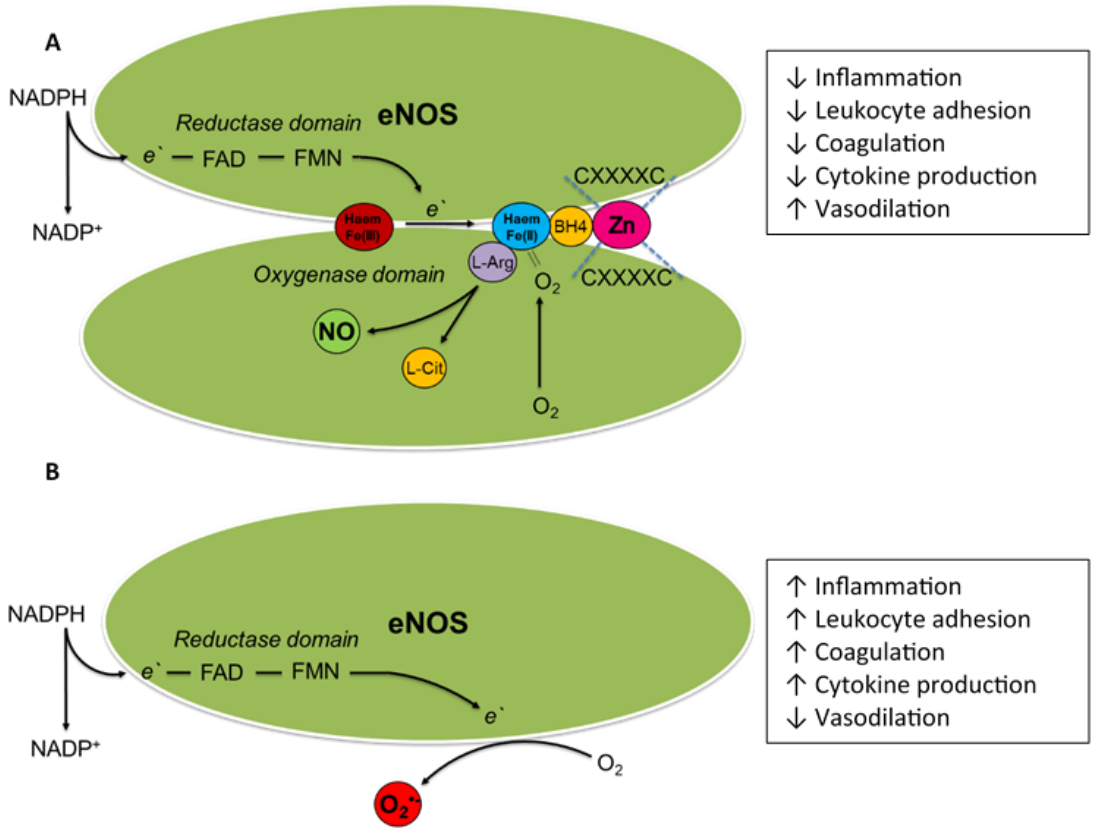

Figure 1.12. Catalytic scheme of NO production by coupled eNOS and $O_2^{\bullet-}$ by uncoupled eNOS. *(A) eNOS dimer as described in Figure 1.9. (B) Uncoupled eNOS exists as a monomer, where the electron is shuttled as in coupled eNOS, but not haem is reduced, instead the electron is scavenged by O_2 to form $O_2^{\bullet-}$.*

Two comparable studies demonstrated that for HOCl and HOSCN exposure to purified HUVEC and HCAEC-derived eNOS resulted in cleavage of the eNOS dimer, oxidation of the Zn-S cluster and overall reduced NO_x levels (indicative of NO production), all indicative of eNOS uncoupling [446, 447]. HOCl-modified LDL induced delocalisation of eNOS from caveolin-1 in HUVEC, which may leave eNOS vulnerable to uncoupling [448]. Yet, evidence has not been obtained for the comparative effect of HOSCN-modified LDL on *in situ* endothelial eNOS activity and expression. Recently, oxidative stress-induced *S*-glutathionylation of conserved Cys residues in the reductase domain has been shown to "switch" eNOS activity, by compromising the reductase FAD- and FMN-binding domains to produce $O_2^{\bullet-}$ [449]. This novel mechanism of eNOS uncoupling, its regulation and relative

contribution to endothelial dysfunction still needs to be elucidated. However, the specificity of HOSCN with Cys could have implications with this glutathionylation-dependent signalling mechanism.

In rabbits fed a high cholesterol diet to produce hypercholesterolaemia, there was increased endothelial $O_2^{\bullet-}$ production and impaired aortic endothelium-dependent vasodilation [450], which was attributed to receptor recognition of LDL [451]. This was later experimentally verified in rabbit aortic [452] and femoral artery vasorelaxation [453], which was shown to be impaired by oxidised LDL. In the porcine coronary artery, oxidised LDL but not native LDL impaired endothelium-dependent vasodilation [454]. A similar finding was also observed with oxidised LDL-, but not native LDL-treated porcine coronary arterioles, which exhibited impaired pressure gradient- and adenosine-mediated vasodilation (both endothelium-dependent) [455], which was supported by another study, with exception of bradykinin-induced vasodilation which was unaffected by oxidised LDL [456]. However, these studies utilised Cu^{2+}- or cell-mediated LDL oxidation and no studies have been published to date describing the effects of MPO-modified LDL.

1.7.2.3. Unfolded Protein Response

The unfolded protein response (UPR) is the pathway involved in the regulation of proteins that are activated when newly synthesised proteins become misfolded and inactive due to endoplasmic reticular (ER) stress (reviewed [457]). Briefly, the role of the UPR is to inhibit the synthesis of proteins, repair protein folding and reverse ER stress [457] (Figure 1.14). The UPR has three distinct branches mediated by inositol requiring kinase-1 (IRE1), activating transcription protein-6 (ATF6) and RNA-activating protein kinase-like ER kinase (PERK) [457]. IRE1 activation leads to splicing of X-box binding protein (XBP1, also the spliced variant; sXBP1), ATF6 activation leads to proteolytic cleavage and translocation to the nucleus

and PERK activation leads to eukaryotic translation initiation factor 2 alpha subunit (eIF2α) phosphorylation; these pathways lead to ER-associated protein degradation and induction of protein folding chaperones [457]. Hence, either the endoplasmic reticulum gets repaired and the cell is rescued, or apoptosis is activated through activation of C/EBP homologous protein (CHOP) through the PERK and/or ATF6 pathway [458].

There is increasing evidence that the accumulation of unfolded proteins is not required for UPR activation [459-461]. This included the induction of UPR by a number of endogenous upstream sources, such as free fatty acids, glucose, homocysteine, angiotensin II and modified LDL (reviewed [462]). Endothelial cells exposed to Cu^{2+}-oxidised LDL activated all three branches of the UPR and induced CHOP and sXBP1 expression, resulting in apoptosis in human microvascular endothelial cells [463, 464]. OxPAPC (a constituent of oxidised phospholipids similar to oxidised LDL) induced the expression of inflammatory markers such as MCP-1, IL-6 and IL-8, which was ablated by genetic silencing of ATF4 and XBP1, indicating that UPR is a regulatory mediator of endothelial inflammation [465]. Whether LDL modified by MPO-derived oxidants induces the UPR in endothelial cells has not been previously demonstrated.

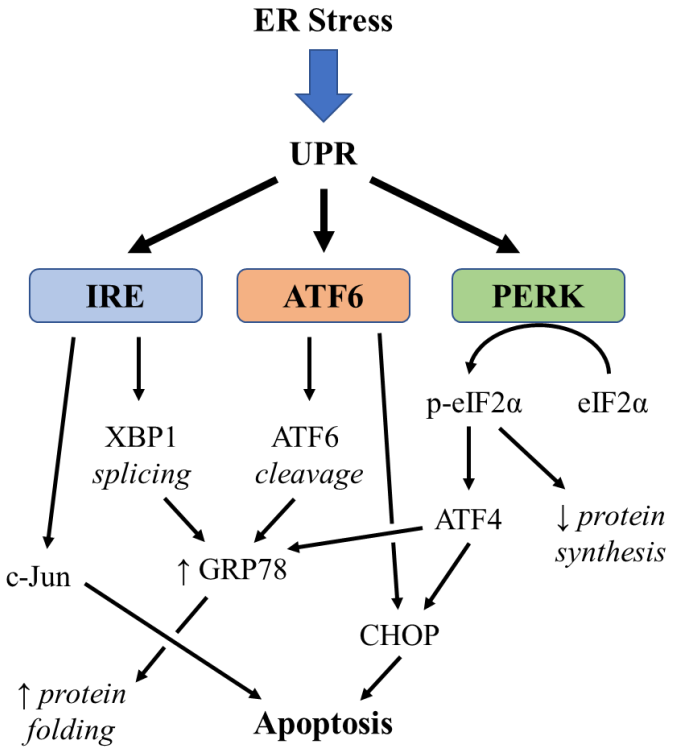

Figure 1.13. Three branches of the UPR. *Scheme summarises the downstream activation of UPR pathways as described in Section 1.7.2.1. Sources cited in the main text.*

1.7.3. Vascular smooth muscle cells

Vascular smooth muscle cells (VSMC) are the effectors of arterial relaxation *via* both endothelium-dependent and independent mechanisms. The dysfunction of smooth muscle cell relaxation is the cause of high blood pressure linked to atherosclerosis and CVD through several pathways including the renin-angiotensin-aldosterone system, proliferation and calcification at lesion sites [4]. These pathways have also shown to be caused by oxidised LDL *in vitro* (reviewed [466]). Cu^{2+}-oxidised LDL induced NF-κB [311] and AP-1 [313] activation in VSMC, thus promoting pro-inflammatory response to oxidised LDL. Additionally, oxidised LDL also induced phosphoinositide 3-kinase (PI_3K)/epithelial growth factor receptor (EGFR)-mediated proliferation in VSMC [467]; a response which is associated with SMC hypertrophy in atherosclerotic lesions [409]. The response of smooth muscle cells to atherogenic stimuli is

complex and displays both pro- and anti-atherogenic properties, which is attributed to the phenotypic plasticity of vascular smooth muscle cells described below.

1.7.3.1. Vascular smooth muscle cell phenotypes

With regard to phenotype, VSMC are highly plastic cells. During angiogenesis (new blood vessel formation from pre-existing vessels) and vasculogenesis (construction of new blood vessels where there are no pre-existing vessels), VSMC are highly migratory and proliferative, and rapidly synthesise ECM components including collagen, elastin and proteoglycans [468]. This stage is also crucial for the development of gap junctions with endothelial cells [469], such as through connexins which are necessary for NO signalling [470]. Contrastingly, migration, proliferation and ECM deposition are slow in established VSMC, signifying their function is solely towards vessel contractility, often termed the "contractile phenotype" [468]. In the event of vascular injury and the resultant inflammation, VSMC can significantly alter their phenotype to aid in vascular repair, termed "synthetic phenotype" [468].

It is beyond doubt that residing VSMC at the sites of vascular injury aid in the repair of the vasculature by altering their phenotype to a highly replicative, migratory and synthetic state [468]. SMC differentiation has strong implications for the development of atherosclerosis. SMC are responsive to inflammatory stimulation and promote inflammation (reviewed [471]). Given that VSMC hyperplasia caused by proliferation and migration is a characteristic of atherosclerotic lesions [4], often termed "remodelling", VSMC phenotypic changes could be integral to vascular repair and be key to monitoring plaque progression and possibly plaque (in)stability. Although referred to as two distinct synthetic and contractile phenotypes, in reality the SMC phenotype will be expressed as a spectrum within the two.

Some studies have shown a causal role of oxidised LDL in the (de)differentiation of VSMC *in vitro*. One study found that VSMC subpopulations responded differently to Cu^{2+}-oxidised

LDL, showing that the "spindle-like" cells had increased liposomal protease activity and accumulated lipids from oxidised LDL, which was not the case with "epithelioid-like" cells, thus indicating phenotypic modulation of SMC in response to oxidised LDL [472]. Cu^{2+}-oxidised LDL also promoted the proliferation and migration of human coronary artery SMC by upregulation of OPN and released matrix metalloprotein-9 (MMP-9) [473], which is also known to promote pro-inflammatory NF-κB and ERK1/2 signalling [474]. Further, oxidised LDL prevented bone marrow-derived SM progenitor cells from differentiation to VSMC by PDGF, shown by reduced gene expression of α-smooth muscle actin (α-SMA) and myocardin, whilst increasing LOX-1 expression, lipid uptake and accumulation [475]. This supports a role for oxidised LDL as a pro-atherogenic stimulus for SMC differentiation. However, the contribution of LDL modified by MPO-derived oxidants in SMC differentiation has not been previously reported.

1.8. Project Outline

Although MPO plays a critical role in the innate immune response to combat pathogens, its misplaced activation and inappropriate generation of oxidants in the vasculature is strongly linked with the development of atherosclerosis. Abundant evidence supports the role of MPO and MPO-derived HOCl in the proatherogenic modification of LDL [53, 476]. HOSCN is also a major product of MPO, yet its role in LDL modification in atherosclerosis is largely unexplored. The reaction of HOSCN and the MPO-H_2O_2-SCN^- system, with LDL modification is of particular relevance to smokers, whom simultaneously exhibit elevated circulating MPO levels [296], SCN^- levels [42, 43], LDL levels [477], and have a greater risk of cardiovascular complications [13, 478] compared to equivalent non-smokers.

Whereas the role of MPO-modified LDL in macrophage "foam cell" formation has been characterised previously [146, 284, 292], considerably less is known on the effects of MPO-

modified LDL on endothelial cells and smooth muscle cells. Similarly, no information is available on LDL modified by HOSCN or the MPO-H_2O_2-SCN^- system in inducing endothelial dysfunction or smooth muscle cell differentiation. The objective of this project therefore is to characterise the physiological effects LDL modified by the MPO-derived oxidants HOCl and HOSCN on endothelial and vascular smooth muscle cells. This is intended to gain a better understanding of the role of SCN^- in the development of atherosclerosis.

1.9. Hypothesis

That LDL modified by MPO-derived oxidants, HOCl and HOSCN, induces vascular cell dysfunction, which will exacerbate inflammation and accelerate inflammatory atherogenesis.

1.10. Aims

The specific project aims are to:

1. Characterise the ability of HOSCN to induce structural modifications to the apoB-100 component of LDL.
2. Determine the cellular uptake of MPO oxidant-modified LDL associated lipids and investigate the effects on inflammatory pathway expression in human endothelial cells.
3. Examine whether each MPO oxidant-modified LDL induces eNOS-dependent endothelial dysfunction in HCAEC *in vitro* and in rat aortic ring segments *ex vivo*.
4. To determine the extent of uptake and cellular reactivity of MPO oxidant-modified LDL with vascular smooth muscle cells.

Chapter 2. Materials and Methods

2.1. Materials and Reagents

All Chemicals were of analytical or higher grade and were purchased from Sigma-Aldrich (Missouri, USA) unless stated otherwise. All aqueous reagents were prepared with nanopure water from a four stage-filtered Milli-Q water system. Phosphate-Buffered Saline (PBS; Amresco; Solon, Ohio) for incubating low-density lipoprotein (LDL; refer to Section 2.3) was treated with Chelex-100 resin (Bio-Rad; Hercules, California) for at least 2 h to remove metal ions, filtered to remove the chelex resin, and then adjusted to pH 7.4 with HCl.

2.2. Generation of myeloperoxidase-derived oxidants

2.2.1. HOCl quantification

HOCl was prepared by diluting a NaOCl stock solution (original concentration of 12.5 % w/v; BDH; Poole, Dorset) with chelated PBS. The concentration of the stock NaOCl was quantified by measuring the absorbance of the stock at pH 11 at 292 nm ($\varepsilon = 350\ M^{-1}\cdot cm^{-1}$) [479]. Stock NaOCl was diluted with chelex-treated PBS immediately prior to use.

2.2.2. HOSCN generation and quantification

HOSCN was produced enzymatically using bovine milk lactoperoxidase (LPO; Calbiochem; San Diego, California) [64, 480]. Briefly, LPO (1.5 – 2 μM) was incubated with 7.5 mM NaSCN in 10 mM potassium phosphate buffer (pH 6.6) and 3.75 μM H_2O_2 was added in five aliquots, 1 minute apart, with a total incubation time of 15 min on ice. Catalase (from bovine liver; 10 μg) was then added to the solution to quench unreacted H_2O_2 and the preparation was incubated for a further 5 min on ice. The preparation was then filtered through a 10 kDa molecular mass cut-off filter (Pall Life Sciences, New York, New York) for 5 min at 10 000 *g* at 4 °C to remove the LPO and catalase.

HOSCN was quantified by 5-thio-2-nitrobenzoic acid (TNB) assay [481]. Briefly, Stock TNB solution was freshly prepared by alkaline hydrolysis of 2 – 2.4 mg DTNB (5,5-dithio-bis-(nitrobenzoic acid)) in 50 mM NaOH. The TNB reagent was then made up by 1:50 dilution of the DTNB stock in chelex-treated 0.1 M sodium phosphate buffer (pH 7.4). Five µL of HOSCN was added to 995 µL of TNB reagent in triplicate and the concentration was determined using the specific molar absorption coefficient of TNB at 412 nm (ε = 14150 M^{-1}**.** cm^{-1}) [481]. The stock HOSCN was then diluted with chelex-treated PBS before incubating with LDL.

2.3. Isolation and oxidation of LDL from plasma

Human blood was taken by a qualified phlebotomist with the donor's consent and under ethics approval (Sydney Local Health District, protocol X12-0375) in accordance with the Declaration of Helsinki, 2000 of the World Medical Association. The collected blood was stored in tubes containing 0.01 mM EDTA (Astral Scientific; Taren Point, NSW), a 1:200 dilution of stock aprotinin from bovine lung (3 – 7 trypsin inhibitor unit/mg protein), 0.04 µM PPACK (a potent, irreversible thrombin inhibitor) and 20 µg**.**mL^{-1} soybean trypsin inhibitor. The plasma was then isolated from whole blood by centrifugation at 3 000 *g* for 20 min at 10 °C. If blood cells were still visible in the plasma, the plasma was replaced into clean tubes and centrifuged again. The plasma was isolated and the density adjusted to 1.24 kg**.**L^{-1} by adding 0.3816 g of KBr per 1 mL of plasma. Density solutions (1.0247, 1.0538, 1.063 and 1.085 kg**.**L^{-1}) were freshly made by combining different volumes of two stock density solutions (1.006 and 1.346 kg**.**L^{-1}) as described in Table 2.1. The final densities were checked gravimetrically and adjusted as appropriate, then degassed under nitrogen. Centrifuged tubes (39.2 mL, Quick-Seal®, 25 × 89 mm polypropylene tubes; Beckman-Coulter, Los Angeles, California) were prepared with 9 mL of each density solution and underlaid with the plasma added in increasing order of density. LDL (ρ 1.019 – 1.050 kg**.**L^{-1}) was isolated using density gradient ultracentrifugation (Optima™ XPN from Beckman-Coulter) using a VTi50 rotor (Beckman,

Palo Alto, California) for 2.5 h at 206 000 *g* at 10 °C [349, 482]. The LDL was then dispensed into new centrifuge tubes, mixed with 1.063 kg**.**L^{-1} density solution and separated from other lipoproteins that may be present in the isolate by a second ultracentrifugation using a Ti70 rotor (Beckman) at 184 000 *g* for 20 h at 10 °C. The LDL was then removed from the centrifuge tubes and dialysed four times for at least 2 h each dialysis in PBS with 1 g**.**L^{-1} EDTA and 0.1 mg**.**L^{-1} chloramphenicol to remove the KBr. The LDL was sterilised through a 0.45 µm filter (Pall Life Sciences) under aseptic conditions and the protein content was measured by bicinchoninic acid (BCA) assay as described in Section 2.5. The LDL was stored in the dark at 4 °C and used within 4 weeks.

Table 2.1. Making density solutions for density gradient ultracentrifugation of LDL from plasma. *Solution A and Solution B are stock density solutions of 1.346 and 1.006 kg**.**L^{-1}, respectively.*

	Volume (mL)	
ρ (kg.**L^{-1})**	**Solution A**	**Solution B**
1.0247	5	85.9
1.0538	12.5	76.37
1.063	10	46.2
1.085	20	66

2.3.1. LDL oxidation

Before oxidation, LDL was desalted through a PD-10 column (GE Healthcare; Barrington, Illinois) to remove the chloramphenicol and EDTA. Apolipoprotein-B100 (apoB-100) concentration was determined using the BCA assay with absorbance read at 562 nm, as detailed in Section 2.5. LDL was diluted in chelated PBS to a concentration of 1.0 mg**.**mL^{-1} apoB-100

(equal to approximately 2 µM apoB-100) prior to incubation with 100 or 250 µM HOSCN or HOCl (equivalent to a 50:1 and 125:1 molar ratio of oxidant: LDL), prepared as described in Section 2.2, at 37 °C and 5 % CO_2 for 24 h, with a control LDL sample incubated under the same conditions without oxidant (control LDL). After incubation, LDL samples were purified through an Amicon (Merck-Millipore; Darmstadt, Hesse) 10 kDa exclusion spin column following the manufacturer's protocol and the protein concentration was remeasured by BCA assay to account for any loss of LDL during the purification step, prior to characterisation or addition to cells as described in Section 2.4 and 2.6, respectively.

2.4. Characterisation of LDL oxidation

2.4.1. ApoB-100 aggregation and fragmentation assessed by SDS-PAGE

The extent of LDL oxidation induced by varying concentrations of HOSCN (0-250 µM) and HOCl (0-250 µM) added to LDL (1.0 mg.mL^{-1}) for 24 h was analysed by sodium dodecyl sulfate-polyacrylamide gel electrophoresis (SDS-PAGE) using a NuPAGE 3-8 % w/v Tris-acetate gel, according to the manufacturer's instructions (Life Technologies; Camarillo, California). Briefly, samples were prepared by adding 2.5 µL of NuPAGE lithium dodecyl sulfate (LDS) buffer and 7.5 µL of nanopure water (or 1 µL of 500 mM DTT in 6.5 µL nanopure water for reduced samples) to a final LDL concentration of 10-20 µg in 20 µL. Samples were left to rest at 21 °C for 30 min before 20 µL of each sample was loaded into a SDS-PAGE gel well. A HiMark 40 – 500 kDa unstained molecular weight ladder (Life Technologies) was run at the same time. Electrophoresis was performed using an Invitrogen XCell SureLock Electrophoresis cell, containing 1X NuPAGE tris-acetate SDS running buffer with running conditions of 80 V for 5 min followed by 120 V for 1.5 h. Gels were stained with Coomassie Brilliant Blue (0.1 % w/v Brilliant Blue G, 40 % v/v ethanol and 10 % v/v acetic

acid) for at least 2 h, then placed in a destain solution (25 % v/v methanol and 10 % v/v acetic acid in nanopure water) under gentle agitation until the gels were adequately destained to allow protein band visualisation. Images of SDS-PAGE gels were then scanned and imaged with SilverFast software (Sarasota, Florida).

2.4.1.1. Silver Stain method

The apoB-100 was separated through SDS-PAGE as described in Section 2.4.1. The gels were submerged in a solution of 50 % methanol and 10 % acetic acid (v/v) for 30 min, then in 5 % (v/v) methanol for 15 min. The gels were then washed three times in deionised water for 5 min each, before incubating with freshly prepared 0.2 $g.L^{-1}$ sodium thiosulfate solution. Excess sodium thiosulfate was washed out for 2 min with deionised, then incubated with 2 $g.L^{-1}$ silver nitrate for 25 min. Excess silver nitrate was washed out for 5 min with deionised water. A development solution of 30 $g.L^{-1}$ sodium carbonate, 4 $mg.L^{-1}$ sodium thiosulfate and 37 % (v/v) formaldehyde was then added until appropriate colour development (1 – 2 min). 14 $g.L^{-1}$ EDTA was added and incubated for 10 min to chelate the silver to stop colour development. The gels were then scanned and imaged using SilverFast software.

2.4.2. Electrophoretic mobility of LDL through agarose gel

The change in electric charge of LDL was assessed empirically by agarose gel electrophoresis and measuring the migration across the gel relative to that of control LDL (i.e. relative electrophoretic mobility; REM). Ten µg of LDL, HOSCN-modified LDL or HOCl-modified LDL were added in 5 separate aliquots to wells in a pre-cast 1 % w/v agarose gels (Helena Laboratories, Mt Waverley, Victoria). The agarose gels were fitted to Ciba Corning gel apparatus containing barbitone buffer (100 mM sodium barbitone, 27 mM barbituric acid

and 12.6 mM EDTA; pH 8.6) at 90 V per gel for 45 min [350]. The REM was measured as the distance migrated by the modified LDL relative to the control LDL.

2.4.3. *De novo* sequencing of apoB-100 fragments by HOSCN-induced oxidation by HOSCN using mass spectrometry

After incubation of LDL with 250 µM HOSCN for 24 h, HOSCN-modified LDL was run through all lanes of a 3-8 % Tris-acetate gel by SDS-PAGE separation, followed up with Coomassie staining and destaining, as described in Section 2.4.1. The subsequent methods for analysing apoB-100 fragmentation by HOSCN described in this section is schematically depicted in Figure 2.1.

2.4.3.1. Trypsin in-gel digestion

The peptide band detected at ~ 97 kDa according to the molecular weight ladder from all sample lanes was pooled together, excised from the gel, diced into approximately 1 mm^3 pieces with a sterile scalpel blade on a glass plate and cleaned with 70 % v/v ethanol. Gel pieces were then transferred to a 2 mL Eppendorf tubes and destained at least three times with 200 µL of 50 % v/v acetonitrile/ 50 % v/v 100 mM ammonium bicarbonate for 10 min each. After the last destain, the liquid was removed and the gel pieces dehydrated with 200 µL of 100 % acetonitrile for 10 min. This was repeated until gel pieces were shrunken and opaque. Cysteines in the peptide were reduced and alkylated to prevent artefactual modification with 5 mM tributylphosphine and 20 mM acrylamide in 100 mM ammonium bicarbonate for 90 min at 21 °C. The liquid was removed and the gel pieces were washed with 100 mM ammonium bicarbonate for 5 min, then three times with 50 % v/v acetonitrile/ 50 % ammonium bicarbonate for 5 min each. The gel pieces were then dehydrated again with 100 % acetonitrile. Acetonitrile was removed, then a 1:80 dilution of 1 $\mu g.mL^{-1}$ mass spectrometry-grade trypsin (Promega;

Fitchburg, Wisconsin) in 100 mM ammonium bicarbonate was incubated with the gel at 4 °C for 30 min for infiltration of trypsin through the gel before trypsin auto-digestion. The gel pieces were then topped up with 100 mM ammonium bicarbonate and digested overnight at 37 °C. The tubes were then sonicated for 10 min, centrifuged briefly and the liquid transferred to a clean 0.65 mL Eppendorf tube. A solution of 50 % v/v acetonitrile and 2 % v/v formic acid was added to the gels, after which the samples were vortexed and sonicated again for 10 min to extract more peptide digests from the gel. This supernatant was then added to the initial digest solution. The volume of peptide solution was concentrated, under vacuum, to approximately 15 µL using a Speedvac Concentrator (John Morris Scientific; Sydney, NSW), and the concentrate was transferred to an autosampler vial and immediately analysed by LC-MS/MS, or otherwise stored at -20 °C.

2.4.3.2. Reductive dimethylation tagging of primary amines

Reductive dimethylation was performed to tag N-terminal primary amines to identify cleavage sites of HOSCN-induced apoB-100 fragmentation [483]. Experimental conditions and procedures were performed as described in Section 2.4.3.1. However, following the reduction and alkylation step, the gel pieces were dried with 100 % acetonitrile, then incubated with 40 mM formaldehyde and 20 mM of freshly prepared cyanoborohydride in water for 1 h at 37 °C. Excess solution was then removed and 100 mM ammonium bicarbonate was added for 5 min to quench the remaining formaldehyde. The ammonium bicarbonate was then removed and the gel pieces were desiccated with 100 % acetonitrile for 5 min. Once dry, trypsin digestion, sample recovery and sample concentration was performed as described in Section 2.4.3.1.

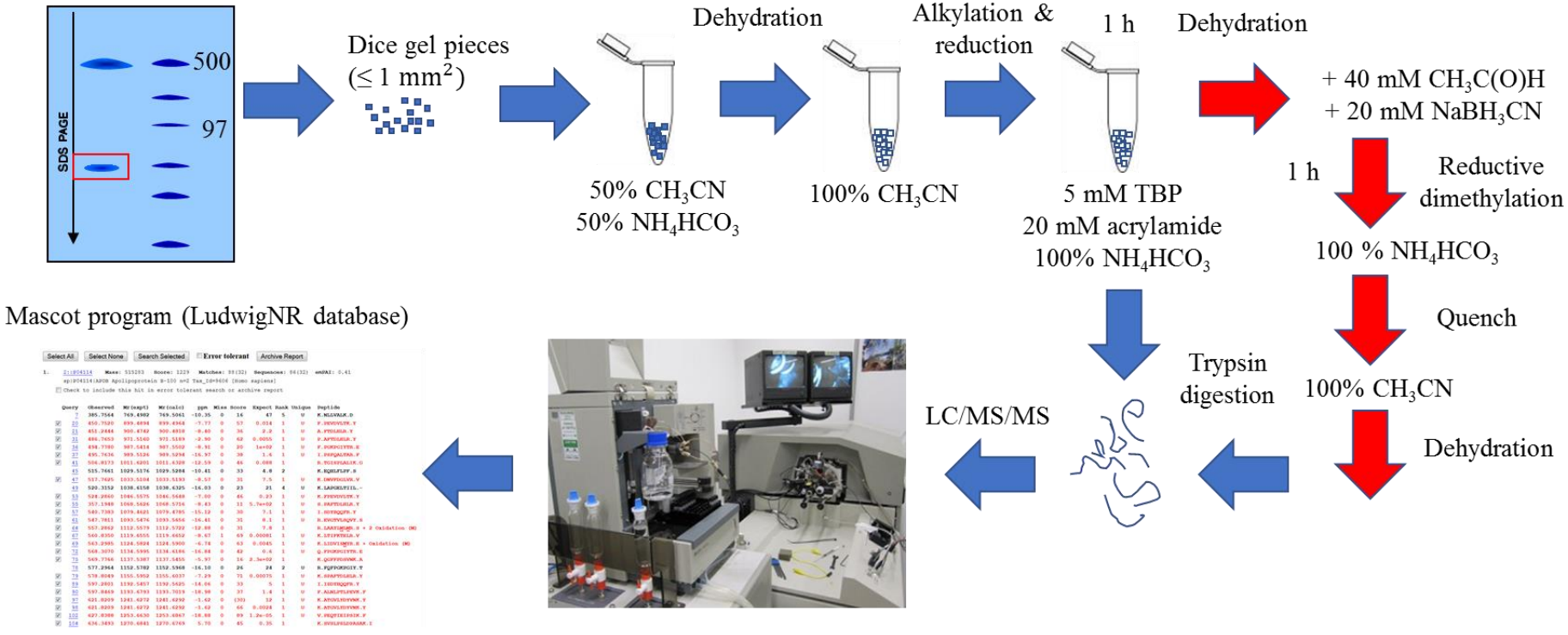

Figure 2.1. Schematic for preparation of HOSCN-modified LDL samples for LC-MS/MS peptide sequencing and N-terminal dimethylation analysis. *Blue arrows indicate pathway for peptide sequencing analysis. Red arrows indicate additional steps for N-terminal dimethylation using 20 mM cyanoborohydride ($NaBH_3CN$) and 40 mM formaldehyde ($CH_3C(O)H$). CH3CN; acetonitrile, NH_4HCO_3; ammonium bicarbonate, TBP; tributylphosphine.*

2.4.3.3. LC-MS/MS

Ten µL of sample was loaded at 20 µL.min^{-1} with MS loading solvent (2 % v/v acetonitrile and 0.2 % v/v trifluoroacetic acid) onto a C8 trap column (Michrom Biosciences, Auburn, California) using an Eksigent AS-1 autosampler connected to a Tempo nanoLC system (Eksigent, Dublin, California). The traps were washed for 3 min before the peptides were washed off the trap at 300 nL.min^{-1} onto a PicoFrit column (75 µm × 100 mm) containing Magic C18AQ resin (Michrom Biosciences). The peptides were then eluted into the QSTAR Elite hybrid quadrupole-time-of-flight mass spectrometer (Applied Biosystems, Foster City, California). MS solvent A (2 % v/v acetonitrile and 0.2 % v/v formic acid) and MS buffer B (98 % v/v acetonitrile and 0.2 % v/v formic acid) were used for the elution gradient of each sample as described in Table 2.1. The eluting peptides were ionised with a 75 µm ID emitter that tapered to 15 µm at 2300 V. An Intelligent Data Acquisition (IDA) analysis was performed, with a mass range of 375 – 1500 Da continuously scanned for peptides of charge state 2^+ - 5^+ with an intensity of more than 30 s^{-1}. The detected peptides were fragmented and the ion products masses were measured over a mass range of 100 – 1500 Da. The precursor peptide masses were then excluded for 15 s.

Table 2.2. Elution gradient for the peptide sequencing analysis of HOSCN-modified LDL fragment.

Time (min)	MS solvent A (%)	MS solvent B (%)
0	95	5
8	50	50
13	20	80
15	20	80
18	95	5

2.4.3.4. Data analysis

MS/MS data files were searched with the Mascot Daemon program through the LudwigNR database (consisting of the UniProt, plasmoDB and Ensembl databases; vQ111. 16,818,973 sequences; 5,891,363,821 residues). The following settings were applied;

- Fixed modification: none.
- Variable modifications: deamidated, propionamide, oxidised methionine.
- Enzyme: semi-trypsin.
- Number of allowed missed cleavages: 3.
- Peptide mass tolerance: ± 100 ppm.
- Fragment mass tolerance: ± 0.2 Da.
- Charge state: 2^+ and 3^+.

The results of the database search were only included if protein hits with at least one unique peptide were detected. Peptide hits with *p*-value > 0.05 were excluded.

2.4.3.5. Inhibition of HOSCN-induced cleavage of apoB-100 with BHT and desferrioxamine

To determine a possible chemical mechanism for HOSCN-induced cleavage of apoB-100, LDL was incubated with 250 µM HOSCN as described in section 2.3.1 in the absence or presence of 200 µM butylated hydroxytoluene (BHT) or 50 µM desferrioxamine (DFO). BHT is an effective scavenger of chemical radicals [484] and can prevent peptide cleavage by HOSCN if it is free radical mediated. DFO is a high-affinity free iron chelator [485] which was added to chelate any haem-derived iron released from LPO during HOSCN-synthesis (as described in Section 2.2.2). As millimolar levels of HOSCN were being generated by LPO in this system, it was a concern that this could potentially cause iron release similar to that reported for HOCl [486]. Such iron cannot be filtered out by a 10 kDa cut-off and if present in

the sample could lead to oxidation of the peptide backbone and amino acid side chains [487]. After incubation, the samples were processed and analysed as described in Section 2.4.1. The band densitometry was analysed using ImageJ software (National Institute of Health open-sourced software).

2.5. Determination of protein concentration by bicinchoninic acid assay

Protein concentration was determined using the bicinchoninic acid (BCA) assay which relies upon protein-mediated stoichiometric conversion of Cu^{+} into Cu^{2+} ions [488]. Diluted samples were compared to a bovine serum albumin (BSA) standard ranging from 0.1 – 1 mg**.**mL^{-1} in a 96 well tissue culture plate (Corning, New York, New York). The BCA reagent (1 % w/v sodium bicinchoninate, 2 % w/v sodium carbonate, 0.16 % w/v sodium tartrate, 0.4 % w/v sodium hydroxide and 0.95 % w/v sodium bicarbonate) and 4 % w/v cupric sulfate solution at a 50:1 ratio. 200 µL of working reagent was transferred to standards and samples, then the plate was incubated at 60 °C for at least 30 min. The absorbance was measured using a plate reader (Sunrise Tecan; Mannedorf, Zurich) at 562 nm and the protein concentration of each sample was determined from the BSA standard curve.

2.6. Cell culture

Human coronary artery endothelial cells (HCAEC) and Human coronary artery smooth muscle cells (HCASMC) were grown in MesoEndo Endothelial Cell Growth Media (Cell Applications; San Diego, California) or Smooth Muscle Growth Media-2 (Lonza; Basel, Basel) respectively; and used from passages 4-6. To prepare suspensions of cells, HCAEC and HCASMC were dissociated with 0.1 % w/v trypsin-EDTA for 1 min at 37 °C and 5 % CO_2 and then trypsin was deactivated with growth media. Cells were pelleted by centrifuge for 5 min at ~232 g, aspirated, resuspended in their respective growth media and a small aliquot of cells

was counted with a haemocytometer. HCAEC (0.5×10^5 cells•mL^{-1}) and HCASMC (1.0×10^5 cells•mL^{-1}) were seeded overnight in their respective growth media. Culture plate wells were then washed twice with PBS before incubation with the different LDL conditions at a concentration of 0.1 mg•mL^{-1} apoB-100 protein in sterile-filtered serum-free defined medium (Cell Applications) supplemented with 5 % v/v foetal bovine serum (FBS) as treatment medium for HCAEC, or basal medium supplemented with 5 % FBS and insulin as treatment medium for HCASMC. At least 3 independent HCAEC and HCASMC donors were used for all experiments.

2.7. Cell viability and activity determination

HCAEC and HCASMC were plated in 12-well plates overnight prior to incubation with LDL, HOSCN-modified LDL or HOCl-modified LDL for 24 h in triplicate. The supernatant was then removed and the cells were washed twice with heat-treated PBS. The cells were lysed with 0.1 % v/v Triton X-100. Cell viability was determined by the lactate dehydrogenase (LDH) kinetic assay. 10 µL of each lysate and supernatant was added separately (after centrifuging at 353 *g* to pellet cell debris) to a 200 µL LDH assay solution of 2.5 mM sodium pyruvate and 0.15 mg•mL^{-1} of reduced nicotinamide adenine dinucleotide (NADH) respectively, in triplicate before recording the change in absorbance at 340 nm (ΔA_{340}). Ten µL of 0.1 % v/v Triton X-100 or cell media in 200 µL of LDH assay solution were used as blanks for the lysate activity and supernatant activity, respectively. Non-viable cells leak LDH into the cell media [489], hence the viability was calculated by comparing the intracellular (lysate) and extracellular (supernatant) LDH activity by measuring the loss of NADH every 5 min over 7 cycles and read with a Tecan Sunrise plate reader. Cell viability was calculated as a fraction of intracellular activity over total activity (i.e. % viability = $100 \times \Delta A_{340}$ [intracellular activity]/ ΔA_{340} [intracellular + extracellular activity]).

Metabolic activity measured by 3-(4,5-dimethylthiazol-2-yl)-2,5-diphenyltetrazolium bromide (MTT) assay. HCAEC and HCASMC were plated in 96-well plates and treated under identical conditions as described in Section 2.6. The cells were then washed twice with heat-treated PBS before 10 µL of MTT (Biotium; Fremont, California), reconstituted in 110 µL of treatment media, was added to the wells and the cells were re-incubated for 4 h at 37 °C and 5 % CO_2 in the dark. The media was then removed and cells washed twice with heat-treated PBS before dissolving the insoluble formazan (formed from the metabolism of MTT by mitochondrial oxidoreductase) in dimethyl sulfoxide (DMSO). The absorbance of the product was then measured at 570 nm with a reference set at 630 nm. Activity within treated cells was expressed as a percentage of the activity present in control cells.

2.8. Assessment of endothelial migration rate by scratch assay

HCAEC were seeded on a 12-well plate as described in Section 2.6. After allowing the cells to adhere for 6 h, a vertical and horizontal scratch was made on the wells with a p200 pipette tip, the debris was washed out with PBS and the cells were treated with control LDL, HOSCN- or HOCl-modified LDL for up to 24 h. Images were taken at the intersection of the vertical and horizontal scratch and the scratch width was measured at the start of treatment (0 h) and at intervals up to 24 h treatment. The cellular migration rate was measured as half the speed of scratch closure rate, as the cells migrate from two sides, doubling the apparent migration rate.

2.9. Quantification of LDL-sourced lipid uptake in endothelial and smooth muscle cells measured by high-performance liquid chromatography (HPLC)

The cellular composition of cholesterol and specific cholesteryl esters (arachidonate, docosahexanoate, linoleate, oleate, palmitate and stearate) was quantified after treatment with LDL as described in Section 2.6. After treatment for 24 or 48 h, cells were washed and lysed

in 1 mL of deionised water, scraped and transferred to glass vials containing 10 µL of 200 mM EDTA and 10 µL of butylated hydroxytoluene (BHT; in ethanol). The cholesterol and cholesterol esters were then separated from apoB-100 by liquid-liquid extraction with 2.5 mL methanol and 5 mL hexane. Each tube was vortexed vigorously and stored at -80 °C. Samples were not stored longer than 4 weeks. Before quantification, the tubes were vortexed again, allowed to fractionate and 4 mL of the hexane (organic) layer was individually transferred to clean glass tubes. The hexane was completely evaporated in a Speedvac Concentrator for 1 h, then the lipid pellet was reconstituted in 200 µL of HPLC mobile phase buffer (HPLC-grade 70 % v/v isopropanol and 30 % v/v acetonitrile; solvent; Merck-Millipore) [490].

Cholesterol and cholesteryl ester standards were used for quantification. One hundred and fifty µL of standard and samples were transferred to individual HPLC vials with inserts for HPLC analysis. Response factors for the cholesterol and cholesteryl esters were formulated to quantify the amounts of cholesterol and cholesteryl esters in each sample against the standards. The samples were run through a Supelco Supercosil LC-18, 25 cm × 4.6 mm × 5 µm HPLC column in a Shimadzu LC-10AT liquid chromatograph system (Kyoto, Japan). The flow rate was set at 1 mL**.**min^{-1} at 25 °C and the constituents were detected by UV absorption at 205 nm (Figure 2.2) [349].

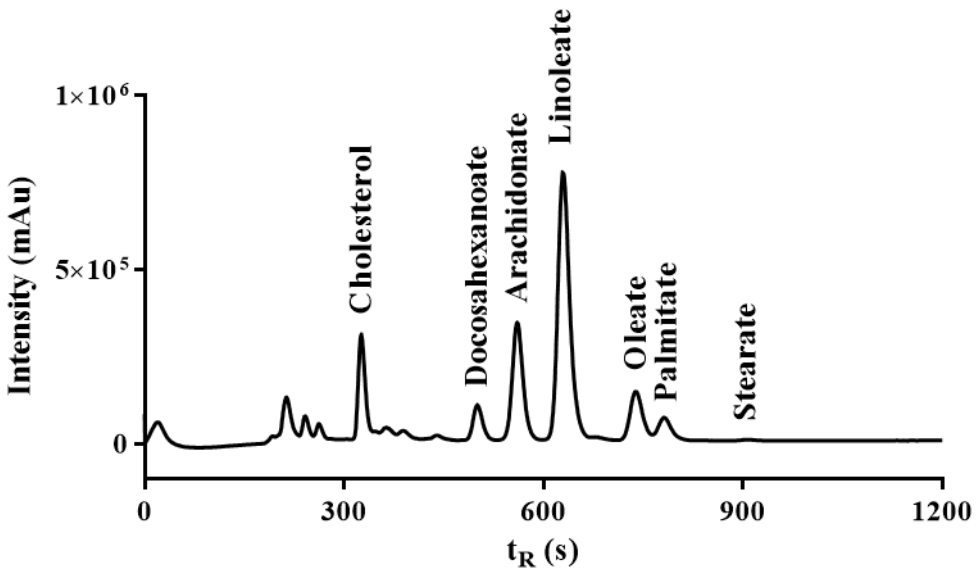

Figure 2.2. Representative HPLC trace of retention peaks of cholesterol and cholesteryl esters. *Representative HPLC trace from 10 µL of 1.0 mg.mL^{-1} LDL. Cholesterol and each cholesteryl ester species can be sufficiently eluted apart for independent or total lipid quantification.*

2.9.1. Lysosomal activity in cells assessed by cysteine-dependent cathepsin enzyme activity

The cysteine-dependent cathepsins (cathepsin B and L enzymes) are known to aid in the digestion of proteins in the lysosome from endocytosed proteins and particles, including LDL [491, 492]. Cells were scraped and lysed in PBS and the suspension was centrifuged at 376 *g* for 5 min at 21 °C to pellet cell debris. Each lysate supernatant was transferred to a clean tube and 25 µL of lysate were added to wells of a 96-well plate. Cathepsin B buffer (100 mM potassium phosphate, 2.5 mM EDTA and 0.005 % v/v Brij35, pH 5.5) or cathepsin L buffer (100 mM monobasic potassium phosphate, 2.5 mM EDTA and 0.005 % v/v Brij35, pH 6) was added to sample wells at 180 µL with the respective fluorescent substrates; 10 µM Z-Arg-Arg-AMC hydrochloride for cathepsin B assay or 10 µM Z-Phe-Arg-AMC hydrochloride for cathepsin L assay (Bachem, Bulbendorf, Switzerland). Cathepsin activity was determined by measuring the fluorescence of the liberated AMC species over 40 min at 1 min intervals using

a SpectraMax M2 fluorescent plate reader (Molecular Devices, Sunnyvale, California) at λ_{ex} 360 nm and λ_{em} 460 nm. The cathepsin enzyme kinetics was measured in the linear phase of enzyme activity.

2.10. RNA isolation and PCR

HCAEC and HCASMC were plated in 12-well plates overnight prior to the addition of LDL or modified LDL (0.1 $mg \cdot mL^{-1}$) and further incubated for 3 or 24 hours. Each well was washed twice with warm PBS before being lysed using 250 µL of BL lysis buffer with thioglycerol (Promega). The lysates were processed and analysed immediately or following storage at -80 °C. RNA extraction was performed using the Promega Reliaprep RNA Miniprep Kit (which supplied all the wash solutions and DNase 1 enzyme) as prescribed by the manufacturer with some alterations, as described below.

2.10.1. RNA isolation

Eighty-five µL of isopropanol was added to fresh or thawed lysates and mixed thoroughly by repeated up-and-down pipetting. Samples were then transferred to spin cartridges supplied with the kit and centrifuged at 14 000 *g* for 30 s. Samples were washed once with 500 µL of RNA wash buffer and centrifuged at 14 000 *g* for 30 s before incubating with 30 µL of DNase solution (24 µL Yellow Core buffer + 3 µL 0.09 M $MnCl_2$ + 3 µL DNase I) for 45 min at room temperature. Samples were then washed with the 200 µL column wash buffer and centrifuged at 14 000 *g* for 30 s. The cartridge was washed with 500 µL of RNA wash buffer and centrifuged at 14 000 *g* for 30 s before washing again with 300 µL of RNA wash buffer and centrifuging at max speed for 2 min to dry the cartridge. Twenty-two µL of RNase-free water was added to the dry spin cartridge and centrifuged at 14 000 *g* for 1 min to extract the RNA into individual microcentrifuge tubes. The concentration of RNA obtained was then measured using a Nanodrop 2000C spectrophotometer (Thermo Scientific; Waltham, Massachusetts) to

measure RNA concentration. The concentration of RNA was normalised to 5 – 10 µg/mL of RNA per sample. Reverse transcription of total cellular RNA was performed using a iScript cDNA synthesis kit under the following conditions; (1) binding of reverse transcriptase to RNA at 25 °C for 5 min, (2) reverse transcription of RNA to cDNA template at 42 °C for 30 min, and (3) denaturing and inactivation of reverse transcriptase at 95 °C for 5 min, using an Eppendorf Mastercycler system (Hamburg, Germany). Non-RT controls were used to test for cDNA contamination. The RNA extraction from cDNA was considered satisfactory if non-RT controls were amplified >10 cycles later than the PCR samples ($1/2^{10}$ or 1/1024-fold) by RT-qPCR (Section 2.9.2). cDNA samples were stored at 4 °C.

2.10.2. Real-time quantitative polymerase chain reaction (qPCR) analysis

Quantification of mRNA expression was performed using qPCR with the primer sequences listed in Table 2.2. Each analysis was performed in triplicate with 2 µL of cDNA sample, 1 µL each of 10 µM forward and reverse primer and the iQ SYBR Green supermix (Bio-Rad) as per the manufacturers' instructions. An initial DNA polymerase activation step was carried out by heating samples to 95 °C for 3 min, followed by denaturation at 95 °C for 30 s, annealing at 60 °C for 30 s and extension at 72 °C for 30 s over 40-50 cycles, followed by denaturing at 95 °C for 2 min. This was performed using either a Bio-Rad CFX96 or CFX384 real-time system with CFX manager 3 software to obtain sample Ct values. For all primer sets tested, a standard curve was generated using serially diluted cDNA to obtain the PCR efficiency. The relative mRNA concentrations in each sample was derived from the Ct values plotted against the standard curve. To verify that only a single product was amplified by PCR, a dissociation curve ranging from 65 – 95 °C with 0.5 °C intervals was generated at the end of the amplification cycle. The genes of interest were calculated based on the Pfaffl method (Equation 1) [493],

with comparison to the 18S ribosomal RNA (18S) and β_2-microglobulin (β2M) housekeeping products.

(1) $$\text{Ratio}=\frac{E^{\Delta Ct(\text{target})}}{E^{\Delta Ct(\text{ref})}}$$

Table 2.3. The forward and reverse primer sequences for qPCR. *All primers were designed using NCBI primer design software and synthesised by GeneWorks (Adelaide, SA).*

Name	Abbreviation	Forward primer sequence (5'-3')	Reverse primer sequence (5'-3')
Intracellular adhesion molecule 1	ICAM-1	GGCTGGAGCTGTTTGAGAAC	ACTGTGGGGTTCAACCTCTG
Vascular cell adhesion molecule 1	VCAM-1	CAGACAGGAAGTCCCTGGAA	TTCTTGCAGCTTTGTGGATG
E-Selectin		GGCAGTTCCGGGAAAGATCA	GTGGGAGCTTCACAGGTAGG
Endothelial nitric oxide synthase	eNOS	CCGGGTCCTGTGTATGGATG	AGTGGGTCTGAGCAGGAGAT
Nuclear factor (erythroid-derived 2)-like 2	Nrf2	GAGCAAGTTTGGGAGGAGCT	GGTTGGGGTCTTCTGTGGAG
Superoxide dismutase 1	SOD-1	AAAGATGGTGTGGCCGATGT	CAAGCCAAACGACTTCCAGC
Haem oxygenase 1	HO-1	TTCAAGCAGCTCTACCGCTC	GGGGCAGAATCTTGCACTTT
Glutamate-cysteine ligase catalytic subunit	Gclc	TCCAGGTGACATTCCAAGCC	GAAATCACTCCCCAGCGACA
Glutamine synthetase	GS	CCCTAGCCGGTTTGTGCTAA	CCAAAGATGCCCAGCTCTGA
Monocyte chemotactic protein 1	MCP-1	AGCCACCTTCATTCCCCAAG	TTGGGTTTGCTTGTCCAGGT
Interleukin 6	IL-6	CCAGAGCTGTGCAGATGAGT	AGCTGCGCAGAATGAGATGA
18S ribosomal subunit	18S	GAGGATGAGGTGGAACGTGT	TCTTCAGTCGCTCCAGGTCT
β2 microglobulin	β2M	AGATGAGTATGCCTGCCGTG	GCGGCATCTTCAAACCTCCA

CCAAT enhancer-binding protein homologous protein	CHOP	GGAGCTGGAAGCCTGGTATG	GCAGGGTCAAGAGTGGTGAAG
Activating transcription factor 4	ATF4	CTTCACCTTCTTACAACCTCTTC	GTAGTCTGGCTTCCTATCTCC
Activating transcription factor 6	ATF6	GTATCAGCAGGAACTCAGG	GTCTTGTGGTCTTGTTATGG
78 kDa glucose-regulated protein	GRP78	TGTTCAACCAATTATCAGCAAAC	TTCTGCTGTATCCTCTTCACCAG
Spliced x-box binding protein 1	sXBP1	GCTGCGTCCGCAGCAGGT	GTCCAGAATGCCCAACAGG
Low-density lipoprotein receptor	LDLR	TACAAGTGGGTCTGCGATGG	TGAAGTCCCCGGATTTGCAG-3’
Scavenger receptor expressed by endothelial cell 1	SREC-1	ATAGAGACAGGGTTTCACCAT GTTA	ATCACCTACAATCTCATCTTC CAGA
Scavenger receptor class A1	SR-A1	TGGACCAAAAGGCCAGAA	ACTTCCCAGCGATCGTCA
Scavenger receptor class B1	SR-B1	CTGTGGGTGAGATCATGTGG	GCCAGAAGTCAACCTTGCTC
Scavenger receptor class B2	SR-B2	GAACCTATTGATGGATTAAA CCC	TCCAGTTACTTGACTTCTG AAC
Lectin-like oxidised low-density lipoprotein receptor 1	LOX-1	GAGAGTAGCAAATTGTTCAGC TCCTT	GCCCGAGGAAAATAGGTAAC AGT
α-smooth muscle actin	α-SMA	CATTGTCCACCGCAAATGCT	GGCCAACGCAAGAAGTTACC
Osteopontin	OPN	AGGCATCACCTGTGCCATAC	GGCCACAGCATCTGGGTATT
S100 calcium-binding protein A4	S100A4	TCTTGGTTTGATCCTGACTGCT	ACTTGTCACCCTCTTTGCCC
Connexin 43	Cx43	TCTTCATGCTGGTGGTGTCC	ACCACTGGTCGCATGGTAAG

Decorin		TGCTTTCTGTTGCAGGTTGG	GTGGGGGTCTTGCTTTTTGG
Olfactomedin-like 3	Olfml3	GGACACACCATGTCCCAGAG	GTTATAGCGGAGGCTGGCAT
Collagen type 1		ACAAGGCATTCGTGGCGATA	ACCATGGTGACCAGCGATAC
Osteocalcin		AGGGAACAATCCCAGCCTTG	CCCTGTTCTAGCCAGTCAGC
Runt-related transcription factor 2	Runx2	CCGGAATGCCTCTGCTGTTA	TGTCTGTGCCTTCTGGGTTC

2.11. Cytokine release from HCAEC by enzyme-linked immunosorbent assay

The release of the cytokines interleukin-1β (IL-1β), interleukin-6 (IL-6) and monocyte chemotactic protein-1 (MCP-1) from HCAEC (after 24 h treatment with LDL as described in Section 2.6) was measured by enzyme-linked immunosorbent assay (ELISA). ELISA kits, including buffers and antibodies for each cytokine, were purchased from PeproTech (Rocky Hill, New Jersey) and performed per the manufacturer's instructions for IL-1β (catalogue number 900-TM95), IL-6 (catalogue number 900-M16) and MCP-1 (catalogue number 900-M31).

The MCP-1 and IL-6 capture antibodies were diluted to 250 ng**.**mL^{-1} and the IL-1β capture antibody was diluted to 1 µg**.**mL^{-1} with PBS, then 100 µL per well of capture antibody was incubated in ELISA microplates (Corning) overnight at 21 °C. The wells were then aspirated and washed four times with 300 µL of wash buffer (0.1 % v/v Tween-20 in PBS), then incubated with 300 µL of fresh block buffer (1 % w/v BSA in PBS) for 1 h at 21 °C. The wells were again washed four times, then 100 µL of cell media sample were incubated at 21 °C for 2 h in triplicate. One hundred µL of standards for IL-1β (0 – 750 pg**.**mL^{-1}), IL-6 (0 – 1.5 ng**.**mL^{-1}) and MCP-1 (0 – 1 ng**.**mL^{-1}) were also incubated in duplicates. The wells were washed again four times and incubated with 100 µL of Streptavidin-HRP (75 ng**.**mL^{-1}) for IL-1β, or Avidin-HRP (1:2000 dilution) for 30 min at 21 °C. The wells were washed again four times and 100 µL of substrate solution (3,3′,5,5′-trimethylbenzidine for IL-1β and 2,2′-azino-bis(3-ethylbenzothiazoline-6-sulfonic acid) for IL-6 and MCP-1) was added to each well. Colour was developed over 20 min incubation at 21 °C, then the absorbance was measured immediately at 450 nm with wavelength correction at 620 nm for IL-1β, or 405 nm with wavelength correction at 650 nm for IL-6 and MCP-1.

2.12. Protein analysis by immunoblot (Western blot)

2.12.1. Preparation of HCAEC lysates for whole cell immunoblot analysis

HCAEC were treated as stated in Section 2.4 and then lysed with radioimmunoprecipitation assay (RIPA) buffer for immunoblot analysis. The protein content of whole cell lysates was measured by BCA assay and normalised to 10-20 µg protein per sample in LDS sample buffer and reducing agent (Life Technologies). The samples were then heat-denatured for 10 min at 70 °C and separated by SDS-PAGE as described in Section 2.8.3.

2.12.2. Preparation of HCAEC lysates for co-immunoprecipitation and immunoblot

The coimmunoprecipitation method was adapted from the manufacturer's protocol for Dynabeads® protein G and used the corresponding immunoprecipitation kit (Life Technologies). HCAEC were lysed with 0.1 % v/v Triton X-100 in tris-buffered saline (TBS) and sonicated for 10 min in iced-water for coimmunoprecipitation experiments to preserve protein-protein interactions. For immunoprecipitation of eNOS, 30 mg of Dynabeads® were magnetically separated from solution, then resuspended in 200 µL solution of PBS, 0.02 % v/v Tween-20 and 1 µg of eNOS antibody (BD Bioscience; San Jose, California; cat. # 610297) for 20 min at 21°C with rotation before each experiment. The beads were magnetically removed from the solution and resuspended with PBS and Tween-20 solution. The beads were magnetically removed from solution and incubated with 100 µL of whole cell lysate for 20 min at 21 °C with rotation to allow binding to the Dynabead®-antibody complex. The leftover unbound lysates (supernatant) were transferred to a clean tube for further analysis with the coimmunoprecipitate. The Dynabead®-antibody-eNOS complex (D-Ab-eNOS) was washed 3 times with 200 µL washing buffer. When the final wash solution was removed, 100 µL of wash

buffer was added and the beads transferred to a clean tube to avoid elution of proteins bound to the tube wall. The solution was removed and the D-Ab-eNOS complex was eluted with a solution of 20 µL elution buffer, 9 µL LDS sample buffer and 1 µL sample reducing agent. Samples were then heat-denatured for 10 min at 70 °C and separated by SDS-PAGE as described in Section 2.9.3.

2.12.3. SDS-PAGE separation and immunoblotting of whole cell lysates and eNOS coimmunoprecipitates

Whole cell lysates and eNOS-coimmunoprecipitates were resolved by SDS-PAGE using a 4-15 % Mini-Protean TGX precast gel in an electrophoresis cell (Bio-Rad). Electrophoresis was performed at 120 V for approximately 1.5 h. For eNOS dimerization, electrophoresis was performed in an ice bath at 4 °C to prevent thermal uncoupling of eNOS. The proteins were transferred to a PVDF membrane over 5.5 min at 20 V using an iBlot 2 system (Life Technologies). The immunoblot membranes were blocked with 5 % w/v bovine serum albumin in TBS with 0.1 % v/v Tween-20 overnight at 4 °C. Blots were incubated with 1:1000 dilution of antibodies for eNOS, p-S1177-eNOS, cav-1 (BD biosciences), LDLR, LOX-1 (Abcam; Cambridge) or β-actin (Santa Cruz; Santa Cruz, California), 1:2000 SR-B1 (Abcam), or 1:500 SR-B2 (BD biosciences) for 2 h at 21 °C. For whole cell and supernatant Western blot, 1:2000 dilution of anti-IgG-HRP-conjugated antibody (Cell Signalling Technology; Beverly, Massachusetts) of the appropriate isotype was incubated for 1 h at 21 °C. For eNOS immunoprecipitation, 1:1000 TrueBlot® Ultra anti-mouse IgG-HRP-conjugated antibody (Rockland; Limerick, Pennsylvania) was used to prevent binding to eluted *unbound* IgG heavy and light chains. Information on the antibodies used are listed in Table 2.3. Chemiluminescence was induced with the enhanced chemiluminescence substrate (Perkin Elmer; Waltham,

Massachusetts), imaged with a ChemiDoc MP (Bio-Rad) imaging system. Band densitometry was ascertained using ImageLab software (Bio-Rad).

Table 2.4. Primary and Secondary antibodies used for immunoblot analysis of HCAEC lysates. *Target antigen, isotype, company and catalogue information of antibodies used for Immunoblot analysis.*

Antigen	Isotype	Antibody company	Catalogue number
eNOS	Mouse	BD biosciences	610297
pS1177-eNOS	Mouse	BD biosciences	612393
Cav-1	Mouse	BD biosciences	610406
β-actin	Mouse	Santa Cruz	Sc-47778
SR-B1	Rabbit	Abcam	ab52629
SR-B2	Mouse	BD biosciences	555453
LDLR	Mouse	Abcam	ab204941
LOX-1	Mouse	Abcam	ab53202
Mouse IgG	Horse	Cell Signaling Technology	7076
Rabbit IgG	Goat	Cell Signaling Technology	7074
Mouse IgG (H&L)*	Rat	Rockland	18-8817-33

* Mouse IgG (H&L) only recognises complete IgG, not unbound light or heavy chains.

2.13. Measurement of eNOS activity

2.13.1. Scintillation counting of ^{3}[H]L-Citrulline converted from ^{3}[H]L-Arginine

The specific activity of eNOS in HCAEC was determined by measuring the total conversion of [^{3}H]-L-Arginine to [^{3}H]-L-Citrulline using a commercial kit (Cayman Chemical, catalogue number 781001, Ann Arbor, Michigan). HCAEC were cultured in 60 mm^{2} petri dishes as described in Section 2.6 for 24 h. Cells were then washed and incubated for 5 min in PBS with 1 mM EDTA, then lightly scraped to non-enzymatically detach cells from the plate. Trypsin was not used to detach cells as eNOS can be bound to the plasma membrane and be deactivated

by trypsin. The detached cells were then centrifuged at 300 *g* for 5 min, the PBS with EDTA was removed and the pellet was lysed in 50 µL homogenisation buffer supplied in the kit. The lysates were stored on ice and the protein content of the lysates were measured by BCA assay as described in Section 2.5. The protein concentrations were normalised to 0.5 $mg{\cdot}mL^{-1}$ for each sample assay. A 50 µL reaction assay mix for each sample was prepared fresh containing 50 mM Tris/HCl (pH 7.4), 1 mM NADPH, 6 µM BH_4, 2 µM FAD, 2 µM FMN, 750 µM $CaCl_2$, 0.2 µM calmodulin and 1 µL (1 $\mu Ci{\cdot}\mu L$) L-[1,2,3,4-^{3}H]-arginine monohydrochloride (Perkin Elmer) and incubated for 1 h at 21 °C. The reaction was stopped by the addition of 400 µL of stop buffer for each reaction. The [^{3}H]-L-citrulline was separated from the unconverted [^{3}H]-L-arginine using an equilibrated resin, 100 µL of resin was added to each reaction. The [^{3}H]-L-citrulline was then eluted from the resin-bound [^{3}H]-L-arginine through spin cups by centrifugation at 20 000 *g* for 30 s.

Two hundred µL of each sample was added to scintillation vials and thoroughly mixed with 5 mL of Ultima Gold scintillation fluid (Perkin Elmer). The radioactivity in each sample was quantified as counts per minute (cpm) averaged over 5 min using a Tri-Carb liquid scintillation counter (Perkin Elmer). A total count (cpm of the reaction mix with stop buffer) and a background count (cpm of reaction mix with stop buffer and equilibrated resin eluted through spin cups) control were used in each experiment. The percentage conversion was calculated by background cpm subtracted from sample cpm compared to the total cpm (Equation 2).

$$(2)\quad \%\ \text{conversion} = \frac{(cpm_{reaction} - cpm_{background})}{cpm_{total}} \times 100$$

2.13.2. Spin trapping of NO and measurement by electron paramagnetic resonance (EPR) spectroscopy

Electron paramagnetic resonance (EPR) spectroscopy is a powerful technique for the sensitive and specific measurement of biological free radicals. The Fe(II)-MGD (N-methyl-D-glucamine dithiocarbamate) method was used to spin trap to trap and directly measure NO released by HCAEC using a modified protocol [494]. HCAEC were cultured and treated for 24 h with LDL treatments as described in Section 2.6. Cells were also treated with LDL that was freshly desalted through a PD-10 column, but not incubated for 24 h at 37 °C and 5 % CO_2, as an additional control. The cells were then washed in PBS and were incubated with the Fe(II)-MGD spin trap (21 μL $Fe(II)SO_4$ + 210 μL MGD + 189 μL PBS with Ca and Mg) at 37 °C and 5 % CO_2 for 36 min. Immediately after incubation, the resulting solution containing the spin trap was then placed in a clean flat cell and the EPR signal was measured. A negative control was performed by incubating the cells in treatment media with 100 μM of the eNOS inhibitor N^5-(1-iminoethyl)-L-ornithine (L-NIO); for 1 h prior to, and during, spin trapping. The EPR signals were acquired by using an EMXplus EPR spectrometer (Bruker) and Xenon software with the following parameters: frequency: 9.8 GHz; centre field: 3420 G; modulation amplitude: 6 G; sweep width: 100 G; gain: 40 dB; power: 25 mW; scans: 15; sweep time: 30 s; and time constant: 20 s. Signal intensity was quantified by double-integration of the signal from 3387 – 3452 G (Figure 2.3).

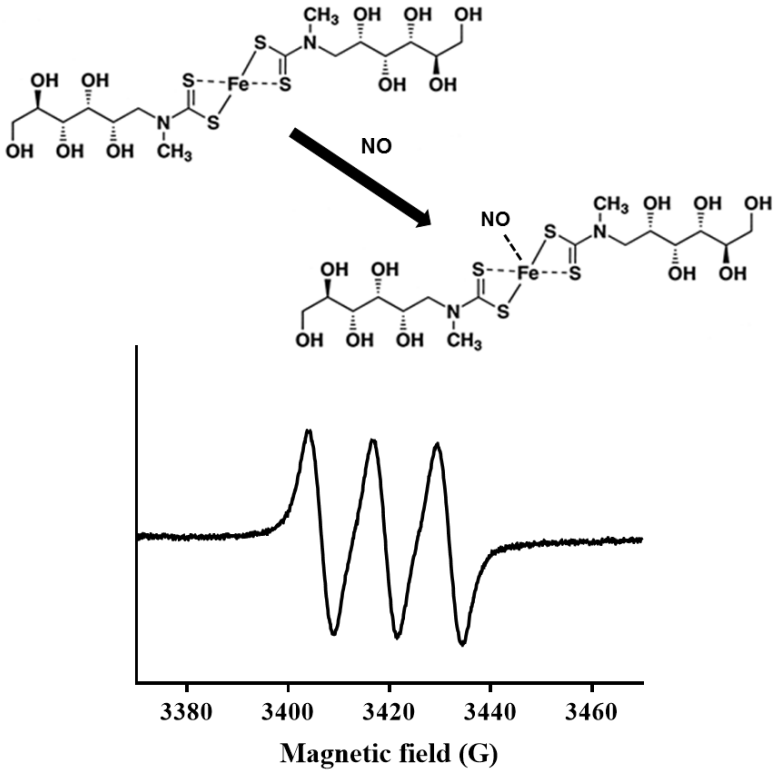

Figure 2.3. Structure and binding of Fe-(MGD)$_2$ spin trap to NO (above) and EPR signal of Fe-(MGD)$_2$-bound NO (below).

2.13.3. Intracellular NO measured by fluorescence of DAF-FM by flow cytometry

The diaminofluorescein probe, 4-amino-5-methylamino-2',7'-difluorofluorescein (DAF-FM) is effective at measuring relative intracellular NO detection. DAF-FM is natively non-fluorescent and cell permeable and is activated by intracellular esterases to a NO-reactive form [495, 496]. DAF-FM then reacts with NO to form the fluorescent benzotriazole derivative with excitation/emission maxima at 494/515 nm. After treating HCAEC for 24 h with oxidised LDL in 12- well plates as described in Section 2.6, HCAEC were washed twice with HBSS supplemented with Ca and Mg. HCAEC were then incubated with 1 μM of DAF-FM in HBSS supplemented with Ca and Mg for 30 min at 37 °C and 5 % CO_2. As DAF-FM is light-sensitive, tissue culture plates were wrapped in foil during incubation and flow cytometry was performed in darkness. HCAEC were then washed twice and incubated with 0.5 mL PBS containing 1

mM EDTA for 5 min before lightly scraping to liberate HCAEC from the plate. The suspension was transferred to a tube to be analysed using the FACSVerse flow cytometer (BD Biosciences) using the FITC laser settings. The FACSVerse was cleaned and quality control was performed before each experiment.

2.13.4. Measurement of cellular $O_2^{\bullet-}$ by DHE oxidation and fluorescence

2.13.4.1. Solutions and preparation of HPLC standards

HPLC-grade acetonitrile (Thermo Scientific) was used to make mobile phase buffers in deionised water from a four stage-filtered Milli-Q system (Merck Millipore). Mobile phase A (10 % v/v acetonitrile in 25 % v/v 0.2 M potassium phosphate buffer pH 2.6) and mobile phase B (60 % v/v acetonitrile in 25 % v/v 0.2 M potassium phosphate buffer pH 2.6) were filtered through a 0.2 µm HPLC filter system.

Stock solutions of 20 mM dihydroethidium (DHE) were prepared in the dark and stored in degassed DMSO at -80 °C. Ethidium bromide (EtBr) and 2-hydroxyethidium (2-OH-E^+; Noxygen, Elzach, Germany) stock were bought commercially and standards were prepared fresh for each experiment. The stock of DHE was diluted to approximately 50 µM in potassium phosphate buffer (pH 7.4) containing 200 µM diethylenetriaminepentaacetic acid (DTPA) and the UV-Vis spectrum was scanned from 200-600 nm in quartz cuvettes to assess the purity and true 2-OH-E^+ concentration. The true concentration of DHE was calculated using the extinction coefficient at 265 nm ($\varepsilon = 1.8 \times 10^4$ M^{-1}•cm^{-1} [497]) and 345 nm ($\varepsilon = 9.75 \times 10^3$ M^{-1}•cm^{-1} [497]) and diluted to 5 µM in mobile phase A. The concentration of 2-OH-E^+ and E^+ were prepared the same and determined using the extinction coefficient at 470 nm ($\varepsilon = 9.4 \times 10^3$ M^{-1}•cm^{-1}

[497]) and 480 nm ($\varepsilon = 5.8 \times 10^3$ $M^{-1}{\cdot}cm^{-1}$ [498]), respectively, and each diluted to 5 µM in mobile phase A. A standard curve was formulated from 1 – 5 µM for each product.

2.13.4.2. HPLC sample preparation

After treatment of HCAEC, the supernatant was replaced with fresh treatment media with 50 µM DHE and incubated for 30 min at 37 °C and 5 % CO_2. As DHE is light-sensitive, tissue culture plates were wrapped in foil during incubation and storage. A 30 min treatment with 50 µM menadione (2.5 mM stock prepared in the dark and stored in degassed DMSO at -80 °C) before incubation with DHE was used as a positive control for $O_2^{\bullet-}$ production [499]. The cells were washed and lightly scraped in 1 mL cold PBS and centrifuged (1000 g for 5 min), the supernatant removed, then the pellet was stored at -80°C for no longer than 1 week before analysis. The samples were lysed with 150 µL of ice-cold PBS with 0.1 % v/v Triton X-100, drawn through a 1 mL syringe ten times. Cell debris were pelleted by centrifugation at 1 000 *g* for 5 min at 4 °C, then 100 µL of supernatant was transferred to a tube containing 100 µL of 0.2 M $HClO_4$ in methanol, vortexed, and allowed to precipitate on ice for 2 h. Meanwhile, 2 µL of each sample was transferred to 200 µL of Bradford reagent (Brilliant Blue G in phosphoric acid and methanol from Sigma-Aldrich) in a 96-well plate for 20 min at 21 °C with BSA standards from 0.5 – 5 $mg{\cdot}mL^{-1}$ to determine the protein concentration. The absorbance for the Bradford assay was measured at 595 nm [500]. After incubation, the protein precipitate was pelleted by centrifugation at 20 000 *g* for 30 min at 4 °C. One-hundred µL of the supernatant was transferred to tubes containing 100 µL of 1 M phosphate buffer pH 2.6 and vortexed for 5 s. The excess buffer and resultant potassium perchlorate precipitate were pelleted by centrifugation at 20 000 *g* for 15 min at 4 °C. One hundred and fifty µL of each sample was then transferred to HPLC vials with 200 µL conical glass inserts and analysed by HPLC immediately.

2.13.4.3. HPLC separation and fluorescence detection of $O_2^{\bullet-}$ products

The samples (50 µL) were separated after injection through a Synergi Polar RP C18 column (250 × 4.6 mm, 4 µM, 80 Å; Phenomenex, Torrance, California), equilibrated with 60 % mobile phase A and 40 % mobile phase B using a Shimadzu LC-10AT liquid chromatograph system with a fluorescence detector (RF-20A XS, Shimadzu). Separation of 2-OH-E^+ and ethidium (E^+) was performed by a linear increase to 100% mobile phase B over 63 min (see Table 2.4) at a flow rate of 0.5 mL•min^{-1}. Products were quantified by fluorescence (DHE; λ_{ex} 358 nm, λ_{em} 440 nm, and 2-OH-E^+ and E^+; λ_{ex} 490 nm, λ_{em} 565 nm). The concentration of 2-OH-E^+ was calculated by peak integration and interpolated from a standard curve, then normalised to cell protein concentration.

Table 2.5. Elution gradient for the analysis of DHE, E^+ and 2-OH-E^+ by HPLC and fluorescence detection.

Time (min)	Mobile phase A (%)	Mobile phase B (%)
0	60	40
30	0	100
40	0	100
45	60	40
63	60	40

2.13.5. eNOS and caveolin-1 localisation in endothelial cells observed by fluorescence microscopy

HCAEC (200 µL of 0.5 × 10^5 cells•mL^{-1}) were seeded onto pre-coated 8-well microscope slides before treating with LDL treatments for 24 h as described in Section 2.6. After treatment, the wells were spiked with 200 µL of 1 % w/v paraformaldehyde (PFA) in PBS for 2 min. The

wells were then aspirated and the cells were fixed to the microscope slide by cross-linking with 1 % PFA for 10 min at 21 °C. The wells were then aspirated and washed with PBS and incubated with 0.1 % Triton X-100 for 5 min to permeabilise the cells. The wells were then washed twice with PBS and then incubated (in a humidified chamber) with 10 % v/v goat serum in PBS for 1 h at 21 °C to block the cells. The wells were then washed twice with PBS for 5 min each, then incubated overnight at 4 °C with 1:200 dilution of primary antibodies in PBS, rabbit monoclonal anti-eNOS (Cell Signalling Technology, catalogue number 9586) and mouse polyclonal anti-cav-1 (BD bioscience, catalogue number 610406) in the humidified chamber. The wells were then aspirated and washed twice with PBS with 0.1 % v/v Tween-20 (PBST) for 5 min each, to wash off excess and non-specific antibody binding. The cells were then incubated with 1:250 dilution of secondary fluorophore-conjugated antibodies, anti-rabbit IgG-AF594 (Abcam, catalogue number ab150080) and anti-mouse IgG-AF488 (Invitrogen, catalogue number A10667, Carlsbad, California) for 30 min at 21 °C in the dark in the humidified chamber. The cells were washed twice with PBST and counterstained with 1 $\mu g \cdot mL^{-1}$ of 4',6-diamidino-2-phenylindole, dihydrochloride (DAPI) for 20 min at 21 °C in the dark in the humidified chamber. The wells were then washed twice with PBS, aspirated and air-dried, then the coverslip was overlaid with Dako S3023 fluorescence mounting media (Agilent Technologies, Santa Clare, California).

The microscope wells were imaged with an Axio Imager.Z2 microscope (Zeiss, Oberkochen, Germany) at 40× magnification. The following excitation/emission spectra for each fluorophore were; DAPI (372/465), AF488 (488/519), AF594 (552/565). The fluorescence of eNOS (AF594) and cav-1 (AF488) were overlayed to visualise the localisation of eNOS and caveolin, with DAPI fluorescence to view cell nuclei.

2.14. Measurement of intracellular calcium levels in endothelial cells

The intracellular calcium levels were measured by utilising the cell permeant, calcium-binding fluorophore, Fluo-4AM (excitation/emission = 494/516 nm [501]). HCAEC were plated onto 6-well plates in triplicate for each 1 h and 24 h treatment with LDL as described in Section 2.6. Ca^{2+}- and Mg^{2+}-free HBSS was used in these experiments. After treatment, cells were washed with HBSS and incubated with 2.5 µM Fluo-4AM for 45 min at 37 °C and 5 % CO_2 in the dark. The wells were then aspirated, washed with HBSS and lightly scraped in 500 µL HBSS to be analysed immediately using the FACSVerse flow cytometer (BD bioscience) with FITC laser settings (excitation/emission = 494/520).

2.15. Neutrophil adhesion to endothelial cells in vitro

2.15.1. Isolation and labelling of leukocytes

Human blood (up to 15 mL into a EDTA-coated vacutainer) was taken on the day of the experiment by a qualified phlebotomist with the donor's consent and under ethics approval (Sydney Local Health District, protocol X12-0375) in accordance with the Declaration of Helsinki, 2000 of the World Medical Association. Equal volumes of blood were carefully overlaid on 4.5 mL of Polymorphprep (Axis-Shield, Oslo, Norway) in two 15 mL Falcon tubes, ensuring whole blood did not mix with the gradient solution. The tubes were centrifuged at 500 *g* for 30 min at 21 °C with no deceleration so as not to disturb the cell bands, and the neutrophil layer were collected into a fresh 15 mL Falcon tube. An equal volume of 0.45 % v/v NaCl saline was mixed with the neutrophils to restore normal osmolality, then the tubes were topped up to 12 mL with 0.1 % v/v NaCl saline and mixed. The tube was centrifuged at 400 *g* for 10 min at 21 °C with maximum deceleration. The supernatant was discarded, then the cells were gently resuspended in 2 mL of red cell lysis buffer and incubated for 15 min at 21 °C in the

dark. The tubes were topped up to 12 mL with HBSS (containing Ca^{2+} and Mg^{2+}) and centrifuged at 400 *g* for 10 min at 21 °C. Red cell lysis was repeated until no further red cells were seen in the neutrophil pellet. Then, the supernatant was removed, cells resuspended in 12 mL of HBSS and centrifuged again at 400 *g* for 10 min at 21 °C. The supernatant (with excess lysis buffer) was removed and the cells were resuspended in 2 mL HBSS.

For analysis of neutrophil adhesion to endothelial cells using fluorescence spectroscopy and microscopy, the leukocytes were labelled with 1 µM of calcein for 20 min at 37 °C and 5 % CO_2, then centrifuged at 400 *g* for 10 min at 21 °C. The supernatant was then discarded to remove excess calcein.

2.15.2. Adhesion assay

HCAEC were plated onto 96-well plates, then treated with LDL for 24 h as described in section 2.6. The cells were then washed with HBSS, aspirated, and 100 µL of neutrophils (10^6 cells**.**mL^{-1}) stained with calcein were added to the cells and incubated for 20 min at 37 °C and 5 % CO_2. The total neutrophil fluorescence (without washing) and adherent neutrophil fluorescence (neutrophils remaining after washing the cells five times with HBSS) were measured in the 96-well plate by fluorescence spectroscopy with an excitation/emission spectrum of 492/515 nm and the percentage was calculated by the difference between the total and adherent neutrophil fluorescence compared to the total fluorescence (Equation 3). The adherence of neutrophils was also qualitatively studied by fluorescence microscopy of the 96-well plates for comparison.

(3) $$\% \text{ adherence} = \frac{(f_{total} - f_{adherent})}{f_{total}} \times 100$$

2.16. Vasodilation of rat aortic segments ex vivo

The physiological consequence of LDL, HOSCN-modified LDL and HOCl-modified LDL was investigated by *ex vivo* treatment of rat aortic segments with 0.1 mg**.**mL^{-1} of each LDL treatment for 1 h in HBSS, or for 24 h in endothelial cell treatment media. The rats used for this study were the control animals sacrificed for other experiments unrelated to this study (Ethics Protocols 2014-020 and 2014-030). This was conducted in accordance with the ARRIVE guidelines, the Australian Code of Practice for the Care and Use of Animals for Scientific Purposes (MSW – Animal Research Act 1985) and certified by the National Health and Medical Research Council of Australia (NHMRC). Rats were acclimatised in cages located at the Heart Research Institute Biological Facilities Centre under environmental enrichment, maintained at 25 ± 2 °C and 40 – 60 % humidity, with access to food and water *ad libitum*.

The thoracic aortae were harvested from eight male Sprague-Dawley rats (weight; 250 – 450 g, 1 h: n = 5, 24 h: n = 3) and rapidly cleaned and stripped of fat and adhered tissue in warm HBSS. The thoracic aorta was cut into four ~ 4 mm length segments and placed in warm HBSS. Each of the four segments were mounted with two pins in 7 mL myograph chambers (Danish Myo Technology, Aarhus, Denmark) maintained at 37 °C and pH 7.4 by continuous bubbling with 95 % O_2 and 5 % CO_2. Myography was recorded and analysed using LabChart 8 software (ADInstruments, Dunedin, New Zealand). Aortic segments were equilibrated to a resting tension of ~15 mN for approximately 15 min, with washout and addition of fresh HBSS. Aortic segments were then washed out and treated with 0.1 mg**.**mL^{-1} LDL or LDL oxidised with either 250 µM HOSCN or HOCl in 7 mL of warm HBSS for 1 h. Untreated ring segments were maintained in HBSS without any added LDL as a control. Rat aortic segments treated for 24 h in endothelial cell treatment media were subject to an initial pre-tension force of 2 mN until equilibrated, then pre-tension force was increased to 4 mN and allowed to equilibrate

again. This was due to the vessels being sensitive to pressure-induced tone (spontaneous periodic contractions which may indicate mechanical vessel injury) when subject to tension forces similar to the 1 h treatment vessels. The treatments were then washed out and replaced with HBSS. A vasoconstrictive dose-response to norepinephrine (NE; 10^{-9} to 10^{-5} M) was measured for each experiment, and a submaximal dose (0.5 - 1 µM NE) was used for preconstriction before performing endothelium-dependent acetylcholine (ACh; 10^{-9} - 10^{-3} M) and endothelium-independent sodium nitroprusside (SNP; 10^{-11} - 10^{-5} M; a NO generator) induced vasodilation experiments. The cumulative dose response curves were generated with four-parameter logistic regression analysis. The EC_{50} and maximum vasodilatory response were analysed between each LDL treatment.

2.17. Statistics

Statistical analyses were performed using GraphPad Prism 7 (GraphPad Software, San Diego, California) with $p < 0.05$ taken for statistical significance. Specific statistics and *post-hoc* tests used in experiments are provided in the Figure legends in the respective Results sections.

Chapter 3. Characterisation of LDL modified by HOSCN and HOCl

3.1. Introduction

Oxidation of the apoB-100 moiety of LDL is a major post-translational modification linked to the development of atherosclerosis [234, 502]. Many different initiators of LDL oxidation have been implicated in atherosclerotic lesion development, including transition metal ions, lipoxygenase, reactive oxygen and nitrogen species, glucose and MPO-derived oxidants, particularly, in the case of the latter: HOCl (see reviews [53, 263, 264, 273, 278, 280, 304, 321, 476, 503, 504]). Transition metal ions, particularly copper, are the most widely utilised agent for the preparation of oxidised LDL used extensively in *in vitro* experiments [303, 304, 318, 375, 505-508]. This type of oxidised LDL is characterised by extensive lipid modifications, such as the loss of polyunsaturated cholesteryl esters and formation of fatty acid hydroperoxides, with the depletion of antioxidants such as α-tocopherol to give free radical intermediates that can potentiate apoB-100 modification [303, 304]. However, it has been questioned as to whether this is a valid model of LDL oxidation, due to the lack of causative evidence of transition metal ion-mediated LDL oxidation in atherosclerotic lesions *in vivo*, where these ions are only present in advanced calcified and complex lesions and at levels lower than that used commonly to modify LDL *in vitro* [322].

Iron ions have also been implicated in atherosclerotic development and shown to potentiate LDL lipid oxidation similar to copper ion-mediated LDL oxidation, albeit at a reduced reactivity compared to copper (Cu^{2+}) ions [323, 375]. In cholesterol-fed rabbits, iron overload did not affect atherosclerotic lesion size [509], while dietary supplementation of copper ions paradoxically decreased atherosclerosis [510, 511]. Contrastingly, atherosclerosis-prone $apoE^{-/-}$ mice with iron overload showed a reduction in atherosclerotic lesion size [327], while C57B mice with copper deficiency showed an exacerbated atherosclerotic state [512]. The majority of studies of people with haemochromatosis and cardiovascular risk have found no significant

association between iron stores (i.e. ferritin, transferrin) [513]. Further, patients with Wilson's disease had reduced LDL levels and no change in LDL oxidisability compared to the control group [319]. This raises further questions as to the relevance of the transition metal ion pathway of LDL oxidation *in vivo*.

In contrast to transition metal ions, the MPO-derived oxidant HOCl predominantly reacts with the apoB-100 moiety of LDL and displays little reactivity with cholesteryl esters or LDL-bound antioxidants at physiologically-relevant concentrations [53]. HOCl reacts directly with apoB-100, which results in the oxidation of a variety of amino acid residues and phospholipid groups including, in order of reactivity: Met > Cys > His ~ N-terminal amine > phosphatidylserine and phosphatidylethanolamine head groups > Trp > Lys > > Tyr > Arg [58, 111, 135, 292]. HOCl-modified epitopes of LDL and 3-Cl-Tyr on LDL have also been detected immunologically in human atherosclerotic lesions [233, 281]. Treatment of LDL with the MPO-H_2O_2-Cl^- system results in extensive modification of Tyr and Trp to form 3-Cl-Tyr and di-oxidised Trp in apoB-100 in the presence of high H_2O_2 concentration of 1 mM, in contrast to reagent HOCl which oxidised predominately Met residues [288]. These data demonstrate that the MPO-H_2O_2-Cl^- system can react in a site-specific manner with apoB-100 due to MPO binding directly to LDL [288].

In contrast, less is known about the modification of LDL by the other major MPO-derived oxidant, HOSCN. Studies of LDL incubated with the MPO-H_2O_2-SCN^- system provided evidence for LDL conjugated diene and lipid hydroperoxide formation [144]. This was supported by Ismael *et al*, who showed some reactivity of reagent and MPO-derived HOSCN with polyunsaturated cholesteryl arachidonate and linoleate components to produce lipid hydroperoxides, 9-HODE and F_2-isoprostanes [146]. Further, the latter study also showed evidence of apoB-100 modification by HOSCN, which differed in reactivity compared to HOCl and cyanate (OCN^-; a decomposition product of HOSCN) with apoB-100. In this study,

evidence was also obtained for the cleavage of apoB-100 by HOSCN in a site-specific manner, though the mechanism of fragmentation and the cleavage site were not identified [146].

3.2. Aims

The aim of the studies in this Chapter was to examine the mechanism and define the cleavage site(s) of HOSCN-induced apoB-100 fragmentation. This is important as identification of a novel HOSCN-derived apoB-100 peptide/protein fragments might be useful as a biomarker to assess the role of HOSCN formation during lesion development *in vivo*.

3.3. Results

3.3.1. Charge modification of LDL

Initial studies were performed to assess the extent of LDL modification by relative electrophoretic mobility (REM); a function of charge modification of LDL measured by the distance travelled through an agarose gel under constant voltage. LDL (1.0 mg**.**mL^{-1}) was incubated with 250 μM HOSCN or HOCl for 24 h at 37 °C, and compared to LDL oxidised by incubation with 5 μM $CuSO_4$, which is commonly used in *in vitro* cell function studies [307-309, 313, 419, 473, 507, 514-530]. The REM was normalised to LDL incubated under identical conditions in the absence of oxidant (referred to as control LDL from hereafter). The REM of LDL incubated with HOSCN was not significantly different to the control LDL (Figure 3.1). In contrast, HOCl-modified LDL migrated significantly further than both control LDL and HOSCN-modified LDL (approximately 183 % versus control LDL). Similarly, Cu^{2+}-modified LDL charge was extensively modified and had an REM of approximately 330 % compared to the control LDL (Figure 3.1). These results reflect differences in the ability of HOCl and HOSCN to modify charged amino acid side chains, including Lys, Arg and His, as unlike HOCl, HOSCN is highly selective towards Cys residues [90, 135, 146, 292, 531]. Meanwhile,

Cu^{2+} ions can react with most LDL constituents, including amino acid residues, lipids and the backbone polypeptides [303, 375, 532].

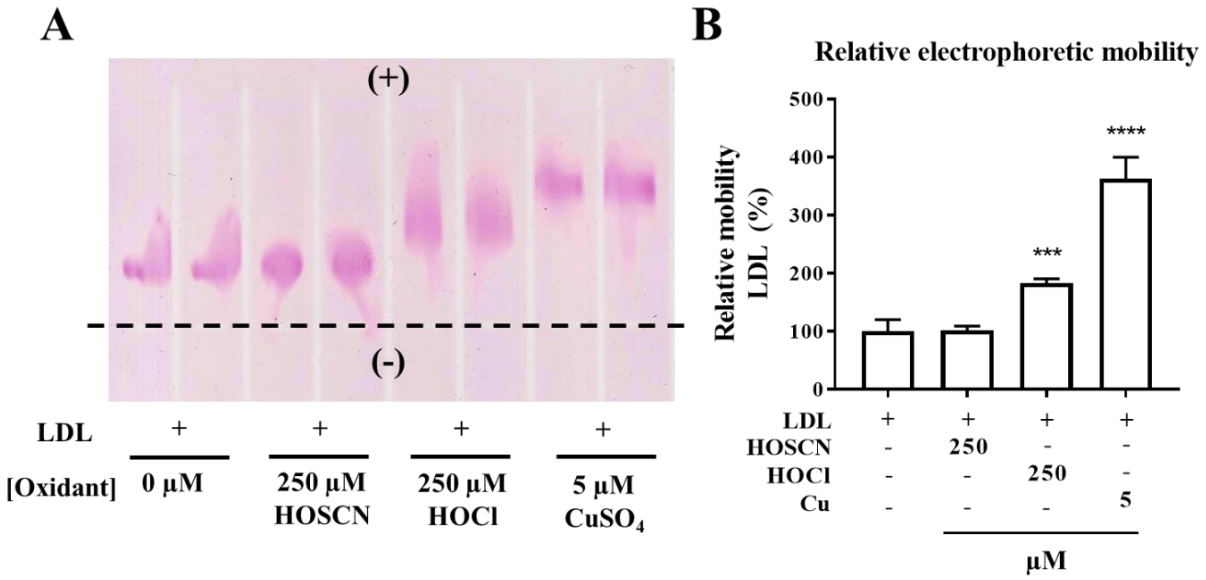

Figure 3.1. Relative Electrophoretic Mobility (REM) of LDL modified by MPO-derived oxidants and $CuSO_4$. *LDL (1.0 mg·mL^{-1}) was incubated with 250 µM HOSCN, 250 µM HOCl or 5 µM $CuSO_4$ for 24 h at 37 °C. (A) Representative REM gel of two independent LDL experiments run through an agarose gel simultaneously. (B) REM of control LDL compared to oxidised LDL species. Migration distance was measured from the origin (dashed line) away from the anode (-) and normalised to control LDL. Bars represent the mean ± SD (n = 4; from two LDL donors). Statistical analysis was performed using one-way ANOVA with Dunnett's multiple comparison test. *** and **** represent significant difference with p < 0.001 and 0.0001, respectively compared to control LDL.*

3.3.2. Structural modifications of apoB-100

The charge modification studies were extended to examine the ability of HOSCN and HOCl to induce structural modifications of apoB-100, such as aggregation and fragmentation of the protein structure. These modifications were examined by SDS-PAGE experiments under reduced and non-reduced conditions after 24 h incubation of LDL with up to 250 µM HOSCN or HOCl or LDL exposed to 5 µM $CuSO_4$. The exposure of LDL to HOSCN or HOCl led to

different types and extents of modification upon comparison of the two oxidants (Figure 3.2). ApoB-100 aggregation (indicated by the bracket in lane 2 and 3, respectively) was observed upon exposure of LDL to both 100 µM or 250 µM HOSCN as seen by the bands appearing above the parent apoB-100 band. This aggregation was also present, but to a lesser extent in the control LDL, most likely due to the mild oxidation seen as a result of the incubation conditions alone. Evidence was also obtained for fragmentation of apoB-100 with HOSCN-modified LDL, indicated by the band stained at approximately 90 kDa (highlighted by the red box). In contrast, LDL modified by 100 or 250 µM HOCl (lanes 4 and 5, respectively) appeared more extensively modified, with visible loss of the parent apoB-100 band, formation of darker, higher molecular mass aggregate bands, and more extensive low molecular-mass bands consistent with protein fragmentation. In some experiments, it was possible to see the 90 kDa fragment evidence with LDL exposure to HOSCN, within the analogous experiments with HOCl, but the visualisation of this band was only seen at 100 µM HOCl doses, and not consistently. This may suggest that HOCl can fragment apoB-100 at the same site as HOSCN, but can further fragment the resultant peptide. Consistent with previously published data [375], LDL exposed to $CuSO_4$ is extensively modified, with the parent apoB-100 protein totally displaced in the gel (lane 6). Cu^{2+}-modified LDL perhaps modified to the extent that Coomassie Blue cannot adequately stain the aggregates or fragments of apoB-100.

To ascertain whether the apoB-100 aggregation upon exposure to HOSCN and HOCl is associated with the formation of disulfide bridging between two Cys residues, identical experiments were performed with samples run under reducing conditions, with the LDL samples pre-treated with 50 µM DTT before running SDS-PAGE in order to break the disulfide bonds. Under reduced conditions, considerable aggregation of the apoB-100 protein was still apparent with treatment of LDL with HOCl and HOSCN, suggesting that aggregation was not dependent on the formation of disulfide bonds and instead involving cross-linking between

other amino acid residues [66, 84, 122]. Likewise, the HOSCN-specific band at approximately 90 kDa was still present (Figure 3.3) [293]. Additionally, in both Figures 3.2 and 3.3, a band just below the parent apoB-100 band appeared (indicated by white arrows) together with the appearance of the HOSCN-modified apoB-100 specific fragment, which was likely the remaining major apoB-100 fragment after cleavage of the peptide by HOSCN.

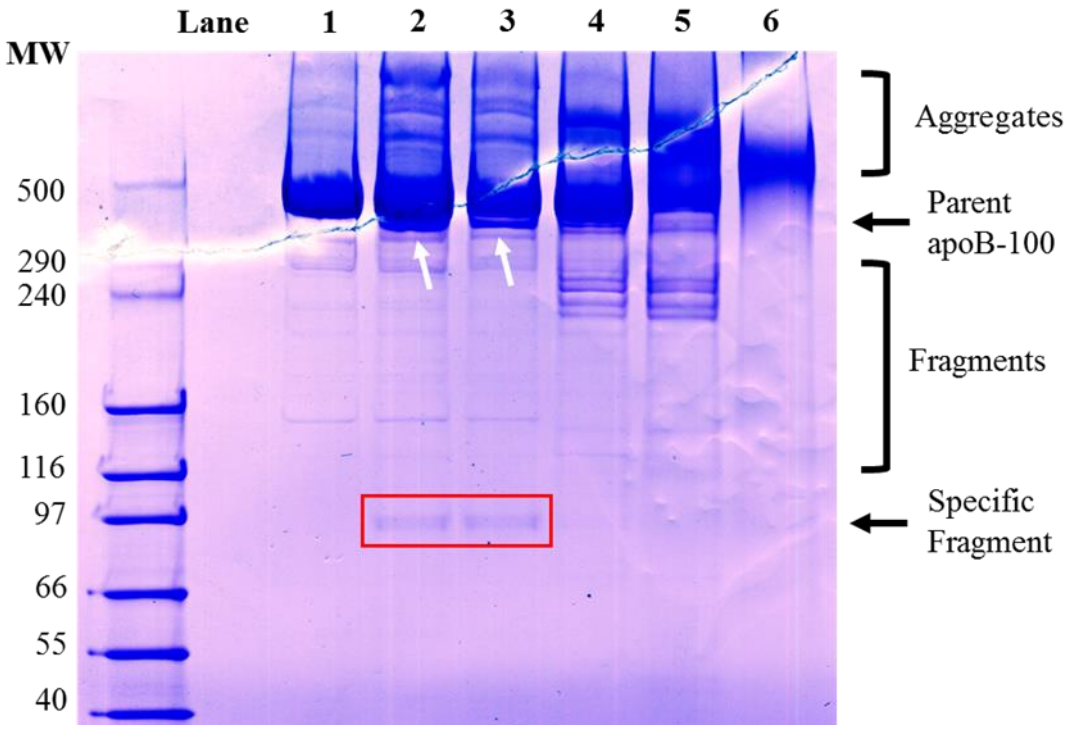

Figure 3.2. Separation of apoB-100 parent, fragment and aggregate peptides by SDS-PAGE from HOSCN- and HOCl-modified LDL under non-reducing conditions. *LDL (1.0 mg•mL^{-1}) was incubated with 100 µM or 250 µM HOSCN or HOCl, or 5 µM $CuSO_4$ for 24 h at 37 °C. 10 µg LDL was added to each lane of the 3 – 8 % Tris-acetate SDS-PAGE gel in each experiment. The peptide bands were stained with Coomassie Blue. A molecular mass ladder is displayed in kDa. LDL was incubated with; Lane 1: no oxidant, lane 2: 100 µM HOSCN, Lane 3: 250 µM HOSCN, Lane 4: 100 µM HOCl, Lane 5: 250 µM HOCl, Lane 6: 5 µM $CuSO_4$. The red box highlights bands specific to HOSCN-modified LDL. Gel is representative of three independent experiments.*

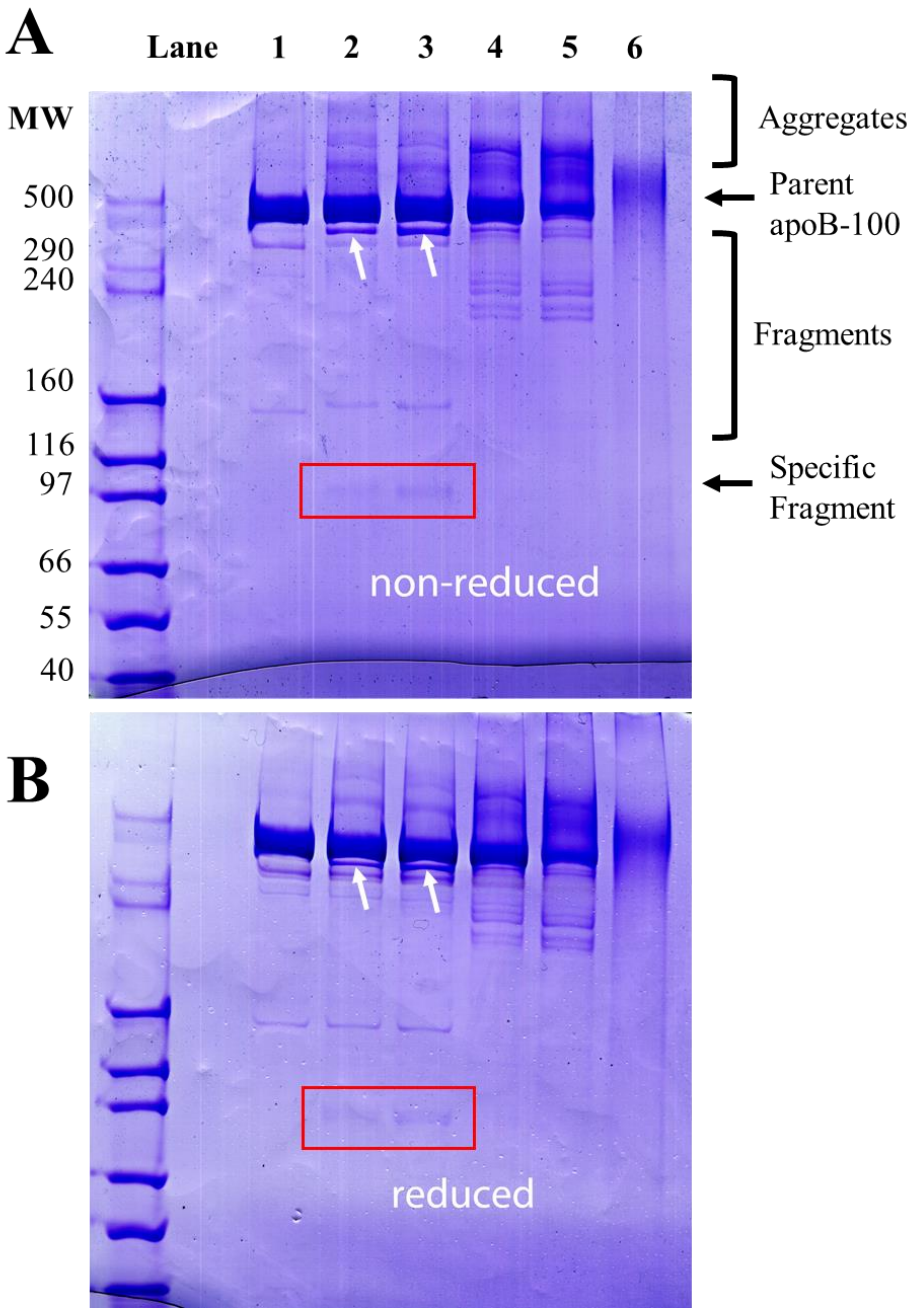

Figure 3.3. Visualisation of apoB-100 parent, fragments and aggregates under non-reduced and reduced conditions by Coomassie staining. *LDL (1.0 mg.mL^{-1}) was incubated with 100 µM or 250 µM HOSCN or HOCl, or 5 µM $CuSO_4$ for 24 h at 37 °C. 10 µg LDL was added to each lane of the 3 – 8 % Tris-acetate SDS-PAGE gel in each experiment under (A) non-reduced conditions, or (B) under reduced conditions with the addition of 50 mM DTT. LDL was incubated with; Lane 1: no oxidant, lane 2: 100 µM HOSCN, lane 3: 250 µM HOSCN, lane 4: 100 µM HOCl, lane 5: 250 µM HOCl, and lane 6: 5 µM $CuSO_4$. Gels are representative of three independent experiments.*

In order to improve the visualisation and resolution of the HOSCN-induced apoB-100 fragment bands, a silver staining protocol was utilised [533]. The silver stain signal can be amplified by extending the exposure of the developing solution to silver ions captured by the peptides to increase sensitivity, while Coomassie blue is a colloid and the stain intensity is dependent on the protein concentration. This results in the silver stain being up to 100-fold more sensitive than Coomassie blue stain [534].

Using the silver staining approach, the smaller fragments of apoB-100 were more easily visualised and the formation of the HOSCN-modified LDL specific fragment at approximately 90 kDa was more clearly distinguished (Figure 3.4 A and B). This fragment band is observed under both reducing and non-reducing conditions, suggesting that site-specific fragmentation is not related to disulfide bond cleavage. Further, this band appears to be a doublet, suggesting the presence of two protein fragments of similar size. These data also showed that this fragment intensity is dependent on HOSCN concentration, while it is not present with the control (Figure 3.4 C). The HOSCN-modified LDL fragment band (indicated by the red box) was also apparent in experiments with 100 µM HOCl-modified LDL (lane 4), but not with 250 µM HOCl-modified LDL (lane 5; Figure 3.3). This is due to a larger number of fragmentation events of apoB-100 with higher concentrations of HOCl, producing more fragments.

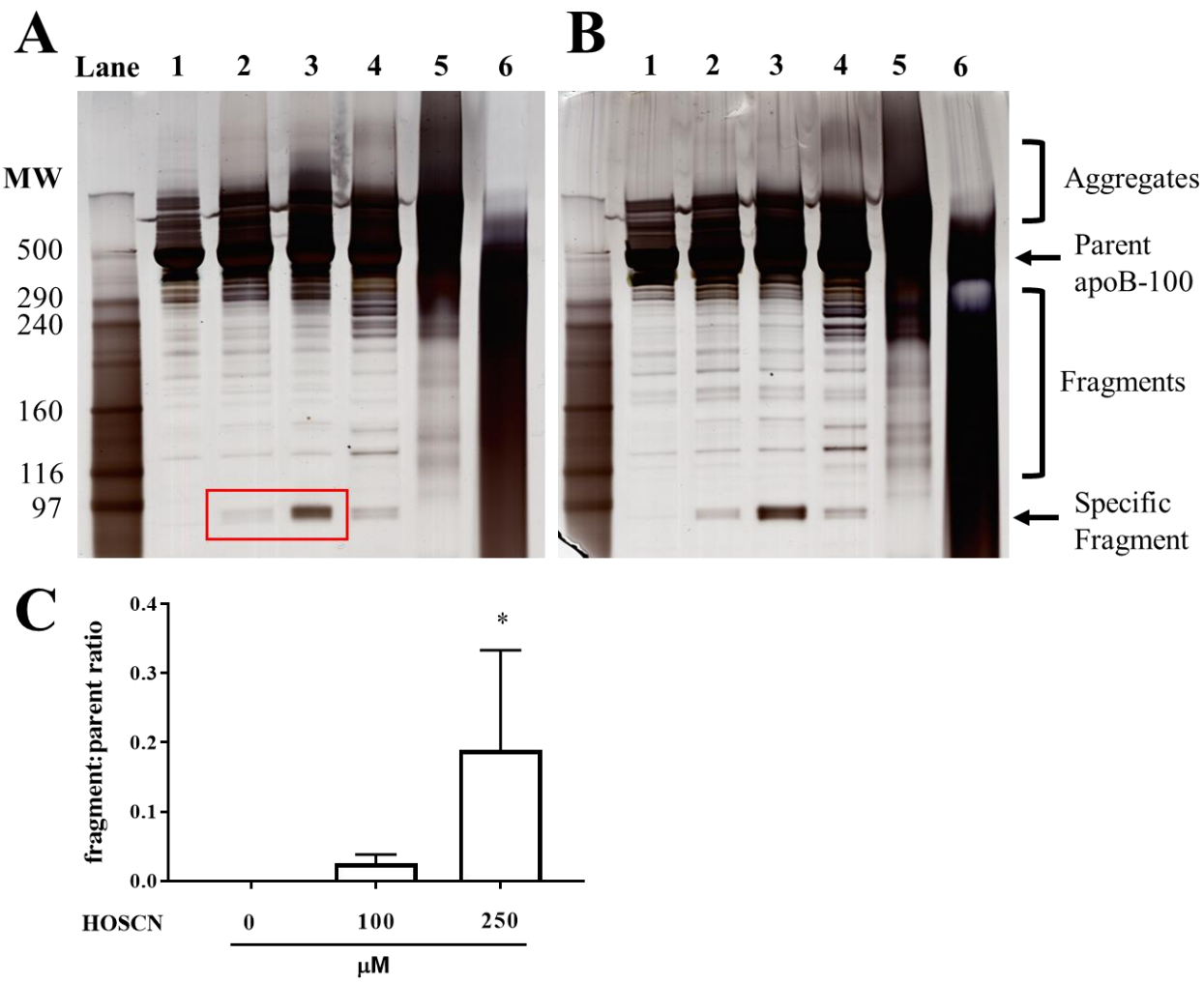

Figure 3.4. Sensitive visualisation of apoB-100 parent, fragments and aggregates under non-reduced and reduced conditions by silver staining. *LDL (1.0 mg.mL^{-1}) was incubated with 100 µM or 250 µM HOSCN or HOCl, or 5 µM $CuSO_4$ for 24 h at 37 °C. 10 µg LDL was added to each lane of the 3 – 8 % Tris-acetate SDS-PAGE gel in each experiment under (A) non-reduced conditions, or under (B) reduced conditions with the addition of 50 mM DTT. LDL was incubated with; Lane 1: no oxidant, lane 2: 100 µM HOSCN, lane 3: 250 µM HOSCN, lane 4: 100 µM HOCl, lane 5: 250 µM HOCl, and lane 6: 5 µM $CuSO_4$. (C) densitometry of apoB-100 fragment (red box):parent ratio. Bars represent the mean ± SD (n = 4). Statistical analysis was performed with one-way ANOVA with Dunnett's multiple comparison test. * represents significance level $p < 0.05$ compared to control LDL.*

3.3.3. HOSCN-modified LDL fragmentation characterisation

It has been shown previously that HOSCN-induced oxidation of LDL associated cholesterol and cholesteryl esters occurred via radical-mediated pathway, and was influenced by the presence of trace transition metal ions [146]. Since the apoB-100 fragmentation by HOSCN was not observed to the same extent as HOCl, which itself may indicate a specific reaction with HOSCN, further experiments were designed to elucidate the chemical mechanism involved in this HOSCN-mediated fragmentation of LDL. This was attained by exposing LDL to 250 μM HOSCN in the presence of a free radical-scavenging compound (BHT) and an iron-chelator (DFO) for 24 h before SDS-PAGE and Coomassie stain analysis (Figure 3.5A). The addition of 50 μM DFO did not reduce the fragmentation of apoB-100 upon HOSCN exposure to LDL, however 200 μM BHT significantly, though not completely, reduced the formation of the fragment band, as shown by the densitometry ratio of the fragment band to the parent band (Figure 3.5B). From these data, free radical-mediated chemistry may be involved in the cleavage of apoB-100 when oxidised by HOSCN.

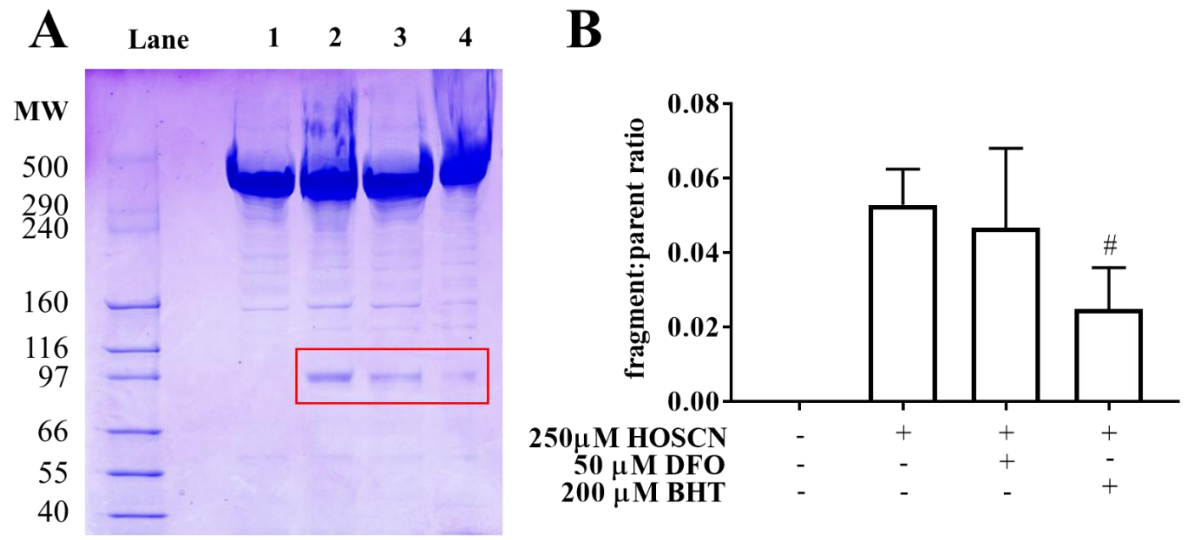

Figure 3.5. LDL incubated with HOSCN and the iron-chelator desferrioxamine (DFO) or the free radical scavenger butylated-hydroxytoluene (BHT). *1.0 mg.mL^{-1} Control LDL (lane 1) or LDL modified by 250 µM HOSCN in the absence (lane 2) or presence of 50 µM DFO (lane 3) or 200 µM BHT (lane 4) for 24 h at 37 °C. (A) Gels were stained with Coomassie Blue. The red box highlights bands specific to HOSCN-modified LDL. (B) Densitometry of the fragment: parent apoB-100 ratio between treatments. Bar represents the mean ± SD (n = 4). One-way ANOVA with Dunnett's multiple comparison test. # represents p < 0.05 compared to LDL incubated with HOSCN only.*

3.3.3.1.a. Sequence of HOSCN-derived apoB-100 fragments

Next, the nature of the cleavage site responsible for the HOSCN-induced apoB-100 cleavage site was examined using a proteomic approach. The proteomics experiments were performed in collaboration with Dr Matthew Padula and Iain Berry at the Proteomics Core Facility at the University of Technology Sydney, who assisted with the experimental design, ran the samples through the LC-MS, and provided guidance regarding data analysis. LDL at 1.0 mg.mL^{-1} was exposed to 250 µM HOSCN for 24 h at 37 °C before separation of the parent protein and fragments by SDS-PAGE. The fragment bands were excised from the gel, free Cys residues were blocked by reduction and alkylation with acrylamide, the fragments were digested using

trypsin and analysed using triple quadrupole time-of-flight LC-MS/MS as described in Section 2.4.3. The peptides were matched to the apoB-100 amino acid sequence through the Mascot Daemon program using the LudwigNR database, as shown in Figure 3.6. Data show that the peptides from the HOSCN-induced fragment band matched two regions of the apoB-100 sequence at the N-terminal (amino acid 1 – 819) and C-terminal (amino acid 3725 – 4563), which were thus named the N-fragment and C-fragment, respectively. The detection of significant peptide sequences was highlighted red in the sequence, while non-significant peptide sequences were highlighted blue.

On comparison of replicate experiments, peptide fragments were detected further in the apoB-100 sequence, up to residue 960 at the N-terminal and up to 3167 at the C-terminal (Figure 3.6). The high scoring peptide sequences (^{950}TEVIPPLIENR^{960} and ^{3167}QSFDLSVK-^{3174}), although statistically significant, needed to be scrutinised in the analysis as there was a large gap in the sequence to the next detected *de novo* peptide, where there were several potential *de novo* tryptic digestion sites possible. The potential tryptic site residues were Lys$^{822, 859, 863, 876, 918, 921, 923, 930}$ and Arg$^{895, 941}$ for the N-fragment, and Lys$^{3778, 3779, 3781, 3202, 3210, 3227, 3229, 3232, 3234, 3237, 3314, 3321, 3344, 3380, 3390, 3524, 3531, 3537, 3568, 3586, 3626, 3630, 3656, 3689}$ and Arg$^{3138, 3206, 3244, 3386, 3389, 3391, 3437, 3507, 3527, 3632, 3638, 3670, 3698, 3699}$, which were not detected in any replicates. Furthermore, the calculated molecular mass of these apoB-100 fragments from residues 1 – 960 and 3617 – 4563, was approximately 106.8 and 160.5 kDa, respectively, which is far greater than the predicted molecular mass of each fragment and the mass difference between the apoB-100 fragments according to the Figures 3.3, 3.4 and 3.5. The next significant peptide detected in all three replicates for the N-terminal apoB-100 fragment was ^{805}TLQGIPQMIGEVIRK^{819} (score: 44) and the C-terminal apoB-100 fragment was ^{3725}VLADKFIIPGLK^{3736} (score: 63). The estimated molecular mass of the N- and C-terminal LDL fragments up to these residues are approximately 91.7 and 96.6 kDa, respectively; which

was in greater agreement with the SDS-PAGE analysis and predicted molecular mass, and in the observed molecular mass difference between the two fragments by SDS-PAGE and silver-stained gels.

1	MDPPRPALLA	LLALPALLLL	LLAGARAEEE	MLENVSLVCP	KDATRFKHLR
51	KYTYNYEAES	SSGVPGTADS	RSATRINCKV	ELEVPQLCSF	ILKTSQCTLK
101	EVYGFNPEGK	ALLKKTKNSE	EFAAAMSRYE	LKLAIPEGKQ	VFLYPEKDEP
151	TYILNIKRGI	ISALLVPPET	EEAKQVLFLD	TVYGNCSTHF	TVKTRKGNVA
201	TEISTERDLG	QCDRFKPIRT	GISPLALIKG	MTRPLSTLIS	SSQSCQYTLD
251	AKRKHVAEAI	CKEQHLFLPF	SYKNKYGMVA	QVTQTLKLED	TPKINSRFFG
301	EGTKKMGLAF	ESTKSTSPPK	QAEAVLKTLQ	ELKKLTISEQ	NIQRANLFNK
351	LVTELRGLSD	EAVTSLLPQL	IEVSSPITLQ	ALVQCGQPQC	STHILQWLKR
401	VHANPLLIDV	VTYLVALIPE	PSAQQLREIF	NMARDQRSRA	TLYALSHAVN
451	NYHKTNPTGT	QELLDIANYL	MEQIQDDCTG	DEDYTYLILR	VIGNMGQTME
501	QLTPELKSSI	LKCVQSTKPS	LMIQKAAIQA	LRKMEPKDKD	QEVLLQTFLD
551	DASPGDKRLA	AYLMLMRSPS	QADINKIVQI	LPWEQNEQVK	NFVASHIANI
601	LNSEELDIQD	LKKLVKEALK	ESQLPTVMDF	RKFSRNYQLY	KSVSLPSLDP
651	ASAKIEGNLI	FDPNNYLPKE	SMLKTTLTAF	GFASADLIEI	GLEGKGFEPT
701	LEALFGKQGF	FPDSVNKALY	WVNGQVPDGV	SKVLVDHFGY	TKDDKHEQDM
751	VNGIMLSVEK	LIKDLKSKEV	PEARAYLRIL	GEELGFASLH	DLQLLGKLLL
801	MGARTLQGIP	QMIGEVIRKG	SKNDFFLHYI	FMENAFELPT	GAGLQLQISS
851	SGVIAPGAKA	GVKLEVANMQ	AELVAKPSVS	VEFVTNMGII	IPDFARSGVQ
901	MNTNFFHESG	LEAHVALKAG	KLKFIIPSPK	RPVKLLSGGN	TLHLVSTTKT
951	EVIPPLIENR	QSWSVCKQVF	PGLNYCTSGA	YSNASSTDSA	SYYPLTGDTR
1001	LELELRPTGE	IEQYSVSATY	ELQREDRALV	DTLKFVTQAE	GAKQTEATMT
1051	FKYNRQSMTL	SSEVQIPDFD	VDLGTILRVN	DESTEGKTSY	RLTLDIQNKK
1101	ITEVALMGHL	SCDTKEERKI	KGVISIPRLQ	AEARSEILAH	WSPAKLLLQM
1151	DSSATAYGST	VSKRVAWHYD	EEKIEFEWNT	GTNVDTKKMT	SNFPVDLSDY
1201	PKSLHMYANR	LLDHRVPQTD	MTFRHVGSKL	IVAMSSWLQK	ASGSLPYTQT
1251	LQDHLNSLKE	FNLQNMGLPD	FHIPENLFLK	SDGRVKYTLN	KNSLKIEIPL
1301	PFGGKSSRDL	KMLETVRTPA	LHFKSVGFHL	PSREFQVPTF	TIPKLYQLQV
1351	PLLGVLDLST	NVYSNLYNWS	ASYSGGNTST	DHFSLRARYH	MKADSVVDLL
1401	SYNVQGSGET	TYDHKNTFTL	SYDGSLRHKF	LDSNIKFSHV	EKLGNNPVSK
1451	GLLIFDASSS	WGPQMSASVH	LDSKKKQHLF	VKEVKIDGQF	RVSSFYAKGT
1501	YGLSCQRDPN	TGRLNGESNL	RFNSSYLQGT	NQITGRYEDG	TLSLTSTSDL
1551	QSGIIKNTAS	LKYENYELTL	KSDTNGKYKN	FATSNKMDMT	FSKQNALLRS
1601	EYQADYESLR	FFSLLSGSLN	SHGLELNADI	LGTDKINSGA	HKATLRIGQD
1651	GISTSATTNL	KCSLLVLENE	LNAELGLSGA	SMKLTTNGRF	REHNAKFSLD
1701	GKAALTELSL	GSAYQAMILG	VDSKNIFNFK	VSQEGLKLSN	DMMGSYAEMK
1751	FDHTNSLNIA	GLSLDFSSKL	DNIYSSDKFY	KQTVNLQLQP	YSLVTTLNSD
1801	LKYNALDLTN	NGKLRLEPLK	LHVAGNLKGA	YQNNEIKHIY	AISSAALSAS
1851	YKADTVAKVQ	GVEFSHRLNT	DIAGLASAID	MSTNYNSDSL	HFSNVFRSVM
1901	APFTMTIDAH	TNGNGKLALW	GEHTGQLYSK	FLLKAEPLAF	TFSHDYKGST
1951	SHHLVSRKSI	SAALEHKVSA	LLTPAEQTGT	WKLKTQFNNN	EYSQDLDAYN
2001	TKDKIGVELT	GRTLADLTLL	DSPIKVPLLL	SEPINIIDAL	EMRDAVEKPQ
2051	EFTIVAFVKY	DKNQDVHSIN	LPFFETLQEY	FERNRQTIIV	VLENVQRNLK
2101	HINIDQFVRK	YRAALGKLPQ	QANDYLNSFN	WERQVSHAKE	KLTALTKKYR
2151	ITENDIQIAL	DDAKINFNEK	LSQLQTYMIQ	FDQYIKDSYD	LHDLKIAIAN
2201	IIDEIIEKLK	SLDEHYHIRV	NLVKTIHDLH	LFIENIDFNK	SGSSTASWIQ
2251	NVDTKYQIRI	QIQEKLQQLK	RHIQNIDIQH	LAGKLKQHIE	AIDVRVLLDQ
2301	LGTTISFERI	NDILEHVKHF	VINLIGDFEV	AEKINAFRAK	VHELIERYEV
2351	DQQIQVLMDK	LVELAHQYKL	KETIQKLSNV	LQQVKIKDYF	EKLVGFIDDA
2401	VKKLNELSFK	TFIEDVNKFL	DMLIKKLKSF	DYHQFVDETN	DKIREVTQRL
2451	NGEIQALELP	QKAEALKLFL	EETKATVAVY	LESLQDTKIT	LIINWLQEAL
2501	SSASLAHMKA	KFRETLEDTR	DRMYQMDIQQ	ELQRYLSLVG	QVYSTLVTYI
2551	SDWWTLAAKN	LTDFAEQYSI	QDWAKRMKAL	VEQGFTVPEI	KTILGTMPAF
2601	EVSLQALQKA	TFQTPDFIVP	LTDLRIPSVQ	INFKDLKNIK	IPSRFSTPEF
2651	TILNTFHIPS	FTIDFVEMKV	KIIRTIDQML	NSELQWPVPD	IYLRDLKVED
2701	IPLARITLPD	FRLPEIAIPE	FIIPTLNLND	FQVPDLHIPE	FQLPHISHTI
2751	EVPTFGKLYS	ILKIQSPLFT	LDANADIGNG	TTSANEAGIA	ASITAKGESK

2801	LEVLNFDFQA	NAQLSNPKIN	PLALKESVKF	SSKYLRTEHG	SEMLFFGNAI
2851	EGKSNTVASL	HTEKNTLELS	NGVIVKINNQ	LTLDSNTKYF	HKLNIPKLDF
2901	SSQADLRNEI	KTLLKAGHIA	WTSSGKGSWK	WACPRFSDEG	THESQISFTI
2951	EGPLTSFGLS	NKINSKHLRV	NQNLVYESGS	LNFSKLEIQS	QVDSQHVGHS
3001	VLTAKGMALF	GEGKAEFTGR	HDAHLNGKVI	GTLKNSLFFS	AQPFEITAST
3051	NNEGNLKVRF	PLRLTGKIDF	LNNYALFLSP	SAQQASWQVS	ARFNQYKYNQ
3101	NFSAGNNENI	MEAHVGINGE	ANLDFLNIPL	TIPEMRLPYT	IITTPPLKDF
3151	SLWEKTGLKE	FLKTTKQSFD	LSVKAQYKKN	KHRHSITNPL	AVLCEFISQS
3201	IKSFDRHFEK	NRNNALDFVT	KSYNETKIKF	DKYKAEKSHD	ELPRTFQIPG
3251	YTVPVVNVEV	SPFTIEMSAF	GYVFPKAVSM	PSFSILGSDV	RVPSYTLILP
3301	SLELPVLHVP	RNLKLSLPDF	KELCTISHIF	IPAMGNITYD	FSFKSSVITL
3351	NTNAELFNQS	DIVAHLLSSS	SSVIDALQYK	LEGTTRLTRK	RGLKLATALS
3401	LSNKFVEGSH	NSTVSLTTKN	MEVSVATTTK	AQIPILRMNF	KQELNGNTKS
3451	KPTVSSSMEF	KYDFNSSMLY	STAKGAVDHK	LSLESLTSYF	SIESSTKGDV
3501	KGSVLSREYS	GTIASEANTY	LNSKSTRSSV	KLQGTSKIDD	IWNLEVKENF
3551	AGEATLQRIY	SLWEHSTKNH	LQLEGLFFTN	GEHTSKATLE	LSPWQMSALV
3601	QVHASQPSSF	HDFPDLGQEV	ALNANTKNQK	IRWKNEVRIH	SGSFQSQVEL
3651	SNDQEKAHLD	IAGSLEGHLR	FLKNIILPVY	DKSLWDFLKL	DVTTSIGRRQ
3701	HLRVSTAFVY	TKNPNGYSFS	IPVKVLADKF	IIPGLKLNDL	NSVLVMPTFH
3751	VPFTDLQVPS	CKLDFREIQI	YKKLRTSSFA	LNLPTLPEVK	FPEVDVLTKY
3801	SQPEDSLIPF	FEITVPESQL	TVSQFTLPKS	VSDGIAALDL	NAVANKIADF
3851	ELPTIIVPEQ	TIEIPSIKFS	VPAGIVIPSF	QALTARFEVD	SPVYNATWSA
3901	SLKNKADYVE	TVLDSTCSST	VQFLEYELNV	LGTHKIEDGT	LASKTKGTFA
3951	HRDFSAEYEE	DGKYEGLQEW	EGKAHLNIKS	PAFTDLHLRY	QKDKKGISTS
4001	AASPAVGTVG	MDMDEDDDFS	KWNFYYSPQS	SPDKKLTIFK	TELRVRESDE
4051	ETQIKVNWEE	EAASGLLTSL	KDNVPKATGV	LYDYVNKYHW	EHTGLTLREV
4101	SSKLRRNLQN	NAEWVYQGAI	RQIDDIDVRF	QKAASGTTGT	YQEWKDKAQN
4151	LYQELLTQEG	QASFQGLKDN	VFDGLVRVTQ	EFHMKVKHLI	DSLIDFLNFP
4201	RFQFPGKPGI	YTREELCTMF	IREVGTVLSQ	VYSKVHNGSE	ILFSYFQDLV
4251	ITLPFELRKH	KLIDVISMYR	ELLKDLSKEA	QEVFKAIQSL	KTTEVLRNLQ
4301	DLLQFIFQLI	EDNIKQLKEM	KFTYLINYIQ	DEINTIFSDY	IPYVFKLLKE
4351	NLCLNLHKFN	EFIQNELQEA	SQELQQIHQY	IMALREEYFD	PSIVGWTVKY
4401	YELEEKIVSL	IKNLLVALKD	FHSEYIVSAS	NFTSQLSSQV	EQFLHRNIQE
4451	YLSILTDPDG	KGKEKIAELS	ATAQEIIKSQ	AIATKKIISD	YHQQFRYKLQ
4501	DFSDQLSDYY	EKFIAESKRL	IDLSIQNYHT	FLIYITELLK	KLQSTTVMNP
4551	YMKLAPGELT	IIL			

	Start – End	*De novo* Peptide sequence	Score
N-terminal	805 – 819	TLQGIPQMIGEVIRK	44
C-terminal	3725 – 3736	VLADKFIIPGLK	63

Figure 3.6. *De novo* tryptic sequence of apoB-100 fragments following HOSCN modification. *(Top) Entire peptide sequence of apoB-100 with detected de novo fragments highlighted red/blue and undetected residues within the fragment sequence highlighted black. Red highlighted fragments had a significant score (E value < 0.05) while blue highlighted fragments had a non-significant score (E value ≥ 0.05). (Bottom) Proposed peptide sequence closest to the true peptide cleavage site. This experiment was replicated three times.*

3.3.3.2. Labelling the N-terminal fragment site by reductive dimethylation

Peptide mapping did not reveal the exact cleavage site, owing to incomplete sequence coverage. Therefore, an in-gel reductive dimethylation labelling of the *N*-terminal amines was performed, prior to excision, improve the identification of the HOSCN-modified apoB-100 cleavage site. This method can be used to determine the cleavage site of the C-fragment, which leaves its N-terminus exposed to dimethylation. As per the fragment sequencing experiment, the same exposure of LDL to HOSCN, separation by SDS-PAGE and in-gel reduction and alkylation was applied. Afterwards, the peptides were exposed to 20 mM cyanoborohydride and 40 mM formaldehyde to dimethylate primary amines as described in Section 2.4.3.1, before trypsin digestion, LC-MS/MS and peptide sequencing. Compared to the sequencing following trypsin digestion, the yields of peptides were significantly reduced following in-gel reductive dimethylation and only ten unique fragments were detected (Table 3.1). Of the ten unique fragments, the last seven fragments in order of apoB-100 sequence were of the C-fragment. Fragment 3767 – 3790 was closest to the suspected fragmentation site, but this fragment was not significant (Score: 44, $p < 0.05$). Regardless, only Lys ε-amine dimethylation and no N-terminal dimethylation of other residues was detected. The likely cause for the reduced fragment yield could be the reduced efficiency of trypsin to digest Lys residues following dimethylation, as the trypsin recognises the positively charged ε-amine group to digest the peptide backbone. This may have left peptides that were too large to exit the gel or be sequenced by the mass spectrometer. The reduced efficacy of trypsin digestion is evidenced by the presence of Lys residues within the fragments 3767 – 3790, 4202 – 4213, 4497 – 4519 and 4552 – 4563 where trypsin did not further fragment the peptides at those Lys sites.

Table 3.1. De novo Peptide sequences of N-fragment and C-fragment peptides following reductive dimethylation of N-terminal and primary amines. *Dimethylated Lys are highlighted in red.*

Start – End	Mr(expt)	Mr(calc)	Score	$P < 0.05$	Peptide
196 – 207	1331.7405	1331.7045	56	Yes	KGNVATEISTER
345 – 356	1444.8775	1444.8402	84	Yes	ANLFNKLVTELR
805 – 818	1569.8998	1569.8549	36	Yes	TLQGIPQMIGEVIR
3767 – 3775	1245.8187	1245.7808	44	No	EIQIYKKLR
3776 – 3790	1615.9206	1615.8821	52	Yes	TSSFALNLPTLPEVK
4107 – 4121	1774.9175	1774.8750	97	Yes	NLQNNAEWVYQGAIR
4122 – 4129	972.5241	972.4876	19	No	QIDDIDVR
4202 – 4213	1437.8175	1437.7769	44	Yes	FQFPGKPGIYTR
4497 – 4519	2956.5751	2956.4858	87	Yes	YKLQDFSDQLSDYYEKFIAESKR
4552 – 4563	1341.8242	1341.7941	26	No	MKLAPGELTIIL

3.4. Discussion

The current study has shown that HOSCN reacts selectively with the apoB-100 moiety of LDL. This was demonstrated by SDS-PAGE, which showed a novel peptide band appearing in LDL samples incubated with HOSCN, indicating selective cleavage of apoB-100 by this oxidant. The formation of this fragment is likely to be free-radical mediated due to the inhibition by the radical scavenger BHT. Peptide sequencing and mapping by LC-MS/MS then revealed this band to be two fragments of similar molecular mass from the terminal ends of apoB-100. The cleavage site of the C-fragment, however, was not resolved by a reductive dimethylation and trypsin digestion approach. This mechanism of selective apoB-100 modification by HOSCN may be of physiological importance in cases of high SCN^- levels in the plasma leading to elevated HOSCN production by MPO. The modification of the apoB-100 moiety of LDL leads to a reduced ability of cells to recognise LDL by the LDLR and altered increased uptake of the modified particle through scavenger receptors (including scavenger receptor class A type 1 (SR-A1), class B type 1 and 2 (SR-B1 and SR-B2), lectin-like oxidised LDL receptor 1 (LOX-1) and SR for endothelial cell type 1 (SREC-1)), which are present on macrophages and endothelial cells, leading to foam cell formation and endothelial

dysfunction, respectively (reviewed [535]) [19, 276, 277, 421]. Additionally, the recognition of modified LDL by these scavenger receptors often leads to activation of pro-inflammatory responses such as MAPK and NF-κB, followed by the consequent release of pro-inflammatory cytokines such as TNF-α and IL-6 [282, 536, 537], leukocyte adhesion molecule expression [538] and caspase 3- and 9-dependent apoptosis [523].

The oxidant concentrations of HOSCN and HOCl incubated with LDL in the experiments of this project are based on calculations of circulating oxidant concentrations *in vivo*. Calculation of these oxidant concentrations were based on, (i) normal levels of circulating neutrophils (5×10^6 cells•mL^{-1}) produce a range of 150 – 425 μM/h HOCl [38, 539], and (ii) that at physiological pH, MPO converts approximately equal proportion of the consumed H_2O_2 to HOSCN and HOCl [39]. *In vitro* exposure of LDL to HOCl and HOSCN led to aggregation and fragmentation of the parent apoB-100 protein, with HOCl also shown to induce significant change in the overall net charge of LDL producing a more negatively charged LDL species. In contrast, no significant change in REM was seen with HOSCN, which agrees with previous data [146]. This can be rationalised by the difference in selectivity of HOSCN and HOCl, with HOSCN targeting free thiols from Cys [145]: whereas the significant change in LDL charge induced by HOCl is likely due to the modification of positively charged apoB-100 residues such as Lys [104, 146, 292, 531, 540], His, another charged amino acid, would likely be another significant target for HOCl reactivity [58].

The difference in the mechanism of apoB-100 modification by hypohalous acids compared to Cu^{2+} were apparent in this study. Modification of LDL by Cu^{2+} significantly altered the charge of LDL compared to the control (similar to previously reported cases [375, 541]) and oxidised LDL to a greater extent than HOCl. Unlike LDL modified by HOSCN or HOCl, which showed distinct parent, fragment and aggregate bands of apoB-100 by SDS-PAGE, the parent apoB-100 band was shifted to a higher molecular mass and there was no distinguishable

aggregate or fragment band of apoB-100 that could be seen by Cu^{2+}-oxidised LDL. It is likely that technical issues in analysing peptide structure by SDS-PAGE gel arise due to the extent of backbone modification of LDL by Cu^{2+}. The lack of resolved silver and Coomassie staining of apoB-100 is likely caused by the universal peptide backbone oxidation by Cu^{2+} [488]. Coomassie blue is a colloidal molecule that binds to basic amino acids (Arg, Lys and His) and to a lesser extent the aromatic amino acids (Phe, Tyr and Trp) [542], which may be modified by Cu^{2+} and impair affinity for Coomassie blue to these residues and prevent binding [304].

3.4.1. Site-specific fragmentation of apoB-100 by HOSCN

A specific fragment band seen at approximately 90 kDa by SDS-PAGE was produced following exposure of LDL to HOSCN, as previously reported by Ismael *et al* [146]. Peptide sequences from the LC-MS/MS study were consistent with the formation of two independent fragments of similar estimated molecular mass (*ca.* 91 to 97 kDa), resulting in the cleavage of a N-fragment and C-fragment. Results also indicated that HOSCN-dependent cleavage of apoB-100 may be free radical-mediated, specifically the inhibition of fragmentation when LDL was exposed to HOSCN in the presence of BHT. Ismael *et al* also demonstrated that the fragment band was not formed when LDL was exposed to OCN^-, indicating that HOSCN degradation did not mediate apoB-100 fragmentation [146]. As the resultant LDL fragmentation from HOSCN was consistent with the formation of a specific N- and C-fragment (as analysed by SDS-PAGE and LC-MS), it was important to determine the amino acid residues located on either side of the fragmentation site as this can help determine the mechanism and peptide environment mediating the specific peptide fragmentation by HOSCN.

The cleavage site could not be determined from the sequence coverage following tryptic digestion as this varied between experiments. Therefore, a reductive dimethylation protocol (adapted from [483]) was utilised to dimethylate the N-terminus of the C-fragment as a non-

physiological tag of the residue at the fragmentation site. This method of terminal amine isotopic labelling of substrates (TAILS) involves the formation of a Schiff base by the reaction of formaldehyde with the amine, which is then reduced by cyanoborohydride to produce the dimethylamine in a very fast reaction, which has no significant side products and does not impact MS/MS peptide sequencing [543], making it a reliable and accurate method of peptide tagging. This approach has applications in differential protein expression, assessing post-translational modifications and protein interactions (reviewed [544]) and has successfully been used to discover substrates of eukaryotic proteases, such as caspases [545], cathepsins [546] and matrix metalloproteins [547, 548], by detecting the loss of the native N-termini. This made it an appropriate approach for identification of fragmentation sites.

In this study, there was a significantly reduced yield of trypsin-digested apoB-100 peptides. Of the peptides detected, Lys ε-dimethylamine groups were detected but no N-terminal dimethylation was observed. As trypsin activity is localised at positively-charged Lys (and Arg) residues of peptides and reductive dimethylation is also known to dimethylate (and neutralise the positive charge of) the Lys ε-amine group [483], it is likely that trypsin was unable to recognise these Lys sites and thus fail to cleave the peptide. Indeed, this has been experimentally verified [549, 550]. This would restrict tryptic digestion at Arg sites and severely impair the capability of obtaining yields of peptides detectable by MS. Using different methods of peptide digestion, such as endoproteinase GluC to cleave Glu sites [551] (and to a lesser extent, Asp [552]) may overcome this limitations of dimethylation tagging, as Glu and Asp sites are not targets of HOSCN reactivity [168] and were not methylated in the peptides we were able to obtain in our experiments.

Other than thiols, HOSCN has previously shown reactivity towards Trp residues [100]. Previously, a study showed that HOSCN was more reactive towards Trp in non-Cys-containing myoglobin (containing haem) compared to apomyoglobin (haem-deficient), but HOSCN did

not react with free Trp or Trp in model peptides (Gly-Trp-Gly or Gly-Lys-Arg-Trp-Gly) [64]. In the current study, neither Cys or Trp can be found near the suspected cleavage site and both residues are of low abundance on apoB-100 [267, 553], the involvement of these residues in formation of the fragments was difficult to determine. However, HOSCN was also found to modify the haem-group of myoglobin [64], which may lead to haem degradation and iron release. This implied that HOSCN reactivity may be altered or modulated by the presence of free iron ions. Ismael *et al* used a free radical scavenger (BHT) and iron chelator (DFO) to examine HOSCN-induced lipid peroxidation of LDL [146]. In this case, DFO partially, yet significantly inhibited lipid hydroperoxide and 9-HODE formation in LDL incubated with 250 μM HOSCN, while BHT completely inhibited the formation of these lipid peroxides and F_2-isoprostane, indicating that lipid peroxidation was *via* free radical-mediated [146]. Results in this Chapter also demonstrate that BHT, but not DFO, significantly reduce apoB-100 fragmentation, which supports a free radical-mediated mechanism. It should be noted that DFO also exhibits free radical-scavenging properties, sometimes leading to the formation of a less reactive DFO radical [554, 555]. This could explain the partial prevention of lipid oxidation products in HOSCN-modified LDL samples and the relatively large variability in fragment: parent apoB-100 ratio when HOSCN-modified LDL was treated with DFO. Nevertheless, together this evidence also confirmed the specific fragmentation of apoB-100 is due to its reactivity with HOSCN.

The inhibition of lipid peroxidation [146] and reduced presence of the specific fragment formed from HOSCN modified LDL by BHT indicates that one-electron, radical-mediated lipid peroxidation is secondary to apoB-100 oxidation and decomposition of peptidyl radicals. This is supported by the detection of apoB-100 modifications before the detection of lipid oxidation products [146] and the distinct lack of products formed between HOSCN and isolated lipids [556]. Unfortunately, the inhibition by BHT is not indicative of a specific radical-

mediated mechanism. HOSCN reactivity with thiol groups has not been previously reported to propagate peptide backbone cleavage. It is still uncertain whether this specific fragmentation of apoB-100 is attributed to the thiol (Cys)-selectivity of HOSCN, though the presence of this specific fragment was verified under thiol-reducing and non-reducing conditions in this study and previously [146]. However, the reaction between HOSCN and thiols can yield RS-SCN intermediates [83], which could decompose to generate thiyl radicals (RS$^{\bullet}$) analogous to RS-Cl to promote lipid oxidation, particularly in the presence of trace transition metal ions. RS$^{\bullet}$ derived from RS-SCN has not been experimentally verified, as RS-SCN has been shown to hydrolyse to RS-OH rather than decomposing via RS$^{\bullet}$ formation [83]. Studies to determine the pathway responsible for radical formation in apoB-100 and LDL lipid species by HOSCN are still required.

Overall, the marked difference in reactivity of HOSCN and HOCl on proteins, as shown with apoB-100, are evident. HOCl exhibits more diverse reactivity with apoB-100 residues, resulting in a higher negative charge, aggregate and fragmentation. In contrast, the thiol-specific oxidant HOSCN, reacts mildly and selectively towards apoB-100, preserving charged amino acid residues while forming distinct fragments. By the aforementioned-results, the chemical and physical modification of apoB-100 by both HOCl and HOSCN form the basis for investigation into the effect these modified LDL species have on cell function and LDL- and scavenger receptor binding. In the next Chapter, the effect of LDL modification by HOSCN and HOCl on endothelial cell processing and inflammatory response is investigated.

Chapter 4. Endothelial uptake and response to LDL modified by HOSCN or HOCl

4.1. Introduction

The accumulation of LDL within the intima of the artery wall leads to the formation of plaques; which is a hallmark of atherosclerosis [262]. This atherosclerotic lesion formation caused by retention of LDL-sourced lipids leads to injury of the endothelium, which consequentially promotes chemotaxis and adhesion of neutrophils and monocytes both through the release of chemokines and cytokines into the vasculature and by the expression of leukocyte adhesion molecules on the endothelium [557, 558]. It has been shown that human atherosclerotic plaques elevated expression of adhesion molecules VCAM-1, ICAM-1 and E-selectin, over lipid-enriched regions of the lesion [557]. As part of the immune response, infiltrating neutrophils release MPO at the site of the atherosclerotic lesion [21], the actions of which can oxidatively modify LDL accumulated in the arterial intima. Indeed, the presence of oxidised LDL in human atherosclerotic lesions has been demonstrated [559] and importantly, HOCl-modified LDL is present at these sites of injury [281, 284, 502]. Additionally, Cu^{2+}-oxidised LDL has been shown to activate NF-κB signalling in endothelial cells [311] to induce neutrophil and monocyte/macrophage adhesion to the endothelium [307, 436, 560]; which is mediated by the expression of ICAM-1, VCAM-1 and E-selectin [307, 433-435]. There is, however, a lack of data on whether LDL modified by MPO-derived oxidants induces adhesion molecule expression on endothelial cells.

Upon invocation of endothelial dysfunction, cells within the vasculature, including endothelial cells, release inflammatory cytokines to facilitate further migration of circulating monocytes/macrophages. One of the most important regulators of this chemotactic process is monocyte chemotactic protein-1 (MCP-1), which is upregulated by endothelial cells to attract monocytes to injury sites and activate them into macrophage differentiation which occur in a MCP-1 concentration-dependent manner [561]. Additionally, it has been shown that the release

of MCP-1 is induced upon exposure of endothelial cells to minimally-modified and Cu^{2+}-oxidised LDL, promoting chemotaxis and adhesion of circulating monocytes [560, 562], independent of leukocyte adhesion molecule expression [560]. Furthermore, interleukin-6 (IL-6) can also be released by endothelial cells, switching the immune response from the early phase of primarily neutrophil adhesion and infiltration to recruitment and subsequent activation of monocytes at inflamed sites [563]. Notably, IL-6 binding to soluble IL-6 receptor (sIL-6R) has also been shown to synergistically promote MCP-1 secretion from endothelial cells pre-treated with oxidised LDL [564]. Given the involvement of MPO and LDL in the progression of atherosclerotic lesions [21, 281], the effect of LDL modified by the MPO oxidants HOSCN and HOCl, on endothelial cell-leukocyte adhesion and cytokine secretion was investigated.

Endothelial dysfunction, in turn, activates a range of response pathways designed to limit cellular damage and restore homeostasis. For example, endoplasmic reticulum (ER) stress initiates the unfolded protein response (UPR) which has previously been shown to be activated in human arterial endothelial cells incubated with Cu^{2+}-oxidised LDL [463-465, 565]. Upon exposure to Cu^{2+}-oxidised LDL, the protein chaperone GRP78 is induced via XBP1 splicing mediated through IRE1 branch activation [464], while an associated oxidised phospholipid, oxPAPC activated both PERK and ATF6 branches of the UPR [566]. Over longer incubation times, the activation of both the IRE1 and PERK branches progressed endothelial cells towards apoptosis in response to Cu^{2+}-oxidised LDL [463, 464, 565]. Activation of the UPR can also lead to the promotion of antioxidant response element (ARE) pathways mediated by nuclear factor (erythroid-derived 2) like-2 (Nrf2) [567, 568]. Upon activation, Nrf2 is cleaved from keap1 and translocates to the nucleus to promote the gene expression of antioxidant response genes, such as haem oxygenase-1 (HO-1) and glutamate-cysteine ligase (Gcl) [569-571]. HO-1 is an inducible haem enzyme that degrades haemoglobin to biliverdin with the release of carbon monoxide (CO) and ferrous iron (Fe^{2+}) [572]. HO-1 activity can be closely coupled

with eNOS activity to preserve eNOS in the coupled state [573], while the CO released by HO-1 is regarded to have anti-atherogenic properties analogous to NO [574, 575]. Furthermore, Gcl ligates Glu and Cys to form L-γ-Glu-L-Cys in the first and rate-limiting step, followed by GSH synthetase (GS) activation, resulting in the synthesis of GSH; a constitutively active cellular antioxidant involved in signalling and redox homeostasis [576]. Together, the components of the ARE pathway work to protect the cell from oxidative injury and preserve endothelial function.

4.2. Aims

The aim of the studies in this Chapter was to assess the degree of cellular uptake of HOSCN- and HOCl-modified LDL associated lipids and the impact of HOSCN- and HOCl-modified LDL upon inflammatory and stress-related signalling pathways, including the UPR and Nrf2, and the alteration of leukocyte adhesion molecule, IL-6 and MCP-1 expression.

4.3. Results

4.3.1. Cell viability and metabolic activity of HCAEC

The extent of endothelial cell viability was initially determined following exposure of HCAEC to modified LDL (1.0 mg.mL^{-1} LDL treated with 0 µM oxidant, or either 250 µM HOSCN or HOCl for 24 h). HCAEC were exposed to 0.1 mg.mL^{-1} of each modified LDL species for both 24 h and 48 h in serum free-defined media with 5 % v/v FBS, before using the lactate dehydrogenase (LDH) assay for cell viability, or the 3-(4,5-dimethylthiazol-2-yl)-2,5-diphenyltetrazolium bromide (MTT) assay for cell metabolic activity (as described in Section 2.7). The LDH assay was used to measure the activity of LDH released into the media compared to the LDH remaining in the cell lysate as an indicator of the proportion of viable (intact) cells [489]. These results were compared to data from the MTT assay, which involves

measuring the conversion of the yellow, soluble MTT substrate to the purple, water-insoluble formazan product by the mitochondria of living cells, which is used as a measure of cellular metabolic activity [577].

No loss in viability was seen when HCAEC were incubated with or without each oxidised LDL species (Figure 4.1A). Similar to the results demonstrated in the LDH assay, there was no significant change in relative formazan production between oxidised LDL treatments after 24 h incubation (Figure 4.1B). At 48 h, whilst there was no change in HCAEC viability between the treatment group, there was a marked increase in formazan production with LDL (both control and oxidised) treatment, although this did not reach statistical significance. Thus, treatment of HCAEC with 0.1 $mg{\cdot}mL^{-1}$ of incubation control LDL, HOSCN- or HOCl-modified LDL species was not cytotoxic to HCAEC, but had a slight stimulatory metabolic effect on the cells.

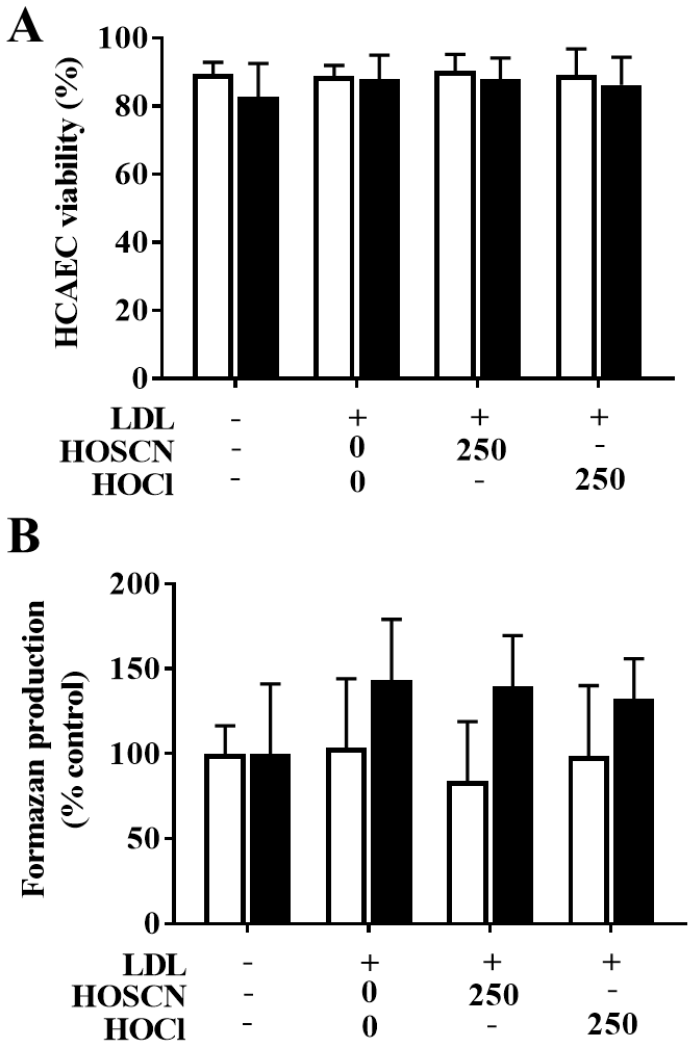

Figure 4.1. Cell viability and activity of HCAEC after incubation with oxidised LDL for 24 h and 48 h. *Firstly, 1.0 mg·mL^{-1} control LDL or LDL incubated with 250 µM HOSCN or 250 µM HOCl were incubated at 37 °C for 24 h. Subsequently, HCAEC were treated with 0.1 mg·mL^{-1} of LDL or (250 µM HOSCN or HOCl) oxidised LDL species at 37 °C for 24 h (white bar) or 48 h (black bar) in treatment medium. (A) Cell viability was measured by the LDH activity assay. (B) Cell activity was measured by the production of formazan (MTT assay). Three independent HCAEC and LDL donors were used. Bars represent the mean ± SD (n = 3). Two-way ANOVA with Dunnett's multiple comparison test between treatment groups and Sidak multiple comparison test between time points. No significant difference between treatments or time points were found.*

4.3.2. Cell Migration

Atherosclerotic injury is known to cause endothelial denudation at the site of the injured vessel and when this occurs, nearby endothelial cells will migrate to the denuded area in an attempt to close the wound [578]. To simulate a wound in the endothelium to assess the effect of MPO oxidant-modified LDL on endothelial cell migration, a scratch was made across a cultured HCAEC monolayer, as described in Section 2.8. The width of the scratch, as an indicator of cell migration, was measured at intervals between 0 and 24 h oxidised LDL treatment or until the scratch closed, for cells in medium alone or incubated with 0.1 $mg{\cdot}mL^{-1}$ of each LDL treatment. The scratch width was measured at four different sites around the scratch intersection indicated by the white arrows in Figure 4.2A. Generally, re-establishment of the endothelial cell monolayer occurred after approximately 18 h across all treatments. Additionally, the average migration rate of the HCAEC was calculated as approximately 2.5 $\mu m{\cdot}h^{-1}$ and likewise did not significantly differ across treatment groups (Figure 4.2B).

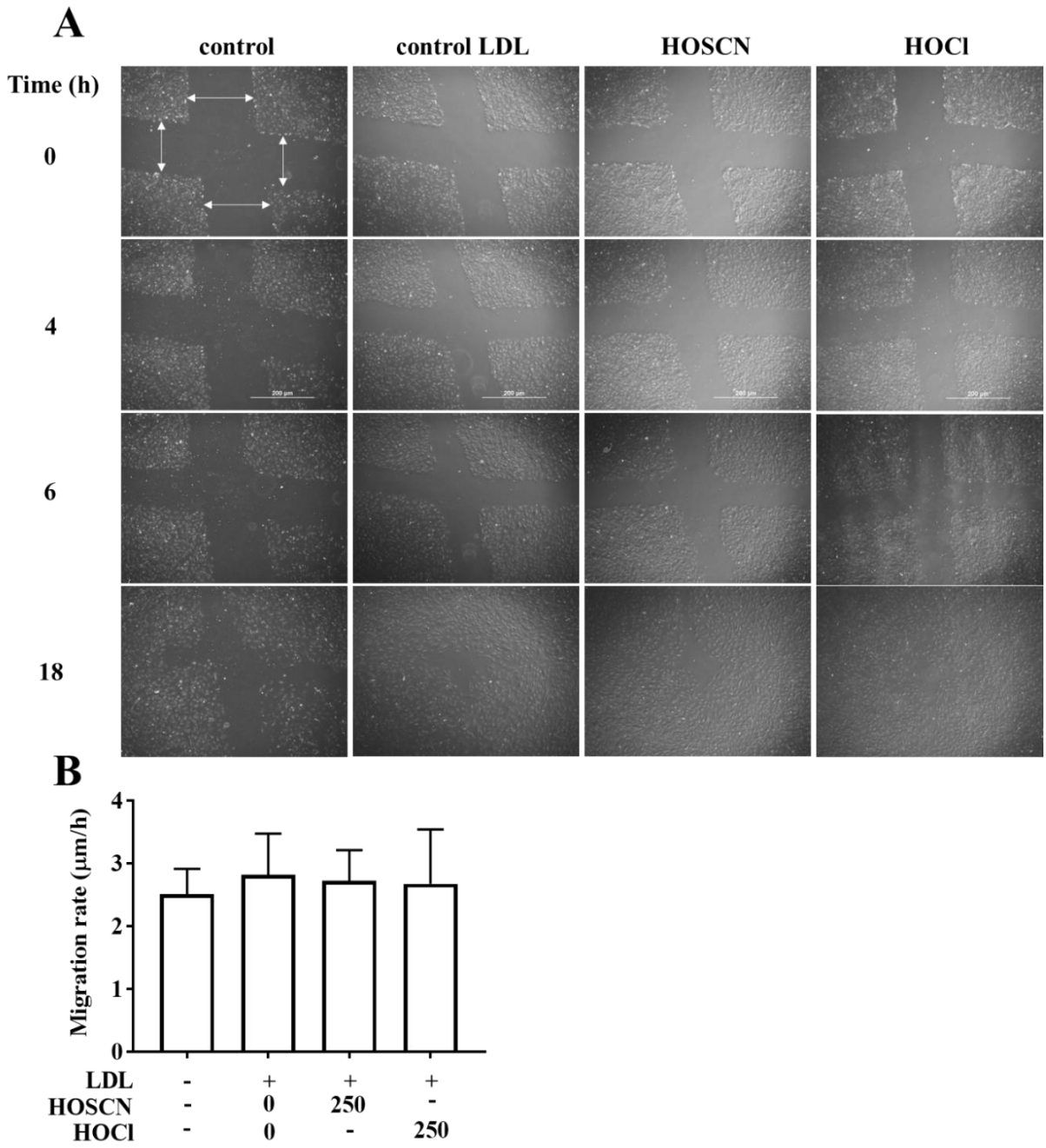

Figure 4.2. Cellular migration rate of HCAEC during incubation with oxidised LDL for 24 h. *Firstly, 1.0 mg·mL^{-1} control LDL or LDL incubated with 250 µM HOSCN or 250 µM HOCl were incubated at 37 °C for 24 h. HCAEC were treated with 0.1 mg·mL^{-1} of LDL or oxidised LDL species at 37 °C for up to 24 h in treatment medium. (A) Scratch width was measured at intervals from 0 h up to 24 h of treatment to calculate the (B) migration rate. Arrows indicate where scratch width was measured in quadruplicate for each sample. Scale bar represent 200 µm. Two independent HCAEC and LDL donors were used. Bars represent the mean ± SD (n = 3). One-way ANOVA with Dunnett's multiple comparison test. No significant difference between treatments or time points was found.*

4.3.3. LDL uptake by HCAEC

Given the aforementioned increases in HCAEC metabolic activity with either control LDL or MPO oxidant-modified LDL treatments, the next experiment assessed the uptake of LDL-sourced lipids by HCAEC. Initial experiments were performed to measure changes in cholesterol and cholesteryl esters following exposure of LDL modified by HOSCN, HOCl or $CuSO_4$, which is reported to be taken up by endothelial cells [579, 580]. After treatment, the LDL associated lipids and cholesterol were extracted and analysed following HPLC separation as described (Section 2.9). As indicated in the HPLC trace of LDL-sourced lipids (Figure 4.3) it was determined that there was no significant loss of cholesterol or cholesteryl esters after incubation with 100 µM or 250 µM HOSCN or HOCl for 24 h at 37 °C. In contrast, LDL incubated with 5 µM $CuSO_4$ for 24 h at 37 °C resulted in a near total depletion of the cholesteryl linoleate, docosahexanoate and arachidonate esters in LDL (Figure 4.3; grey line). This is consistent with previous reports showing extensive lipid modifications and oxidation on exposure to $CuSO_4$ [266, 375].

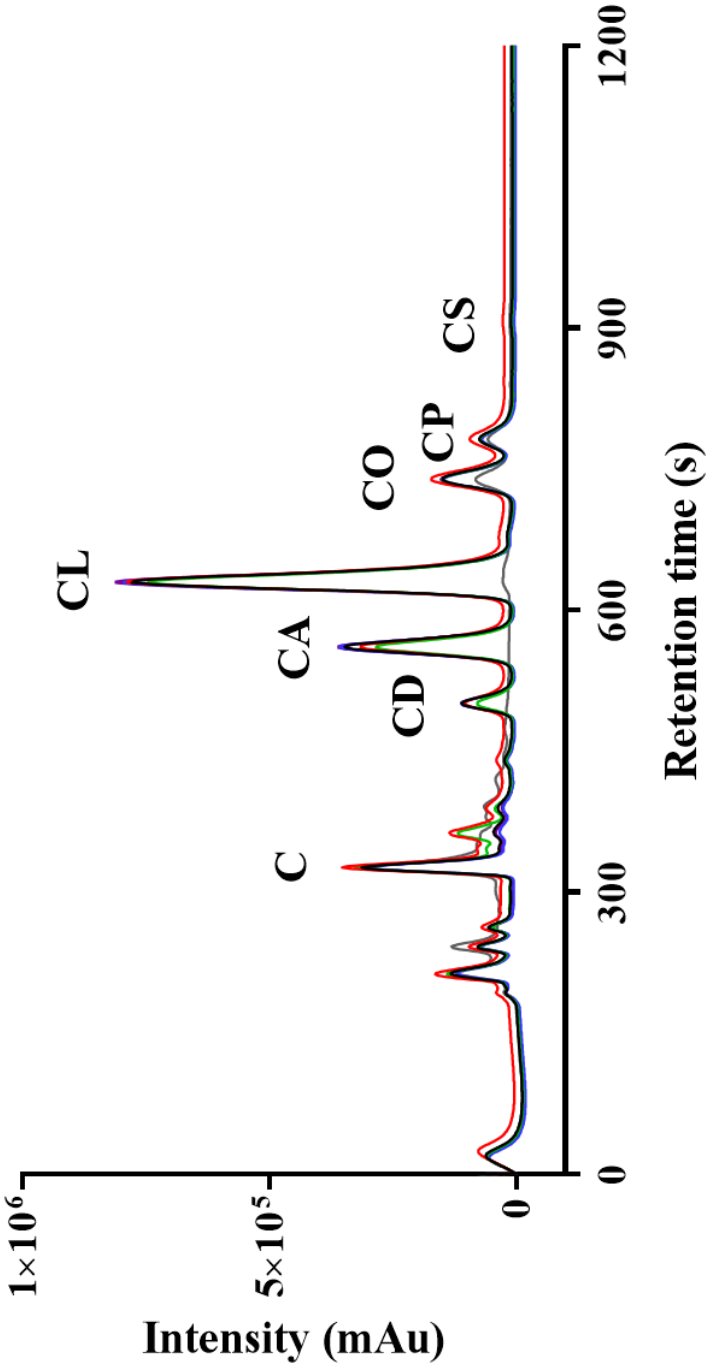

Figure 4.3. Representative HPLC trace of cholesterol and cholesteryl ester separation from 10 µg LDL. *1.0 mg·mL^{-1} control LDL (black) or LDL modified by 100 µM HOSCN (red), 250 µM HOSCN (green), 100 µM HOCl (blue), 250 µM HOCl (purple) or 5 µM $CuSO_4$ (grey) for 24 h at 37 °C. The labels for each peak are (C) Cholesterol; (CD) Cholesteryl docosahexanoate; (CA) Cholesteryl arachidonate; (CL) Cholesteryl linoleate; (CO) Cholesteryl oleate; (CP) Cholesteryl palmitate; (CS) Cholesteryl stearate. Data are representative of three independent experiments.*

Having demonstrated that LDL modified by MPO oxidants HOSCN or HOCl does not significantly lead to a loss of native cholesterol or cholesteryl esters, the next experiments similarly measured the content of cholesterol and cholesteryl esters in HCAEC following exposure to each type of modified LDL. Cholesterol and cholesteryl ester uptake by HCAEC was measured following the incubation of cells with medium alone or either control LDL, HOSCN- or HOCl-modified LDL for 24 h and 48 h (Figure 4.4A). Whether in the presence or absence of LDL or each MPO oxidant-modified LDL, there was an increase in total cholesterol content within HCAEC between 24 and 48 h. In the control LDL-treated group, this increase was found to be statistically significant (shown by #) and was paralleled with a reproducible, but non-significant increase in the proportion of intracellular cholesteryl esters (Figure 4.4B). No significant changes were observed between treatments within each time point. When the time-dependent accumulation of the total cholesterol was expressed as the difference between 24 and 48 h measurements, there was a significant accumulation of total cholesterol with all LDL treatments compared to the control (Table 4.1). LDL cholesterol and cholesteryl ester uptake was also measured in HCAEC exposed to Cu^{2+}-oxidised LDL, however the near-complete depletion of native cholesteryl esters following exposure to Cu^{2+} (Figure 4.3) made this HPLC method inappropriate to measure uptake of Cu^{2+}-oxidised LDL. Overall, prolonged *in vitro* exposure of HCAEC to each LDL treatment resulted in an accumulation of cholesterol, however this was independent of LDL modification by MPO.

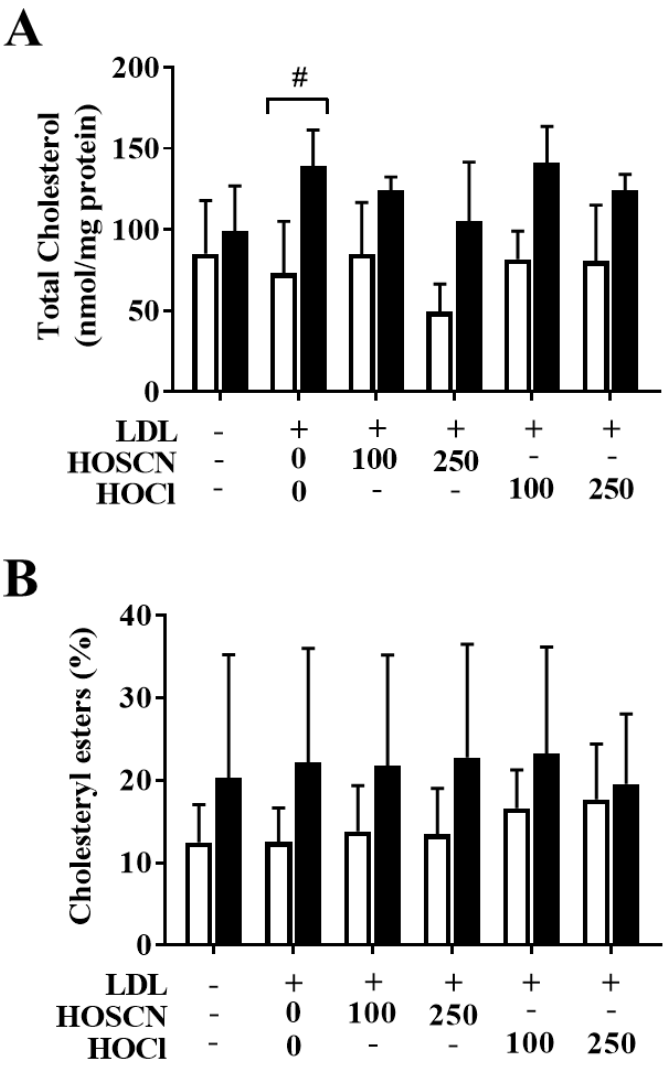

Figure 4.4. Total cholesterol and cholesteryl ester levels of HCAEC after incubation with oxidised LDL. *Firstly, 1.0 mg•mL^{-1} control LDL or LDL incubated with 100 or 250 µM HOSCN, or 100 or 250 µM HOCl were incubated at 37 °C for 24 h. HCAEC were treated with 0.1 mg•mL^{-1} of LDL or oxidised LDL species at 37 °C for 24 h (white bar) or 48 h (black bar) in treatment media. Cholesterol and cholesteryl esters were normalised to cellular protein concentration as assessed by the BCA assay. Total cholesterol represents the sum of the free cholesterol and the cholesteryl esters detected by HPLC in the HCAEC lysate samples (A). Cholesteryl esters are represented as a percentage of the total cholesterol measured in HCAEC lysates (B). Three independent HCAEC and LDL donors were used. Bars represent the mean ± SD (n = 3). Two-way ANOVA with Dunnett's multiple comparison test between treatment groups and Sidak multiple comparison test between time points. # represent p < 0.05 between 24 and 48 h time point.*

Table 4.1. Difference in total cellular cholesterol in HCAEC between 24 h and 48 h incubation with MPO oxidant-modified LDL. *The change in intracellular lipids was calculated between 24 h and 48 h incubation times (ΔIntracellular lipid) from the data in Figure 4.4A to compare the change in intracellular lipids due to LDL uptake, independent of lipids already present in the cells. One-way ANOVA with Holm-Sidak multiple comparison test. * and ** represent p < 0.05 and 0.01 respectively compared to the control.*

LDL treatment	ΔIntracellular lipid (mean ± SD)	Significance
Control	14.1 ± 4.7	
Control LDL	66.0 ± 19.7	**
100 μM HOSCN-LDL	39.3 ± 8.7	*
250 μM HOSCN-LDL	55.9 ± 19.3	**
100 μM HOCl-LDL	59.2 ± 11.1	**
250 μM HOCl-LDL	43.7 ± 11.1	*

4.3.3.1. Scavenger receptor expression in HCAEC

The removal of modified proteins, including oxidised LDL, from the circulation is mediated by scavenger receptors expressed on cells of the vasculature [421]. There are several different scavenger receptors that are present on endothelial cells that have been reported to bind to modified LDL for removal from the circulation and transcytosis to the intima [535]. As there was no apparent increased uptake of cholesterol and cholesteryl esters by HCAEC after incubation with each modified LDL species compared to the control, the expression of various endothelial scavenger receptors was assessed.

HCAEC were incubated with each MPO-oxidant modified LDL or Cu^{2+}-modified LDL (0.1 $mg{\cdot}mL^{-1}$ apoB-100) for 3 or 24 h, at which time the relative mRNA expressions of LDL

receptor (LDLR) and scavenger receptors were measured by qPCR relative to the expression of constitutive genes 18S ribosomal subunit and β_2-microglobulin (β2M) for normalisation. Compared to non-treated HCAEC, expression of LDLR was decreased following exposure to each MPO oxidant-modified LDL for 24 h (Figure 4.5). Scavenger receptor class A 1 (SR-A1), SR class B 2 (SR-B2, also known as CD36) and scavenger receptor for endothelial cell 1 (SREC-1) were unchanged across LDL treatments at both the 3 and 24 h time points analysed (Figure 5.5). In contrast, the expression of the scavenger receptors SR-B1 and LOX-1 were decreased following exposure to MPO oxidant-modified LDL (Figure 4.6). Compared to control, SR-B1 was significantly decreased after 24 h incubation with 250 µM HOCl-modified LDL whilst the mRNA expression of the LDL receptor (LDLR) was decreased in all HCAEC exposed to either control LDL or MPO oxidant-modified, reaching statistical significance across all MPO oxidant-modified LDL treatments. Similarly, LOX-1 expression was also decreased following MPO oxidant-modified LDL exposure but this did not reach statistical significance. In contrast, there was no significant changes in LDLR expression in HCAEC treated with Cu^{2+}-modified LDL treatment. However, the expression of LOX-1 with Cu^{2+}-modified LDL was significantly increased following 3 h incubation time, but decreased to basal levels following increased treatment time (24 h).

After having demonstrated that each MPO oxidant-modified LDL can reduce the expression of scavenger receptors SR-B1 and LDLR after 24 h incubation with HCAEC, we next assessed the protein expression after 24 h incubation with control LDL, (250 µM oxidant) HOSCN- or HOCl-modified LDL by Western blot (Figure 4.7). However, no changes in SR-B1 and LDLR protein expression were observed relative to the β-actin loading control. Similarly, no changes in SR-B2 protein expression was observed. The expression of LOX-1 was also probed, but no LOX-1 protein expression in HCAEC was detected by the Western blot techniques employed in this study (data not shown).

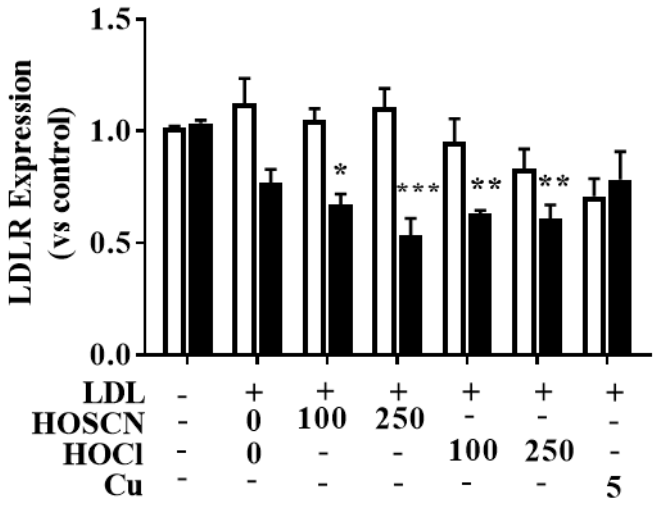

Figure 4.5. HCAEC LDLR mRNA expression measured by qPCR after incubation with LDL modified by HOSCN, HOCl or $CuSO_4$. *Firstly, 1.0 mg·mL^{-1} control LDL or LDL modified by 100 or 250 µM HOSCN, 100 or 250 µM HOCl, or 5 µM $CuSO_4$ at 37 °C for 24 h. HCAEC were treated with 0.1 mg·mL^{-1} of LDL or oxidised LDL species at 37 °C for 3 h (white bar) or 24 h (black bar) in treatment medium. LDLR mRNA expression was normalised to 18S and β2M as housekeeping genes. Two independent HCAEC and three independent LDL donors were used. Bars represent the mean ± SD (n = 3). Two-way ANOVA with Dunnett's multiple comparison test between treatment groups and Sidak multiple comparison test between time points. *, ** and *** represent p < 0.05, 0.01 and 0.001 respectively compared to their respective control.*

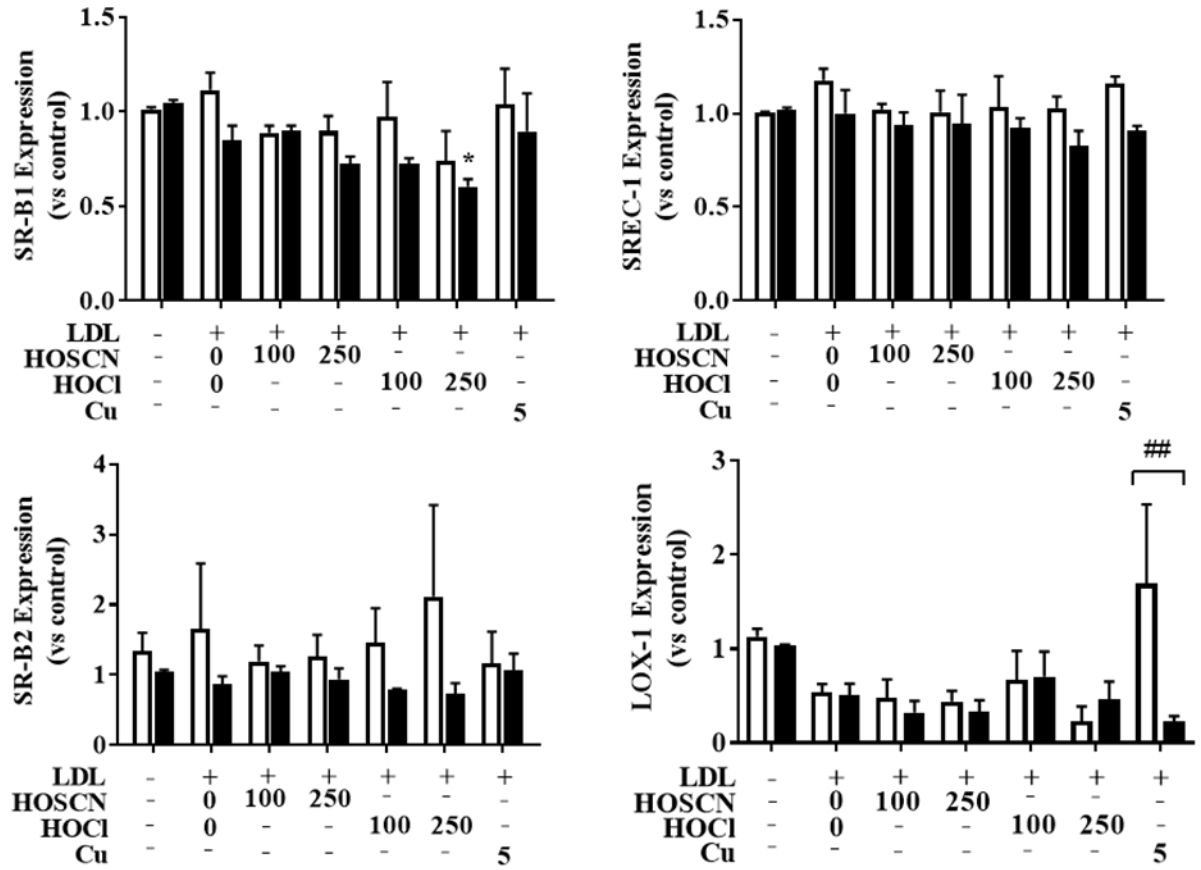

Figure 4.6. HCAEC scavenger receptor mRNA expression measured by qPCR after incubation with LDL modified by HOSCN, HOCl or $CuSO_4$. *Firstly, 1.0 mg.mL^{-1} control LDL or LDL modified by 100 or 250 µM HOSCN, 100 or 250 µM HOCl, or 5 µM $CuSO_4$ at 37 °C for 24 h. HCAEC were treated with 0.1 mg.mL^{-1} of LDL or oxidised LDL species at 37 °C for 3 h (white bar) or 24 h (black bar) in treatment medium. Scavenger receptor mRNA expression was normalised to 18S and B2M as housekeeping genes. Two independent HCAEC and three independent LDL donors were used. Bars represent the mean ± SD (n = 3). Two-way ANOVA with Dunnett's multiple comparison test between treatment groups and Sidak multiple comparison test between time points. * represent p < 0.05 respectively compared to their respective control. ## represent p < 0.01 respectively between 24 and 48 h time point.*

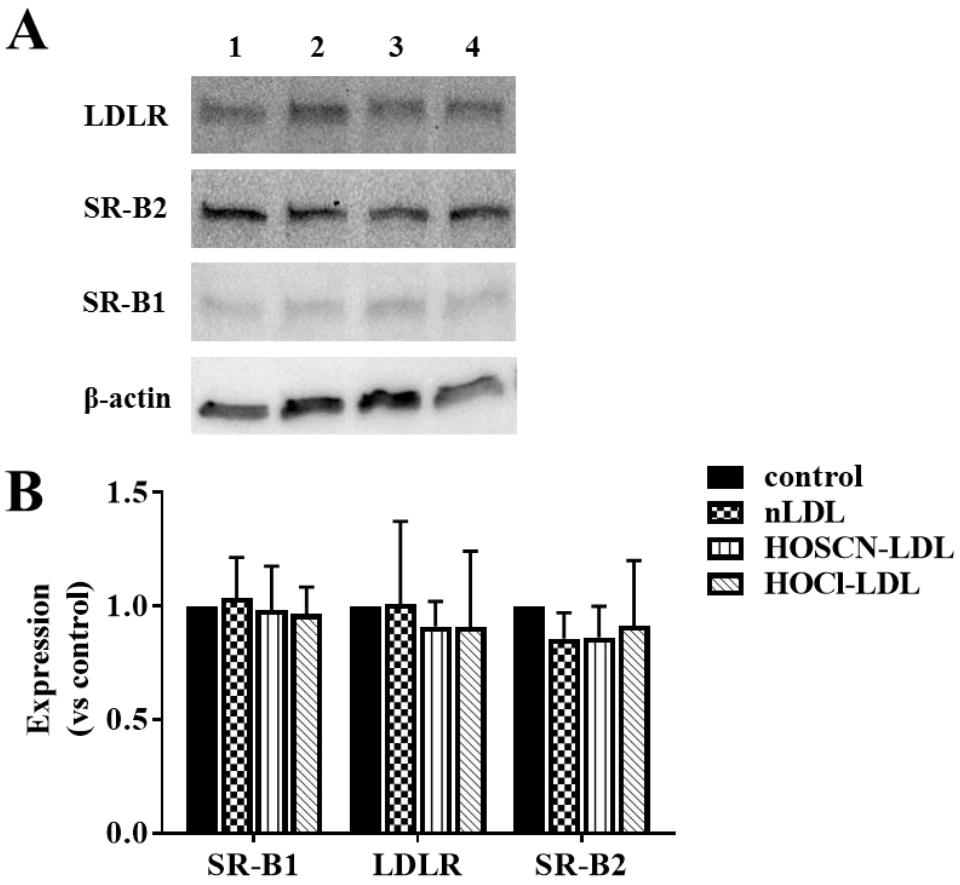

Figure 4.7. HCAEC LDLR and scavenger receptor protein expression of SR-B1 and SR-B2 measured by Western blot after incubation with LDL modified by HOSCN or HOCl. *Firstly, 1.0 mg.mL^{-1} control LDL or LDL incubated with 250 µM HOSCN or 250 µM HOCl were incubated at 37 °C for 24 h. HCAEC were treated with 0.1 mg.mL^{-1} of LDL or oxidised LDL species for 37 °C for 24 h in treatment medium. (A) Representative Western blots of SR-B1, SR-B2, LDLR and β-actin, column 1: control without LDL, column 2: control LDL, column 3: LDL modified by HOSCN, column 4: LDL modified by HOCl. LOX-1 was not detected in any blots when using two independent LOX-1 antibodies. (B) Expression of scavenger receptors measured by densitometry, relative to the control; control (black), control LDL (chequered), HOSCN-LDL (vertical line) and HOCl-LDL (diagonal line). Scavenger receptor protein expression was normalised to β-actin as the housekeeping protein. Three independent HCAEC and LDL donors were used. Bars represent the mean ± SD (n = 3). Two-way ANOVA with Dunnett's multiple comparison test between treatment groups and Sidak multiple comparison test between time points. No statistical difference was found between treatments.*

4.3.3.2. Cys-dependent cathepsin activity

Cathepsins are a family of lysosomal protease enzymes that hydrolyse the peptide bonds of proteins [581]. The Cys-dependent cathepsins (named due to the cathepsin activity depending on the Cys residue in the active site) are heavily implicated in cardiovascular disease with cathepsins capable of degrading LDL, which decreases cholesterol efflux from macrophages and propagates foam cell formation (reviewed [581]). In addition, (MPO- and Cu^{2+}-) oxidised LDL has been reported to alter cathepsin activity in macrophages, which compromises the ability of cells to process LDL [582, 583]. Endothelial cells also contain cathepsin B and L, which are important for neovascularisation [584-586] and, like macrophages, may be involved in the degradation of oxidised LDL in endothelial cells to prevent apoptosis [587], though other physiological consequences of this still remains uncertain.

Given the finding that intracellular cholesterol increased, while scavenger receptor protein expression was unchanged after incubation with LDL modified by HOSCN or HOCl, the activity of Cys-dependent cathepsins B and L to assess lysosomal function after 24 h treatment of the cells was then assessed. Cathepsin L activity was approximately 5.6-fold higher than cathepsin B in HCAEC under control conditions as measured at 24 h (Figure 4.8A). Treatment of cells with 0.1 $mg{\cdot}mL^{-1}$ of control LDL, 250 µM HOSCN-modified LDL or 250 µM HOCl-modified LDL, did not significantly alter cathepsin B or L activity in the HCAEC compared to the untreated control cells (Figure 4.8B).

In summary, there was a time-dependent accumulation of cholesterol in HCAEC exposed to control LDL or MPO oxidant-modified LDL *in vitro* that was concurrent with a reduction in LDLR mRNA, but not protein expression, which was significant for each MPO oxidant-modified LDL. Similarly, HOCl-modified LDL significantly reduced the mRNA expression of

SR-B1, whilst other scavenger receptors and Cys-dependent cathepsin activity remained unaffected by LDL treatment.

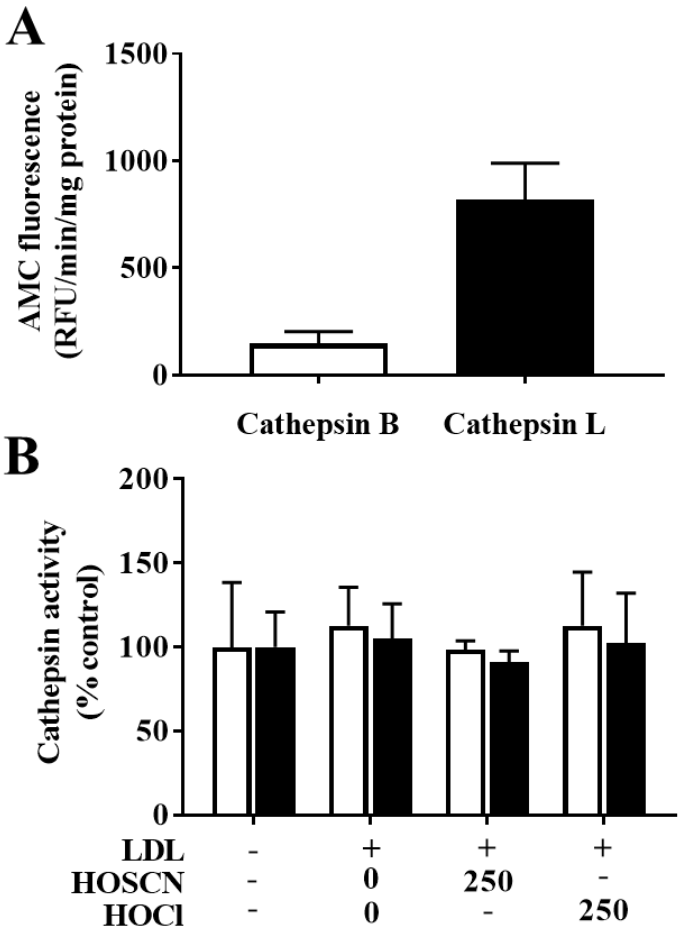

Figure 4.8. Cys-dependent cathepsin (B & L) activity in HCAEC treated with LDL modified by HOSCN or HOCl. *Firstly, 1.0 mg•mL^{-1} control LDL or LDL modified by 250 µM HOSCN or 250 µM HOCl at 37 °C for 24 h. HCAEC were treated with 0.1 mg•mL^{-1} of LDL or oxidised LDL species at 37 °C for 24 h in treatment medium. (A) Comparison of the activity of Cathepsin B and L in control HCAEC measured by the rate of release of the fluorescent AMC compound from the proteolytic degradation of the cathepsin substrates (Z-Arg-Arg-AMC and Z-Phe-Arg-AMC, respectively) measured at 360 and 460 nm. Fluorescence was normalised to cell protein measured by the BCA assay. (B) Cathepsin B (white bars) and cathepsin L (Black bars) activity was measured in the cell lysate similarly to A and normalised to the respective control. Three independent HCAEC and two independent LDL donors were used. Bars represent the mean ± SD (n = 4). One-way ANOVA with Dunnett's multiple comparison test. No statistical difference was found between treatments.*

4.3.3.3. Leukocyte adhesion molecule expression

Given that exposure of HCAEC to LDL was not causing extensive toxicity or altered lipid profiles, the next series of experiments sought to investigate whether MPO oxidant-modified LDL induced an inflammatory or stress response in HCAEC. Given the previous data that showed other types of modified LDL can promote inflammation by altering adhesion molecule expression and cytokine/chemokine release [433, 435, 588-590], initial studies assessed ICAM-1, VCAM-1 and E-selectin expression. As demonstrated in Figure 4.9, following incubation of HCAEC for 3 h or 24 h with 0.1 mg.mL^{-1} control LDL, 100 µM or 250 µM HOSCN- or HOCl-modified LDL, no significant change in ICAM-1, VCAM-1 or E-selectin expression was observed. In comparison, the expression of ICAM-1, VCAM-1 and E-selectin were induced by stimulation with 0.2 mg.mL^{-1} TNF-α within 3 h and maintained at a significantly elevated level over the 24 h incubation. The elevated expression at 3 and 24 h (respectively) compared to the respective controls were as follows; ICAM-1 (9.6- and 4.8-fold), VCAM-1 (15.5- and 3.8-fold) and E-selectin (27- and 4-fold).

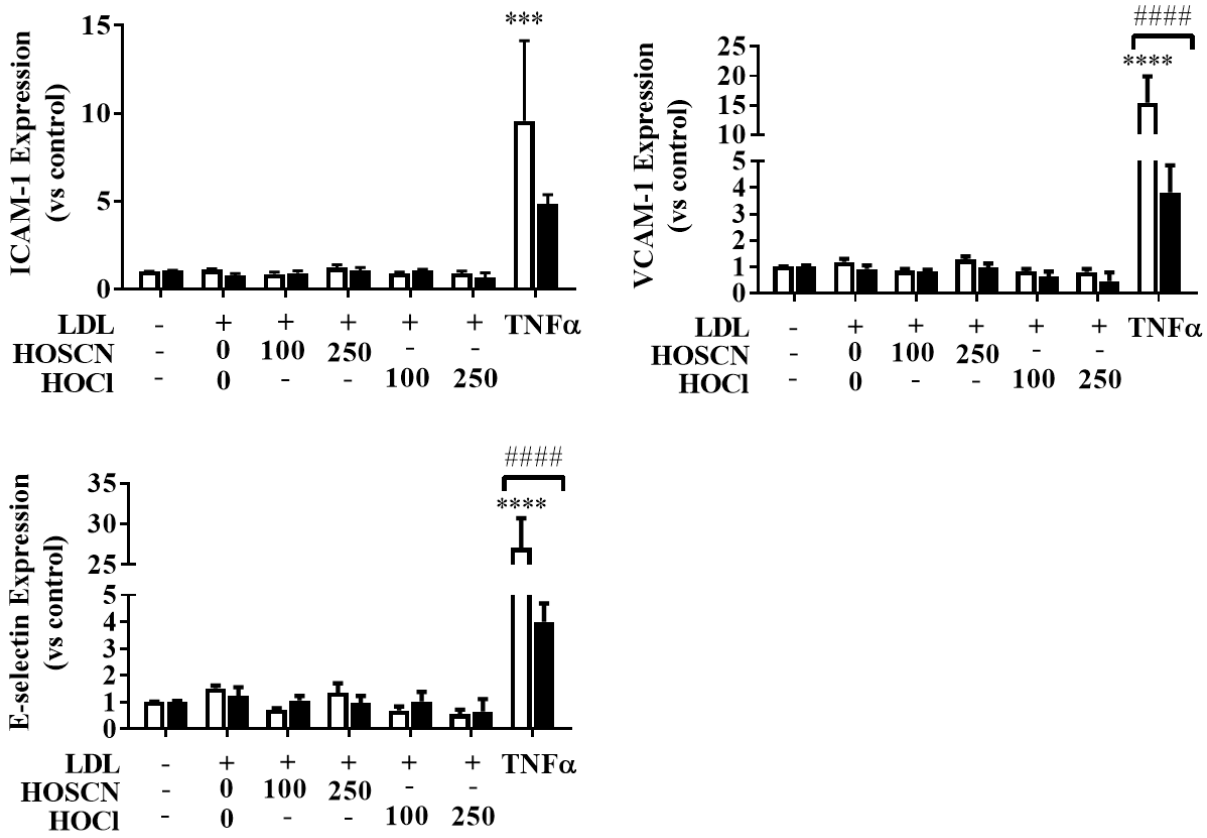

Figure 4.9. HCAEC leukocyte adhesion molecule mRNA expression measured by qPCR after incubation with LDL modified by HOSCN or HOCl. *Firstly, 1.0 mg.mL^{-1} control LDL or LDL modified by 100 or 250 µM HOSCN, 100 or 250 µM HOCl for 24 h at 37 °C. HCAEC were treated with 0.1 mg.mL^{-1} of LDL or oxidised LDL species at 37 °C for 3 h (white bar) or 24 h (black bar) in treatment medium. A 21 h control incubation followed by 3 h treatment with TNF-α (0.2 ng.mL^{-1}) totalling 24 h was used as a positive control for leukocyte adhesion molecule gene expression. Expression was normalised to 18S and β2M as housekeeping genes. Three independent HCAEC and LDL donors were used. Bars represent the mean ± SD (n = 3). Two-way ANOVA with Dunnett's multiple comparison test between treatment groups and Sidak multiple comparison test between time points. *** and **** represent p < 0.001 and 0.0001 respectively compared to their respective control. #### represents p < 0.0001 between 24 and 48 h time point.*

4.3.3.3.a. Neutrophil adhesion to endothelial cells

Functional assessment of HCAEC adhesion molecule expression was next undertaken by a neutrophil adhesion assay. The adhesion of human neutrophils to HCAEC following incubation with 0.1 mg.mL^{-1} control LDL, (250 μM oxidant) HOSCN- or HOCl-modified LDL for 24 h was performed under static conditions *in vitro*. Neutrophils were stained with 1 μM calcein for visualisation during microscopy and to quantify the adhesion of neutrophils through the measurement of the calcein fluorescence emission.

As shown in Figure 4.10A, neutrophils are clearly distinguishable from HCAEC due to the calcein fluorescence. The neutrophils adherent to HCAEC after treatment was quantified by the fluorescence measured before and after five washes with PBS to remove non-adherent cells. The population of adherent neutrophils (%) was calculated as the ratio of the fluorescence after five washes compared to before washing. In confirmation of the HCAEC adhesion molecule mRNA data above, there was no significant change in the population of neutrophils adherent to HCAEC following treatment with each type of modified LDL. This was calculated to be between 10.6 % (control) and 13 % (HOCl-modified LDL; Figure 4.10B), indicating that under the conditions employed in this study, MPO-modified LDL is not an independent inducer of endothelial cell-dependent leukocyte adhesion.

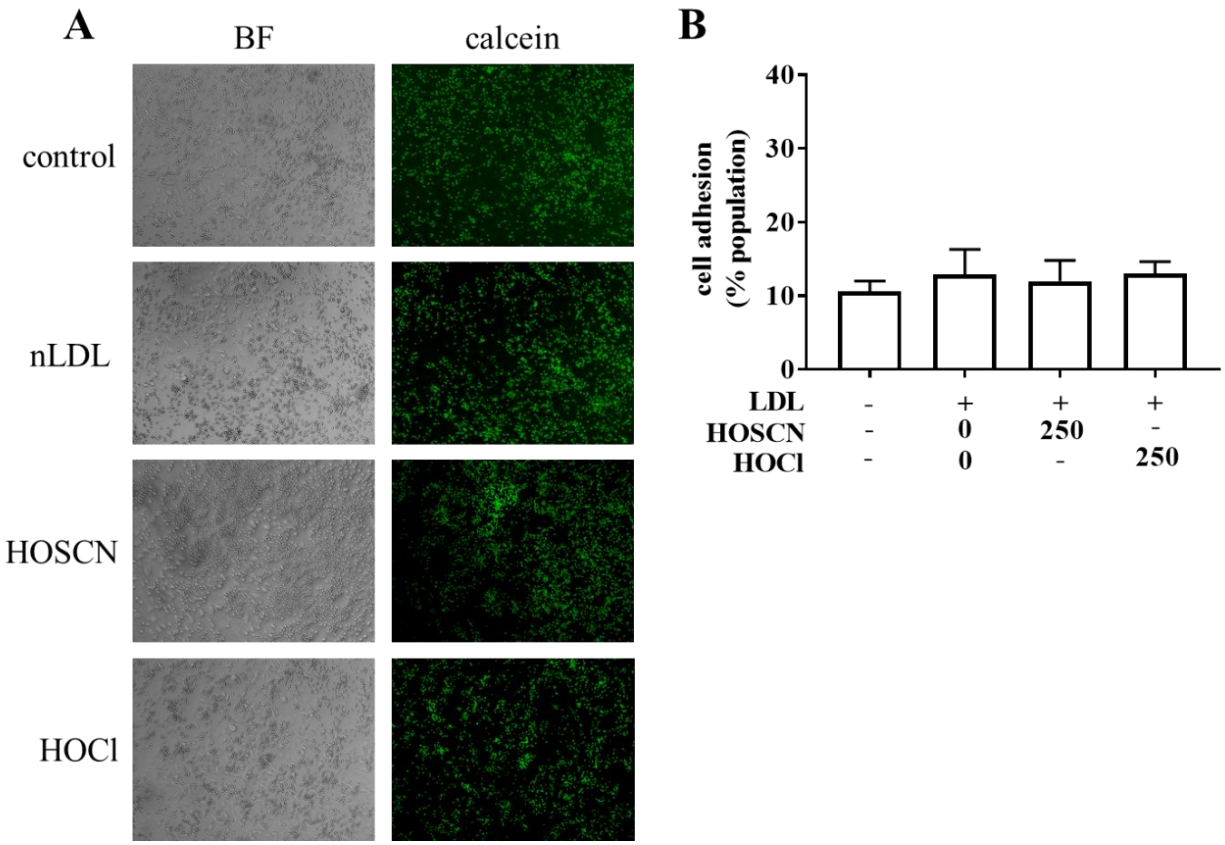

Figure 4.10. Neutrophil adhesion to HCAEC after incubation of HCAEC with LDL modified by HOSCN or HOCl. *Firstly, 1.0 mg.mL^{-1} control LDL or LDL modified by 250 µM HOSCN or 250 µM HOCl at 37 °C for 24 h. HCAEC were treated with 0.1 mg.mL^{-1} of LDL or oxidised LDL species at 37 °C for 24 h in treatment medium. Neutrophils were stained with 1 µM calcein for fluorescence measurement at 492 and 515 nm for live neutrophil adhesion to HCAEC. HCAEC and neutrophils were incubated together for 30 min prior to removal of non-adherent neutrophils with repeated rinsing. (A) Representative brightfield (left) and fluorescence (calcein: right) microscopic images of neutrophils adherent to HCAEC after washing. (B) Percentage adhesion of neutrophils after 24 h LDL treatment to HCAEC and 20 min incubation of neutrophils to HCAEC. Two independent HCAEC and LDL donors were used. Bars represent the mean ± SD (n = 3). One-way ANOVA with Dunnett's multiple comparison test. No statistical difference was found between treatments.*

4.3.3.4. IL-6 and MCP-1 expression and secretion

Although neutrophil adhesion to HCAEC was not enhanced by incubation with MPO oxidant-modified LDL, IL-6 released by endothelial cells can lead to switching of neutrophil infiltration to the recruitment of monocytes [563] and concurrent secretion of MCP-1 to attract monocytes to the site of inflammation [561]. The next set of experiments investigated whether expression of chemotactic cytokines MCP-1 and IL-6 was upregulated in HCAEC.

In Figure 4.11A and B, respectively, expression of both IL-6 and MCP-1 was significantly upregulated by exposure of HCAEC to 0.2 ng**.**mL^{-1} TNF-α, which was used as a positive control. However, after incubation with LDL modified by either (100 μM or 250 μM oxidant) HOSCN or HOCl for 3 or 24 h, no significant change in IL-6 (Figure 4.11A) or MCP-1 (Figure 4.11B) mRNA expression was observed compared to the control.

Similarly, incubation of HCAEC with 0.1 mg**.**mL^{-1} control LDL or LDL modified by (250 μM oxidant) HOSCN or HOCl for 24 h did not result in alteration of the levels of IL-6 (Figure 4.12A) and MCP-1 (Figure 4.12B) secreted from HCAEC following 24 h incubation compared to the respective controls. In summary, these data implicate a lack of monocyte recruitment response by endothelial cells exposed to each MPO oxidant-modified LDL.

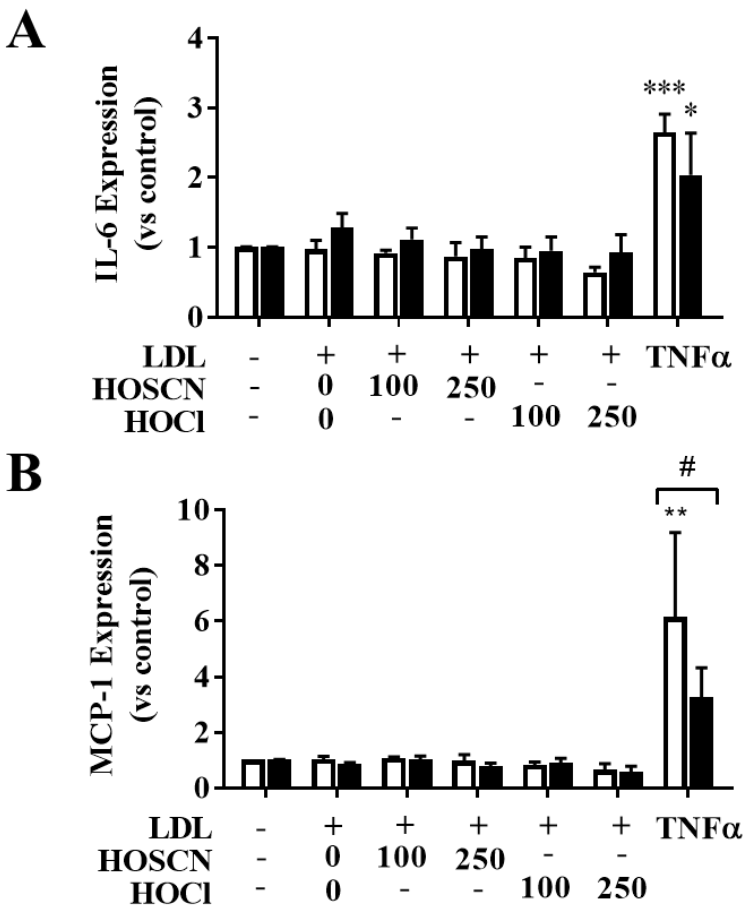

Figure 4.11. HCAEC mRNA expression of cytokines IL-6 and MCP-1 measured by qPCR after incubation with LDL modified by HOSCN or HOCl. *Firstly, 1.0 mg•mL^{-1} control LDL or LDL modified by 100 or 250 µM HOSCN, 100 or 250 µM HOCl at 37 °C for 24 h. HCAEC were treated with 0.1 mg•mL^{-1} of control LDL or oxidised LDL species at 37 °C for 3 h (white bar) or 24 h (black bar) in treatment medium. A 21 h control incubation followed by 3 h treatment with TNF-α (0.2 ng•mL^{-1}) totalling 24 h was used as a positive control for IL-6 (A) and MCP-1 (B) gene expression. Expression was normalised to 18S and β2M as housekeeping genes. Three independent HCAEC and LDL donors were used. Bars represent the mean ± SD (n = 3). Two-way ANOVA with Dunnett's multiple comparison test between treatment groups and Sidak multiple comparison test between time points. * and *** represent p < 0.05 and 0.001 respectively compared to their respective control. No statistical difference was found between time points.*

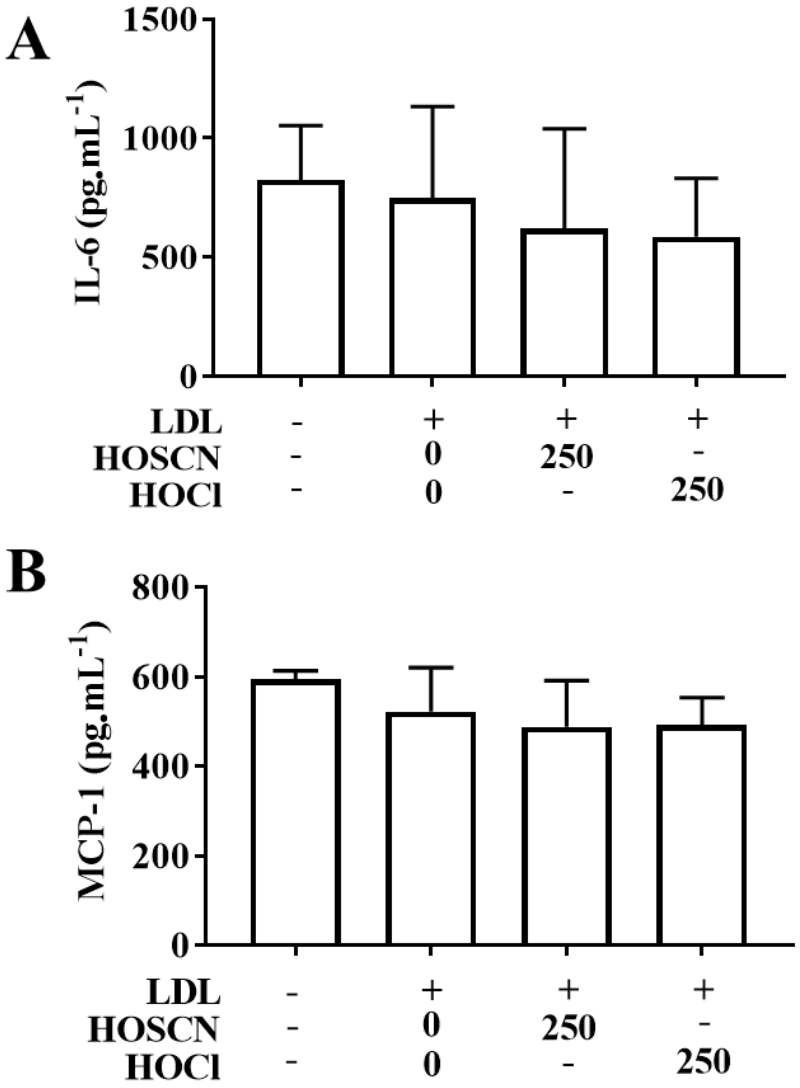

Figure 4.12. HCAEC protein expression of cytokines IL-6 and MCP-1 measured by ELISA after incubation with LDL modified by HOSCN or HOCl. *Firstly, 1.0 mg.mL^{-1} control LDL or LDL modified by 250 µM HOSCN or 250 µM HOCl at 37 °C for 24 h. HCAEC were treated with 0.1 mg.mL^{-1} of LDL or oxidised LDL species at 37 °C for 24 h in treatment medium. The treatment media from untreated and treated HCAEC was collected after 24 h to measure IL-6 (A) and MCP-1 (B) released from HCAEC. Three independent HCAEC and LDL donors were used. Bars represent the mean ± SD (n = 3). One-way ANOVA with Dunnett's multiple comparison test. No statistical difference was found between treatments.*

4.3.4. Stress response pathways in HCAEC

4.3.4.1. Unfolded protein response

ER stress is a key response of vascular cells to oxidised LDL in the development of atherosclerotic lesions (reviewed [591]). ER stress triggers that activation of the UPR, which is an integrated signalling pathway designed to restore cellular homeostasis or failing that, trigger cell death by apoptosis, which involved activation of the effector protein CHOP [458]. The UPR consist of three separate pathways termed PERK, IRE1 and ATF6 (as described in Chapter 1, see Figure 1.14), which are activated following dissociation of the chaperone GRP78 from the ER membrane [592]. Thus, in situations of ER stress, the mRNA expression of UPR genes, activating transcription factor-4 (ATF4), 78 kDa glucose-regulating protein (GRP78), spliced X-box binding protein-1 (sXBP1) and CHOP are induced leading to synthesis of the respective proteins [457]. Tunicamycin (TM) was used as a positive control, as it is promotor of UPR by blocking the N-linked glycosylation of proteins [593], leading to the accumulation of unglycosylated proteins and subsequent induction of ER stress and the UPR. The expression of ATF4, GRP78, sXBP1and CHOP mRNA was significantly upregulated when cells were stimulated with 5 $\mu g.mL^{-1}$ TM (Figure 4.13). The elevated expression at 3 and 24 h (respectively) compared to the respective controls were as follows; CHOP (69- and 6.6-fold), ATF4 (2.7- and 1.9-fold), GRP78 (7.4- and 3.7-fold) and sXBP1 (4- and 1.2-fold).

The mRNA expression of activating transcription factor-6 (ATF6) was not upregulated with TM treatment. However, ATF6 is constitutively expressed and inactive until accumulation of misfolded proteins results in the proteolytic cleavage of ATF6 and translocation to the nucleus [594]. Thus, ATF6 activity in the activation of the UPR may not be dependent on the induction of gene expression. The expression of ATF4, GRP78, sXBP1 and CHOP induced by TM decreased significantly between 3 and 24 h treatment, indicating the induced gene expression

of UPR by TM is a relatively fast and acute response in this case. This has also been demonstrated in other studies with human endothelial cells exposed to (5 – 10 μg**.**mL^{-1}) TM for 4 – 6 h, which upregulated ATF4, CHOP, GRP78 and splicing of XBP1 [465, 592, 595]. However, the aforementioned studies did not extend the TM exposure to 24 h to compare to the results of this Chapter. Having shown that HCAEC have the capacity to invoke the UPR, these studies were extended by exposing HCAEC with LDL modified by either HOSCN or HOCl under conditions described above. However, in each case no significant changes in the above mentioned UPR genes were apparent after 3 or 24 h incubation of the HCAEC with each oxidised LDL. This suggests that HCAEC exposed to oxidised LDL, under these experimental conditions at least, does not invoke these cellular responses.

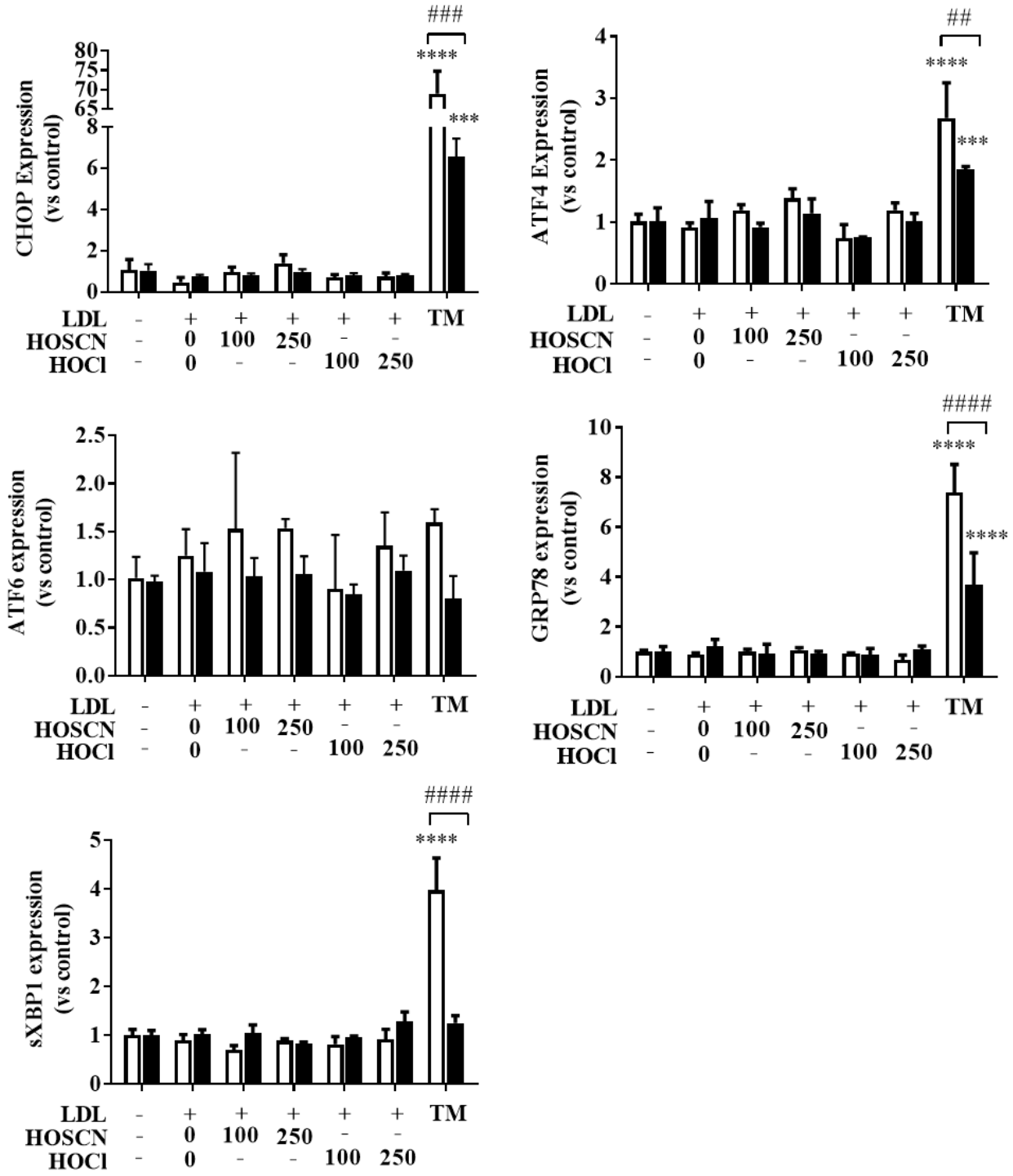

(Figure description continued next page)

Figure 4.13. HCAEC mRNA expression of unfolded protein response (UPR) genes measured by qPCR after incubation with LDL modified by HOSCN or HOCl. *Firstly, 1.0 mg•mL^{-1} control LDL or LDL modified by 100 or 250 µM HOSCN, 100 or 250 µM HOCl at 37 °C for 24 h. HCAEC were treated with 0.1 mg•mL^{-1} of LDL or oxidised LDL species at 37 °C for 3 h (white bar) or 24 h (black bar) in treatment medium. Incubation with tunicamycin (TM; 5 µg•mL^{-1}) for 3 or 24 h was used as a positive control for UPR gene expression. Bars represent the mean ± SD (n = 3). Expression was normalised to 18S and β2M as housekeeping genes. Two-way ANOVA with Dunnett's multiple comparison test between treatment groups and Sidak multiple comparison test between time points. *, **, *** and **** represent p < 0.05, 0.01, 0.001 and 0.0001 respectively compared to their respective control. ##, ### and #### represent p < 0.01, 0.001 and 0.0001 respectively between 24 and 48 h time point.*

4.3.4.2. Antioxidant response element genes

Previous studies have also shown that oxidised LDL species, including LDL oxidised by HOCl, can induce Nrf2 activation [596, 597]. Activation of Nrf2 leads to upregulated expression of antioxidant genes, including GS, Gclc and HO-1 [569, 570, 598]. As shown in Figure 4.14, incubation of HCAEC with 0.1 mg•mL^{-1} of control LDL, or LDL incubated with 100 µM or 250 µM HOSCN or HOCl for 3 or 24 h, mRNA expression of Nrf2, GS and Gclc was not significantly changed. However, incubation with 100 µM and 250 µM HOSCN-modified LDL for 3 h significantly increased HO-1 expression by 1.7- and 2.9-fold, respectively, compared to the control. This increased mRNA expression returned to control levels after 24 h treatment. In contrast, HOCl-modified LDL did not significantly induce HO-1 expression after 3 h, but did significantly elevate HO-1 mRNA expression (approximately 1.5-fold) compared to the control after 24 h exposure to (250 µM oxidant) HOCl-modified LDL.

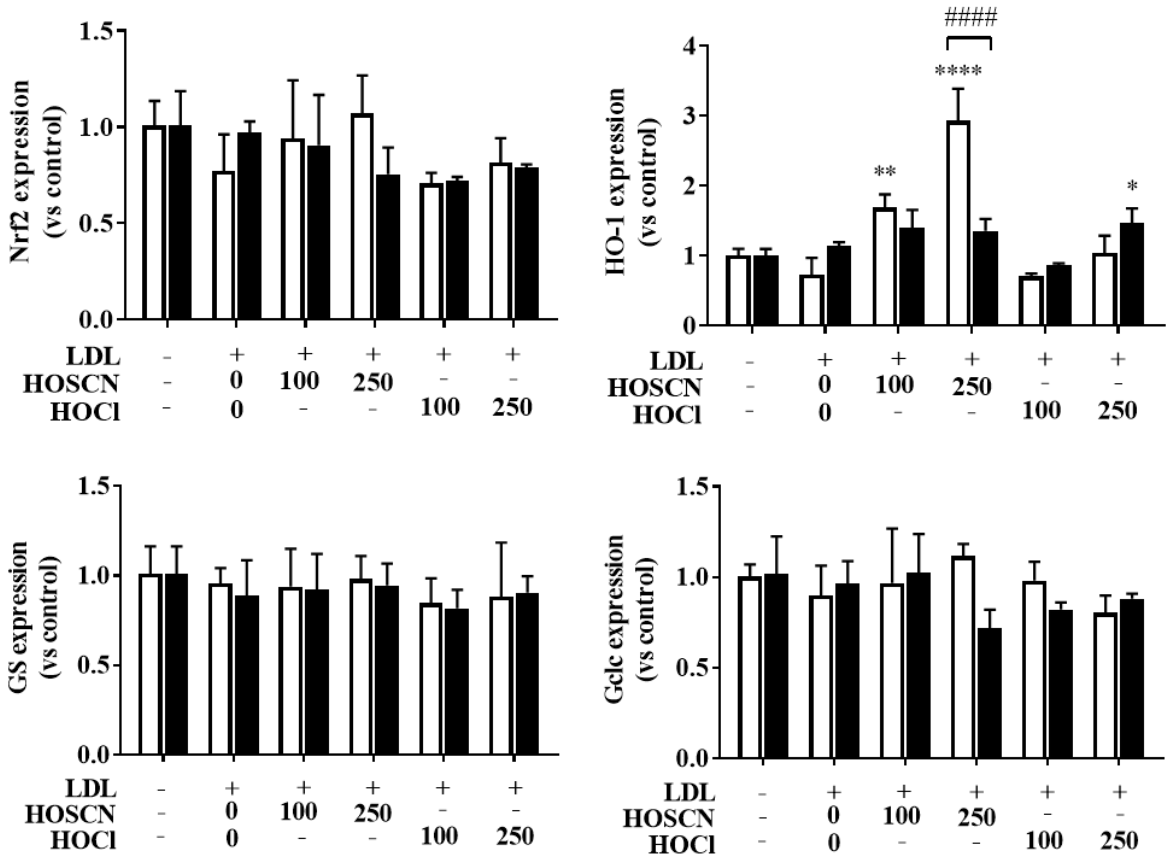

Figure 4.14. HCAEC mRNA expression of antioxidant response genes measured by qPCR after incubation with LDL modified by HOSCN or HOCl. *Firstly, 1.0 mg•mL^{-1} control LDL or LDL modified by 100 or 250 µM HOSCN, 100 or 250 µM HOCl at 37 °C for 24 h. HCAEC were treated with 0.1 mg•mL^{-1} of LDL or oxidised LDL species at 37 °C for 3 h (white bar) or 24 h (black bar) in treatment medium. Expression was normalised to 18S and β2M as housekeeping genes. Three independent HCAEC and LDL donors were used. Bars represent the mean ± SD (n = 3). Two-way ANOVA with Dunnett's multiple comparison test between treatment groups and Sidak multiple comparison test between time points. *, **, *** and **** represent p < 0.05, 0.01, 0.001 and 0.0001 respectively compared to their respective control. ## and #### represent p < 0.01 and 0.0001 respectively between 24 and 48 h time point.*

These studies were extended by examination of the protein expression of HO-1 by Western blotting. Initial studies showed that following exposure of HCAEC to 0.1 mg.mL^{-1} LDL modified by HOSCN or HOCl (250 μM oxidant) for 24 h, there was a large induction of HO-1 protein expression (Figure 4.15, *n* = 2). Regardless of the 2.9-fold spike in HO-1 mRNA expression after 3 h treatment with (250 μM oxidant) HOSCN-modified LDL, which returned to similar levels induced by HOCl-modified LDL after 24 h exposure, HOCl-modified LDL induced considerably greater HO-1 protein expression than the equivalent HOSCN-modified LDL after 24 h exposure. However, the lack of reproducibility, which may be due to HCAEC donor variation or problems with the current Western blot procedure, makes interpretation of this result difficult. Overall, these experiments show the antioxidant response to MPO oxidant-modified LDL may involve induction of HO-1, but this study was not conclusive.

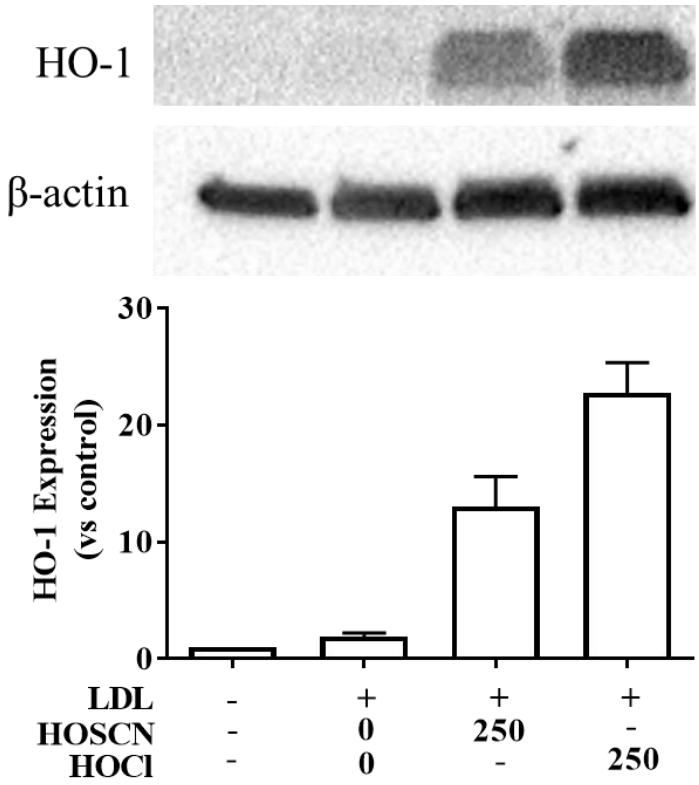

Figure 4.15. HCAEC protein expression of HO-1 after incubation with LDL modified by HOSCN or HOCl. *Firstly, 1.0 mg.mL^{-1} control LDL or LDL modified by 250 μM HOSCN or HOCl at 37 °C for 24 h. HCAEC were treated with 0.1 mg.mL^{-1} of LDL or oxidised LDL species for 24 h at 37 °C. Bars represent the mean ± SD (n = 2).*

4.4. Discussion

The experiments in this Chapter involved the *in vitro* exposure of HCAEC to LDL after the lipoprotein had been incubated with up to 250 μM HOSCN or HOCl, which is believed to be achievable under physiological conditions as it has previously been shown that plasma SCN^- concentrations in smokers have been detected up to 250 μM [42]. The impact of exposure of HOSCN- or HOCl-modified LDL upon HCAEC was assessed in terms of cytotoxicity, metabolic activity, lipid uptake and induction of pro-inflammatory and stress-related pathways in endothelial cells. The extent of cholesterol and cholesteryl ester accumulation, even at prolonged incubation times (48 h), did not significantly differ to the control, with no alteration in viability, metabolic activity or cell migration in this study. This is likely related to a lack of change in scavenger receptor expression. Further, no overall change in expression of leukocyte adhesion molecules, cytokines, or UPR and ARE pathway signalling molecules was observed, apart from HO-1 being stimulated by HOSCN-modified LDL.

In this study, no evidence was obtained for cell death, whereas previous data have shown that Cu^{2+}- or cell-dependent oxidised LDL induced apoptosis in endothelial cells *in vitro* [514, 523, 599, 600]. In HCAEC exposed to Cu^{2+}-oxidised LDL, apoptosis was associated with the downregulation of bcl-1 protein and induced caspase activation by the independent activation of protein kinase C or protein tyrosine kinase [514, 523]. However, LDL modified by HOSCN or HOCl in this study did not induce significant cell death in HCAEC following up to a 48 h incubation time. This is likely due in large part to the difference in the extent and nature of LDL modification seen with reactivity of MPO oxidants compared to Cu^{2+} ions to LDL. Cu^{2+}-modified LDL is largely characterised by extensive lipid oxidation [303], which has been shown to cause endothelial cell apoptosis [514, 523, 526, 601]. In contrast, MPO oxidants display more limited reactivity with the lipid moiety of LDL, except at high molar excesses

[53]. In the studies which used a higher molar ratio of HOCl to LDL (2000: 1), apoptosis was induced in macrophages [602, 603], therefore extensively modified LDL particles are required to elicit this response, which may also be the case for endothelial cells.

4.4.1. LDL uptake and scavenger receptor expression

The increase in intracellular lipid (Δintracellular lipid) concentration in HCAEC over time was significantly greater after incubation with control LDL and each MPO oxidant-modified LDL compared to cells incubated without LDL. However, there was no difference in intracellular lipids between HCAEC treated with these different forms of LDL. HCAEC exposed to LDL for longer incubation times may have led to cell-mediated modification of LDL by lipoxygenases [341]. As lipoxygenases target the arachidonate and linoleate moiety of LDL [335, 336], and hypohalous acids used at the concentrations of this study did not significantly deplete native arachidonate and linoleate levels (shown in Figure 4.3), measuring these cholesteryl esters post-incubation with cells could be performed to determine if cell-mediated oxidation of LDL occurred, as well as if MPO-modified LDL upregulates lipoxygenase activity. Further, the use of serum-supplemented treatment media which would contain lipids may mask the uptake of the MPO oxidant-modified LDL. The use of lipoprotein-deficient serum would remove this potential limitation and future experiments could be optimised for these experimental conditions.

Endothelial cells express several classes of scavenger receptors that have classically been associated with elevated uptake and accumulation of LDL-sourced lipids in macrophages [421]. HOCl-modified LDL (400:1 molar ratio of HOCl to apoB-100) binding to SR-B1 and SR-B2 has been shown to be competitive to Cu^{2+}-oxidised LDL in THP-1 monocytes [604] and suggests that uptake of LDL modified by HOCl by endothelial cells may be *via* scavenger receptors. This is supported by another study which found that immunological blocking of SR-

B2 largely inhibited adhesion of polymorphonuclear leukocytes to HUVEC that was induced by exposure to HOCl-modified LDL [438]. However, alterations in the gene or protein expression of these SR-B1 and SR-B2 was not investigated in those studies. Yet, the expression of scavenger receptors was mostly unaltered in the current study, with a modest downregulation of SR-B1 after 24 h incubation with HOCl-modified LDL. This contrast may be due to the higher HOCl: apoB-100 ratio in those previous studies (approximately 400:1 [604], and up to 2716:1 [438]) compared to the current study (up to 125:1) resulting in greater extent of modification of the LDL. This is pertinent when the REM of HOCl-modified LDL is compared from those studies (*cf.* 2.1-fold [604] and 7.2-fold [438]) to the current study (approximately 1.8-fold; Figure 3.1), despite the fact that the LDL was incubated for only 40 min to 1 h in those studies, while LDL was incubated for 24 h in the current study.

Cu^{2+}-oxidised LDL may have induced a rapid response in upregulating LOX-1 expression, but the expression was highly variable, and only significant following 3 h incubation, with downregulation to below control levels by 24 h exposure. This contradicts a similar study in HCAEC, which did observe mRNA and protein upregulation of LOX-1 following 24 h incubation to 0.04 mg**.**mL^{-1} Cu^{2+}-oxidised LDL [518]. This difference could be attributed to Cu^{2+}-oxidised LDL inducing greater extent of apoptosis in HCAEC at 0.1 mg**.**mL^{-1} Cu^{2+}-oxidised LDL in that study [518], which was also the concentration used in the current study to assess scavenger receptor expression. However, no data was obtained in this current study for comparing the cell toxicity of Cu^{2+}-modified LDL when treated to HCAEC.

Interestingly, the LDLR mRNA expression was downregulated after 24 h treatment with HOCl- and HOSCN-modified LDL, but not Cu^{2+}-oxidised LDL. This may be related to the extensive lipid modification observed, as Cu^{2+}-oxidised LDL is depleted of native cholesterol and cholesteryl ester content, as shown in Figure 4.3. LDLR expression is transcriptionally regulated by the sterol regulatory element-binding proteins (SREBP), which is inhibited by

LDL uptake, but the LDLR protein is also recycled back to the plasma membrane after dissociating from LDL [605]. The LDLR was shown to have a long half-life of 25 h in human fibroblasts [606], which could be similar in endothelial cells. The reduction in LDLR mRNA may indicate a negative feedback of LDLR synthesis to counteract the LDLR recycling to reach cholesterol homeostasis. However, downregulation of the LDLR was only apparent at the mRNA but not protein level. In this case, 24 h may not have been enough time to observe a downregulation in LDLR protein expression due to the long half-life of the protein.

HOSCN- and HOCl-modified LDL were shown to reduce cathepsin B and L activity in mouse J774A.1 macrophages [582], but this was not the case in this study of HCAEC, which exhibited no change in cathepsin B or L activity upon incubation with similar types of modified LDL. Cathepsins are important lysosomal and endosomal proteases that digest biomolecules taken up by endocytosis [581]. Overall, the unchanged cathepsin B and L activity and SR expression after uptake of MPO oxidant-modified LDL could exhibit competent processing of the modified LDL by endosomal digestion. Alternatively, the modified LDL species may be transported by transcytosis to embed under the endothelium, which has been shown to be LDLR- and SR-mediated [607], and which occurs *in vivo* [608, 609] and has been modelled *in vitro* [607, 609]. The transport of LDL and oxidised LDL through the cell by endocytosis or transcytosis was not interrogated in this study, but future investigation into these transport pathways could gauge the extent of the role of cathepsins in LDL or MPO oxidant-modified LDL processing in endothelial cells.

4.4.2. Leukocyte adhesion and inflammatory cytokines

Multiple studies have shown that vascular inflammation can be endothelial cell-mediated by modulating the adhesion of leukocytes, which can be induced by pro-inflammatory cytokines [610] or alterations in vascular shear stress/disturbed flow [307, 611, 612]. However,

in this study, incubation of HCAEC with HOSCN- or HOCl-modified LDL for up to 24 h did not alter expression of several well-established mediators of cell adhesion, or adhesion of neutrophils to the endothelial monolayer. These findings contradict some previous studies utilising Cu^{2+}-oxidised LDL [307, 433-435, 613]. However, the literature is conflicted regarding the ICAM-1 and VCAM-1-dependent monocyte–endothelial adhesion, with some reports finding no induction of either VCAM-1 or ICAM-1 when endothelial cells are exposed to Cu^{2+}-oxidised LDL [433, 560, 589, 614]. In respect to HOCl-modified LDL, one study by Kopprasch *et al* found that leukocyte adhesion was elevated when HUVEC were co-incubated with either RAW 264.7 murine macrophages or isolated human neutrophils exposed to native LDL and HOCl-modified LDL [438]. However, this study also noted that HUVEC incubated with native or HOCl-modified LDL alone prior to incubation with RAW 264.7 cells had no change in cell adhesion, except for a modest significant increase in adhesion when incubated with heavily modified LDL (2716:1 molar ratio of HOCl to apoB-100) [438]. Furthermore, antibody inhibition of the leukocyte SR-B2 completely blocked native LDL-induced adhesion and significantly reduced HOCl-modified LDL-induced adhesion of HUVEC and leukocytes when co-incubated with LDL [438]. Not only did the adhesion depend on the extent of LDL modification by HOCl, but also on the presence of leukocytes and CD-36-dependent uptake of LDL.

The uptake of Cu^{2+}-oxidised LDL by monocytes and macrophages induces the release of IL-6 and TNF-α [610], which can stimulate adhesion molecule expression in endothelial cells as shown by the TNF-α-induced positive control. In this study, HCAEC were incubated with control LDL and LDL modified by HOSCN or HOCl prior to incubation with human isolated neutrophils, and the molar excess of HOCl used to modify LDL was comparatively modest (125:1 rather than 2516:1 molar ratio [438]), which is in agreement with the findings by Kopprasch *et al* [438]. However, endothelial cells can also modulate neutrophil infiltration by

secreting IL-6 and transition to monocyte infiltration by the release of MCP-1 [563, 615]. In this study, no changes in IL-6 or MCP-1 mRNA or protein were detected following up to 24 h incubation with MPO oxidant-modified LDL. Thus, uptake of either HOSCN- or HOCl-modified LDL alone does not induce pro-inflammatory proteins in HCAEC under the conditions employed in this study.

4.4.3. UPR and ARE genotypic expression

In recent years, ER stress has been causally linked to endothelial dysfunction and atherosclerosis (reviewed [462, 616, 617]). The two major transport destinations of native LDL cholesterol in the cell are the ER and the plasma membrane by endosomal transport, which is mediated by lysosome-associated membrane protein type 2 (LAMP-2; [618]). The ER plays a critical role in lipid metabolism in the cell and disturbance in lipid metabolism can lead to ER stress [619]. One of the possible causal factors linked to UPR-induced endothelial dysfunction has been exposure to oxidised LDL, which is based upon the observations that the Cu^{2+}-oxidised form, but not control LDL, can induce ER stress in human and animal endothelial cells *in vitro* as well as in mouse overexpressing the 150-kDa oxygen-regulated protein or $apoE^{-/-}$ and $apoE^{-/-}$/AMPK$\alpha 2^{-/-}$ mice fed a high-fat diet *in vivo* [464, 620]. Incubation of HUVEC *in vitro* with Cu^{2+}-oxidised LDL was shown to lead to an upregulation of GRP78, XBP1, IRE-1 and PERK protein expression mediated by LOX-1-dependent induction of ER stress [565] and lead to apoptosis induced by CHOP activity [463]. The effect of MPO oxidant-modified LDLs upon ER stress and UPR in endothelial cells has not been reported. The results of this study show that LDL modified by up to 250 μM HOSCN or HOCl did not induce mRNA expression of UPR components in HCAEC.

The difference between LDL modified by HOCl or HOSCN and other modified forms of LDL in part relates to difference in the extent of lipid modification. The reaction of HOCl with

phospholipids in LDL (such as phosphatidylserine and phosphatidylethanolamine) is competitive with apoB-100 oxidation by HOCl, but likely only becomes a major product at very high molar ratios (approximately 2.4 % HOCl consumption by lipids in LDL at 200:1 molar ratio HOCl:apoB-100 [135]), whereas in this study, a maximum of 125:1 molar ratio was used. Incubation of HUVEC and human aortic endothelial cells (HAEC) with isolated oxidised phospholipids instead of oxidised LDL activated the ATF4 branch of the UPR [465, 566, 621, 622]. This oxidised phospholipid-mediated induction of UPR was in parallel with increased expression of inflammatory mediators such as IL-6, IL-8 and MCP-1, and antioxidant genes such as HO-1, NADPH quinone dehydrogenase-1 (NQO-1) and Gclc/m [566, 622], strongly linking the ER stress and activation of the UPR and inflammatory response in endothelial cells exposed to oxidised phospholipids.

In the current study, no evidence for Nrf2 upregulation was found following exposure to HOSCN- or HOCl-modified LDL, but evidence for induction of HO-1 mRNA expression by HOSCN-modified LDL was observed. There was a stronger upregulation of HO-1 mRNA expression following incubation with HOSCN-modified LDL than after incubation with HOCl-modified LDL (*cf.* three-fold expression after 3 h with HOSCN-modified LDL vs 1.5-fold expression after 24 h treatment with HOCl-modified LDL). Initial results showed that regardless of the difference in HO-1 mRNA expression following exposure to HOSCN- or HOCl-modified LDL, HO-1 protein expression was upregulated by both MPO oxidant-modified LDL species (n = 2), but unfortunately this was not reproducible upon further replication and further work is required to assess alterations in HO-1 expression.

There is some evidence that exposure of endothelial cells to the MPO-H_2O_2-halide system can lead to HO-1 activation. A study by Porubksy *et al* found that HO-1 gene expression was significantly upregulated in human proximal tubular cells following 4 – 8 h exposure of HOCl-modified LDL [437]. Yet, proximal tubular cells are not of vascular origin and the HOCl: LDL

ratio was higher than in the current study (*cf*. 1:400 vs 1:125 LDL: HOCl ratio, respectively). Another study by Daher *et al* found that MPO-oxidised LDL (likely by chlorinating activity) induced HO-1 mRNA expression in the absence of apoptosis in HUVEC [623], however the authors did not investigate the protein expression. HUVEC and HAEC incubated with 3 – 300 μM HOCl for 24 h induced mRNA expression and synthesis of HO-1 and subsequent elevated CO production which were associated with increased cell viability [624]. In macrophages, incubation with enzymatic MPO-modified LDL induced Nrf2-dependent activation of HO-1 and Gclm mRNA expression and synthesis to a larger extent than Cu^{2+}-oxidised LDL [597]. However, there was no change in the mRNA expression of ARE genes Nrf2, Gclc and GS in the current study.

Daher *et al* also noted the co-expression of microRNA-22 (miR-22) with HO-1 following incubation with enzymatic MPO-modified LDL, which has recently been demonstrated to interact with the 3′-untranslated region (3′-UTR) of HO-1 mRNA to supress translation [625]. Given the findings by Daher *et al*, HCAEC exposed to HOSCN- or HOCl-modified LDL in this study may have induced miR-22 expression, which could explain the difficulty in replicating induction of the HO-1 protein following treatment with MPO oxidant-modified LDL in the current study. Induction of HO-1 and production of CO is an important redox feedback mechanism in the cell [626]. Stimulation of HO-1 activity and expression in vascular endothelial cells by oxidised LDL has again been attributed to the oxidised (phospho)lipid moiety of oxidised LDL [596, 627]. Fatty acid hydroperoxides strongly stimulated HO-1 mRNA and protein expression in HAEC and renal epithelial cells [627]. Similarly, exposure of HAEC to oxPAPC lead to upregulated HO-1 expression and activity through activation of Nrf2 [596]. Additionally, pre-stimulation of HO-1 activity in a co-culture of endothelial and smooth muscle cells prior to treatment with cell-modified LDL significantly inhibited monocyte adhesion, this was replicated with exposure to oxPAPC which also upregulated HO-

1, but not with exposure to native LDL [628]. Although this was not examined in the current study, the phospholipids of LDL can be oxidised by HOCl at concentrations used in the current study [135] and could explain the induction of HO-1. However, HOSCN-modified LDL also induced HO-1 mRNA and protein expression in this study, and though HOSCN does not react with phospholipids [147], HOSCN elicits a greater extent of oxidation of other lipid species in LDL compared to HOCl [146] which may also be inductive of HO-1 expression. Additionally, HO-1 mRNA expression was strongly induced by LDL modified by HOSCN and not HOCl, which suggests induction of HO-1 could be through different pathways between the two oxidised LDL epitopes.

4.4.4. Limitations

The quantification of cellular RNA and protein expression, cellular lipid content and cathepsin activity after exposure to LDL modified by HOSCN or HOCl represent static measures at 3 and 24 h treatment. These results cannot be interpreted as time-dependent responses to LDL modified by either HOSCN or HOCl. Repeating these experiments over shorter incubation intervals may detect acute fluxes in expression or protein activity in endothelial cells which may have been missed. HO-1 protein expression also was not reproducible and requires further experiments.

4.5. Conclusion

Overall, this Chapter demonstrates that the uptake of each type of MPO oxidant-modified LDL did not significantly alter pro-inflammatory mechanisms in HCAEC. Scavenger receptor protein expression was not significantly altered, but for the exception of downregulation of SR-B1 mRNA following incubation with HOCl-modified LDL. Further, LDLR mRNA, though not protein, expression was significantly downregulated by exposure to LDL modified by either HOSCN or HOCl. Leukocyte adhesion molecule expression, neutrophil adhesion and cytokine

(IL-6 and MCP-1) expression were also unchanged following incubation with MPO oxidant-modified LDL. These data contrast with the literature that exhibited the pro-inflammatory effects of other modified forms of LDL (Cu^{2+}- or cell-mediated). Concerning anti-inflammatory mechanisms, HO-1 mRNA was significantly upregulated by HOSCN-modified LDL, while both HOSCN- and HOCl-modified LDL could induce HO-1 protein expression. This would suggest that MPO oxidant-modified LDL may influence redox signalling pathways in HCAEC. These data highlight the importance of the extent of LDL modification reflected by the concentration of oxidant utilised on the nature of the cellular responses observed. The current study was extended to examine the role of LDL modified by either HOSCN or HOCl in inducing endothelial dysfunction; a key contributor to atherosclerosis.

Chapter 5. LDL modified by HOSCN or HOCl causes eNOS dysfunction in endothelial cells

5.1. Introduction

Atherosclerosis is characterised by the narrowing and stiffening of arteries. Disease progression is recognised by a loss in vascular endothelial function [629] and chronic inflammation [630], arising from LDL accumulation in the arterial intima [631]. Endothelial dysfunction in arteries is an early hallmark of atherosclerosis [629], which is defined by the reduction in eNOS activity and the consequent decrease in NO production, leading to impaired arterial distensibility [408] (Figure 5.1). Given that NO is a potent vasodilator, the reduction in eNOS activity resulting in endothelial dysfunction and impaired arterial vasorelaxation *in vivo* has been implicated as having a key role in atherosclerosis [408]. Coupled eNOS exists as a dimeric enzyme which produces NO *via* one-electron reduction of the haem centre to catalyse the conversion of L-Arg to NO and L-Cit [632]. Uncoupling of the eNOS dimer results in disrupted electron-transport, leading to direct reduction of O_2 to $O_2^{\bullet-}$ instead of producing NO [633]. This one-electron oxidation leading to $O_2^{\bullet-}$ formation can further deplete NO by the formation of peroxynitrite ($ONOO^-$), which itself is a potent oxidant that can cause further damage is capable of further exacerbating endothelial dysfunction [446].

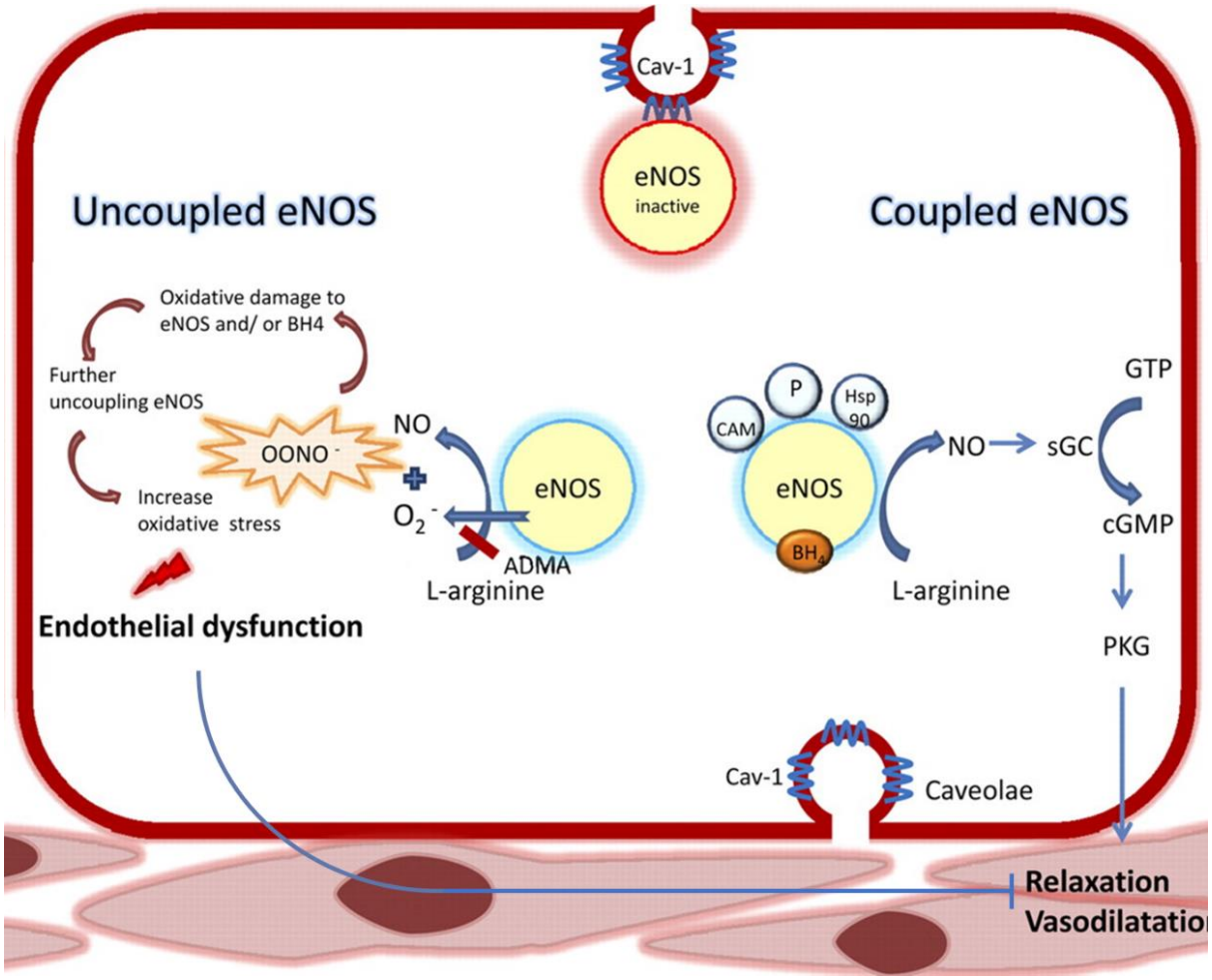

Figure 5.1. Endothelial dysfunction is linked to eNOS uncoupling and impaired vasodilation (adapted from [634]). *eNOS as a functional dimer (coupled eNOS) is activated by binding to calmodulin (CaM), heat shock protein 90 (hsp90), residue phosphorylation and cofactor BH_4 to convert L-Arg to L-Cit and NO. NO activates soluble guanylyl cyclase (sGC) to cyclise GMP to cGMP, which activates protein kinase G (PKG) to promote vasodilation by smooth muscle. Coupled eNOS can be inactivated by binding to cav-1. Uncoupled eNOS does not function as a dimer and leads to the production of $O_2^{\bullet-}$, which can react with NO to reduce NO bioavailability and impair vasodilation. The reaction of $O_2^{\bullet-}$ and NO also produces the potent oxidant $ONOO^-$. The production of $O_2^{\bullet-}$ and $ONOO^-$ increases oxidative stress which can further uncouple eNOS in a vicious cycle to further cement endothelial dysfunction.*

It is well established that LDL oxidation is a key factor in atherosclerotic lesion development through numerous pathways (reviewed [280, 631]) and there is strong evidence to implicate oxidised LDL as a causal factor in endothelial dysfunction by its effect on eNOS *in vitro* [448, 516, 635]. This is further supported by evidence that exposure to oxidised LDL impairs the endothelium-dependent vasodilatory capacity of animal aortae *ex vivo* [455, 636, 637]. Despite this knowledge that oxidised LDL can perturb endothelial function, there is still debate regarding the precise mechanisms responsible.

The presence of eNOS has been found to be predominantly localised to the caveolae within endothelial cells [638]. Caveolin-1 (cav-1; named after the caveolae) is one of the proteins known to negatively regulate eNOS activity by blocking the Ca^{2+}-dependent, calmodulin (CaM)-mediated electron transport to the eNOS oxidase domain [639]. The importance of cav-1-dependent eNOS regulation is also supported by studies using cav-$1^{-/-}$ mice, which demonstrated significantly greater capacity for endothelium-dependent vasodilation and eNOS hyperactivity compared to their wild type counterparts [640, 641]. Furthermore, alterations in the cellular compartmentalisation of eNOS can also alter the production of NO by endothelial cells *in vitro* [448, 516], which can be mediated by endocytosis of caveolae [642-644]. It has previously been shown that incubation of porcine pulmonary aortic endothelial cells with Cu^{2+}-oxidised LDL, but not native LDL, resulted in delocalisation of eNOS and cav-1 from the caveolae to the cytosol, which also reduced acetylcholine (ACh)-stimulated eNOS activity without reducing total eNOS expression or phosphorylation [516]. Similarly, treatment with HOCl-modified LDL has been shown to delocalise eNOS from cav-1 and impair eNOS activity in HUVEC, the occurrence of which was proposed to leave eNOS vulnerable to uncoupling [448]. In addition, eNOS activity is also positively or negatively regulated by several post-translational modifications, including phosphorylation, acylation, *S*-nitrosylation and acetylation [645, 646].

As of yet, the comparative effect of LDL modified by physiological levels of the MPO-derived oxidants HOSCN or HOCl on eNOS activity has not been elucidated. This is significant in light of the presence of higher circulating concentrations of SCN^- in smokers [42, 43], which can shift MPO activity to significant production of HOSCN [39]. In this study, we hypothesised that LDL modified by HOCl and HOSCN would cause endothelial dysfunction by uncoupling eNOS, leading to the reduction in NO production in HCAEC *in vitro*.

5.2. Aims

The aim of the studies in this Chapter was to examine whether LDL modified by the MPO-derived oxidants HOCl and HOSCN could alter the endothelial production of NO via influencing the activity of eNOS. This was assessed *in vitro* using HCAEC as a model, and *ex vivo*, using rat aortic segments.

5.3. Results

5.3.1. NO production

HCAEC were treated with LDL (0.1 $mg.mL^{-1}$) modified by HOSCN or HOCl (100 or 250 μM) for 24 h before assessing intracellular NO levels by DAF-FM fluorescence using flow cytometry. DAF-FM is a very weakly fluorescent, cell-permeable molecule which reacts with NO, to form a highly fluorescent benzotriazole derivative, with an excitation and emission maximum of 495 nm and 515 nm, respectively [647]. On visual assessment of the distribution of the DAF-FM fluorescence histograms in all three experimental replicates, a Gaussian (normal) distribution was not observed in all treatment groups (Figure 5.2A – D). This made the mean of total DAF-FM fluorescence an inappropriate descriptive statistic for analysis of NO levels by this method, as the cell population was bimodal in all three experimental replicates. Therefore, the DAF-FM fluorescence was categorised into two populations;

"percentage-negative" (P_0) and "percentage-positive" (P_1), and the percentage of the parent population (P) represented in each category was calculated [648]. This showed that compared to the control, a significantly lower proportion of P_1 cells were detected in HCAEC following treatment with LDL exposed to 250 μM HOSCN or LDL exposed to HOCl (100 or 250 μM), corresponding with a significant increase in P_0 cells (Figure 5.3).

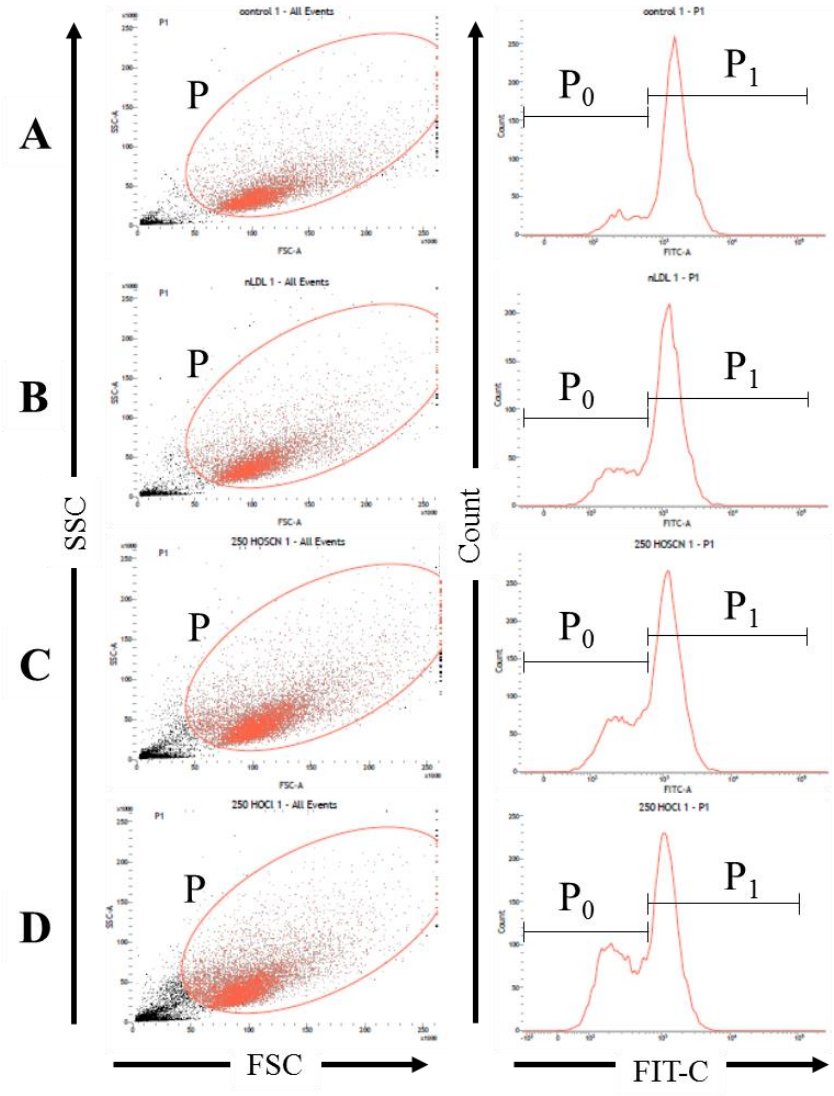

Figure 5.2. Intracellular measurement of DAF-FM fluorescence by flow cytometry to measure NO levels in HCAEC after incubation with LDL modified by HOSCN or HOCl. *1.0 mg·mL^{-1} control LDL or LDL modified by 100 or 250 µM HOSCN or 100 or 250 µM HOCl for 24 h. HCAEC were treated with 0.1 mg·mL^{-1} of LDL or oxidised LDL species for 24 h at 37 °C. After treatment, HCAEC were incubated with 1 µM DAF-FM for 30 min at 37 °C to react with intracellular NO. Representative flow cytometry forward-scatter (FSC) and side-scatter (SSC) plots and DAF-FM fluorescence (FIT-C) histograms are shown; (A) control, (B) control LDL, (C) 250 µM HOSCN-modified LDL and (D) 250 µM HOCl-modified LDL. Data are representative of three independent experiments*

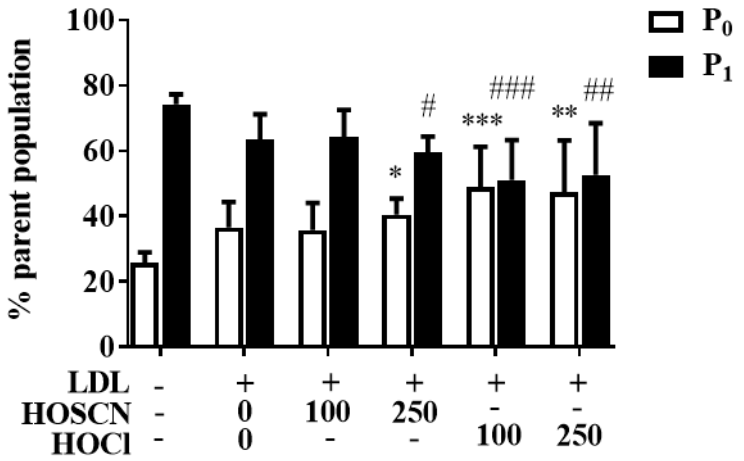

Figure 5.3. Proportion of low fluorescence and high fluorescence cell populations following 24 h exposure to LDL modified by HOSCN or HOCl. *DAF-FM fluorescence quantified by the percentage of parent population (P) of the FIT-C histogram, with the low fluorescence population (P_0; white bars) and high fluorescence population (P_1; black bars). Two-way ANOVA with Dunnett's multiple comparison test between treatment groups and the control (n = 3). *, ** and *** represent p < 0.05, 0.01 and 0.001, respectively compared to the control for low fluorescence population. #, ## and ### represent p < 0.05, 0.01 and 0.001, respectively compared to the control for high fluorescence population.*

These studies were extended to examine the effect of each modified LDL on NO release. To quantify the amount of NO produced by HCAEC following 24 h treatment with MPO oxidant-modified LDL, the iron-dithiocarbamate ($Fe(MGD)_2$) spin trap was used to trap NO [649], which results in the formation of a $Fe(MGD)_2$-NO complex that can be detected by EPR. This method was verified using the NO donor, spermine NONOate in the absence of cells prior to every experiment, as a positive control, which had a characteristic hyperfine splitting of 13.2 G and g-value of 2.04 (Figure 5.4A). Then, to ensure that the $Fe(MGD)_2$-NO signal was dependent on eNOS activity in HCAEC, 100 μM of the eNOS inhibitor, N^5-(1-iminoethyl)-L-ornithine dihydrochloride (L-NIO) was incubated with untreated HCAEC prior to addition of the spin trap. L-NIO significantly decreased the $Fe(MGD)_2$-NO signal compared to the corresponding HCAEC control (Figure 5.4B). Therefore, the EPR signal detected following incubation with HCAEC was dependent on eNOS-dependent NO production.

Incubation of HCAEC with LDL modified by HOSCN or HOCl (100 or 250 μM) for 24 h resulted in a significant reduction in the EPR signal of the $Fe(MGD)_2$-NO adduct compared to the non-treated cells, consistent with a decrease in NO production by the cells (Figure 5.4C). A loss in EPR signal intensity was also observed with control LDL. The relative abundance of NO detected by EPR is proportional to the EPR signal intensity and hence can be quantified by determining the area under the curve of the signal. Since the EPR trace is the derivative of the $Fe(MGD)_2$-NO signal, NO detection was quantified by double integration of the signal from 3387 G and 3452 G. This analysis showed that the NO released from HCAEC was significantly reduced following 24 h incubation with both the control LDL and all subsequent MPO oxidant-modified LDL treatments (Figure 5.4D).

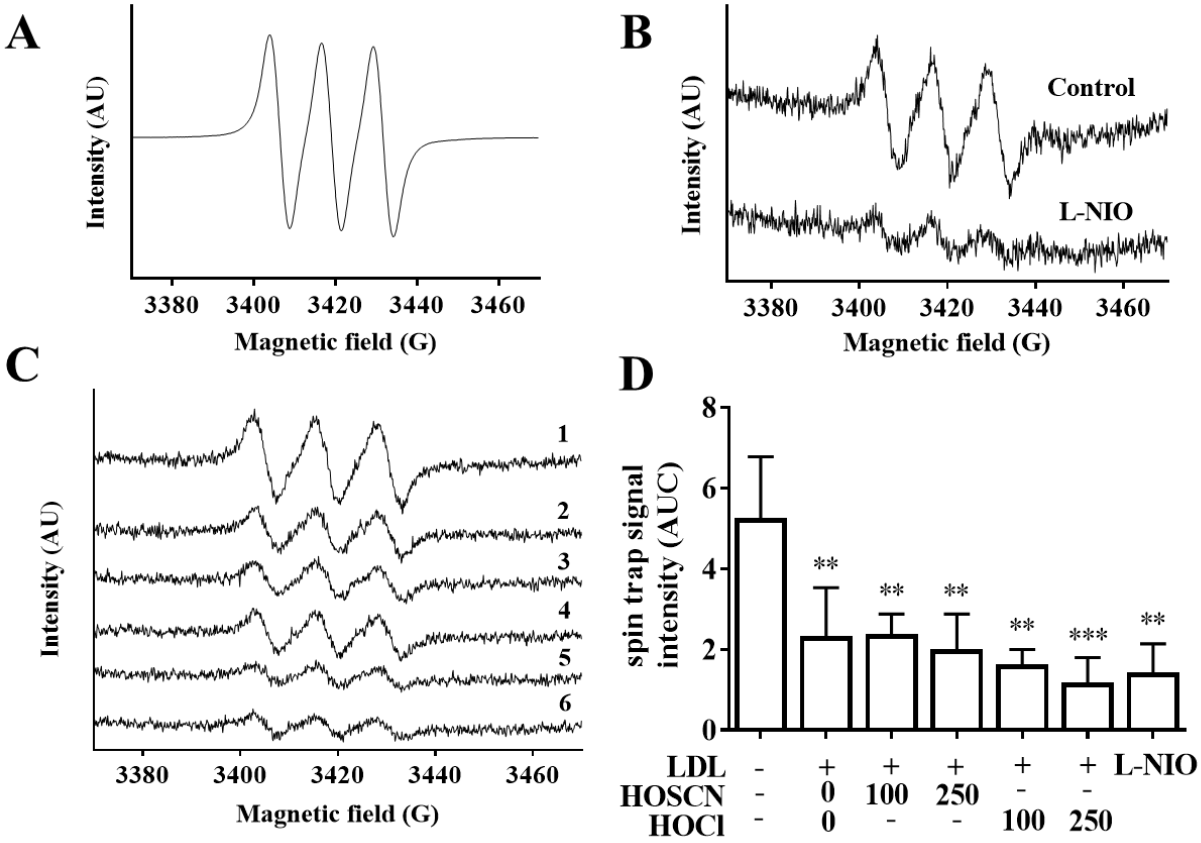

Figure 5.4. Spin trapping of NO by iron-dithiocarbomate complex $Fe(MGD)_2$ measured by EPR spectroscopy from HCAEC after incubation with LDL modified by HOSCN or HOCl. *1.0 mg·mL^{-1} control LDL or LDL modified by 100 or 250 µM HOSCN or 100 or 250 µM HOCl for 24 h. HCAEC were treated with 0.1 mg·mL^{-1} of LDL or oxidised LDL species for 24 h at 37 °C. After treatment, HCAEC were incubated with the spin trap $Fe(MGD)_2$ for 36 min at 37 °C to bind with NO. Representative EPR spectra; (A) $Fe(MGD)_2$-NO spin trap using the NO donor spermine NONOate, (B) signal inhibition by the eNOS inhibitor, L-NIO, and (C) NO released from HCAEC after each 24 h incubation of; (1) control, (2) control LDL, (3) 100 µM HOSCN, (4) 250 µM HOSCN, (5) 100 µM HOCl, (6) 250 µM HOCl. (D) Area under the curve (AUC) of the EPR spectra to measure proportionate NO production from HCAEC after treatment. Data represent mean ± SD (n = 3). One-way ANOVA with Dunnett's multiple comparison test between treatment groups and control. ** and *** represent p < 0.01 and 0.001 respectively, compared to control.*

5.3.2. eNOS activity and expression

As endothelial production of NO is dependent on eNOS activity, these studies were extended to measure eNOS activity by assessing the conversion of ^{3}[H]arginine to ^{3}[H]citrulline. As demonstrated in Figure 5.5, incubation of HCAEC with either HOCl- or HOSCN-modified LDL resulted in the reduction of ^{3}[H]citrulline produced, (when compared to cells exposed to control LDL) indicative of reduced eNOS activity. Furthermore, the demonstrated decrease in eNOS activity was dose-dependent on the concentration of HOSCN or HOCl used to modify LDL, and was shown to be more markedly decreased with the HOSCN-modified LDL compared to the HOCl-modified LDL, with the ^{3}[H]citrulline produced decreasing to approximately 37 % of the control for the HOSCN-modified LDL and 55 % of control for the HOCl-modified LDL, when LDL was modified by 250 μM of HOSCN or HOCl. These results support the reduced NO production by HCAEC detected by EPR following 24 h MPO oxidant-modified LDL treatment, although the reduction in NO synthesis following 24 h exposure to control LDL was not reflected in a similar reduction in eNOS activity by ^{3}[H]citrulline detection. This is likely due to higher variability between experimental replicates. Together however, these data indicate that there is a reduced capability for eNOS to synthesise NO after treatment with HOSCN- and HOCl-modified LDL.

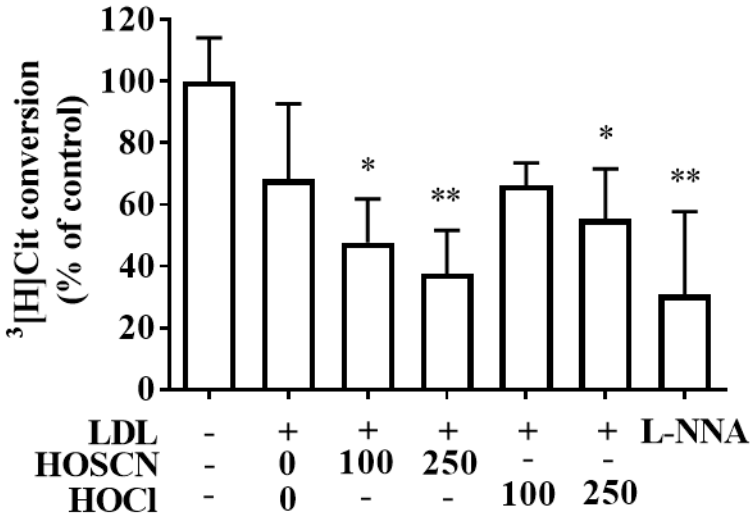

Figure 5.5. Enzymatic activity of eNOS in HCAEC measured by the conversion of ^{3}[H]-L-arginine to ^{3}[H]-L-citrulline after incubation with LDL modified by HOSCN or HOCl. *1.0 mg•mL^{-1} control LDL or LDL modified by 100 or 250 µM HOSCN or 100 or 250 µM HOCl for 24 h. HCAEC were treated with 0.1 mg•mL^{-1} of LDL or oxidised LDL species for 24 h at 37 °C. ^{3}[H]citrulline is separated from unreacted ^{3}[H]arginine by charge affinity chromatography using an equilibrated resin. ^{3}[H]citrulline levels were determined using liquid scintillation counting compared to that of the total reaction mixture and then normalised to the control. Data represent the mean ± SD (n = 3). One-way ANOVA with Dunnett's multiple comparison test between treatment groups and control. * and ** represent p < 0.05 and 0.01 respectively compared to control LDL.*

To determine the mechanism involved in modified LDL-induced loss in eNOS activity and subsequent decrease in NO production, eNOS mRNA and protein expression was assessed by qPCR normalised to the expression of the 18S and β2M housekeeping genes, and Western blotting normalised to β-actin normalising protein, respectively. No change in eNOS mRNA expression was observed when HCAEC were incubated with control LDL or LDL modified by HOCl for 3 or 24 h (Figure 5.6A). In comparison, HCAEC incubated with LDL modified by 250 µM HOSCN significantly upregulated mRNA expression of eNOS at both 3 and 24 h time points (Figure 5.6A). Next, Western blot experiments were performed to determine both the total eNOS expression and activating phosphorylation site Ser^{1177} of eNOS (which is Akt-

dependent and promotes NO synthesis [650]). From these experiments, no significant change in total eNOS or eNOS phosphorylation was observed after 24 h incubation with control LDL or MPO oxidant-modified LDL relative to the β-actin loading control (Figure 5.6B and C). Given that electron transfer between the monomers of the homodimeric form of eNOS is necessary for L-Arg catalysis and NO production [651], further assessment of the dimer-to-monomer ratio of eNOS to assess the coupling state of eNOS was also undertaken. Following 24 h exposure to LDL modified by 250 μM HOSCN, there was a significant decrease in the expression of the dimer: monomer ratio of eNOS compared to the HCAEC exposed to untreated control or incubation control LDL (Figure 5.6D). A similar trend in eNOS uncoupling was also observed within HCAEC exposed to HOCl-oxidised LDL, although this did not reach statistical significance (Figure 5.6D).

Given these results, it was prudent to assess the extent of eNOS phosphorylation following shorter incubation times with LDL modified HOSCN or HOCl was further analysed in a preliminary time-course plotting MPO oxidant-modified LDL exposure over 1, 3 and 24 h on the extent of eNOS S^{1177} phosphorylation (Figure 5.7). Following HCAEC exposure to oxidised LDL for either 1, 3 or 24 h exposure, the data demonstrated that there was no clear difference in the proportion of phosphorylated eNOS between LDL treatments. These data suggest that it is therefore unlikely that LDL modified by HOSCN or HOCl decreases eNOS activity through disruption of eNOS phosphorylation, at the very least with respect to phosphorylation occurring at the S^{1177} residue.

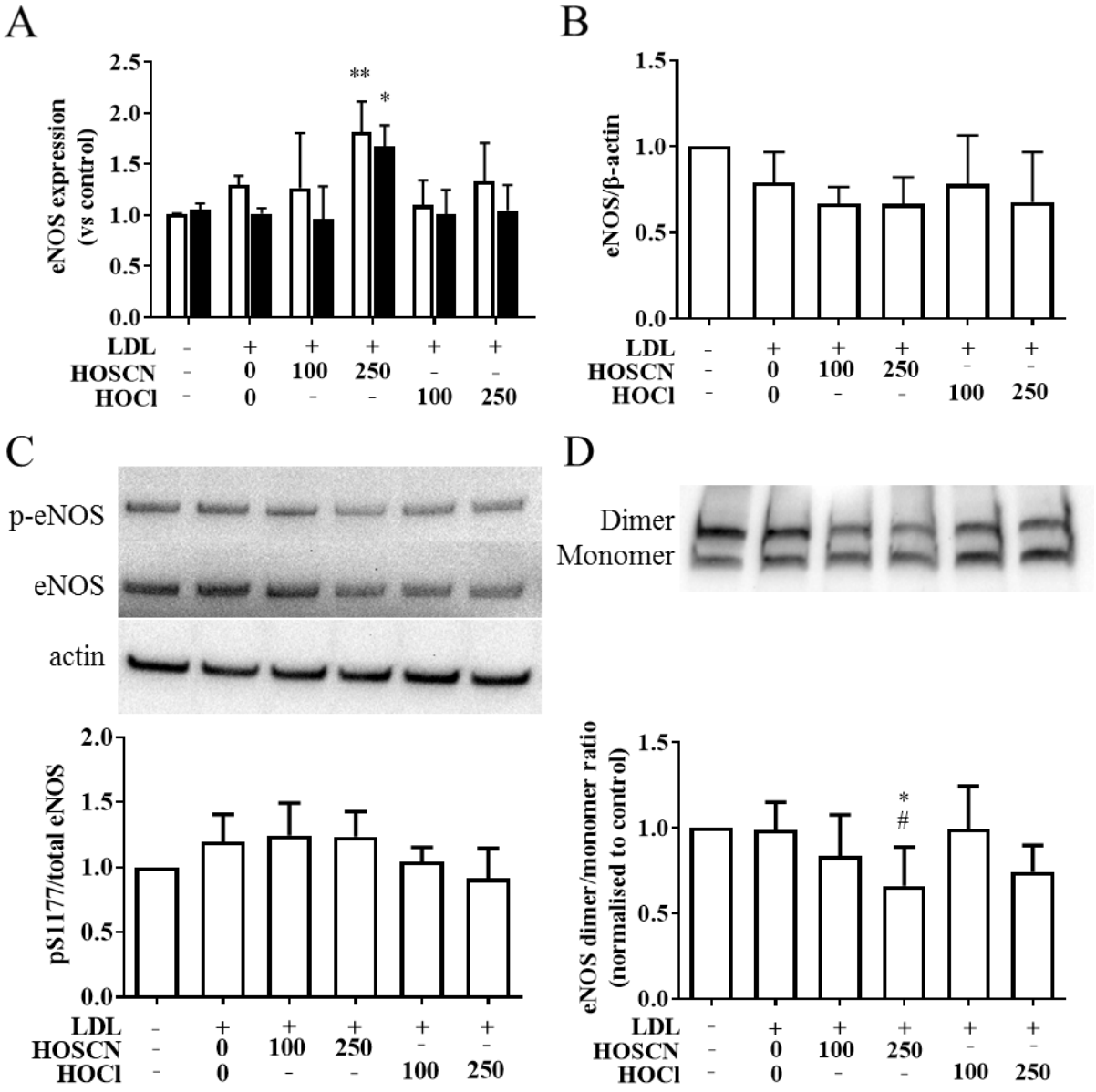

Figure 5.6. Expression, post-translational modification and uncoupling of eNOS in HCAEC after incubation with LDL modified by HOSCN or HOCl. *1.0 mg•mL^{-1} control LDL or LDL modified by 100 or 250 µM HOSCN or 100 or 250 µM HOCl for 24 h. HCAEC were treated with 0.1 mg•mL^{-1} of LDL or oxidised LDL species for 24 h at 37 °C. (A) eNOS mRNA expression following 3 h (white bar) and 24 h (black bar) incubation with each LDL treatment was normalised to 18S and β2M normalising genes (n = 3). (B, C) eNOS normalisation to β-actin loading control and phosphorylation of S^{1177}-eNOS (p-eNOS; n = 3). (D) eNOS coupling assessed by the dimer: monomer ratio of eNOS (n ≥ 3). Representative blots are displayed on top of and in line with the bar graph labels. One-way ANOVA with Dunnett's multiple comparison test between treatment groups and control LDL. * represent p < 0.05 compared to control LDL.*

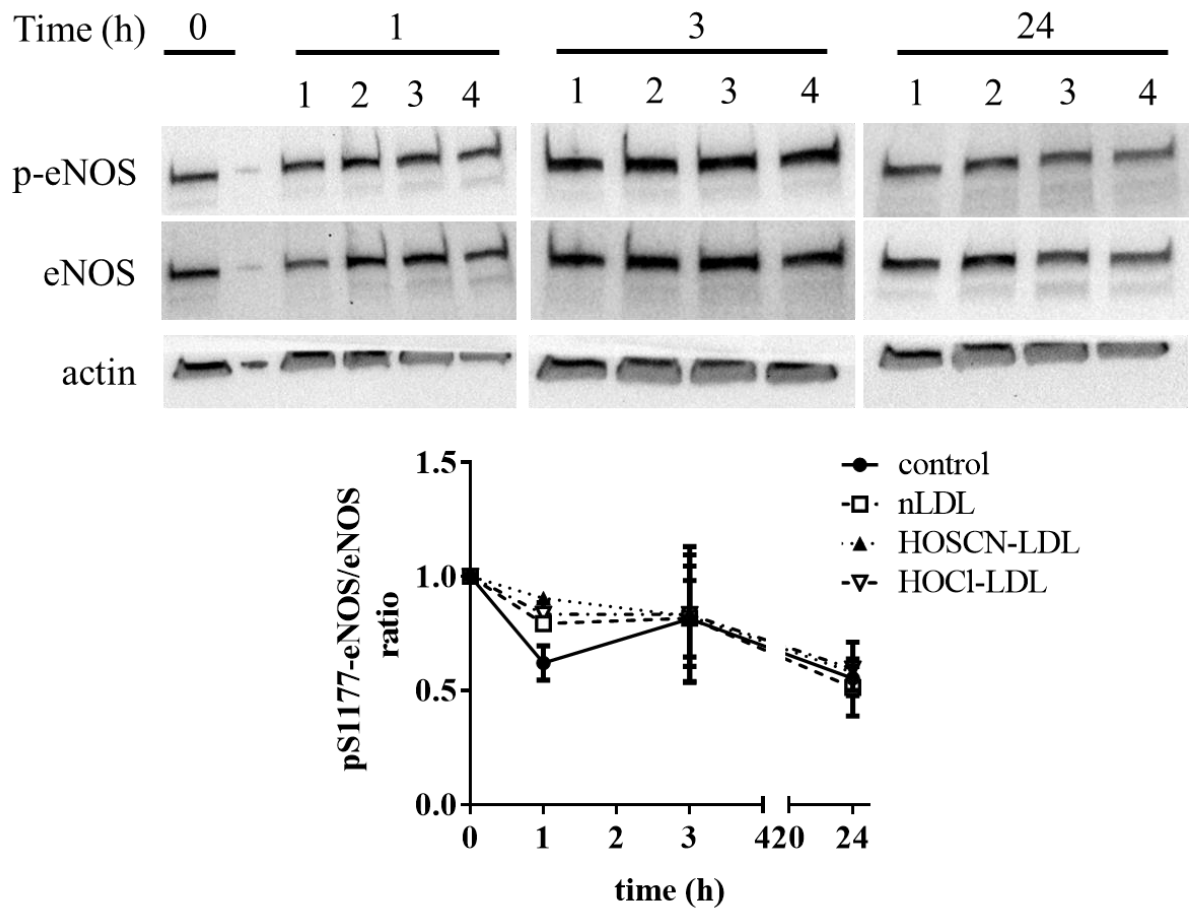

Figure 5.7. Time-course of S1177 phosphorylation of eNOS in HCAEC after incubation with LDL modified by HOSCN or HOCl. *1.0 mg•mL^{-1} control LDL or LDL modified by 100 or 250 µM HOSCN or 100 or 250 µM HOCl for 24 h. HCAEC were treated with 0.1 mg•mL^{-1} of LDL or oxidised LDL species for 1, 3 or 24 h at 37 °C. β-actin was used as a loading control. Representative blots are labelled as; (1) control, (2) control LDL, (3) LDL modified by 250 µM HOSCN, and (4) LDL modified by 250 µM HOCl (n = 2).*

5.3.3. $O_2^{\bullet-}$ production in HCAEC

Uncoupling of eNOS results in the failure of eNOS to catalyse a reaction with O_2 and L-Arg to form NO and L-Cit, decreasing NO production but favouring the reduction of O_2 to $O_2^{\bullet-}$, which, in addition to reducing NO levels can also lead to formation of a potent oxidant $ONOO^-$ [633]. Due to the eNOS uncoupling observed following incubation of HCAEC with HOSCN-modified LDL, $O_2^{\bullet-}$ production was next investigated by measuring the formation of 2-OH-E^+ following supplementation of DHE to the cells. DHE oxidation and fluorescence is commonly used to detect the production of $O_2^{\bullet-}$ by the formation of the specific product 2-OH-E^+. As 2-OH-E^+ has a similar fluorescence profile to E^+ which is not specific to reaction with $O_2^{\bullet-}$ [652], HPLC was further used to separate and quantify these products (retention time of 2-OH-E^+ ~ 23 min and E^+ ~ 25 min; Figure 5.8A).

HCAEC were incubated with each modified LDL treatment for 24 h, before addition of DHE and further incubated for 30 min to assess $O_2^{\bullet-}$ formation. HCAEC were then lysed and subjected to HPLC separation of DHE, 2-OH-E^+ and E^+, and fluorescent detection of 2-OH-E^+ was undertaken to determine if there was any alteration to $O_2^{\bullet-}$ production, as previously described [653, 654]. No change in 2-OH-E^+ formation was observed on exposure of HCAEC to either HOCl- or HOSCN-modified LDL compared to the cells exposed to control LDL alone, whilst HCAEC incubated with menadione as a positive control [655] had nearly double the 2-OH-E^+ formation (hence, $O_2^{\bullet-}$ production) after 30 min (Figure 5.8B). This supports that $O_2^{\bullet-}$ produced by HCAEC is not increased when measured for a defined period of 24 h after treatment with LDL modified by MPO-derived oxidants under the conditions employed in this study.

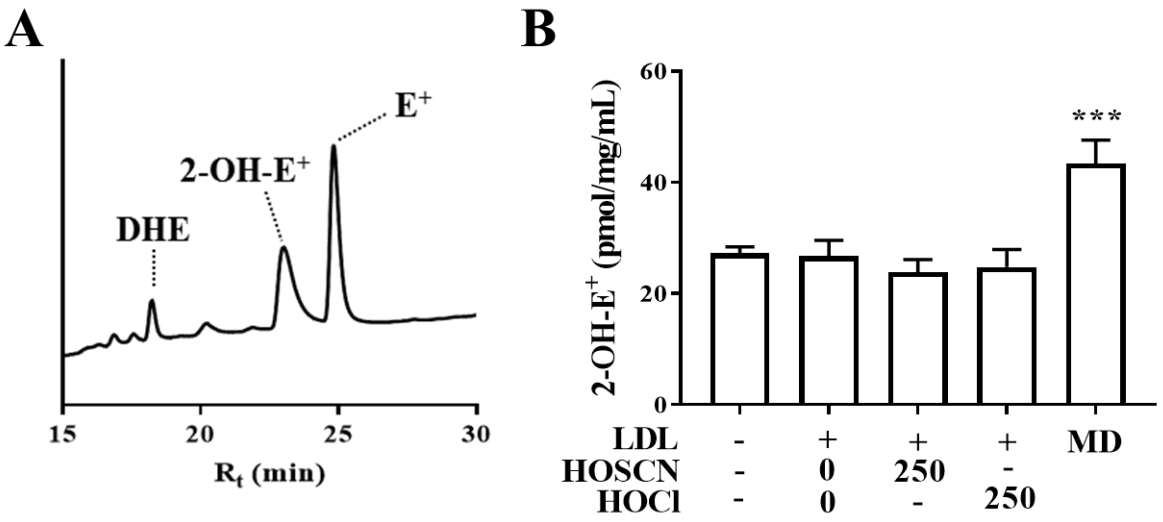

Figure 5.8. Detection of $O_2^{\bullet-}$ in HCAEC following 24 h incubation with LDL modified by HOSCN or HOCl. *1.0 mg•mL^{-1} control LDL or LDL modified by 250 µM HOSCN or 250 µM HOCl for 24 h. HCAEC were treated with 0.1 mg•mL^{-1} of LDL or oxidised LDL species for 24 h at 37 °C. (A) Representative HPLC and fluorescence trace of DHE, 2-OH-E$^+$ and E$^+$ separation. (B) Quantification of 2-OH-E$^+$ fluorescence by area under the curve analysis, normalised to cellular protein measured by BCA assay. MD represents menadione exposure for 30 min. Data represent the mean ± SD (n = 3). One-way ANOVA with Dunnett's multiple comparison test. *** represent p < 0.001 respectively compared to the control.*

The extent of 3-nitroTyr formation on proteins in HCAEC following incubation with MPO oxidant-modified LDL was also measured by Western blot (Figure 5.9) to assess any increase in the production of $ONOO^-$ due to eNOS uncoupling [351, 352]. From those experiments, there was no discernible evidence for increased 3-nitroTyr formation following exposure to LDL modified by MPO-derived oxidants. However, as the results presented here were performed *ad hoc* from the Western blot of the supernatant run-off of the eNOS co-immunoprecipitation experiments described above, there is likely a loss of cellular protein that could unduly influence these results. Additionally, a positive control for the detection of 3-nitroTyr (e.g. nitrated albumin) has not been used to confirm the efficiency of the 3-nitryoTyr

antibody. Hence experiments must be repeated prior to any definitive interpretation of the data presented.

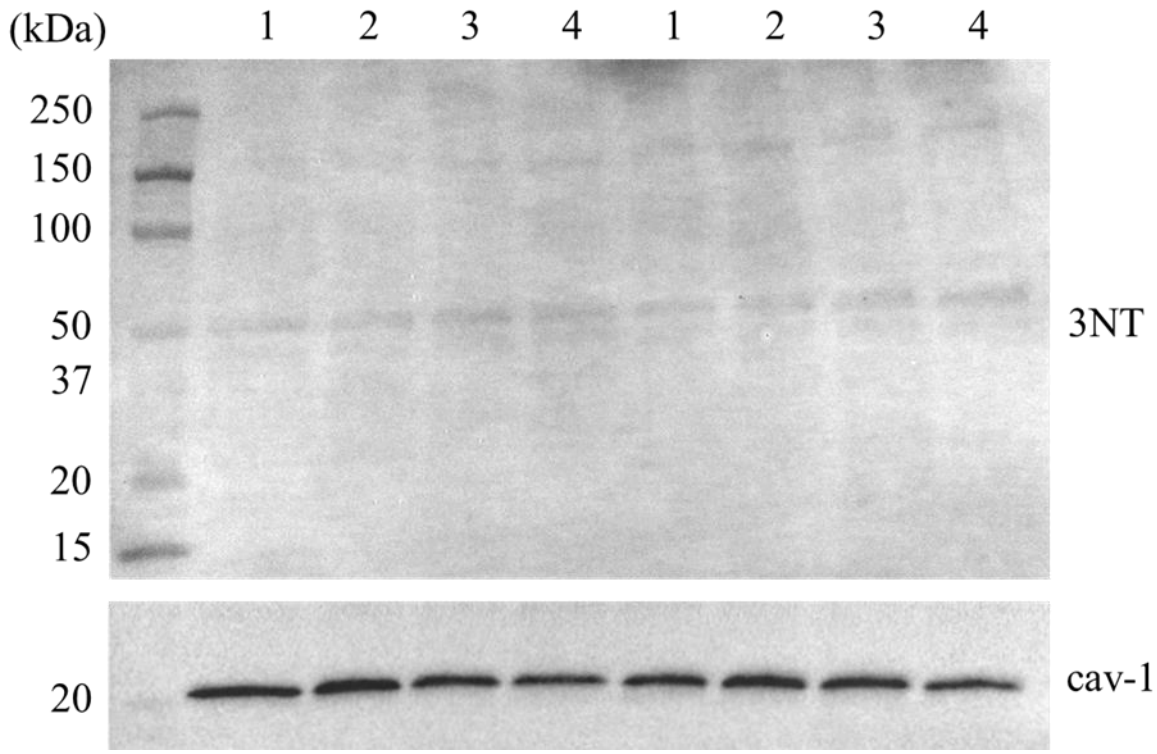

Figure 5.9. No changes in 3-nitroTyr formation in HCAEC exposed to LDL modified by HOSCN or HOCl for 24 h. *1.0 mg.mL^{-1} control LDL or LDL modified by 250 µM HOSCN or 250 µM HOCl for 24 h. HCAEC were untreated (lane 1 and 5) or treated with 0.1 mg.mL^{-1} of control LDL (lane 2 and 6) or LDL modified by HOSCN (lane 3 and 7) or HOCl (lane 4 and 8) for 24 h at 37 °C. The production of ONOO^{-} was assessed by Western blot and immunodetection of 3-nitroTyr (3NT) in the supernatants of the co-immunoprecipitation experiments of cav-1 and eNOS. Representative blot of two independent experiments under high chemiluminescence exposure shows no detectable changes in 3-nitroTyr formation.*

5.3.4. eNOS and cav-1 in HCAEC

Plasma membrane-bound eNOS is particularly concentrated in the caveolae of endothelial cells [656]. Caveolae are rich in the structural and functional protein cav-1, which has been shown to functionally reduce eNOS activity by direct binding [639]. However, this is contradicted in a study of HUVEC, which showed that reduced eNOS activity in response to exposure to LDL modified by HOCl was linked to eNOS delocalisation from the plasma membrane independent of eNOS binding to cav-1 [448]. To confirm the involvement of cav-1 in our model, we next studied cav-1 binding and localisation of eNOS in HCAEC, a cell lineage of physiologically relevant vascular origin, in response to LDL modified by HOCl or HOSCN. Firstly, cav-1 and eNOS colocalisation was assessed by immunofluorescence microscopy (Figure 5.10). Following incubation for 24 h with or without control LDL, eNOS and cav-1 colocalisation was diffuse in the cell, likely throughout the plasma membrane. In contrast, cells incubated with HOSCN- and HOCl-modified LDL generally showed some cellular redistribution of eNOS and cav-1 in some cells, where discrete speckling of colocalised eNOS and cav-1 were observed in the cytoplasm (indicated by the white arrows in Figure 5.10). This likely reflected internalisation of the caveolae from the plasma membrane into the cytoplasm, in which eNOS may be bound to the caveolae and inactivated.

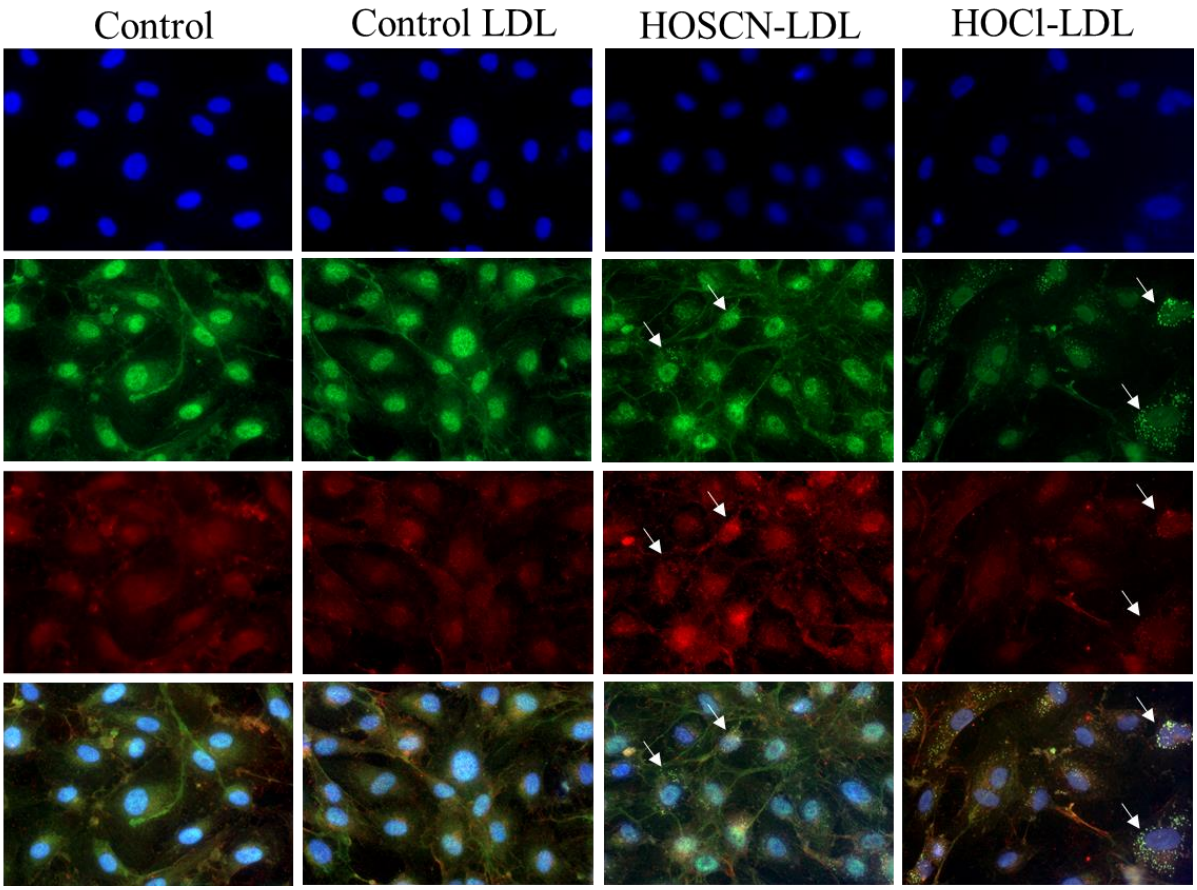

Figure 5.10. Fluorescence microscopic colocalisation of cav-1 and eNOS in HCAEC after incubation with LDL modified by HOSCN or HOCl. *1.0 mg.mL^{-1} control LDL or LDL modified by 250 µM HOSCN or 250 µM HOCl for 24 h. HCAEC were treated with 0.1 mg.mL^{-1} of LDL or oxidised LDL species for 24 h at 37 °C. Columns represent different treatments labelled control, control LDL, 250 µM HOSCN modified LDL and 250 µM HOCl modified LDL. Rows represent staining for the nucleus with DAPI (blue), cav-1 (green), eNOS (red) and the merged image on the bottom. White arrows indicate colocalised fluorescence of eNOS and cav-1 in HCAEC treated with LDL modified by either HOSCN or HOCl. This experiment was replicated three times.*

Next, the binding of cav-1 and eNOS was assessed by cav-1 co-immunoprecipitation by Western blot following immunoprecipitation using an antibody against eNOS. In Figure 5.11, in both eNOS and cav-1 immunoprecipitates (IP: eNOS and IP: cav-1), there were other bands detected by Western blot at approximately 25 and 50 kDa, which is likely the IgG light and heavy chain of the eNOS and cav-1 antibodies of the respective immunoprecipitate. In the IP: eNOS, eNOS was detected, but cav-1 chemiluminescence could not be confirmed because the cav-1 protein is detected at 21 – 24 kDa; approximately the same molecular weight of the IgG light chain (IgG_L). This is shown by the IP: cav-1, which had more intense chemiluminescence at the cav-1 and IgG_L. Therefore, chemiluminescent detection of the immunoprecipitates was performed by substituting the conventional secondary HRP-conjugated antibody for an antibody that only detects the intact (non-denatured) IgG.

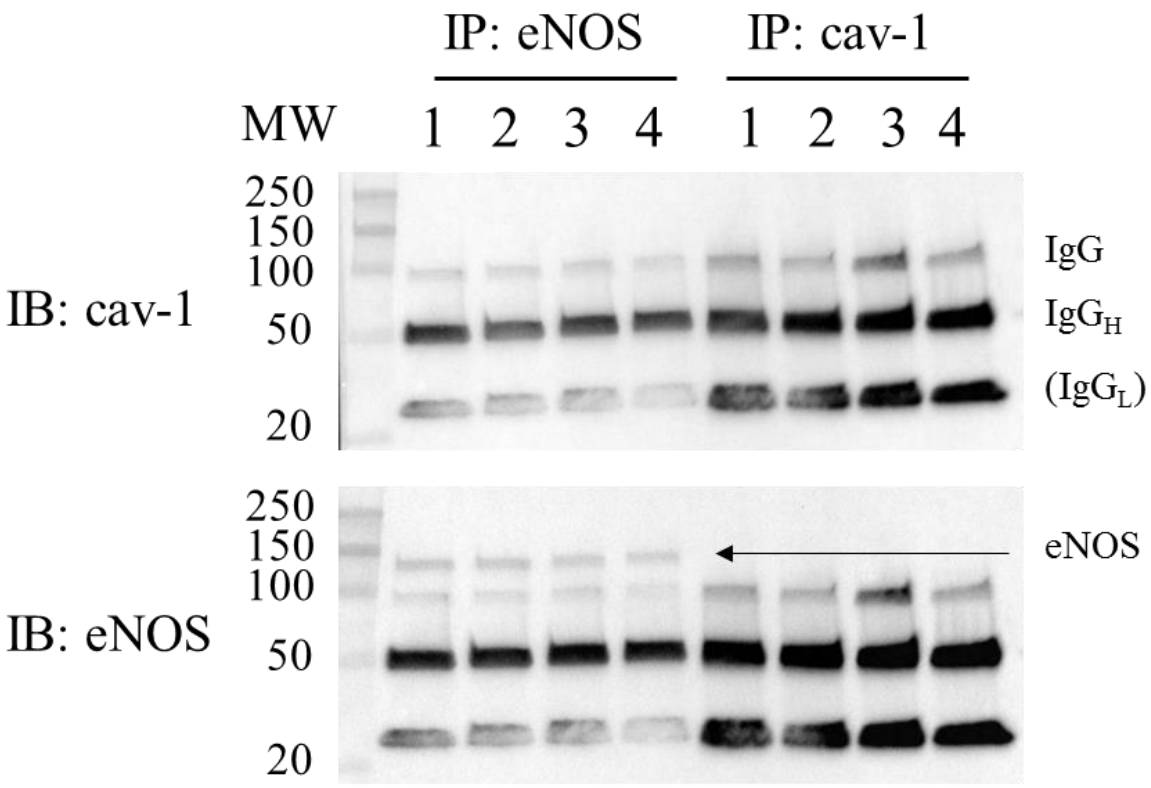

Figure 5.11. IgG contamination in coimmunoprecipitation of cav-1 and eNOS in HCAEC after incubation with LDL modified by HOSCN or HOCl. *1.0 mg•mL^{-1} control LDL or LDL modified by 250 µM HOSCN or 250 µM HOCl for 24 h. HCAEC were treated with; lane 1: no LDL, lane 2: control LDL, lane 3: 250 µM HOSCN-modified LDL, lane 4: 250 µM HOCl-modified LDL. Each LDL treatment was at a concentration of 0.1 mg•mL^{-1} for 24 h at 37 °C. Both immunoprecipitation (IP) of eNOS and cav-1 was performed to isolate from cell lysates and an immunoblot (IB) of eNOS and cav-1 was performed. Intact IgG, and the heavy (IgG$_H$) and light (IgG$_L$) chains sourced from the eNOS and cav-1 IP antibodies were detected and contaminated the immunoblots. This blot is representative of three independent experiments.*

The co-immunoprecipitation results suggest that reduced eNOS activity and NO production in HCAEC by LDL modified by MPO-derived oxidants was not related to altered cav-1-eNOS binding. This is demonstrated through comparison of the IP: eNOS and lysate supernatant blots in the eNOS immunoblot (IB: eNOS) which indicate that immunoprecipitation was efficiently achieved with comparable amounts of eNOS immunoprecipitated from the lysates and low amounts of residual eNOS detected in the lysate supernatant and only following high chemiluminescence exposure. However, in the corresponding immunoblot of cav-1 (IB: Cav-1) in the IP: eNOS, no detectable cav-1 was co-immunoprecipitated with eNOS following 24 h incubation of the HCAEC with control LDL or MPO oxidant-modified LDL, where all the cav-1 detected was in the lysate supernatant, unbound to eNOS (Figure 5.12). These results are disparate to the former fluorescence microscopy which demonstrated that cav-1 and eNOS were colocalised in the cytosol of cells following exposure to LDL modified by HOSCN or HOCl.

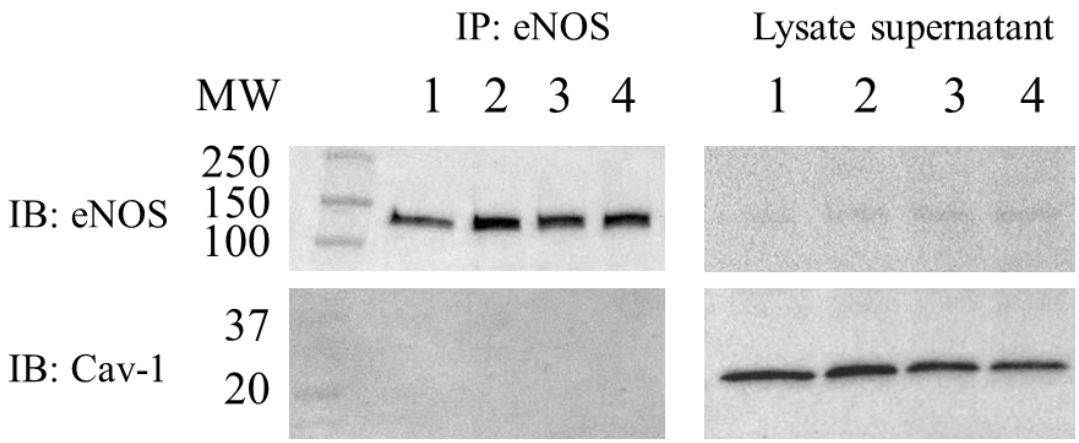

Figure 5.12. Coimmunoprecipitation of cav-1 and eNOS in HCAEC after incubation with LDL modified by HOSCN or HOCl. *1.0 mg•mL^{-1} control LDL or LDL modified by 250 µM HOSCN or 250 µM HOCl for 24 h. HCAEC were treated with; lane 1: no LDL, lane 2: control LDL, lane 3: 250 µM HOSCN-modified LDL, lane 4: 250 µM HOCl-modified LDL for 24 h at 37 °C. IP: immunoprecipitate, IB: immunoblot. Cell lysate supernatant shows the presence of cav-1 after eNOS IP. No cav-1 was detected to be coimmunoprecipitated with eNOS. Blots are representative of three independent experiments.*

5.3.5. Intracellular Ca^{2+} levels in HCAEC

Increases in intracellular calcium levels are a positive regulator of eNOS activity by activating CaM, which then binds to eNOS to promote electron shuttling through the reductase domain to reduce the haem group [657]. Intracellular calcium levels were next assessed in HCAEC incubated with each modified LDL treatment for 1 and 24 h. Specifically, cells were incubated with the fluorescent probe Fluo-4AM; a membrane-permeable which upon binding to Ca^{2+} has an absorption and emission spectra of 488 and 516 nm, respectively [501], following 1 h and 24 h incubation with MPO oxidant-modified LDL. The fluorescence upon Fluo-4AM binding to intracellular Ca^{2+} was measured by flow cytometry.

The representative flow cytometry histogram displays a slight right-shift of the fluorescent population in HCAEC incubated for 24 h with LDL modified by 250 μM HOSCN or HOCl (Figure 5.13A), compared to the non-treated control cells, indicating increased cytosolic Ca^{2+} accumulation. Although quantification of the geometric mean fluorescence of Fluo-4AM within the cells demonstrated no significant increase in intracellular Ca^{2+} following either 1 h or 24 h incubation with control LDL or LDL modified by 250 μM HOSCN or HOCl LDL compared to the control (Figure 5.13B). These data indicate that changes in total intracellular calcium levels are not likely to be involved in altered NO production and eNOS activity in HCAEC.

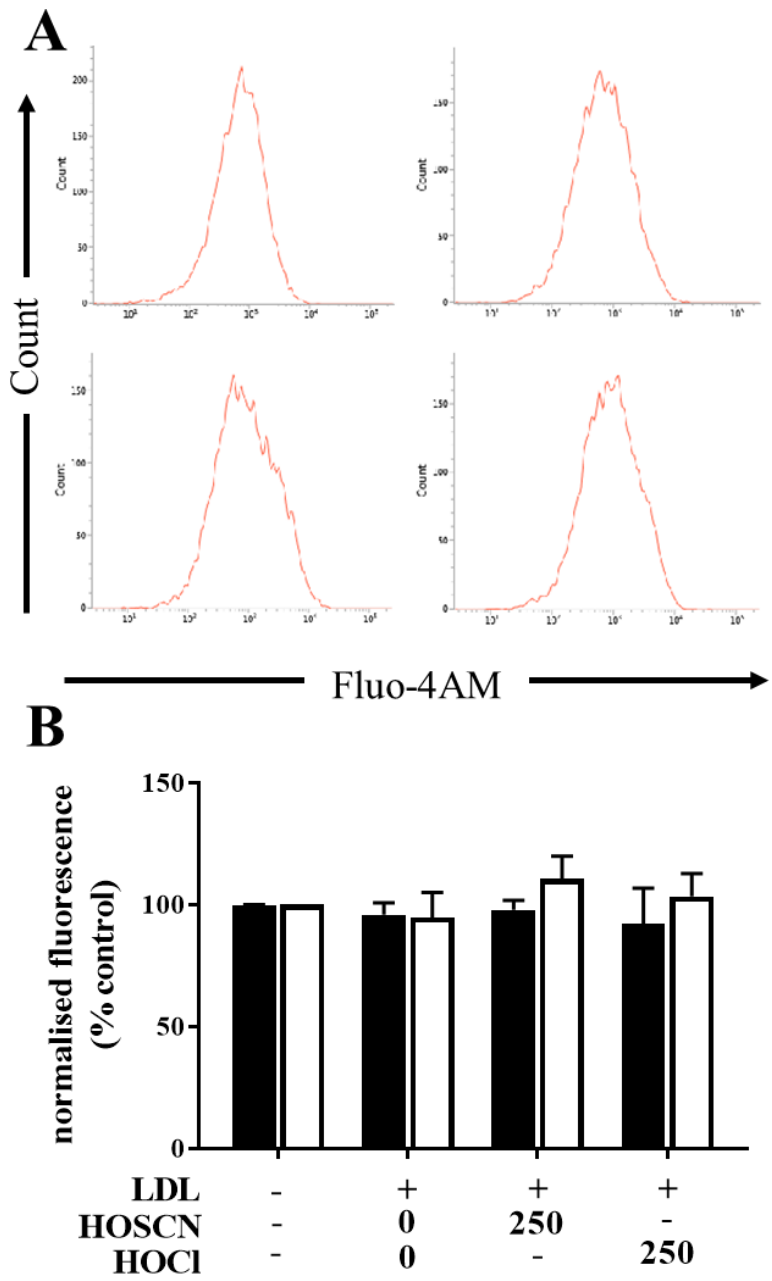

Figure 5.13. Intracellular Ca^{2+} levels in HCAEC incubated with control LDL, HOSCN- and HOCl-modified LDL. *1.0 mg.mL^{-1} control LDL or LDL modified by 250 µM HOSCN or 250 µM HOCl for 24 h. HCAEC were treated with 0.1 mg.mL^{-1} of control LDL or LDL modified by 250 µM HOSCN or HOCl for 1 h (black) or 24 h (white) at 37 °C. (A) Representative histograms of Fluo-4AM fluorescence measured in 24 h treated samples by flow cytometry; top-left; control, top-right; control LDL, bottom-left; HOSCN-modified LDL, bottom-right; HOCl-modified LDL. (B) Geometric mean of the Fluo-4AM fluorescence normalised to the control. Data represent the mean ± SD (n = 3). One-way ANOVA with Dunnett's multiple comparison test.*

5.3.6. Rat aortic ring myography

The impairment of eNOS activity and subsequently reduced NO production *in vivo* plays a key role in endothelial dysfunction in the progression of atherosclerosis [658], therefore the study was extended to consider the effect of LDL modified by HOSCN or HOCl on vasorelaxation using pre-constricted rat aortic tissue. Rat aortic vessel vasodilation was assessed by wire myography following 1 h incubation with (250 μM oxidant) HOSCN- or HOCl-modified LDL *ex vivo*. Figure 5.14A shows the control aortic segment preconstricted with NE (10^{-9} – 10^{-5} M) and dilated with increasing doses of ACh (10^{-8} – 10^{-3} M) until a return to baseline tension was achieved. The sub-maximal dose of 1 μM NE was used for pre-constriction in each experiment prior to ACh- and SNP-induced vasodilation.

Using a non-linear regression model of ACh-induced vasodilation, it was found that control segments reached a maximum vasodilation (E_{max}) of approximately 94 % (Figure 5.14B). Following a 1 h incubation of the aortic segments with control LDL, the E_{max} was mildly, but non-significantly reduced to approximately 81.4 %. However, incubation of the aortic segments with HOSCN-modified LDL or HOCl-modified LDL for 1 h resulted in impaired endothelium-dependent E_{max} of approximately 61.6 % and 59.3 %, respectively. This reached statistical significance for both HOSCN- and HOCl-modified LDL compared to the untreated segments, but not compared to the control LDL. Endothelium-independent vasodilation was also assessed using SNP; a pharmacological NO donor that directly stimulates smooth muscle relaxation [659]. In contrast to the ACh-induced vasodilation, SNP-induced vasorelaxation responses following preconstriction with NE, were not significant different between the control and all LDL treatments (control: 99.4 %, control LDL: 99.5 %, HOSCN-modified LDL: 93.3 % and HOCl-modified LDL: 98.8 %; Figure 5.12C). This suggests that the impaired vasodilation observed with modified LDL was endothelium-dependent.

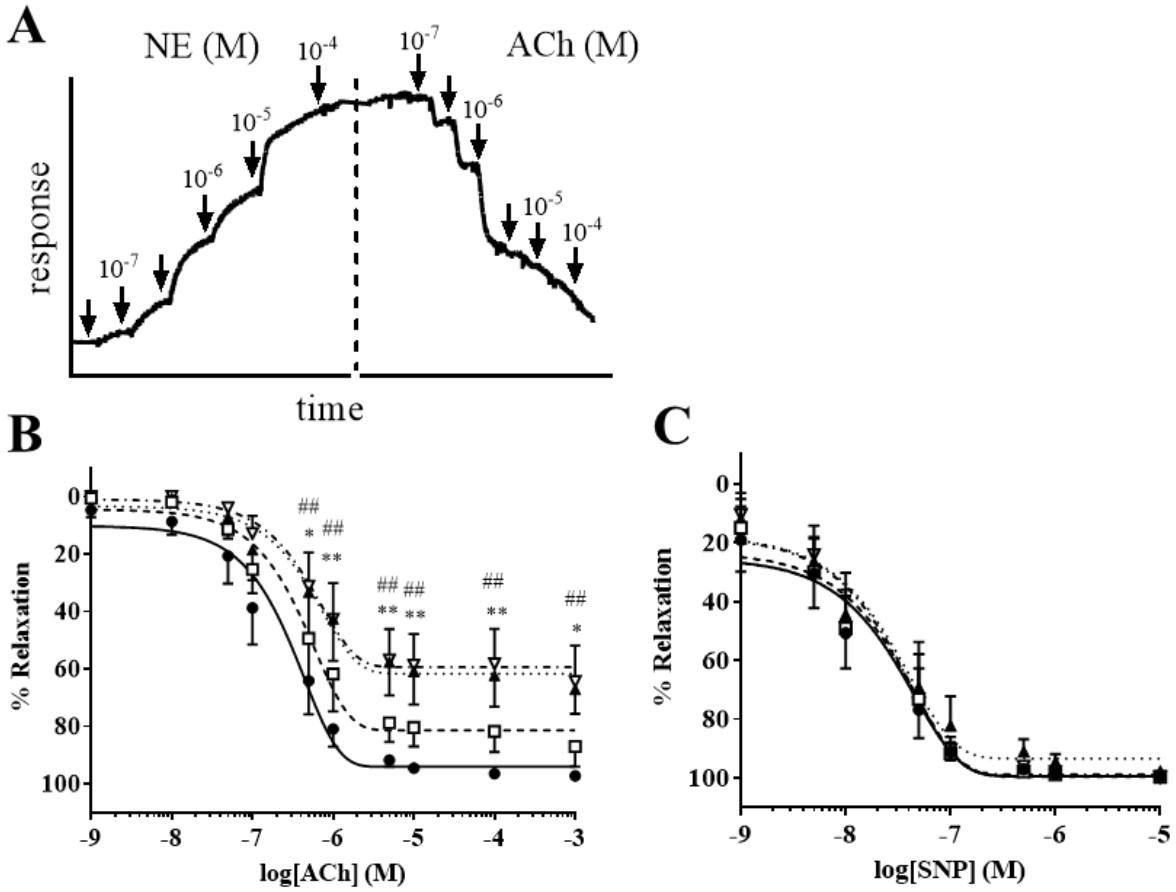

Figure 5.14. Vasodilation dose-response of rat aortic segments to acetylcholine and sodium nitroprusside following incubation with LDL modified by HOSCN or HOCl for 1 h. *1.0 mg•mL^{-1} control LDL or LDL modified by 250 µM HOSCN or 250 µM HOCl for 24 h. Sprague-Dawley Rat aortic rings were treated with 0.1 mg•mL^{-1} of LDL or LDL modified by 250 µM HOSCN or HOCl for 1 h in HBSS at 37 °C. (A) Representative example of a myographic trace of rat aortic segment vasoconstricted with increasing doses of NE (5 × 10^{-7} to 1 × 10^{-4} M) and vasodilated with increasing doses of ACh (1 × 10^{-7} to 1 × 10^{-4} M). Rat aortic segments were preconstricted with a submaximal dose of NE and relaxation was assessed by accumulative doses of (B) ACh (10^{-9} to 10^{-3} M) and (C) SNP (10^{-9} to 10^{-5} M). Symbols represent (●) control, (□) control LDL, (▲) 250 µM HOSCN-modified LDL and (▽) 250 µM HOCl-modified LDL. Non-linear dose-response curves; (solid line) control, (dashed line) control LDL, (dotted line) 250 µM HOSCN-modified LDL and (dashed and dotted line) 250 µM HOCl-modified LDL. Data represent the mean ± SE (n = 5). Two-way ANOVA with Dunnett's multiple comparison test. * and ** represents significant difference (p < 0.05 and 0.01, respectively) between HOSCN-modified LDL compared to the control. ## represents significant difference (p < 0.01) between HOCl-modified LDL compared to the control.*

Rat aortic segments were also incubated with LDL modified by 250 μM HOSCN or HOCl for 24 h in endothelial treatment media in order to align the time points used for the *in vitro* experiments with HCAEC to the *ex vivo* setting. Unlike the SNP-dependent dose-response curve, a non-linear dose-response model could not be obtained for ACh-dependent vasodilation. This was due to the large variance of the response to ACh-induced vasodilation at each dose of ACh between each experiment following the extended incubation time.

The dilation of the control segment was largely reduced to approximately 60 % of the maximum level and there was no significant difference between the control LDL or LDL modified by MPO oxidants compared to the control (Figure 5.15A). Like the treatment of vessels for 1 h, the endothelium-independent vasodilation stimulated by SNP was not affected by incubation with MPO oxidant-modified LDL for 24 h (Figure 5.15B). This confirmed that the impaired ACh-induced relaxation was due to endothelial dysfunction. However, the large reduction in the maximum relaxation in the control after 24 h compared to 1 h incubation, suggests that prolonged *ex vivo* incubation of the vessel may have damaged the endothelium.

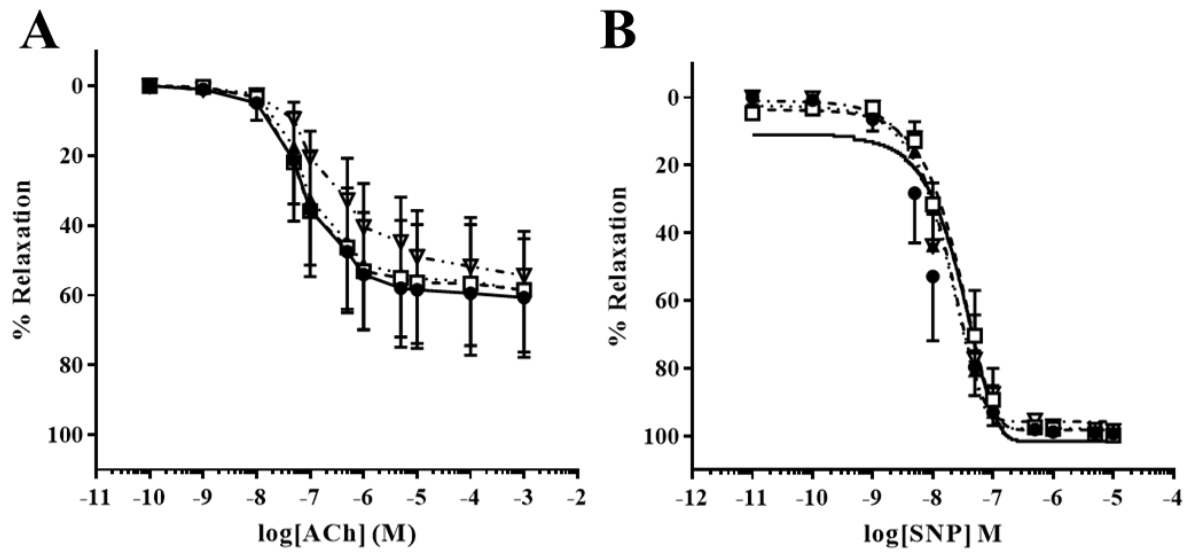

Figure 5.15. Vasodilation dose-response of rat aortic segments to acetylcholine and sodium nitroprusside following incubation with LDL modified by HOSCN or HOCl for 24 h. *1.0 mg•mL^{-1} control LDL or LDL modified by 250 µM HOSCN or 250 µM HOCl for 24 h. Sprague-Dawley Rat aortic rings were treated with 0.1 mg•mL^{-1} of LDL or LDL modified by 250 µM HOSCN or HOCl for 24 h in endothelial cell treatment media at 37 °C. Rat aortic segments were preconstricted with a submaximal dose of NE and relaxation was assessed by accumulative doses of (A) ACh (10^{-10} to 10^{-3} M) and (B) SNP (10^{-11} to 10^{-5} M). Symbols represent (●) control, (□) control LDL, (▲) 250 µM HOSCN-modified LDL and (▽) 250 µM HOCl-modified LDL. Non-linear dose-response curves for SNP-dependent vasodilation; (solid line) control, (dashed line) control LDL, (dotted line) 250 µM HOSCN-modified LDL and (dashed and dotted line) 250 µM HOCl-modified LDL. Data represent the mean ± SE (n = 3). Two-way ANOVA with Dunnett's multiple comparison test.*

5.4. Discussion

Endothelial dysfunction is a key process in the development of atherosclerosis. A major attribute of endothelial dysfunction has been the reduction in eNOS-dependent vasodilation, due to the reduced bioavailability of NO, causing the characteristic arterial stiffening in atherosclerosis [407, 629, 658, 660]. The disruption of endothelium-dependent NO and vasodilation by some forms of oxidised LDL, particularly Cu^{2+}-oxidised LDL, is well established [408, 661]. The most commonly studied form of oxidised LDL is LDL modified by Cu^{2+} ions (5 – 10 μM), which forms an extensively-modified particle with reactive lipid oxidation products. In contrast, few studies have investigated effects of LDL modified directly by MPO or by its oxidant product HOCl upon endothelial cells, though there is evidence for this type of modified LDL in both the diseased tissue and the circulation of people with atherosclerosis [233, 290]. Additionally, the contribution of the other major MPO-derived oxidant, HOSCN, to the modification of LDL and the effect of HOSCN-modified LDL on endothelial function remains to be characterised. This is significant in light of the correlation between plasma SCN^- (the precursor of HOSCN) levels and foam cell formation in early atherosclerotic development in smokers [254, 662] as well as the link to coronary artery disease, future myocardial infarction and death [255].

The results of this Chapter clearly demonstrate that LDL modified by HOSCN or HOCl causes endothelial dysfunction by impairing eNOS activity and subsequently decreased NO production. LDL modified by HOSCN or HOCl induced eNOS uncoupling after 24 h, as shown by a loss of the functional eNOS dimer, but did not alter S^{1177} eNOS phosphorylation or eNOS protein expression. One difference was that HOSCN-modified LDL significantly elevated eNOS mRNA expression, while HOCl-modified LDL did not; possibly indicating an independent cell response to HOSCN-modified LDL. However, $O_2^{\bullet-}$ production was not

elevated, nor was there increased detection of 3-nitroTyr to indicate reduction of NO by $O_2^{\bullet-}$ to produce $ONOO^-$. Fluorescence microscopic analysis of cav-1 as a key regulator of eNOS activity showed there was increased presence of eNOS colocalised with cav-1 in the cytosol following exposure to LDL modified by either HOSCN or HOCl, but despite this, immunoprecipitation of eNOS following exposure to these LDL treatments did not show cav-1 binding. Regardless, when extended to treating intact rat aortic segments *ex vivo*, LDL modified by either (250 μM oxidant) HOSCN or HOCl significantly impaired eNOS-dependent vasodilation.

Therefore, this study shows for the first time that LDL modified by HOSCN alters eNOS gene expression and functionality, decreases the endothelial production of NO and impairs the endothelium-dependent vasodilation. In comparison, the effect of HOSCN-modified LDL on eNOS activity and NO production are similar to or, in some cases, greater than that seen in with LDL modified by HOCl.

5.4.1. Regulation of endothelial cell NO production, eNOS expression, uncoupling and vessel relaxation

Both intracellular and extracellular NO levels were reduced by incubation of HCAEC with either control LDL or each type of MPO oxidant-modified LDL. That is, a significant reduction of NO production was measured after 24 h incubation with control LDL, HOSCN-modified LDL and HOCl-modified LDL compared to the untreated control as determined by direct measurement using both flow cytometry and EPR analysis. Similar results were seen on measuring eNOS activity in terms of the formation of ^{3}[H]citrulline. The observed effects were independent of intracellular calcium levels as assessed by Fluo-4AM fluorescence, or changes in the phosphorylation of the Ser^{1177} residue of eNOS, which is known to promote NO production [663]. In this case, the difference in ^{3}[H]citrulline formation between treatments

was larger than the difference in NO detected by EPR between the treatments. Conditions were slightly different in the two experiments; EPR was performed following 30 min incubation at 37 °C with the $Fe(MGD)_2$ spin trap to adduct with NO produced by intact HCAEC, while eNOS activity was measured by ^{3}[H]citrulline formation over the course of 1 h at 21 °C in HCAEC lysates. Although both methods are highly sensitive to changes in eNOS activity, it is speculated that this difference arises from the eNOS activity being measured in cell lysates, while the detection of NO in the supernatant by EPR was from intact cells directly after treatment. Intact cells will maintain structural and protein-protein interactions which can regulate eNOS activity, which is unlikely to be the case in cell lysates. Additionally, EPR provides a direct measure of NO, which could be influenced by other factors though the signal was significantly decreased by the specific inhibitor L-NIO, other factors could influence the NO adduct stability. However, the measurement of ^{3}[H]citrulline formation incorporates several sample processing steps, which take time and add to the sources of experimental error, as can be the case with commercial kits. Nevertheless, collectively the results demonstrate a reduction in eNOS activity with a concurrent decrease in NO production in HCAEC following incubation with control LDL or MPO oxidant-modified LDL. Similar effects have also been shown in previous studies that demonstrated eNOS activity was sensitive to other types of oxidised LDL [664].

No change in total intracellular Ca^{2+} levels was detected by Fluo-4 AM fluorescence measured by flow cytometry. However, a limitation to note is that flow cytometry is not sensitive to measuring Ca^{2+} flux in cells over time. Early fluctuations in Ca^{2+} influx seconds to minutes after initial exposure to LDL modified by MPO-derived oxidants were not measured. It may also be pertinent to assess possible alterations in Ca^{2+} localisation in endothelial cells, as a spike in Ca^{2+} flux to the cytosol may not only come from the influx of extracellular Ca^{2+},

but from release of Ca^{2+} from granules or organelles inside the cell [665]. This could be investigated by fluorescence confocal microscopy and would be valuable in future studies.

One major difference between the treatment of HCAEC with LDL modified by HOSCN or HOCl was treatment with the former resulted in the approximately two-fold upregulation of the eNOS mRNA after both 3 h and 24 h treatment, though this did not translate to an increase in eNOS protein expression after 24 h when measured by Western blot. This difference in mRNA gene expression after treatment with HOSCN- compared to control LDL and HOCl-modified LDL could be indicative of a disparate response of endothelial cells to these different LDL species. Determining the mechanism of uptake of LDL modified by either HOSCN or HOCl could explain this difference, however the current study did not determine endothelial cell receptor binding to HOSCN- or HOCl-modified LDL. The reaction of HOSCN with LDL lipids to form linoleate-derived oxidation products, which are formed significantly at HOSCN concentrations as low as 50 μM per 1 $mg{\cdot}mL^{-1}$ LDL, but do not form at significant levels when LDL was exposed to HOCl [146], have been shown to modulate eNOS mRNA expression. Linoleate-derived oxidation products, such as 13-hydroperoxyoctadecadienoate (13-HODE) have been demonstrated to increase eNOS mRNA expression in BAEC [666]. However, this also translated to upregulated eNOS protein expression and proportionate increase in activity [666], which was not observed in this study with HOSCN-modified LDL. It could also be possible that parallel post-transcriptional regulatory mechanisms, such as eNOS antisense RNA (called NOS3AS or sONE) could be activated which prevent the translation of eNOS protein by compromising eNOS mRNA stability [667]. Alternatively, a number of microRNAs (small ~22 nucleotide non-coding single-stranded RNA) including miRNA-24 [668] and miRNA-27 [669] are known to post-transcriptionally regulate eNOS expression. The current study did not investigate on eNOS sense-antisense or miRNA interactions, hence future studies

interrogating the effects of HOSCN-modified LDL or related products (e.g. 13-HODE) in these pathways could be of interest.

In each case, the extent of eNOS uncoupling, rather than phosphorylation aligned with the reduced eNOS activity and $NO^{\bullet}$ production. However, no change in $O_2^{\bullet-}$ production was detected upon measuring the formation of 2-OH-E^+ following addition of DHE and further incubation in HCAEC at the same time point. One study by Fleming *et al* observed increased reactive oxygen species production in HUVEC incubated for 24 h with Cu^{2+}-oxidised LDL [524]. The reactive oxygen species produced was assumed to be $O_2^{\bullet-}$, but the luminol chemiluminescence detection utilised in that study is known to detect other reactive oxygen species and thus it is not a conclusive measure of $O_2^{\bullet-}$ [670, 671]. Regardless, this was concurrent with increased Akt phosphorylation and T^{495} dephosphorylation, and reduced downstream PKC phosphorylation and activity, while CaM binding was unaltered [524]. Similar to this study, the same authors also observed no change in S^{1177} phosphorylation, while eNOS became delocalised from the plasma membrane into the cytosol. Perturbations in $O_2^{\bullet-}$ production in endothelial cells exposed to (non-MPO-mediated) oxidised LDL leading to eNOS uncoupling have also been causatively linked to LOX-1 binding (reviewed [672]). It is also founded that other types of oxidised LDL can activate MAPK and PKC-mediated pathways, which can influence eNOS phosphorylation and alter $O_2^{\bullet-}$ production [664, 673]. The role of these pathways in the altered NO production of HCAEC exposed to HOSCN- and HOCl-modified LDL in these experimental conditions was not assessed, however, no changes in scavenger receptor expression nor evidence of sterol accumulation via modified LDL uptake were apparent on comparison to control LDL, as described in the previous Chapter (Section 4.3.3.1; Figure 4.5 and 4.6).

A limitation for the measurement of $O_2^{\bullet-}$ production in the current study is that $O_2^{\bullet-}$ was measured over a defined time-period of 30 min following 24 h treatment of HCAEC with

modified LDL. Altered flux in reactive oxygen species production can rapidly occur in endothelial cells in response to other types of oxidised LDL [672], so it is possible that increased $O_2^{\bullet-}$ production as a result of eNOS uncoupling could be induced by MPO oxidant-modified LDL in early response phases of endothelial cells. The lack of change in $O_2^{\bullet-}$ detected also does not seem to be due to scavenging of $O_2^{\bullet-}$ by NO to form $ONOO^-$, as no change in the formation of 3-nitroTyr (a marker of $ONOO^-$ reactivity) in HCAEC was observed by immunodetection using Western blot. However, it would be useful to confirm these data in experiments in the absence of conditions pertaining to co-immunoprecipitation. Currently, no comparative studies have been undertaken to determine the effect of MPO-derived oxidation of LDL on $ONOO^-$ formation in endothelial cells. However, one study by Steffen *et al* demonstrated that MPO-derived nitration of LDL (with a MPO-H_2O_2-NO_2^- system) promoted carbonylation, nitration (by detection of 3-nitroTyr) and 4-hydroxynonenal (4-HNE; lipid peroxidation product) modification of cellular proteins in BAEC and HUVEC [674]. However, this was related to an increase in $O_2^{\bullet-}$ production, downregulation of eNOS expression and concurrent upregulation of iNOS, overall increasing NO production in endothelial cells [674], likely leading to $ONOO^-$ formation; none of which was observed in the current study. Given that increased NO and $O_2^{\bullet-}$ production and 3-nitroTyr formation were observed in that study [674], while NO was decreased and $O_2^{\bullet-}$ was unchanged in this study, it is likely no significant $ONOO^-$ formation was induced by HOSCN- or HOCl-modified LDL.

The lack of altered $O_2^{\bullet-}$ production could also be related, at least in part, by the reliance of eNOS activity upon endogenous cofactors, like BH_4, which bind to haem and L-Arg to facilitate NO release [445]. In the catalytic process, BH_4 is oxidised to the $BH_3^{\bullet}$ radical, which can be recovered to BH_4 with ascorbate and eNOS itself in a $BH_4/BH_3^{\bullet}$ redox cycle [675]. In the current study, eNOS coupling was impaired by HOSCN-modified LDL and to a lesser extent with HOCl-modified LDL, so depletion or displacement of BH_4 may be an important

factor in modulating eNOS activity in MPO-oxidant modified LDL due to reduced cycling of $BH_3^{\bullet}$ to BH_4, but this was not assessed. Further, $O_2^{\bullet-}$ production can be dependent on the equilibrium between BH_4 and the oxidised product BH_2, where BH_4 favours NO production while BH_2 promotes production of $O_2^{\bullet-}$, mediated by uncoupled eNOS activity and independent of the L-Arg concentration [444]. Small trials of acute BH_4 supplementation were found to improve endothelial function in the brachial artery and coronary artery of hypercholesterolaemia patients [676, 677] and the brachial artery of long-term smokers [678]. Further, a small double-blind, randomised trial of acute and chronic BH_4 supplementation in patients with hypercholesterolaemia indeed showed a benefit towards endothelial function with increased NO and decreased $O_2^{\bullet-}$ production [679]. These results suggest that the inflammation and elevated LDL levels that contributed to endothelial dysfunction could be partially reversible by administration of eNOS cofactors. However, the contribution of BH_4 to eNOS (re)coupling in these studies are difficult to determine, as BH_4 is not eNOS specific and can act as general antioxidant through redox cycling, such as ascorbate as described above. Notably, in the study by Nuszkowski *et al*, the loss of eNOS activity in HUVEC incubated with LDL modified by HOCl was not due to changes in BH_4 levels or binding to eNOS [448].

5.4.2. Caveolae and cav-1

Cav-1 has been shown to regulate eNOS specifically inhibiting eNOS activity resulting in an inhibition of NO-dependent vascular distensibility *in vivo* [680]. As caveolae are key structures for the endocytosis of LDL and oxidised LDL from the circulation [656, 681-683], the effect of MPO oxidant-modified LDL upon eNOS may involve cav-1-linked eNOS inactivation [684-686]. In HCAEC, the data presented supports alterations in cellular compartmentalisation of eNOS in response to HOSCN- and HOCl-modified LDL, which was more pronounced on exposure to the latter. eNOS appeared to colocalise with cav-1 based on immunofluorescence detection, in contrast to a previous study in HUVEC, where there was no

change in cav-1 localisation alongside eNOS [448]. However, cav-1 did not co-immunoprecipitate with eNOS, indicating that no direct binding of cav-1 to eNOS was demonstrable. Disruption of the interaction between eNOS and cav-1 proteins resulting from the experimental conditions used to precipitate and resolubilise the cell lysates for analysis cannot be ruled out. The current study analysed total cav-1-eNOS binding in the cell, however separating the cellular compartments (caveolae, plasma membrane and Golgi apparatus) from the cytosol for individual analysis may be helpful for determining the intracellular fate of eNOS following exposure to MPO oxidant-modified LDL. This has been performed in previous studies that individually analysed cav-1-eNOS binding in the plasma membrane and the cytosol [448, 687].

Further experiments are required to focus on the effects of HOSCN- and HOCl-modified LDL on the caveolae which may be mediated by the scavenger receptor binding and/or membrane cholesterol content, in order to determine if cav-1 plays a direct role in eNOS uncoupling, or mediates transport of eNOS (along with other caveolae-bound proteins) to other cellular compartments for degradation or functional repurposing. This redistribution of eNOS has been characterised as a response to changes in the physicochemical properties of the plasma membrane, independent of eNOS myristoylation or palmitoylation [448]. This was previously observed with Cu^{2+}-oxidised LDL [516, 682], which ilicited the cytosolic translocation of eNOS as a response to cholesterol depletion in the caveolae, which was prevented by blocking oxidised LDL binding to CD36 [682]. This could be pertinent to HOCl-modified LDL, which has been shown to bind to the same receptor in HUVEC [604], though this has not been examined in HCAEC. Interestingly, HDL was able to reverse delocalisation of eNOS and cav-1 from the caveolae induced by SR-B1-mediated binding of oxidised LDL, resulting in restoration of ACh-stimulated eNOS activity [688]. This was due to preventing loss of cholesterol by HDL donating cholesterol to the caveolar membrane [688]. Whereas, native

LDL alone, albeit at very high concentrations, was shown to promote promote caveolar localisation of eNOS by the promotion of stress fibres by Ras homolog gene family, member A (RhoA) [689].

Uncoupling of eNOS has been shown to be in large part dependent on its interaction with cav-1. Although studies with cav-$1^{-/-}$ mice have exhibited a profound effect of cav-1 upon eNOS functionality [640, 641], the role of cav-1 in cardiovascular system is complex, as deficiency in cav-$1^{-/-}$ in mice also resulted in cardiomyopathies not directly related to eNOS functionality [690, 691]. Instead this appears to be linked to inflammation, as p42/44 MAPK is activated in cardiac fibroblasts of mice lacking cav-1 [691]. Wunderlich *et al* hypothesised that a lack of cav-1 to regulate eNOS leads to an overproduction of NO, thus causing nitrosative stress [692]. This was supported by their observation that young cav-$1^{-/-}$ mice exhibit cardiohypertrophy linked to severely reduced cardiac output, together with enhanced eNOS activity and elevated staining of nitrotyrosine in cardiac tissue [692]. Further, cav-$1^{-/-}$ mice had elevated vascular $O_2^{\bullet-}$ production, which was prevented by endothelial denudation, supplementation with BH_4 (but not tetrahydroneopterin; an analogue of BH_4 unrelated to eNOS activity) or the pharmacological eNOS inhibitor, L-NAME [693]. Together, this evidence links a lack of cav-1 to increased uncoupling of eNOS, oxidative (and nitrosative) stress, tissue damage and cardiac remodelling, which may be a unique oxidative scenario to cardiac tissue as this contradicts the previous findings in peripheral arteries [640, 641]. The colocalisation, but lack of binding of cav-1 and eNOS observed in the current study following treatment with MPO oxidant-modified LDL is difficult to compare to studies using cav-$1^{-/-}$ mice, as the effect of MPO-modified LDL or hypercholesterolaemia on atherosclerosis is these strains are unknown. However, the findings that $O_2^{\bullet-}$ levels remained unchanged while NO production was decreased may indicate that cav-1-dependent endocytosis may lead to inactivation and degradation of the eNOS dimer, but not the resultant $O_2^{\bullet-}$ production by uncoupling.

5.4.3. Rat aortic segment vasodilation

The relevance and significance of the findings from the *in vitro* studies with HCAEC were assessed using an *ex vivo* rat model. Under similar experimental conditions to previous studies that used native LDL, Cu^{2+}- or cell-modified LDL [451, 455, 456], incubation of rat aortic segments with 0.1 mg**.**mL^{-1} LDL modified by HOSCN or HOCl for 1 h caused a significant reduction in ACh-(endothelium-)dependent vasodilation, with no effect on endothelium-independent vasodilation (measured by the response to SNP). LDL modified by either 250 μM HOSCN or HOCl, which significantly decreased eNOS activity and NO production in HCAEC *in vitro*, significantly reduced endothelium-dependent (ACh-induced) vasodilation, but did not alter aortic vasodilation induced by SNP, meaning the impaired arterial distensibility was due to effects on the endothelium and not the underlying smooth muscle. These results have not been reported in the literature previously for HOSCN- or HOCl-modified LDL, and are in line with what was expected based on the *in vitro* findings in HCAEC exposed to the MPO oxidant-modified LDL.

Although treatment with the control LDL significantly reduced NO production in HCAEC *in vitro*, endothelium-dependent vasodilation was not significantly lower in rat aortae stimulated with ACh following exposure to control LDL. Another previous study has shown that 0.5 mg**.**mL^{-1} control LDL also did not impair endothelium-dependent vasodilation in porcine coronary arterioles [455], supporting the findings here. This indicates that although LDL can modulate eNOS activity, this does not interfere as much with ACh signaling to promote NO production in the endothelium compared to HOSCN- or HOCl-modified LDL. This could be attributed to eNOS remaining coupled when endothelial cells were exposed to control LDL, compared to the increased uncoupling seen with exposure to HOSCN- or HOCl-modified LDL, which was demonstrated in the current study in HCAEC *in vitro*.

An aspect of endothelium-derived vasodilation that has not been addressed in the preceding experiments, factors that can influence vasodilation. is the role other endothelium-derived vasodilators. Endothelium-derived hyperpolarising factor (EDHF) is proposed to be released as a compensatory mechanism by endothelial cells to maintain vascular tone should NO production be impaired [694]. NO production was reduced by over 50 % from exposure to HOSCN-modified LDL and 75 % from HOCl-modified LDL as shown by EPR (Figure 5.4), but ACh-dependent vasodilation was only reduced by approximately 40 % by both modified LDL species. This difference may be related to EDHF which is also released by rat vessels in response to stimulation by ACh [695]. Therefore, it would be helpful to perform experiments to measure the release of EDHF in response to modified LDL-induced endothelial dysfunction.

5.5. Conclusions

Together, the data in this study support a role for both HOSCN- and HOCl-modified LDL in decreasing NO production, which translated to impaired endothelium-dependent arterial distensibility in functioning rat aortic vessels by inducing endothelial dysfunction. The comparable decreases in NO production and vasodilation induced by exposure to LDL modified by both HOSCN and HOCl is significant, as there is evidence to support the beneficial effects of SCN^-, which may slow lesion development in atherosclerosis, evidenced by HOSCN-modified LDL not being taken up by macrophages to the same extent as HOCl-LDL [146, 290]. This may have detrimental implications in smokers who have augmented levels of plasma SCN^- and are burdened by increased endothelial dysfunction. This also highlights the need to interrogate other mechanistic pathways to better understand how SCN^- promoting HOSCN formation rather than HOCl influences disease progression, where there can be detrimental or beneficial aspects depending on the inflammatory situation (e.g. thiol availability, MPO activity, presence of lipids) in atherosclerosis or other chronic inflammatory conditions. Although MPO oxidant-modified LDL did not affect vascular smooth muscle relaxation in a

short incubation time, as they are protected by the endothelium, LDL and oxidised LDL can be transported through the endothelium over time to embed in the intimal layer [608, 685, 686, 696], where smooth muscle cells can be directly exposed to oxidised LDL. Therefore, the effect of MPO oxidant-modified LDL on vascular smooth muscle cells was investigated in the following Chapter.

Chapter 6. Smooth muscle cell uptake and response to MPO oxidant-modified LDL

6.1. Introduction

Vascular smooth muscle cells (VSMC) have been implicated in the progression of atherosclerotic plaques by several mechanisms, including foam cell formation and ECM synthesis, the latter of which can lead to the establishment of a fibrous cap and eventually calcification (reviewed [697]). It has been demonstrated that VSMC can take up modified LDL, which accumulates to an extent comparable to macrophage foam cells [475, 698-700]. Notably, in Watanabe heritable hyperlipidaemic rabbits, a greater proportion of foam cells were of SMC origin than macrophage origin in advanced lesions, evidenced by cell-specific monoclonal antibodies (*cf.* 45 % and 30 %, respectively [701]). This has also been shown in atherosclerotic plaques of human coronary arteries, demonstrating that intimal SMC can transform into foam cells [702]. SMC, like endothelial cells and macrophages, express multiple classes of scavenger receptors; such as LOX-1, SR-A and CD36, for which all have demonstrated affinity for Cu^{2+}-oxidised LDL and can promote the intracellular accumulation of lipids [306, 703-705]. However, current evidence for a role of LDL modified by MPO-derived oxidants in VSMC foam cell formation has not been established.

It is generally accepted that the major role of VSMC in the development of atherosclerosis relates to aiding in vascular remodelling (reviewed [697]). VSMC can do this due to their heterogeneity; being able to switch from a contractile phenotype, which mediates vascular contractility in healthy vessels, to a synthetic phenotype, which promotes SMC proliferation, migration, and production of synthetic proteins to aid in repair of the injured vessel [706]. The change in phenotype results in drastic structural and functional changes, where contractile SMC have high abundance of myofilaments for vessel contraction, while synthetic SMC have a high number of synthetic organelles and sparse myofilaments [706, 707]. This is mediated by an array of alterations in gene expression (Figure 6.1).

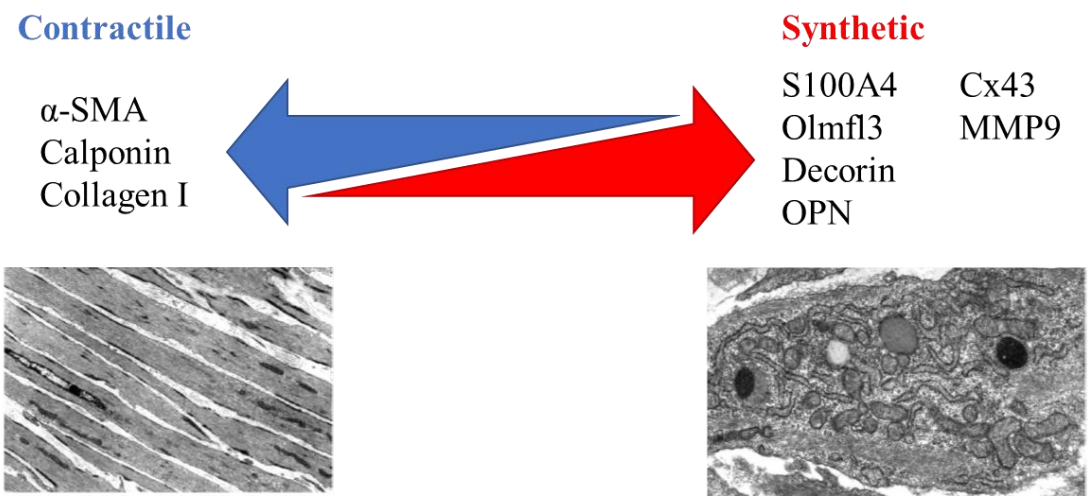

Figure 6.1. Contractile and Synthetic phenotype markers and morphology. *Common markers of VSMC contractile and synthetic phenotypes which were assessed in this current study. Contractile VSMC display a highly striated morphology due to the large abundance of myofilaments (image adapted from [706]), while synthetic phenotypes lose the majority of myofilaments and have a high number of synthetic organelles (image adapted from [707]).*

Muscle contraction-associated genes/proteins, α-smooth muscle actin (α-SMA), smooth muscle-myosin heavy chain (SMMHC) and calponin are constitutively highly expressed in mature contractile VSMC and modulate vasorelaxation/contraction [469, 708-710]. These contractile genes are downregulated upon switching to synthetic-state [711-713]. Osteopontin (OPN); a bone-associated extracellular structural protein with similar role to other structural ECM proteins, is upregulated in the synthetic VSMC [714]. The expression of connexin-43 (Cx43), the primary gap junction protein expressed in VSMC [715], is also upregulated in synthetic SMC [716]. Cx43 upregulation also correlates with increased proliferation and migration of VSMC [711], which was reduced in Cx43 knockdown rat in a balloon angioplasty-model of intimal hyperplasia [717]. Of particular relevance to atherosclerosis, decorin, a dermatan sulfate proteoglycan that links adjacent collagen proteins to form collagen matrices [718]; is highly expressed in arterial SMC [719] and is localised in atherosclerotic lesions [720, 721], particularly near lipid/lipoprotein deposits [722, 723]. An increase in decorin expression also accompanies a shift of less collagen III production and greater collagen I production in

synthetic VSMC [724] and aids in linking LDL to collagen I, providing a mechanism of retaining LDL in lesions [722, 723]. The Ca-binding protein S100A4 is also expressed in synthetic ("rhomboid-shaped") proliferating SMC and human atheromas [725], and was demonstrated to promote proliferation and migration through receptor for advanced glycation end products (RAGE)-dependent NF-κB activation in human pulmonary artery SMC [726, 727]. Recently, olfactomedin-like 3 (Olfml3), a gene encoding a family of proteins with olfactomedin domains which is also involved in cell cycle regulation and tumorogenesis [728], was shown not to be expressed in contractile VSMC subpopulation, but was upregulated in a synthetic subpopulation VSMC which promoted cell proliferation [729].

Calcification; a process of mineralisation of cells/tissue, which is involved in advanced atherosclerotic plaques [730], is positively correlated to an increased risk of MI [731] concurrent with plaque instability [732]. VSMC uptake of oxidised LDL has also been linked to calcification [733, 734]. The synthetic phenotype protein, OPN negatively modulates calcification [735-737], and is found highly expressed in calcified regions of human atherosclerotic plaques near cholesterol depositions and macrophages/smooth muscle cells [738]. OPN inhibits apatite crystallisation to perturb mineralisation, and hence plays a key role in preventing vascular calcification [739]. Conversely, calcification is promoted by the expression of calcification factors, core binding-factor subunit α-1/runt-related transcription factor-2 (Cbfa1/Runx2) and osteocalcin [740, 741]. Unlike in bone, where a loss of decorin is associated with collagen fibril mineralisation [742], decorin expression in synthetic VSMC eventually promotes calcification [741, 743] and is colocalised with calcium deposits in atherosclerotic lesions of sudden coronary death patients [743]. Bovine aortic SMC (BASMC) undergoing calcification had reduced expression of α-SMA and SM22α and upregulation of OPN and osteocalcin, which was followed by Cbfa1 upregulation and corroborated *in vivo* in calcified arterial SMC from $MGP^{-/-}$ mice that exhibit spontaneous arterial calcification [744].

Changes to SMC phenotype, including in response to LDL, could represent a synthetic phenotype transition to stabilise the atherosclerotic plaque and aid in vessel repair. Notably, myosin, myocardin and α-SMA (associated with myofilaments) and calponin expression decreased in VSMC in response to Cu^{2+}- and Fe^{2+}-oxidised LDL [475, 703, 745], which also upregulated expression of toll-like receptor 4 (TLR4), and the scavenger receptors LOX-1 and CD36 in VSMC [475, 703]. Together these studies indicate oxidised LDL promoting a transition away from a contractile phenotype and lipid accumulation, although the expression of classic synthetic markers (such as OPN, decorin, S100A4, Olfml3 and Cx43) have not been assessed following exposure to oxidised LDL. Further, there is currently a lack of data on the role of MPO- or MPO oxidant-modified LDL in modulating VSMC phenotype.

6.2. Aims

The aim of the preliminary studies in this Chapter, using human coronary artery smooth muscle cells (HCASMC) as a model, was to compare HOSCN-modified LDL with HOCl-modified LDL with regard to the degree of LDL uptake, cell viability and gene expression of contractile, synthetic and calcification markers.

6.3. Results

6.3.1. Cell viability and metabolic activity

The effect of each modified LDL on cell viability was determined in HCASMC following exposure to 0.1 mg**.**mL^{-1} modified LDL (prepared from a stock of 1.0 mg**.**mL^{-1} LDL treated without oxidant, or either 250 µM HOSCN or HOCl for 24 h) in a similar manner to that reported in Chapter 4 for HCAEC. HCASMC (seeded at 0.1×10^6 cells**.**mL^{-1}) were exposed to each type of modified LDL species for 24 h and 48 h in SMC basal media supplemented with insulin and 5 % v/v FBS, before performing the LDH assay for cell viability, or the MTT assay

for cell metabolic activity (as described in Section 2.7). Viability was unaltered when HCASMC were incubated with or without control LDL, or HOSCN- or HOCl-modified LDL for 24 or 48 h (Figure 6.2A). Formazan production was also unaltered by treatment with HOSCN- or HOCl-modified LDL treatments after 24 h incubation (Figure 6.2B). Compared to 24 h treatment, there was a general increase in formazan production in the control and LDL treatment groups after 48 h incubation, but this was not statistically different, whilst there was high variability between the HCASMC donors. In summary, HCASMC treated with 0.1 mg.mL^{-1} of incubation control LDL, HOSCN- or HOCl-modified LDL remained viable, while there was a slight stimulatory metabolic effect, similar to the response by HCAEC (refer to Figure 4.1).

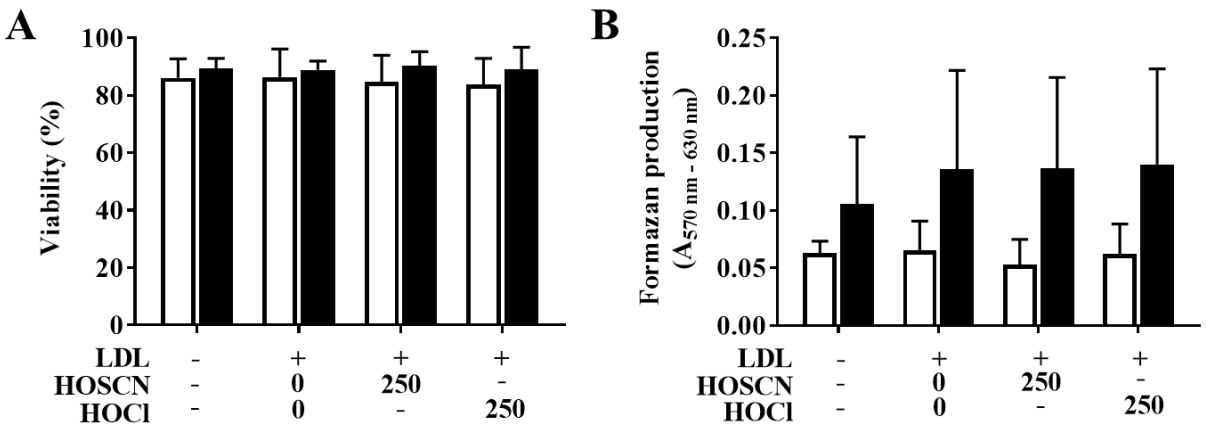

Figure 6.2. Cell viability and activity of HCASMC after incubation with oxidised LDL for 24 h and 48 h. *Firstly, 1.0 mg.mL^{-1} control LDL, or LDL incubated with 250 µM HOSCN or 250 µM HOCl, were incubated at 37 °C for 24 h. Subsequently, HCASMC were treated with 0.1 mg.mL^{-1} of LDL or (250 µM HOSCN or HOCl) oxidised LDL species at 37 °C for 24 h (white bar) or 48 h (black bar) in treatment medium. (A) Cell viability was measured by the LDH activity assay. (B) Cell activity was measured by formazan production (MTT assay). Three independent HCASMC and LDL donors were used. Bars represent the mean ± SD (n = 3). Two-way ANOVA with Dunnett's multiple comparison test between treatment groups and Sidak multiple comparison test between time points. No significant difference between treatments or time points were found.*

6.3.2. Uptake of MPO oxidant-modified LDL

Several studies have shown that human and rat VSMC accumulate lipids following exposure to several forms of modified LDL, including Cu^{2+}-oxidised, which led to foam cell formation *in vitro* [698, 746, 747]. Yet, whether VSMC challenged with LDL modified by MPO or MPO-derived oxidants contributes to lipid accumulation remains to be established. Therefore, given the lack of toxicity and increases in HCASMC metabolic activity following incubation with either control LDL or each MPO oxidant-modified LDL, the next experiment assessed the accumulation of lipids by HCASMC. Cholesterol and cholesteryl ester uptake by HCASMC was measured following the incubation of cells with treatment medium (basal medium supplemented with 5 % FBS and insulin, without growth factors) alone, or with medium with either control LDL, HOSCN- or HOCl-modified LDL, for 24 h and 48 h.

Intracellular lipid levels were increased in HCASMC incubated with the incubation control LDL at both 24 and 48 h time points, however there was no considerable difference between the control and MPO oxidant-modified LDL treatments (Figure 6.3A). At both 24 and 48 h measurements, the proportion of cholesteryl esters in the cell was augmented in incubation control- and MPO oxidant-modified LDL compared to the no LDL-control, but this varied between HCASMC donors and was not significant (Figure 6.3B). However, the time-dependent accumulation of intracellular lipid, expressed as the difference in lipid levels between 24 and 48 h measurements (ΔIntracellular lipids), was generally decreased between the 24 and 48 h time points within each treatment. This suggests that intracellular lipids were not accumulating in the cells upon exposure to LDL for up to 48 h (Table 6.1).

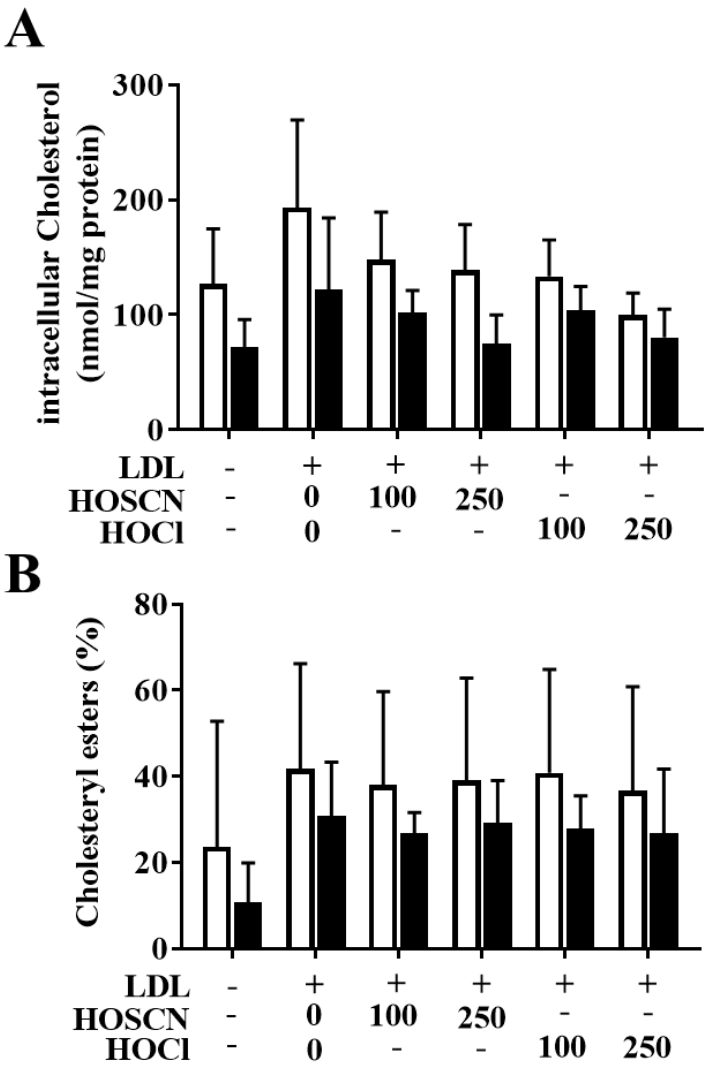

Figure 6.3. Total cholesterol and cholesteryl ester levels of HCASMC after incubation with oxidised LDL. *Firstly, 1.0 mg.mL^{-1} control LDL, or LDL incubated with 100 or 250 µM HOSCN, or 100 or 250 µM HOCl, were incubated at 37 °C for 24 h. HCASMC were treated with 0.1 mg.mL^{-1} of LDL or oxidised LDL species at 37 °C for 24 h (white bar) or 48 h (black bar) in treatment media. Cholesterol and cholesteryl ester content were normalised to cellular protein concentration as assessed by the BCA assay. Total cholesterol represents the sum of the free cholesterol and the cholesteryl esters detected by HPLC in the HCASMC lysate samples (A). Cholesteryl esters are represented as a percentage of the total cholesterol measured in HCAEC lysates (B). Three independent HCASMC and LDL donors were used. Bars represent the mean ± SD (n = 3). Two-way ANOVA with Dunnett's multiple comparison test between treatment groups and Sidak multiple comparison test between time points. No significant differences were found between 24 and 48 h time point.*

Table 6.1. Difference in total cellular cholesterol in HCASMC between 24 h and 48 h incubation with MPO oxidant-modified LDL. *The change in intracellular lipids was calculated between 24 h and 48 h incubation times (ΔIntracellular lipid) from the data in Figure 6.2A to compare the change in intracellular lipids due to LDL uptake, independent of lipids already present in the cells. One-way ANOVA with Holm-Sidak multiple comparison test. No significant differences were found compared to the control.*

LDL treatment	ΔIntracellular lipid (mean ± SD)	Significance
Control	-59.92 ± 53.24	NS
Control LDL	-71.15 ± 74.24	NS
100 μM HOSCN-LDL	-45.79 ± 38.92	NS
250 μM HOSCN-LDL	-64.14 ± 67.10	NS
100 μM HOCl-LDL	-29.19 ± 31.02	NS
250 μM HOCl-LDL	-19.36 ± 36.00	NS

6.3.3. SMC phenotype gene expression

6.3.3.1. Contractile markers

The uptake of oxidised LDL by VSMC has been linked to reduced expression of contractile markers concurrent with increased proliferation [475, 703], indicative of a shift from contractile to synthetic phenotype. However, these studies were performed in a Cu^{2+}-modified LDL model [475, 703] and the comparative effect of LDL modified by MPO-derived oxidants has not been reported. Therefore, both contractile and synthetic phenotype markers were examined following 24 and 48 h treatment of HCASMC with LDL modified by HOSCN or HOCl (250 μM, 24 h). No significant alterations were observed the mRNA expression of the contractile markers α-SMA or calponin following 24 h incubation of the cells with each LDL.

However, after 48 h treatment, HOSCN- and HOCl-modified LDL reduced α-SMA mRNA expression and all LDL treatments reduced calponin mRNA expression in the HCASMC compared to the respective no LDL control (Figure 6.4A and B). The mRNA expression of α-SMA and calponin was increased between 24 and 48 h time points in the cells in the absence of LDL, though this was only significant for calponin expression (shown by #), while α-SMA was not significant ($p = 0.10$). This result indicates that LDL, and to a greater extent HOSCN- and HOCl-modified LDL, halted the mRNA expression of both α-SMA and calponin. In contrast, no change in collagen I was observed between treatments at 24 or 48 h time points (Figure 6.4C).

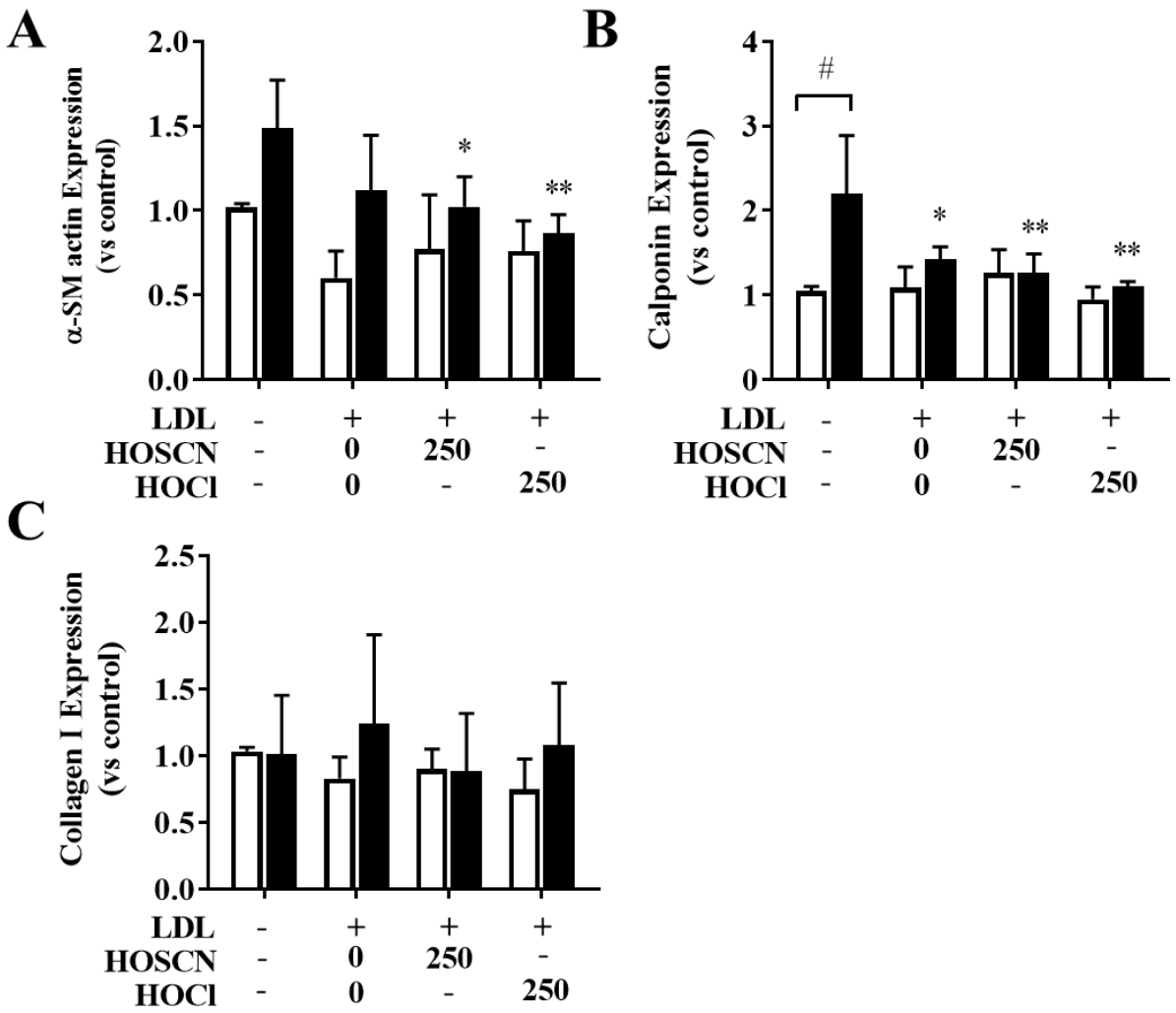

Figure 6.4. Gene expression of contractile phenotype-associated genes in HCASMC following exposure to LDL modified by HOSCN or HOCl. *1.0 mg•mL^{-1} control LDL or LDL modified with 250 µM HOSCN or 250 µM HOCl for 24 h. HCASMC were treated with 0.1 mg•mL^{-1} of control LDL or oxidised LDL species for 24 h (white bar) or 48 h (black bar) at 37 °C before measuring the mRNA expression of (A) α-SMA, (B) calponin and (C) collagen 1 by qPCR. Expression was normalised to 18S and β2M as housekeeping genes. Three independent HCASMC and LDL donors were used. Bars represent the mean ± SD (n = 3). Two-way ANOVA with Dunnett's multiple comparison test between treatment. * and ** represent p < 0.05 and 0.01, respectively, compared to the control. # represents p < 0.05 compared to 24 and 48 h time points.*

6.3.3.2. Synthetic markers

Studies were undertaken to corroborate the alteration in contractile marker expression with the expression of synthetic markers. The HCASMC were treated with HOSCN- or HOCl-modified LDL as in Section 6.3.3.1, before determining the mRNA expression of synthetic markers OPN, Olfml3, S100A4, Cx43, decorin and MMP9. There was no difference in OPN mRNA expression between the non-treated LDL control and control LDL treatments after 24 or 48 h exposure, nor was there a difference between the time points within those treatments (Figure 6.5A). In contrast, HCASMC exposed to HOSCN- and HOCl-modified LDL displayed a time-dependent elevation in OPN mRNA expression, which reached significance following 48 h exposure. Olfml3 expression was not altered between treatments after 24 h incubation, but was elevated in the non-treated HCASMC between 24 and 48 h incubation, though this was not significant ($p = 0.081$; Figure 6.5B). However, upon exposure to HOSCN-modified LDL, Olfml3 expression remained unchanged at both 24 and 48 h incubation and the expression of Olfml3 was significantly reduced compared to the respective control after 48 h. This trend was also observed to a lesser extent with HOCl-modified LDL, but this was not significant ($p = 0.0502$). S100A4 expression in the HCASMC between 24 and 48 h incubation remained unchanged in the control and control LDL treatment groups, but was increased on exposure of the cells to HOSCN- and HOCl-modified LDL, though these changes were not significant ($p = 0.2860$ and 0.1549, respectively; Figure 6.5C). Other synthetic phenotype markers, Cx43, decorin and MMP-9 were unaltered in all treatment groups at both 24 and 48 h time points (Figures 6.5D – F).

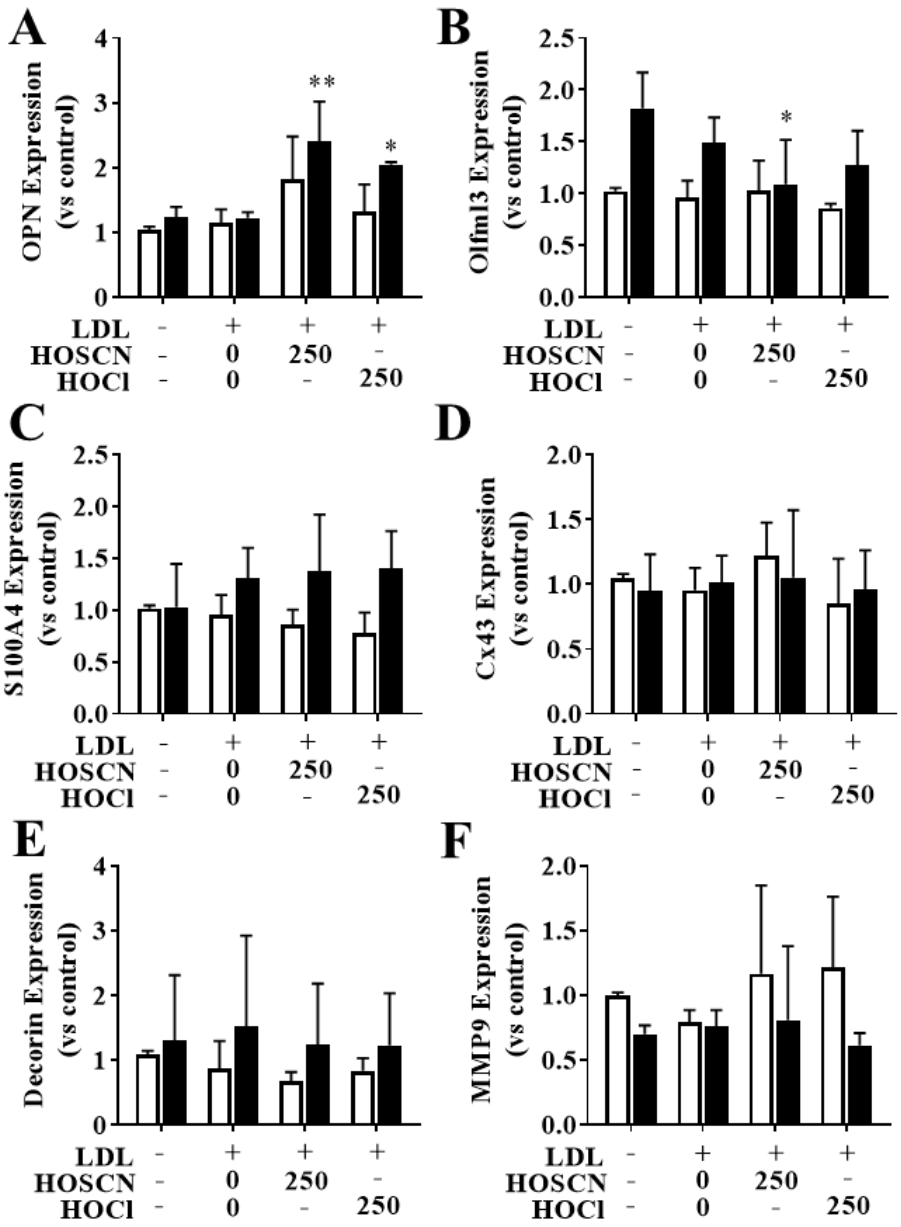

Figure 6.5. Gene expression of synthetic phenotype-associated genes in HCASMC following exposure to LDL modified by HOSCN or HOCl. *1.0 mg•mL^{-1} control LDL, or LDL modified with 250 µM HOSCN or 250 µM HOCl for 24 h. HCASMC were treated with 0.1 mg•mL^{-1} of control LDL or oxidised LDL species for 24 h (white bar) or 48 h (black bar) at 37 °C before measuring the mRNA expression of (A) OPN, (B) S100A4, (C) Cx43, (D) decorin, (E) Olfml3 and (F) MMP-9 by qPCR. Expression was normalised to 18S and β2M as housekeeping genes. Three independent HCASMC and LDL donors were used. Bars represent the mean ± SD (n = 3). Two-way ANOVA with Dunnett's multiple comparison test between treatment groups. * and ** represent p < 0.05 and 0.01, respectively, compare to the control.*

6.3.3.3. Calcification markers

The synthetic phenotype-associated protein, OPN plays a key role in the calcification of VSMC [736, 737, 748] and was shown to be upregulated following 48 h incubation with HOSCN- and HOCl-modified LDL (Figure 6.5A). Therefore, the expression of calcification markers, osteocalcin and Runx2 were measured following 24 and 48 h incubation of HCASMC with each type of modified LDL. No significant alteration in osteocalcin was observed at either time point (Figure 6.6A). In general, Runx2 expression increased between the 24 and 48 h incubation times between all treatment groups, which nearly approached significance with HOCl-modified LDL treatment ($p = 0.053$; Figure 6.6B). However, this was due to the decrease in Runx2 expression with HOCl-modified LDL compared to the control after 24 h incubation, whereby the Runx2 mRNA expression levels became equal across all treatments by 48 h.

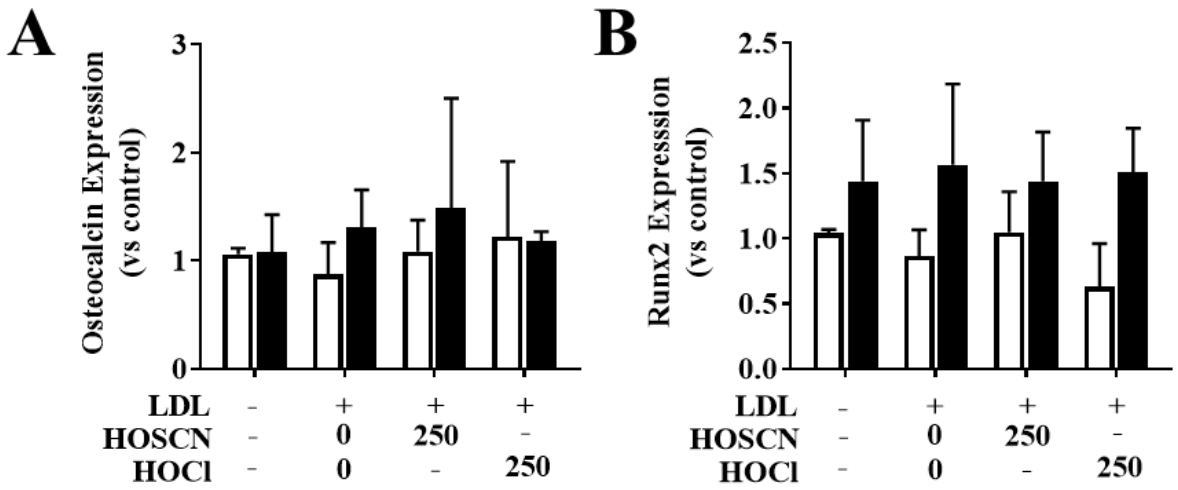

Figure 6.6. Gene expression of calcification-associated genes in HCASMC following exposure to LDL modified by HOSCN or HOCl. *1.0 mg.mL^{-1} control LDL, or LDL modified with 250 µM HOSCN or 250 µM HOCl for 24 h. HCASMC were treated with 0.1 mg.mL^{-1} of control LDL or oxidised LDL species for 24 h (white bar) or 48 h (black bar) at 37 °C. Expression was normalised to 18S and β2M as housekeeping genes. Three independent HCASMC and LDL donors were used. Bars represent the mean ± SD (n = 3). Two-way ANOVA with Dunnett's multiple comparison test between treatment groups.*

6.4. Discussion

The experiments in this Chapter examined the *in vitro* exposure of HCASMC to LDL oxidised with either 250 µM HOSCN or HOCl, which is believed to be achievable under physiological conditions [42]. These oxidised LDL treatments did not result in cytotoxicity, as measured by the LDH; nor was any modulation of metabolic activity as determined using the MTT assay; nor did these forms of oxidised LDL promote excessive accumulation of lipids in HCASMC with up to 48 h exposure. Despite this, the contractile genes α-SMA and calponin, were not as highly expressed following 48 h exposure to HOSCN- or HOCl-modified LDL compared to the 48 h control, while the synthetic gene OPN was significantly upregulated by 48 h exposure to both HOSCN- and HOCl-modified LDL compared to the control, which has not been reportedly previously. However, other synthetic and calcific genes were not altered.

Overall, the expression array of phenotype markers did not change significantly enough to demonstrate a strong oxidized-LDL induced transition of VSMC phenotype to a synthetic or calcific state under the conditions employed in this study.

Whilst there was a modest rise in intracellular cholesterol levels when HCASMC were exposed to incubation control LDL, the results of the current study do not support the excessive accumulation of cholesterol upon exposure to each MPO oxidant-modified LDL. This contrasts with other previous studies, where rat thoracic aortic- and bone marrow-derived SMC exposed to Cu^{2+}-oxidised LDL at similar concentrations for 24 to 48 h formed into foam cells, as measured by Oil Red O staining or quantification by a fluorescence enzymatic assay [475, 746, 747]. As LDLR mRNA expression was reduced in endothelial cells, as shown in Chapter 4, a similar mechanism may have been in action upon exposure of HCASMC to incubation control- and MPO oxidant-modified LDL. This notion is supported by a prior study that showed that LDLR expression in HCASMC was sensitive to lipid loading, as 25 $\mu g \cdot mL^{-1}$ of native LDL significantly reduced LDLR mRNA and protein expression under both inflammatory (LPS-stimulated) and non-inflammatory conditions [700]. VSMC-derived foam cell formation is also linked to synthetic transdifferentiation [699].

In the current study, only OPN was significantly elevated following exposure to each MPO oxidant-modified LDL over the course of 48 h. Olfml3 mRNA expression was lower following incubation with HOSCN- and HOCl-modified LDL, while S100A4 expression inclined towards increased expression by the same treatments. Pericytes, highly proliferative cells which can originate from VSMC lineages, express Olfml3 to promote angiogenesis, which is important to vascular remodelling [729]. However, pericytes also highly express α-SMA together with Olfml3; the expressions of which are linked as Olfml3 silencing reduced α-SMA expression and proliferation [729]. The same expression pattern was also observed between α-SMA and Olfml3 in this current study. However, in the current study, the slight increase of

S100A4 mRNA expression with exposure to HOSCN- or HOCl-modified LDL over 24 and 48 h closely reflected the increased production of formazan as an indicator of proliferation. Elevated S100A4 expression has been detected in "rhomboid" (synthetic) pulmonary artery SMC, but not "spindle" (synthetic) SMC under hypoxia *in vitro*, which was associated with augmented proliferation and migration by NF-κB activation [727, 749]. Further, in a calf animal model of hypoxic pulmonary hypertension, blockade of S100A4 and RAGE attenuated SMC migration [750]. However, it has not been previously reported if oxidised LDL could promote S100A4-mediated responses in SMC.

The synthetic VSMC phenotype, particularly linked to the expression of OPN and decorin, also cross-functionally promotes VSMC calcification. However, in the current study, elevated OPN mRNA expression upon exposure to HOSCN- and HOCl-modified LDL was not reciprocated with decorin, Runx2 or osteocalcin expression, indicating that calcification was not an active process following exposure to LDL modified by HOSCN or HOCl. Several studies have shown that acetylated LDL [733], Cu^{2+}-oxidised LDL [734, 751], or oxidised LDL-associated lipids (7-ketocholesterol [752]) induced calcification in human arterial SMC. This is concurrent with an upregulation of OPN and Cbfa1/Runx2 expression [753], which are co-localised in advanced atherosclerotic lesions and are crucial to calcification [713]. Exposure of human aortic SMC to 7-ketocholesterol was shown to induce calcification linked to the loss of lysosomal function [752]. However, the reaction of HOCl with cholesterol does not form 7-ketocholesterol [135, 298], and while HOSCN can react with LDL-derived lipids, whether this leads to formation of 7-ketocholesterol has not yet been reported [146]. Therefore, other mechanisms of LDL oxidation may be relevant to promoting calcification.

6.4.1. SMC transdifferentiation/calcification: a matter of time?

A possible limitation faced in this study is the relatively short incubation time of up to 48 h of the HCASMC to LDL treatments when compared to other *in vitro* studies. Several other studies have investigated SMC phenotype transitions over the course of between 6 to 28 days [711, 717, 719, 725, 740, 743, 744, 754, 755], including those studies investigating the impact of modified LDL [475, 733, 734] or related oxidation products [752, 753], on SMC transdifferentiation and calcification. The proliferation of rabbit arterial and venous SMC did not significantly increase in culture until the fifth day of treatment in conditioned media [719]. Further, arterial SMC were less proliferative than the venous counterpart [719] and may be slower to transdifferentiate. Downregulation of α-SMA and SM22α, upregulation of OPN and osteocalcin, and calcification, were not induced until day 7 of incubation with organic phosphate (β-glycerophosphate) in BASMC, with the exception of Cbfa1 expression upregulated at day 3 of treatment [744]. This was similar to two independent studies exposing human VSMC to Cu^{2+}-oxidised LDL, though decorin expression was almost completely abated at day 4 of treatment [734, 751]. In light of this, as the gene expression of contractile markers, α-SMA and calponin were stunted, and the expression of the synthetic marker OPN was elevated by exposure to LDL modified by HOSCN or HOCl in this study. This could be an early indicator of phenotype shift that is still in a transitionary stage at a shorter incubation time of 48 h.

The cases for which SMC differentiation was studied in accordance with 24 and 48 h time points was that this was previously enough of an incubation period for with oxidised LDL induced foam-cell formation. Specifically, in bone marrow-derived SM progenitor cells (SMPC; mesenchymal cells that are differentiated to smooth muscle-like cells over 30 days), exposure to 25 – 100 $\mu g \cdot mL^{-1}$ DiI-labelled Cu^{2+}-oxidised LDL, equivalent LDL concentration

to this current study, significantly reduced α-SMA and myocardin expression within 48 h of incubation [475]. When HCASMC were exposed to low levels (4 – 15 $\mu g \cdot mL^{-1}$) of Cu^{2+}-modified LDL (less than the 100 $\mu g \cdot mL^{-1}$ of HOSCN- or HOCl-modified LDL used in the current study), there was an induction of up to 3-fold greater proliferation (measured by fluorochrome incorporation into DNA during replication) and migration, which receded at concentrations > 7.5 $\mu g \cdot mL^{-1}$ [703]. This was concurrent with an approximate 70 % reduction in calponin and SM22α, and 40 % reduction in α-SMA protein expression, which was linked to NF-κB, stimulated the production of G-CSF and GM-CSF and subsequently stimulated monocytes and macrophages to release MCP-1 when cultured in the medium of the VSMC treated with oxidised LDL [703]. The results of that study showed that 24 h exposure to Cu^{2+}-oxidised LDL induced a pro-inflammatory response and promoted switching to a synthetic phenotype. It is difficult to predict if a similar outcome would have been observed if this current study utilised an equivalent 0.1 $mg \cdot mL^{-1}$ Cu^{2+}-oxidised LDL by the finding that significant cell death was incurred at 0.1 $mg \cdot mL^{-1}$ Cu^{2+}-oxidised LDL [703], which was not the case upon exposure to HOSCN- or HOCl-modified LDL in the current study. In that case, investigating whether comparatively lower concentrations of HOSCN- or HOCl-modified LDL would induce these proliferative and phenotypic changes observed in Cu^{2+}-oxidised LDL-treated SMC would be more determinative.

Although a degree of phenotype switching was observed, SMC-derived foam cell formation was not investigated in that study. Additionally, S100A4 stimulation of VSMC also activates NF-κB to promote proliferation, migration, and production of cytokines MCP-1 and IL-6 [727, 749]. Regardless, these studies demonstrated the transdifferentiation of (bone marrow- and vascular-derived) SMC by oxidised LDL, but did not investigate the expression of synthetic phenotype markers; such a study has yet to be reported in the literature. Given the trending, but non-significant increase in S100A4 mRNA expression and formazan production in this current

study, longer exposure to HOSCN- or HOCl-modified LDL may have resulted in a greater extent of altered S100A4 expression and/or significant proliferation.

6.4.2. Limitations and conclusion

There are key limitations to this study that need to be acknowledged. One issue that is likely present in this study is subculturing the cells through multiple cell divisions in growth medium to achieve confluence may have shifted the HCASMC to a more synthetic phenotype [756, 757]. Although HCASMC were incubated with LDL treatments in the absence of growth factors, the cells may have been in a mixture of cell-cycle phases before treatment, while contractile VSMC are usually in the G_0 phase of mitosis [758]. This variable may be somewhat controlled by the preincubation of HCASMC for several days in nutrient media (such as Dulbecco's Modified Eagle's Media) in the absence of growth factors and serum to return cells to G_0 phase (referred to as synchronisation) [475, 741]. Another limitation is the gene expression variations between primary cell donors, which may make the use of three HCASMC donors too few to assess gene expression alterations. The three HCASMC donors were all of male origin, but of different ages and races. Although the variation was not attributed to one particular donor for each gene, using different donors but normalising for also age and race may reduce the variation in response to HOSCN- and HOCl-modified LDL. Further, as per the discussion in Section 6.4.1, investigating longer treatment times (e.g. 7 – 14 days) may better assess phenotypic changes in HCASMC.

Overall, this study showed for the first time that LDL modified by HOSCN or HOCl upregulated OPN mRNA expression *in vitro*, though this did not cause VSMC foam cell formation or a change in VSMC phenotype over 48 h. Additionally, LDL modified by either HOSCN or HOCl inhibited the upregulation of α-SMA and calponin, indicating that the contractile phenotype of VSMC was impaired. Further higher-powered studies are required to

corroborate whether exposure to LDL modified by MPO over longer terms can significantly elevate levels of intracellular LDL-derived lipids and evoke a synthetic SMC phenotype mediated by OPN and S100A4 upregulation in SMC transdifferentiation.

Chapter 7. General Discussions and Future Directions

7.1. Overview

The research performed in this Thesis was designed to explore the role of the MPO-derived oxidants, HOSCN and HOCl, in the modification of LDL and whether such modifications lead to impaired vascular endothelial and SMC function. Oxidised LDL is a key component of atherosclerotic plaques, and is proposed to be critical in the initiation and progression of atherosclerosis [759]. MPO is likely to be an important pathway to LDL oxidation, whereby neutrophils infiltrate the intima of atherosclerotic plaques and release MPO during the inflammatory response. Notably, functional MPO has been shown to colocalise in human atherosclerotic plaques with LDL modified by HOCl [233, 234, 284]. The development of atherosclerotic plaques leads to arterial stiffening by impaired endothelium-dependent dilation of arteries, termed endothelial dysfunction [760]. The severity of endothelial dysfunction can be independently predicted by measuring the circulating levels of MPO [761], lending further support to a central role for the enzyme in the development of atherosclerosis. Concomitant with endothelial dysfunction are alterations in VSMC function, linked to a phenotypic shift, which causes hyperplasia and vascular remodelling [697]. However, a role of MPO as a driver for altered VSMC function in vascular inflammation and atherosclerosis has yet to be established. Given the evidence for MPO-derived oxidants in the promotion of atherosclerosis by altering several vascular cell functions, such as endothelial dysfunction and macrophage foam cell formation [146, 292, 446, 447], this could be a key pathway to target for pharmacological therapy, and such therapy is likely to have a wide range of beneficial effects for preventing atherosclerosis and its related cardiovascular complications.

Several studies have shown that elevated MPO levels are associated with the severity of atherosclerosis and are an independent predictor and risk factor of coronary artery disease (CAD) [235, 236, 238-241] and acute coronary syndromes (ACS) [245-247]. Given that MPO

is present in atherosclerotic lesions [21], and shown to be active by the detection of chlorinated products on LDL and other biomolecules [141, 233, 284] indicates that MPO is not just a marker, but is enzymatically active in producing the reactive oxidant HOCl. Several studies have demonstrated a capacity of HOCl and MPO-chlorinating activity to modify LDL, altering the functionality in diverse ways relevant to atherosclerosis [53, 111, 288, 290, 293, 762, 763]. However, the role of HOSCN, the other major MPO-derived product formed under physiological conditions, in the onset and progression of atherosclerosis has not been well characterised. This is related to the lack of a distinct biomarker for HOSCN reactivity, which has made elucidating the role of HOSCN formation *in vivo* difficult. Regardless, HOSCN production by MPO is believed to be relevant in smokers, who compared to non-smokers have significantly elevated circulating levels of the precursor, SCN^- [42, 43, 296, 297, 764], together with a significantly lower presence of chlorinated products [120]. This implicates a shift from production of HOCl to HOSCN in smokers, who concurrently exhibit accelerated atherosclerotic lesion development [254]. Augmented HOSCN production in smokers is also implicated in inducing LDL modification *in vivo*, with the thoracic and abdominal aorta of smokers exhibited substantial macrophage infiltration and foam cell formation correlating with elevated plasma SCN^- levels [253], together with elevated levels of the lipid peroxidation markers malondialdehyde- and 4-hydroxynonenal (4-HNE)-modified Lys [254], compared to the respective samples from non-smokers. However, experiments in atherosclerosis-prone mice that express human MPO demonstrate reduced lesion development when supplemented with SCN^- in their drinking water, implicating HOSCN formation by MPO in this case, as protective [261]. Considering this discrepancy, investigating whether LDL modified by HOSCN can alter vascular function, by inducing endothelial dysfunction and/or SMC transdifferentiation, may shed light on whether elevated HOSCN production is a detrimental or protective factor in the progression of atherosclerosis.

The results in this study have demonstrated that LDL modified by either HOCl or HOSCN induced endothelial dysfunction by impairing eNOS activity, and reduced endothelium-dependent vasodilation of rat aortae *ex vivo*. Further, HOSCN- and HOCl-modified LDL influenced the expression of some phenotype markers in a vascular smooth muscle cell model (HCASMC), which could demonstrate a long-term response to LDL modified by MPO-derived oxidants.

7.2. HOSCN-induced apoB-100 fragmentation

HOSCN and HOCl induced modification to LDL, after 24 h exposure, albeit to very different extents. Oxidation of LDL by 250 μM HOCl led to formation of a more negatively charged LDL particle, with extensive aggregation and fragmentation of apoB-100. Conversely, oxidation of LDL by 250 μM HOSCN also led to aggregation, but with selective fragmentation of apoB-100, with no significant alteration in LDL charge. This is attributed to a free radical-dependent pathway as it was significantly abated by concurrent incubation with the anti-oxidant BHT. This fragmentation had been observed previously [146], but identification and sequencing had not been performed to identify the molecular weight and cleavage site of the apoB-100-derived peptides. A peptide mass-mapping approach with LC-MS/MS showed that HOSCN caused fragmentation of apoB-100, leading to cleavage of the C- and N-termini of the protein. From these studies, it was apparent that two peptides with similar molecular-mass (approximately 91.7 and 96.6 kDa for the N- and C-terminal fragment, respectively) were formed, though experiments to locate the specific cleavage site were not successful.

The N- and C-terminal fragments produced following exposure of LDL to HOSCN were calculated to have a pI of 7.59 and 5.19, respectively, making it possible in theory to purify each fragment from the rest of the LDL molecule by 2D-PAGE for additional analysis. Complete separation of the terminal fragments and the remaining middle fragment, from intact

apoB-100, would allow for more extensive proteomic analysis of the individual fragments and other chemical modifications. From previous studies, it has been reported that high circulating SCN^- levels correspond to an elevation of malondialdehyde- and 4-HNE-modified Lys residues on LDL [254]. This type of LDL modification has been shown to mediate oxidised lipid-dependent protein cross-linking [507, 765, 766]. Future studies could therefore characterise both the cleavage site and post-translational modifications of apoB-100, particularly lipid-derived oxidation products. The formation of 4-HNE by HOSCN could explain why apoB-100 aggregation was not prevented or reversed by DTT and could potentially serve as a biomarker to assess HOSCN formation *in vivo*. But a caveat to any interpretation in this manner would be that 4-HNE can be formed by several chemical pathways and is not a specific product of HOSCN-mediated oxidation [767].

A further implication for the specific fragmentation of apoB-100 by HOSCN is related to changes to the recognition of LDL by the LDLR and/or scavenger receptors. In this study, it was shown that only the LDLR expression was downregulated, though only at the mRNA level, while no changes were observed in scavenger receptors SR-B1, SR-B2, LOX-1 or SREC-1 on exposure of HCAEC to HOSCN-modified LDL. Moreover, no increase in LDL uptake following exposure to HOSCN-modified LDL was seen in either HCAEC or HCASMC. Previous studies have tested several potential binding sites, and discerned that two basic regions of the LDLR are important in binding to apoB-100, named site A (L^{3147} - G^{3157}) and site B (Q^{3359} - S^{3369}) [267, 768-770], the latter being essential to apoB-100 binding to the LDLR [771]. However, these regions are well outside where the apoB-100 is likely to be cleaved by HOSCN (in proximity to residue 3725, based on LC-MS/MS sequence of the C-terminal fragment). Therefore, the LDLR binding domain is not likely removed after exposure to HOSCN. Further, truncation of the C-terminus is able to increase the binding strength of apoB-100 to the LDLR [771], which may be relevant to LDL modified by HOSCN (or HOCl, which

also induced fragmentation of the apoB-100, though not in a site-specific manner). As the LDLR is recycled back to the plasma membrane after dissociating from LDL in the endosome [605], stronger binding of HOSCN- or HOCl-modified LDL to the LDLR may prolong the recycling process and hold the LDL-LDLR complex in the cell longer, which might dysregulate lipid metabolism in the cell. The reduced expression of LDLR mRNA following exposure to HOSCN- or HOCl-modified LDL may be a negative feedback mechanism to reduce transcriptional LDLR expression by sterol-dependent response elements, such as inhibiting SREBP binding to the LDLR promotor region [772]. A future study could examine the binding of HOSCN- or HOCl-modified LDL to LDLR, for example, by performing a competitive binding assay to the LDLR using labelled LDL (e.g. DiI-, I^{125}-) modified by HOSCN or HOCl.

7.3. Stress signalling induced by HOSCN- or HOCl-modified LDL

Several studies have observed detrimental effects of oxidised LDL (most commonly LDL modified by Cu^{2+}) on endothelial function, finding that oxidised LDL promoted pro-inflammatory cell adhesion molecule expression [307, 433-435, 613], impaired eNOS function [455, 516, 524] and induction of cell death by apoptosis [514, 523, 599, 600]. Similarly, HOCl-modified LDL has been shown in previous work to impair eNOS function by delocalising eNOS from the plasma membrane [448]. However, the role of HOSCN-modified LDL on endothelial function has not been previously reported. This may be of significance, as the difference in molecular reactivity of HOSCN and HOCl on LDL may alter the cellular response to these modified LDL species.

Cu^{2+}-modified LDL has been previously demonstrated to cause an increase in arginase 2 activity and expression, which reduced L-Arg availability to competitively decrease eNOS activity in HCAEC, as the rate of L-Arg consumption by arginase 2 is almost 200-fold greater compared to consumption by eNOS [773]. This was demonstrated further to influence NO

production in rat aortic segments *ex vivo* [773]. This was further supported by a more recent study that showed arginase 2 translocated from the mitochondria to the cytoplasm, in the absence of changes to mitochondrial membrane potential, leading to consumption of L-Arg [774]. Induction of arginase 2 to compete with eNOS for L-Arg may be of relevance to HCAEC exposed to HOSCN- or HOCl-modified LDL, based on the observation of a reduction of eNOS activity and NO detection, together with the absence of increased $O_2^{\bullet-}$, which normally accompanies eNOS uncoupling (Figure 7.2). In addition to depleting L-Arg stores, increases in arginase 2 activity also result in increased urea production, which could contribute to pro-atherogenic protein carbamylation, as the increase in urea formation also increases cyanate levels in the cell [255]. However, it is not clear if HOSCN- or HOCl-modified LDL alter arginase 2 expression or translocation in endothelial cells. Further, arginase $2^{-/-}$/apoE$^{-/-}$ double-knockout mice had a reduced atherosclerotic plaque burden and improved endothelium-dependent vasodilation compared to apoE$^{-/-}$ mice [774], which further exemplifies the negative role of arginase 2 on endothelial function and lesion development. Moreover, it is also not clear as to what effect the exposure of HCAEC to native LDL has on arginase 2 activity [773], as the current study showed that the control LDL also reduced NO production in HCAEC.

Cu^{2+}-oxidised LDL-induced arginase 2 activation was also shown to be downstream of LOX-1 mediated uptake of the modified LDL in HAEC (Figure 7.1), as arginase 2 activation by oxidised LDL was completely ablated by antibody blocking of LOX-1 [775]. This was also demonstrated to be LOX-1-dependent in primary endothelial cell culture of LOX-$1^{-/-}$ mice, which did not exhibit translocation of arginase 2 when exposed to Cu^{2+}-oxidised LDL [774]. Additionally, this led to increased ROS production, measured by DHE oxidation fluorescence, which was prevented by inhibiting eNOS with L-NAME, implicating eNOS uncoupling-related $O_2^{\bullet-}$ production induced by arginase 2 activation by oxidised LDL [775]. The current study did not confirm whether LDL modified by HOSCN or HOCl is taken up by LOX-1 in

HCAEC which would verify a role of LOX-1 and help assess if arginase 2 induction is involved in reduced NO production observed in HCAEC exposed to HOSCN- or HOCl-modified LDL. To determine this, the comparative level of arginase 2 in the cytoplasm and mitochondria following exposure of HCAEC to HOSCN- or HOCl-modified LDL in the presence or absence of LOX-1 inhibitors would need to be assessed and corroborated by measuring cellular urea content and the extent of resultant protein, all in conjunction with measuring NO production to assess alterations in eNOS activity.

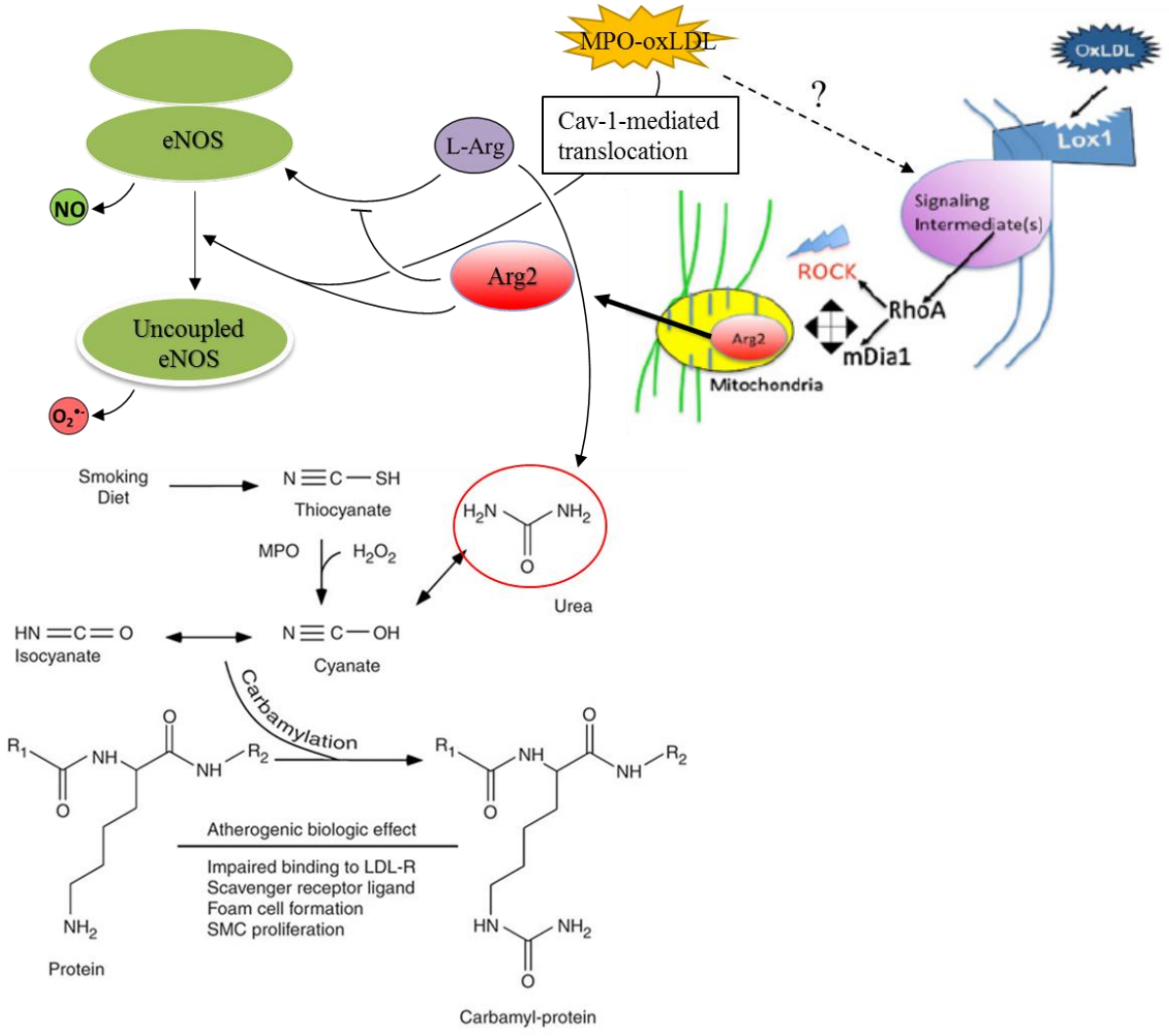

Figure 7.1. Proposed schematic for the potential interplay between MPO oxidant-modified LDL, endothelial dysfunction and protein carbamylation propagated by arginase 2 (Arg2) (Adapted from [255, 775] and Figure 1.13). *Scheme described in the accompanying text.*

In the current study, treatment of HCAEC with HOSCN-modified LDL resulted in increased mRNA expression of both eNOS and HO-1 after 24 h exposure, whereas these gene expression changes were not apparent following exposure to HOCl-modified LDL. This corresponded with significantly lower NO production, which was attributed to decreased eNOS activity following exposure of HCAEC to HOSCN-modified LDL. However, HOCl-modified LDL still impaired eNOS activity and NO production in HCAEC, and induced HO-1 protein expression to a similar extent as HOSCN-modified LDL. This difference in gene expression between the two oxidant-modified LDL treatments, whilst still exhibiting the same extent of eNOS dysfunction and HO-1 expression, is attributed to differences in cellular response pathway activation to the uptake of HOSCN-modified LDL compared to HOCl-modified LDL. This could be related to the differences in the nature and extent of LDL modification in each case.

To date, no work has reported the effect of HOSCN-modified LDL on eNOS expression, while in agreement with the current study, a previous study reported that eNOS activity was reduced, in the absence of altered eNOS mRNA or protein expression following incubation of HUVEC with HOCl-modified LDL [448]. This at first seemed contrary to studies exposing cultured endothelial cells to Cu^{2+}-oxidised LDL, where concentrations of Cu^{2+}-modified LDL at 0.05 – 0.1 mg**.**mL^{-1} caused a significant reduction in eNOS mRNA and protein expression [776, 777]. However, lower concentrations of 0.01 mg**.**mL^{-1} Cu^{2+}-oxidised LDL resulted in upregulation of eNOS mRNA expression [776], whilst also displacing eNOS from the plasma membrane [516]. It is likely that this concentration-dependent regulation of eNOS gene expression is linked to the cytotoxicity of Cu^{2+}-modified LDL, which causes significant cell death at concentrations of 0.05 – 0.1 mg**.**mL^{-1} in cultured endothelial cells [523, 599, 600]. However, cell viability was not investigated in the previous studies that found Cu^{2+}-oxidised LDL reduced eNOS gene expression [776, 777]. This is a limitation, particularly if reduced expression of eNOS mRNA is a result of increased cell death.

Increased HO-1 expression is seen as a protective mechanism which can ameliorate endothelial dysfunction by several actions (Figure 7.2). In endothelial cells exposed to Cu^{2+}-oxidised LDL or TNF-α, bilirubin production through the conversion of biliverdin (released by HO-1-degradation of haem) by biliverdin reductase, improves arterial vasodilation and reduces VCAM-1, MCP-1 and macrophage colony-stimulating factor (MCSF) gene and protein expression [778, 779]. Under oxidative stress, increased NOX activity and $O_2^{\bullet-}$ production is also abated by induction of HO-1 [780], both by the formation of CO, biliverdin and bilirubin to directly scavenge $O_2^{\bullet-}$ [781, 782], and by HO-1 promoting the expression of SOD and catalase to detoxify $O_2^{\bullet-}$ and H_2O_2, respectively [783, 784]. Additionally, the subsequent CO released also acts as a NO analogue, aiding in vascular relaxation by activating sGC [575, 785, 786]. Further, HO-1 and eNOS are linked by the shared compartmentalisation and interaction with cav-1 in endothelial cell caveolae [787], where the HO-1 protein disrupts eNOS-cav-1 interactions and promotes eNOS phosphorylation to increase NO production and restore endothelial function [788].

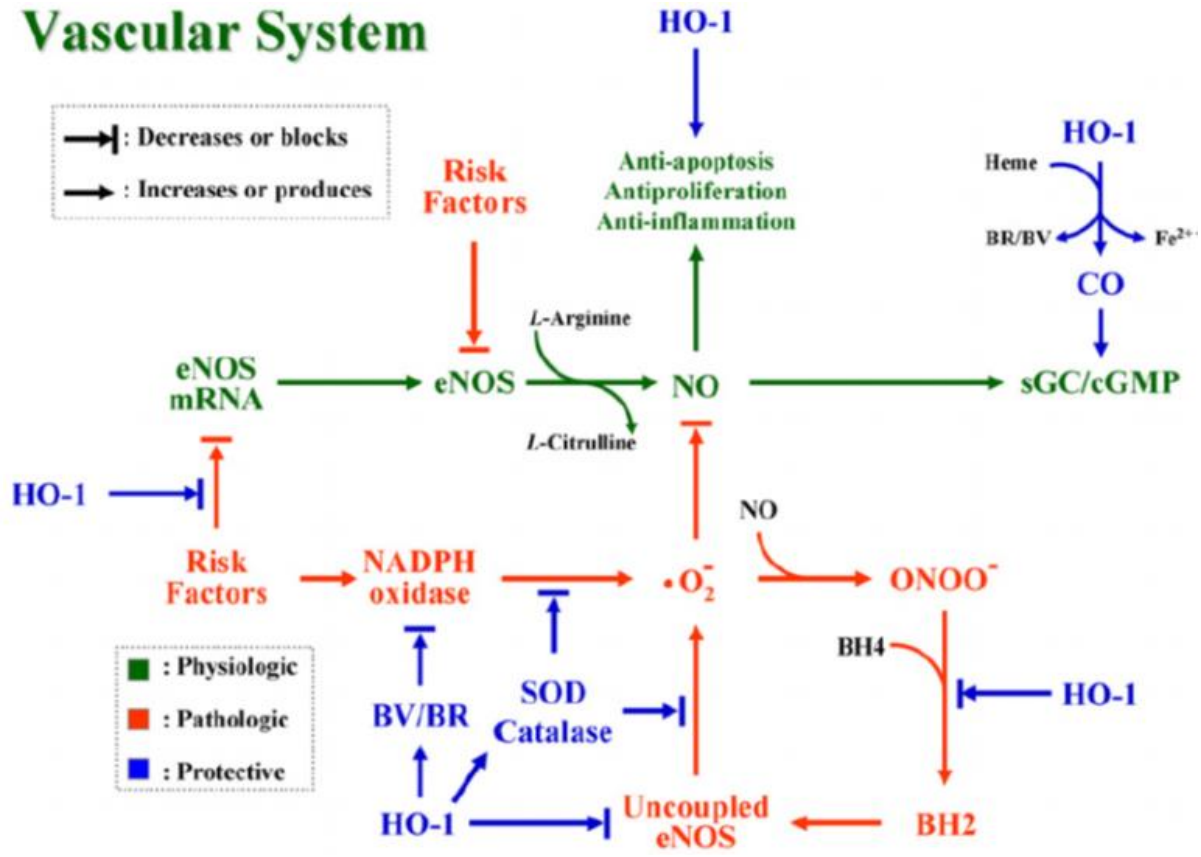

Figure 7.2. The role of HO-1 in ameliorating eNOS dysfunction in endothelial cells (adapted from [789]). *Risk factors (e.g. TNF-α, ROS, Cu^{2+}-oxidised LDL, LPS) that may alter eNOS expression, reduce NO production and cause eNOS dysfunction can be abated by HO-1 activity. HO-1 can inhibit $O_2^{\bullet-}$ production (and subsequent $ONOO^-$ formation) by inhibiting both NOX and eNOS uncoupling, in addition to upregulating SOD and catalase to scavenge $O_2^{\bullet-}$. Additionally, CO produced by HO-1 can activate sGC to produce cGMP analogous to NO and aid in vascular relaxation.*

When HCAEC were exposed to HOSCN- or HOCl-modified LDL for 3 or 24 h, there was no significant change in mRNA expression of leukocyte adhesion molecules ICAM-1, VCAM-1 or E-selectin, or the inflammatory cytokine MCP-1. Based on the previous studies outlined above, the results of the current study indicate that HO-1 induction may have limited the response of adhesion molecules and MCP-1 expression in HCAEC after exposure to HOSCN- or HOCl-modified LDL. However, assessment of eNOS-cav-1 binding in HCAEC by immunoprecipitation did not reveal that eNOS was bound to cav-1 after 24 h incubation with

HOSCN- or HOCl-modified LDL, and so the role of HO-1 induction in this regard cannot be determined. One complication in investigating the role of cav-1 is that cultured endothelial cells are reported to contain up to 1000-fold fewer caveolae than vascular endothelial cells *in situ* [642] with the majority of cav-1 localised to the perinuclear region in culture [790]. This may be of relevance to the *in vitro* experiments in the current study which demonstrated that eNOS colocalised, but did not bind to cav-1 in the cytosol of HCAEC following treatment with HOSCN- or HOCl-modified LDL. Having fewer caveolae in endothelial cells would affect cav-1 compartmentalisation and its function to regulate eNOS activity by binding. Although exposure to HOSCN- or HOCl-modified LDL reduced NO production and uncoupled eNOS in HCAEC, no significant change in $O_2^{\bullet-}$ or 3-nitroTyr formation was observed. There is a limitation to this finding, as alterations in the flux in $O_2^{\bullet-}$ can rapidly occur in endothelial cells from eNOS uncoupling in response to oxidised LDL [672]. In this case, $O_2^{\bullet-}$ was measured over a defined period of 30 min following 24 h treatment of HCAEC with HOSCN- or HOCl-modified LDL. Therefore, it would be helpful if the measurement of $O_2^{\bullet-}$ were performed in real time to detect flux, which has been performed with HAEC using fluorescence spectroscopy optimised for specifically detecting 2-OH-E^+ without the need for HPLC separation [791]. However, lack of alteration in $O_2^{\bullet-}$ production could be due to HO-1 scavenging and/or the subsequent activation of SOD [781-784], with the role of LDL modified by HOSCN or HOCl in SOD/catalase expression in endothelial cells was not investigated in the current study.

Specificity protein-1 (SP-1) and activator protein-1 (AP-1) are transcription factors that bind to the promotor region of the eNOS gene to upregulate eNOS mRNA expression [668, 792-796]. Native and Cu^{2+}-oxidised LDL, and the related oxidation product lysophosphatidylcholine, have been shown to enhance SP-1 and AP-1 binding to the respective eNOS promotor region [797, 798], whilst conversely inflammatory agents such as H_2O_2 and LPS have been shown to reduce eNOS basal gene expression by inhibiting SP-1 activity [799,

800]. Furthermore, both AP-1 and SP-1 together mediate the expression of ATP-binding cassette-1 [801], an important cholesterol efflux protein that regulates intracellular cholesterol levels. The HO-1 gene promotor also contains AP-1 and SP-1-specific binding sites that promote HO-1 mRNA expression [802-806], independent of the ARE (i.e. Nrf2 translocation). The significantly large elevation in HO-1 mRNA expression following 24 h exposure to HOSCN-modified LDL in the absence of upregulation of other ARE genes (GS, Gclc, Nrf2) indicate that HO-1 upregulation occurred via an Nrf2 independent mechanism in conjunction with upregulation in eNOS mRNA. However, Nrf2 translocation has not been investigated in the current study, and so this pathway cannot be fully ruled out. Regardless, no study to date has reported the role of (MPO-derived) oxidised LDL in the signalling of AP-1 and SP-1 to promote eNOS and HO-1 transcriptional upregulation. This translocation pathway is circumstantially implicated in HCAEC as a response to HOSCN-modified LDL in the current study and provides a basis for future investigation, as it may be important for determining how the cells respond differently to HOSCN- and HOCl-modified LDL. The activation of these transcription factors can be determined by measuring the translocation to the nucleus (Western blot detection of AP-1, SP-1 and Nrf2 in the nuclear and cytosolic fractions of cells) and by using a dual luciferase reporter system. Additionally, a gel mobility shift assay to determine binding of AP-1, SP-1 and Nrf2 to their matching promotor sequence could also be performed to confirm the translocation and promotion of gene upregulation of the upstream proteins. This could lead to identifying specific therapeutic mechanisms for preventing endothelial dysfunction induced by the uptake of oxidised LDL.

AP-1 and SP-1 also regulate gene transcription in VSMC. As described in Chapter 6, HCASMC incubated with either HOSCN- or HOCl-modified LDL exhibited increased OPN gene expression, and it may be that HOSCN- and HOCl-modified LDL may alter VSMC gene expressions via AP-1 or SP-1 signalling as well. Cu^{2+}-oxidised LDL has also been reported to

induce AP-1 and SP-1 activation in VSMC [313, 807]. It was later found that AP-1 transcription factor c-fos expression and activity was increased, subsequently along with proliferation, in the VSMC of aged New Zealand rabbits compared to young rabbits [808]. This may be linked to the transition in VSMC phenotype, as AP-1 activation leads to upregulation of OPN in VSMC [809], which is associated with transition to a synthetic (proliferative) phenotype. However, this was under hyperglycaemic conditions [809] and AP-1-induced OPN upregulation has not yet been linked to oxidised LDL.

7.4. Endothelial dysfunction caused by LDL modified by MPO-derived oxidants linked to SMC transdifferentiation?

VSMC play an integral role in the development and complication of atherosclerotic plaques by the increase in proliferation and heterogenic transdifferentiation eventually leading to vascular remodelling and calcification [466, 697, 699, 737, 758, 810, 811]. These VSMC responses to the vascular environment are influenced in large part by the endothelium (reviewed [812]). For example, EC-SMC gap junctions are formed by Cx43, but also Cx37, 40 and 45, to facilitate the spread of hyperpolarisation between EC and SMC during vasodilation [813, 814]; this has the advantage of not needing to directly stimulate all cells by hyperpolarising factors (e.g. ACh) to induce a general vasodilatory response.

An endothelial-SMC co-culture system showed that endothelial cells prevented the conversion of SMC to a synthetic phenotype, characterised by their lower proliferation, spindle-shaped appearance and lack of “hill and valley” growth behaviour under electron microscopy, but no mechanism was ascertained [815]. However, in an atherogenic environment, reduced NO production leads to an increase in proliferation of VSMC, where previous studies have shown that NO-donors inhibited DNA replication and proliferation by arresting the cell cycle of VSMC [816-818]. Bovine aortic endothelial cells transfected to over-

express eNOS largely reduced the proliferation of co-cultured bovine aortic smooth muscle cells through NO production [819]. These findings are congruent with highly proliferative SMC being more receptive to NO signalling by the increased expression of gap junction proteins (Cx43) to help facilitate cross-talk of NO signalling between the endothelium and smooth muscle (reviewed [470]). The role of NO as an effector of VSMC phenotype has been attributed to protein kinase G (PKG) activity and subsequent cGMP formation [820, 821], and activation of the phosphoinositol 3-kinase/Akt pathway [822]. This evidence seems to support NO being able to promote the contractile phenotype of SMC, however, little is known about the role NO has on modulating SMC contractile and synthetic markers.

The finding that endothelium-dependent, but not endothelium-independent vasorelaxation was impaired in *ex vivo* rat aortic segments treated with HOSCN- or HOCl-modified LDL, while the modified LDL particles did not alter the expression of Cx43 in HCASMC, indicate that oxidised LDL may alter VSMC function indirectly by causing endothelial dysfunction. Though, it should be noted that Cx37, Cx40 and Cx45 were not assessed in the current study and the role of these connexins should also be investigated in future studies. This could be performed by the co-culture of SMC under endothelial cells to assess the role of MPO-derived oxidant-modified LDL-induced eNOS uncoupling on SMC proliferation and phenotype, and whether this is linked to higher expression of connexins. Further, the endothelial cell layer could be replaced with fresh, untreated HCAEC to restore eNOS activity and NO production, to see if the SMC revert to a contractile phenotype.

Although no markers for HOSCN are known, characterisation of LDL modification in human MPO-transgenic apoE$^{-/-}$ mice compared to apoE$^{-/-}$ only mice supplemented with or without SCN^- in a normal or high cholesterol diet would provide valuable information on whether high plasma SCN^- levels are deleterious to LDL modification *in vivo*. This study could be extended to assess vasorelaxation in the mouse arteries *in situ* or *ex vivo*, which would

validate the finding in the current study that rat aortic rings treated with HOSCN-modified LDL *ex vivo* cause a loss in vasorelaxation, and whether SMC phenotype is affected by these conditions *in vivo*. In a mouse model expressing human MPO, Morgan and colleagues demonstrated that SCN^- supplementation significantly reduced plaque formation in human MPO transgenic $LDLR^{-/-}$ mice [261]. A limitation of this study [261] is that it is not clear whether SCN^- is influencing lesion formation by altering the ratio of HOCl: HOSCN formed. Additional characterisation of the extent of HOCl-induced oxidation is required, particularly as SCN^- was used extensively as an anti-hypertensive agent, at similar final plasma concentrations [56, 823].

7.5. Study limitations

A limitation of the current study is that LDL was modified by reagent HOCl and HOSCN rather than a MPO-H_2O_2-halide enzymatic system. This is an important distinction, as the selectivity of isolated oxidants does not necessarily match modifications caused by an enzymatic system owing to ability of MPO to bind to LDL [288]. For example, reagent HOCl (up to 1:50 LDL: HOCl ratio) mostly oxidised Met residues on LDL, with several oxidised Trp and only two Cl-Tyr residues [288]. In contrast, in the same study using an equivalent MPO-H_2O_2-Cl^- system, resulted in the oxidation of significantly fewer Met residues and only one Cl-Tyr and no Trp oxidation were detected [288]. This also applies to HOSCN and an MPO-H_2O_2-SCN^- system, as exposing LDL to the MPO-H_2O_2-SCN^- (200 μM SCN^-) system did not cause fragmentation of the apoB-100 C- and N-termini and 9-HODE formation was considerably less than that observed with reagent HOSCN [146]. Therefore, future studies should perform comparative investigations of vascular dysfunction caused by LDL modified by MPO-H_2O_2-halide systems to alleviate this limitation.

The *ex vivo* rat aortic vasodilation model used in the current study also has drawbacks. Although both HOSCN- and HOCl-modified LDL impaired endothelium-dependent vasorelaxation, the exposure of rat aortae to LDL modified by HOSCN or HOCl *ex vivo* for only a short time (1 h) does not adequately imitate the physiologically context. What should be drawn from this experiment is validation to explore an animal model of high vascular MPO activity and its relation to LDL modification and endothelial dysfunction in blood vessels *in vivo*.

7.6. Conclusions

The results of this Thesis highlight the differences in cellular responses to LDL that has been modified by either HOSCN or HOCl at oxidant concentrations likely to be pathologically relevant to inflammation in atherosclerosis. The selective fragmentation of LDL by HOSCN may become more prevalent as MPO activity shifts to producing HOSCN when plasma SCN^- levels are elevated, such as in smokers. This significant post-translational modification may have physiological consequences and/or serve as a surrogate marker for HOSCN reactivity *in vivo*, which requires further investigation.

An increasing number of studies have found that elevated plasma SCN^- levels can have beneficial anti-inflammatory effects and reduce the severity and extent of inflammatory disease, including lesion development [55, 56, 261], though it is not clear if this is related to modification of LDL or other proteins by HOSCN instead of HOCl. Although both HOSCN- and HOCl-modified LDL caused endothelial dysfunction by impairing NO bioavailability, resulting in reduced vasodilation *ex vivo*, the upregulation of HO-1 in eNOS mRNA in HCAEC following exposure to HOSCN-modified LDL could be a pathway to reduce atherogenesis in response to the decrease in NO production. This suggests a cellular response to HOSCN-modified LDL that is distinct to the response to HOCl-modified LDL, which may have a

protective effect on endothelial cells. Likewise, it has been previously shown that HOSCN-modified LDL is not taken up as avidly as HOCl-modified LDL by macrophages [146]. Investigations of the role of SCN^-, both as an exogenous antioxidant and a substrate for MPO producing HOSCN, in cell signalling pathways that maintain health and promote disease are still required.

References

1. Abdo, A.I., et al., 2017, Low-density lipoprotein modified by myeloperoxidase oxidants induces endothelial dysfunction. *Redox Biol* **13**: p. 623-32.
2. AIHW, *Cardiovascular disease mortality: Trends at different ages*, in *Cardiovascular Series*, A.I.o.H.a.W. (AIHW), Editor. 2010, AIHW: Canberra.
3. Libby, P., 2012, Inflammation in atherosclerosis. *Arterioscler Thromb Vasc Biol* **32**(9): p. 2045-51.
4. Ross, R., 1999, Mechanisms of Disease - Atherosclerosis - An inflammatory Disease. *N Engl J Med* **340**(2): p. 115-26.
5. Davies, M.J. and A. Thomas, 1984, Thrombosis and acute coronary-artery lesions in sudden cardiac ischemic death. *N Engl J Med* **310**(18): p. 1137-40.
6. AIHW, *Trends in coronary heart disease mortality: age groups and populations*, in *Cardiovascular Disease Series*, A.I.o.H.a.W. (AIHW), Editor. 2014, AIHW: Canberra.
7. Li, Y., et al., 2017, Risk factors between intracranial-extracranial atherosclerosis and anterior-posterior circulation stroke in ischaemic stroke. *Neurol Res* **39**(1): p. 30-5.
8. Mercuro, G., et al., 2010, Gender determinants of cardiovascular risk factors and diseases. *J Cardiovasc Med* **11**(3): p. 207-20.
9. Banerjee, A., 2012, A review of family history of cardiovascular disease: Risk factor and research tool. *Int J Clin Pract* **66**(6): p. 536-43.
10. Dauchet, L., et al., 2006, Fruit and vegetable consumption and risk of coronary heart disease: A meta-analysis of cohort studies. *J Nutrit* **136**(10): p. 2588-93.
11. Guzmán, M.A., 2010, Diet and chronic diseases: INCAP studies of atherosclerosis and coronary heart disease. *Food Nutr Bull* **31**(1): p. 141-51.
12. Bassett, C.M., et al., 2009, Trans-fatty acids in the diet stimulate atherosclerosis. *Metabolism* **58**(12): p. 1802-8.
13. Chelland Campbell, S., R.J. Moffatt, and B.A. Stamford, 2008, Smoking and smoking cessation -- the relationship between cardiovascular disease and lipoprotein metabolism: A review. *Atherosclerosis* **201**(2): p. 225-35.
14. Steffen, B.T., et al., 2012, Obesity modifies the association between plasma phospholipid polyunsaturated fatty acids and markers of inflammation: The Multi-Ethnic Study of Atherosclerosis. *Int J Obesity* **36**(6): p. 797-804.
15. Lakoski, S.G., et al., 2011, The relationship between inflammation, obesity and risk for hypertension in the Multi-Ethnic Study of Atherosclerosis (MESA). *J Hum Hypertens* **25**(2): p. 73-9.
16. Pearson, T.A., et al., 2003, Markers of inflammation and cardiovascular disease: Application to clinical and public health practice: A statement for healthcare professionals from the centers for disease control and prevention and the American Heart Association. *Circulation* **107**(3): p. 499-511.

17. Libby, P. and G.K. Hansson, 2015, Inflammation and immunity in diseases of the arterial tree: players and layers. *Circ Res* **116**(2): p. 307-11.

18. Nussbaum, C., et al., 2013, Myeloperoxidase: a leukocyte-derived protagonist of inflammation and cardiovascular disease. *Antioxid Redox Signal* **18**(6): p. 692-713.

19. Hopkins, P.N., 2013, Molecular biology of atherosclerosis. *Physiol Rev* **93**(3): p. 1317-542.

20. Hansson, G.K., P. Libby, and I. Tabas, 2015, Inflammation and plaque vulnerability. *J Intern Med* **278**(5): p. 483-93.

21. Daugherty, A., et al., 1994, Myeloperoxidase, a catalyst for lipoprotein oxidation, is expressed in human atherosclerotic lesions. *J Clin Invest* **94**(1): p. 437-44.

22. Klebanoff, S.J., 1968, Myeloperoxidase-halide-hydrogen peroxidase antibacterial system. *J Bacteriol* **95**(6): p. 2131-8.

23. Lloyd, M.M., et al., 2013, Comparative reactivity of the myeloperoxidase-derived oxidants hypochlorous acid and hypothiocyanous acid with human coronary artery endothelial cells. *Free Radic Biol Med* **65**: p. 1352-62.

24. Rayner, B.S., D.T. Love, and C.L. Hawkins, 2014, Comparative reactivity of myeloperoxidase-derived oxidants with mammalian cells. *Free Radic Biol Med* **71**: p. 240-55.

25. Carlsson, J., Y. Iwami, and T. Yamada, 1983, Hydrogen peroxide excretion by oral streptococci and effect of lactoperoxidase-thiocyanate-hydrogen peroxide. *infect Immun* **40**(1): p. 70-80.

26. Slungaard, A. and J.R. Mahoney Jr, 1991, Thiocyanate is the major substrate for eosinophil peroxidase in physiologic fluids: Implications for cytotoxicity. *J Biol Chem* **266**(8): p. 4903-10.

27. Cheng, G., et al., 2008, Identification and characterization of VPO1, a new animal heme-containing peroxidase. *Free Radic Biol Med* **45**(12): p. 1682-94.

28. Kimura, S., et al., 1987, Human thyroid peroxidase: Complete cDNA and protein sequence, chromosome mapping, and identification of two alternatively spliced mRNAs. *Proc Natl Acad Sci* **84**(16): p. 5555-9.

29. Hansen, N.E., et al., 1976, Neutrophilic granulocytes in acute bacterial infection: Sequential studies on lysozyme, myeloperoxidase and lactoferrin. *Clin Exp Immunol* **26**(3): p. 463-8.

30. Cross, A.R. and A.W. Segal, 2004, The NADPH oxidase of professional phagocytes—prototype of the NOX electron transport chain systems. *Biochim Biophys Acta* **1657**(1): p. 1-22.

31. McCord, J.M. and Fridovic.I, 1969, Superoxide Dismutase - An Enzymatic Function for Erythrocuprein (Hemocuprein). *J Biol Chem* **244**(22): p. 6049-55.

32. Zeng, J. and R.E. Fenna, 1992, X-ray crystal structure of canine myeloperoxidase at 3 Å resolution. *J Molec Biol* **226**(1): p. 185-207.

33. Davies, M.J., 2010, Myeloperoxidase-derived oxidation: mechanisms of biological damage and its prevention. *J Clin Biochem Nutr* **48**(1): p. 8-19.

34. Furtmuller, P.G., et al., 2006, Active site structure and catalytic mechanisms of human peroxidases. *Arch Biochem Biophys* **445**(2): p. 199-213.

35. Furtmüller, P.G., U. Burner, and C. Obinger, 1998, Reaction of Myeloperoxidase Compound I with Chloride, Bromide, Iodide, and Thiocyanate. *Biochemistry* **37**(51): p. 17923-30.

36. Paumann-Page, M., et al., 2013, Inactivation of human myeloperoxidase by hydrogen peroxide. *Arch Biochem Biophys* **539**(1): p. 51-62.

37. Sullivan, J.L., 1981, Iron and the sex difference in heart disease risk. *Lancet* **317**(8233): p. 1293-4.

38. Weiss, S.J., et al., 1982, Chlorination of taurine by human neutrophils. Evidence for hypochlorous acid generation. *J Clin Invest* **70**(3): p. 598-607.

39. van Dalen, C.J., et al., 1997, Thiocyanate and chloride as competing substrates for myeloperoxidase. *Biochem J* **327**(2): p. 487-92.

40. Ashby, M.T., A.C. Carlson, and M.J. Scott, 2004, Redox buffering of hypochlorous acid by thiocyanate in physiological fluids. *J Am Chem Soc* **126**(49): p. 15976-7.

41. Nagy, P., J.L. Beal, and M.T. Ashby, 2006, Thiocyanate is an efficient endogenous scavenger of the phagocytic killing agent hypobromous acid. *Chem Res Toxicol* **19**(4): p. 587-93.

42. Morgan, P.E., et al., 2011, High plasma thiocyanate levels in smokers are a key determinant of thiol oxidation induced by myeloperoxidase. *Free Radic Biol Med* **51**(9): p. 1815-22.

43. Spagnolo, A., et al., 1988, Serum thiocyanate levels as an objective measure of smoking habits in epidemiological studies. *Eur J Epidemiol* **4**(2): p. 206-11.

44. Kettle, A.J. and C.C. Winterbourn, 1997, Myeloperoxidase: A key regulator of neutrophil oxidant product. *Redox Rep* **3**(1): p. 3-15.

45. Nagy, P., G.N.L. Jameson, and C.C. Winterbourn, 2009, Kinetics and Mechanisms of the Reaction of Hypothiocyanous Acid with 5-Thio-2-nitrobenzoic Acid and Reduced Glutathione. *Chem Res Toxicol* **22**(11): p. 1833-40.

46. Ashby, M.T., *Hypothiocyanite*, in *Inorganic/Bioinorganic Reaction Mechanisms*. 2012. p. 263-303.

47. Saude, E.J., et al., 2004, NMR analysis of neutrophil activation in sputum samples from patients with cystic fibrosis. *Magn Reson Med* **52**(4): p. 807-14.

48. Henderson, J.P., et al., 2003, Phagocytes produce 5-chlorouracil and 5-bromouracil, two mutagenic products of myeloperoxidase, in human inflammatory tissue. *J Biol Chem* **278**(26): p. 23522-8.

49. Takeshita, J., et al., 2006, Myeloperoxidase generates 5-chlorouracil in human atherosclerotic tissue: a potential pathway for somatic mutagenesis by macrophages. *J Biol Chem* **281**(6): p. 3096-104.

50. Henderson, J.P., et al., 2001, Production of brominating intermediates by myeloperoxidase. A transhalogenation pathway for generating mutagenic nucleobases during inflammation. *J Biol Chem* **276**(11): p. 7867-75.

51. Heinecke, J.W., 2000, Eosinophil-dependent bromination in the pathogenesis of asthma. *J Clin Invest* **105**(10): p. 1331-2.

52. Pattison, D.I., M.J. Davies, and C.L. Hawkins, 2012, Reactions and reactivity of myeloperoxidase-derived oxidants: differential biological effects of hypochlorous and hypothiocyanous acids. *Free Radic Res* **46**(8): p. 975-95.

53. Malle, E., et al., 2006, Modification of low-density lipoprotein by myeloperoxidase-derived oxidants and reagent hypochlorous acid. *Biochim Biophys Acta* **1761**(4): p. 392-415.

54. Chandler, J.D., et al., 2013, Nebulized thiocyanate improves lung infection outcomes in mice. *Brit J Pharmacol* **169**(5): p. 1166-77.

55. Nedoboy, P.E., et al., 2014, High plasma thiocyanate levels are associated with enhanced myeloperoxidase-induced thiol oxidation and long-term survival in subjects following a first myocardial infarction. *Free Radic Res* **48**(10): p. 1256-66.

56. Chandler, J.D. and B.J. Day, 2015, Biochemical Mechanisms and Therapeutic Potential of the Pseudohalide Thiocyanate in Human Health. *Free Radic Res* **49**(6): p. 695-710.

57. Arnhold, J., et al., 2006, Kinetics and thermodynamics of halide and nitrite oxidation by mammalian heme peroxidases. *Eur J Inorg Chem* **2006**(19): p. 3801-11.

58. Pattison, D.I. and M.J. Davies, 2001, Absolute rate constants for the reaction of hypochlorous acid with protein side chains and peptide bonds. *Chem Res Toxicol* **14**(10): p. 1453-64.

59. Storkey, C., M.J. Davies, and D.I. Pattison, 2014, Reevaluation of the rate constants for the reaction of hypochlorous acid (HOCl) with cysteine, methionine, and peptide derivatives using a new competition kinetic approach. *Free Radic Biol Med* **73**: p. 60-6.

60. Curtis, M.P., A.J. Hicks, and J.W. Neidigh, 2011, Kinetics of 3-chlorotyrosine formation and loss due to hypochlorous acid and chloramines. *Chem Res Toxicol* **24**(3): p. 418-28.

61. Pattison, D.I. and M.J. davies, 2004, Kinetic analysis of the reactions of hypobromous acid with protein components: Implications for cellular damage and use of 3-bromotyrosine as a marker of oxidative stress. *Biochemistry* **43**(16): p. 4799-809.

62. Skaff, O., D.I. Pattison, and M.J. Davies, 2009, Hypothiocyanous acid reactivity with low-molecular-mass and protein thiols: absolute rate constants and assessment of biological relevance. *Biochem J* **422**(1): p. 111-7.

63. Skaff, O., et al., 2012, Selenium-containing amino acids are targets for myeloperoxidase-derived hypothiocyanous acid: determination of absolute rate constants and implications for biological damage. *Biochem J* **441**(1): p. 305-16.

64. Hawkins, C.L., et al., 2008, Tryptophan residues are targets in hypothiocyanous acid-mediated protein oxidation. *Biochem J* **416**(3): p. 441-52.

65. Storkey, C., et al., 2012, Preventing protein oxidation with sugars: scavenging of hypohalous acids by 5-selenopyranose and 4-selenofuranose derivatives. *Chem Res Toxicol* **25**(11): p. 2589-99.

66. Ronsein, G.E., et al., 2014, Cross-linking methionine and amine residues with reactive halogen species. *Free Radic Biol Med* **70**: p. 278-87.

67. Peskin, A.V., et al., 2009, Oxidation of methionine to dehydromethionine by reactive halogen species generated by neutrophils. *Biochemistry* **48**(42): p. 10175-82.

68. Pereira, W.E., et al., 1973, Chlorination studies .2. Reactions of aqueous hypochlorous acid with alpha amino-acids and dipeptides. *Biochim Biophys Acta* **313**(1): p. 170-80.

69. Drozdz, R., J.W. Naskalski, and J. Sznajd, 1988, Oxidation of amino acids and peptides in reaction with myeloperoxidase, chloride and hydrogen peroxide. *Biochim Biophys Acta* **957**(1): p. 47-52.

70. Stadtman, E.R., J. Moskovitz, and R.L. Levine, 2003, Oxidation of methionine residues of proteins: Biological consequences. *Antioxid Redox Signal* **5**(5): p. 577-82.

71. Pattison, D.I., C.L. Hawkins, and M.J. Davies, 2009, What are the plasma targets of the oxidant hypochlorous acid? A kinetic modeling approach. *Chem Res Toxicol* **22**(5): p. 807-17.

72. Levine, R.L., et al., 1999, Methionine residues may protect proteins from critical oxidative damage. *Mechan Ageing Dev* **107**(3): p. 323-32.

73. Kim, G., S.J. Weiss, and R.L. Levine, 2014, Methionine oxidation and reduction in proteins. *Biochim Biophys Acta* **1840**(2): p. 901-5.

74. Hawkins, C.L. and M.J. Davies, 2005, Inactivation of protease inhibitors and lysozyme by hypochlorous acid: Role of side-chain oxidation and protein unfolding in loss of biological functions. *Chem Res Toxicol* **18**(10): p. 1600-10.

75. Hawkins, C.L. and M.J. Davies, 2005, The role of aromatic amino acid oxidation, protein unfolding, and aggregation in the hypobromous acid-induced inactivation of trypsin inhibitor and lysozyme. *Chem Res Toxicol* **18**(11): p. 1669-77.

76. Vissers, M.C.M. and C.C. Winterbourn, 1987, Myeloperoxidase-dependent oxidative inactivation of neutrophil neutral proteinases and microbicidal enzymes. *Biochem J* **245**(1): p. 277-80.

77. Lee, B.C., et al., 2009, Functions and evolution of selenoprotein methionine sulfoxide reductases. *Biochim Biophys Acta* **1790**(11): p. 1471-7.

78. Drazic, A. and J. Winter, 2014, The physiological role of reversible methionine oxidation. *Biochim Biophys Acta* **1844**(8): p. 1367-82.

79. Beal, J.L., S.B. Foster, and M.T. Ashby, 2009, Hypochlorous acid reacts with the N-terminal methionines of proteins to give dehydromethionine, a potential biomarker for neutrophil-induced oxidative stress. *Biochemistry* **48**(46): p. 11142-8.

80. Magon, N.J., et al., 2015, Oxidation of calprotectin by hypochlorous acid prevents chelation of essential metal ions and allows bacterial growth: Relevance to infections in cystic fibrosis. *Free Radic Biol Med* **86**: p. 133-44.

81. Lloyd, M.M., et al., 2008, Hypothiocyanous acid is a more potent inducer of apoptosis and protein thiol depletion in murine macrophage cells than hypochlorous acid or hypobromous acid. *Biochem J* **414**(2): p. 271-80.

82. Aune, T.M., E.L. Thomas, and M. Morrison, 1977, Lactoperoxidase-catalyzed incorporation of thiocyanate ion into a protein substrate. *Biochemistry* **16**(21): p. 4611-5.

83. Barrett, T.J., et al., 2012, Inactivation of thiol-dependent enzymes by hypothiocyanous acid: role of sulfenyl thiocyanate and sulfenic acid intermediates. *Free Radic Biol Med* **52**(6): p. 1075-85.

84. Fu, X., D.M. Mueller, and J.W. Heinecke, 2002, Generation of intramolecular and intermolecular sulfenamides, sulfinamides, and sulfonamides by hypochlorous acid: A potential pathway for oxidative cross-linking of low-density lipoprotein by myeloperoxidase. *Biochemistry* **41**(4): p. 1293-301.

85. Harwood, D.T., A.J. Kettle, and C.C. Winterbourn, 2006, Production of glutathione sulfonamide and dehydroglutathione from GSH by myeloperoxidase-derived oxidants and detection using a novel LC-MS/MS method. *Biochem J* **399**(1): p. 161-8.

86. Raftery, M.J., et al., 2001, Novel intra- and inter-molecular sulfinamide bonds in S100A8 produced by hypochlorite oxidation. *J Biol Chem* **276**(36): p. 33393-401.

87. Thomas, E.L., 1981, Lactoperoxidase-catalyzed oxidation of thiocyanate - Equilibria between oxidized forms of thiocyanate. *Biochemistry* **20**(11): p. 3273-80.

88. Davies, M.J. and C.L. Hawkins, 2000, Hypochlorite-induced oxidation of thiols: Formation of thiyl radicals and the role of sulfenyl chloride intermediates. *Free Radic Res* **33**(6): p. 719-29.

89. Ashby, M.T. and H. Aneetha, 2004, Reactive sulfur species: Aqueous chemistry of sulfenyl thiocyanates. *JACS* **126**(33): p. 10216-7.

90. Aune, T.M. and E.L. Thomas, 1978, Oxidation of protein sulfyhdryls by products of peroxidase-catalyzed oxidation of thiocyanate ion. *Biochemistry* **17**(6): p. 1005-10.

91. Hawkins, C.L., D.I. Pattison, and M.J. Davies, 2003, Hypochlorite-induced oxidation of amino acids, peptides and proteins. *Amino Acids* **25**(3-4): p. 259-74.

92. Mieyal, J.J. and P.B. Chock, 2012, Posttranslational modification of cysteine in redox signaling and oxidative stress: Focus on S-glutathionylation. *Antioxid Redox Signal* **16**(6): p. 471-5.

93. Carr, A.C., et al., 2001, Comparison of low-density lipoprotein modification by myeloperoxidase-derived hypochorous and hypobromous acids. *Free Radic Biol Med* **31**(1): p. 62-72.

94. Fu, X.Y., et al., 2006, Specific sequence motifs direct the oxygenation and chlorination of tryptophan by myeloperoxidase. *Biochemistry* **45**(12): p. 3961-71.

95. Fu, X., et al., 2004, Oxidative cross-linking of tryptophan to glycine restrains matrix metalloproteinase activity: specific structural motifs control protein oxidation. *J Biol Chem* **279**(8): p. 6209-12.

96. Zheng, L., et al., 2004, Apolipoprotein A-I is a selective target for myeloperoxidase-catalyzed oxidation and functional impairment in subjects with cardiovascular disease. *J Clin Invest* **114**(4): p. 529-41.

97. Peng, D.Q., et al., 2005, Tyrosine modification is not required for myeloperoxidase-induced loss of apolipoprotein A-I functional activities. *J Biol Chem* **280**(40): p. 33775-84.

98. Peng, D.Q., et al., 2008, Apolipoprotein A-I tryptophan substitution leads to resistance to myeloperoxidase-mediated loss of function. *Arterioscler Thromb Vasc Biol* **28**(11): p. 2063-70.

99. Hadfield, K.A., et al., 2013, Myeloperoxidase-derived oxidants modify apolipoprotein A-I and generate dysfunctional high-density lipoproteins: comparison of hypothiocyanous acid (HOSCN) with hypochlorous acid (HOCl). *Biochem J* **449**(2): p. 531-42.

100. Bonifay, V., et al., 2014, Tryptophan oxidation in proteins exposed to thiocyanate-derived oxidants. *Arch Biochem Biophys* **564**: p. 1-11.

101. Stewart, M. and C. Nicholls, 1972, A kinetic study of the acid autoxidation of tryptophan. *Aust J Chem* **25**(10): p. 2139-44.

102. Pattison, D.I. and M.J. davies, 2005, Kinetics analysis of the role of histidine chloramines in hypochlorous acid mediated protein oxidation. *Biochemistry* **44**(19): p. 7378-87.

103. Pattison, D.I. and M.J. Davies, 2006, Evidence for rapid inter- and intramolecular chlorine transfer reactions of histamine and carnosine chloramines: Implications for the prevention of hypochlorous-acid-mediated damage. *Biochemistry* **45**(26): p. 8152-62.

104. Nightingale, Z.D., et al., 2000, Relative reactivity of lysine and other peptide-bound amino acids to oxidation by hypochlorite. *Free Radic Biol Med* **29**(5): p. 425-33.

105. Pattison, D.I. and M.J. Davies, 2006, Reactions of myeloperoxidase-derived oxidants with biological substrate: Gaining insight into human inflammatory diseases. *Curr Med Chem* **13**(27): p. 3271-90.

106. Peskin, A.V. and C.C. Winterbourn, 2001, Kinetics of the reactions of hypochlorous acid and amino acid chloramines with thiols, methionine, and ascorbate. *Free Radic Biol Med* **30**(5): p. 572-9.

107. Summers, F.A., et al., 2008, Identification of plasma proteins that are susceptible to thiol oxidation by hypochlorous acid and N-chloramines. *Chem Res Toxicol* **21**(9): p. 1832-40.

108. Hawkins, C.L. and M.J. Davies, 1998, Hypochlorite-induced damage to proteins: formation of nitrogen-centred radicals from lysine residues and their role in protein fragmentation. *Biochem J* **332**: p. 617-25.

109. Hawkins, C.L. and M.J. Davies, 1998, Reaction of HOCl with amino acids and peptides: EPR evidence for rapid rearrangement and fragmentation, reactions of nitrogen-centred radicals. *J Chem Soc Perkin Trans* **9**: p. 1937-45.

110. Hawkins, C.L. and M.J. Davies, 2005, The role of reactive N-bromo species and radical intermediates in hypobromous acid-induced protein oxidation. *Free Radic Biol Med* **39**(7): p. 900-12.

111. Hazell, L.J., M.J. Davies, and R. Stocker, 1999, Secondary radicals derived from chloramines of apolipoprotein B-100 contribute to HOCl-induced lipid peroxidation of low-density lipoprotein. *Biochem J* **339**: p. 489-95.

112. Hawkins, C.L., D.I. Pattison, and M.J. Davies, 2002, Reaction of protein chloramines with DNA and nucleosides: evidence for the formation of radicals, protein–DNA cross-links and DNA fragmentation. *Biochem J* **365**: p. 605-15.

113. Hawkins, C.L. and M.J. Davies, 2001, Hypochlorite-induced damage to nucleosides: Formation of chloramines and nitrogen-centred radicals. *Chem Res Toxicol* **14**(8): p. 1071-81.

114. Fu, S., et al., 2000, Reactions of hypochlorous acid with tyrosine and peptidyl-tyrosyl residues give dichlorinated and aldehydic products in addition to 3-chlorotyrosine. *J Biol Chem* **275**(15): p. 10851-8.

115. Aldridge, R.E., et al., 2002, Eosinophil peroxidase produces hypobromous acid in the airways of stable asthmatics. *Free Radic Biol Med* **33**(6): p. 847-56.

116. Chakraborty, S., Y. Cai, and M.A. Tarr, 2014, In vitro oxidative footprinting provides insight into apolipoprotein B-100 structure in low-density lipoprotein. *Proteomics* **14**(21-22): p. 2614-22.

117. Bergt, C., et al., 2004, Lysine residues direct the chlorination of tyrosines in YXXK motifs of apolipoprotein A-I when hypochlorous acid oxidizes high density lipoprotein. *J Biol Chem* **279**(9): p. 7856-66.

118. Winterbourn, C.C., 2002, Biological reactivity and biomarkers of the neutrophil oxidant, hypochlorous acid. *Toxicology* **181**: p. 223-7.

119. Whiteman, M. and J.P. Spencer, 2008, Loss of 3-chlorotyrosine by inflammatory oxidants: implications for the use of 3-chlorotyrosine as a bio-marker in vivo. *Biochem Biophys Res Commun* **371**(1): p. 50-3.

120. Talib, J., et al., 2012, High plasma thiocyanate levels modulate protein damage induced by myeloperoxidase and perturb measurement of 3-chlorotyrosine. *Free Radic Biol Med* **53**(1): p. 20-9.

121. Heinecke, J.W., et al., 1993, Dityrosine, a specific marker of oxidation, is synthesised by the myeloperoxidase-hydrogen peroxide system of human neutrophils and macrophages. *J Biol Chem* **268**(6): p. 4069-77.

122. Heinecke, J.W., 2002, Tyrosyl radical production by myeloperoxidase: a phagocyte pathway for lipid peroxidation and dityrosine cross-linking of proteins. *Toxicology* **177**(1): p. 11-22.

123. Gross, A.J. and I.W. Sizer, 1959, The oxidation of tyramine, tyrosine, and related compounds by peroxidase. *J Biol Chem* **234**(6): p. 1611-4.

124. Sealy, R.C., et al., 1985, The electron-spin resonance-spectrum of the tyrosyl radical. *J Am Chem Soc* **107**(12): p. 3401-6.

125. Schrauzer, G.N., 2000, Selenomethionine: A review of its nutritional significance, metabolism and toxicity. *J Nutrit* **130**(7): p. 1653-6.

126. Carroll, L., et al., 2015, Reactivity of selenium-containing compounds with myeloperoxidase-derived chlorinating oxidants: Second-order rate constants and implications for biological damage. *Free Radic Biol Med* **84**: p. 279-88.

127. Assmann, A., K. Briviba, and H. Sies, 1998, Reduction of Methionine Selenoxide to Selenomethionine by Glutathione. *Arch Biochem Biophys* **349**(1): p. 201-3.

128. Krause, R.J. and A.A. Elfarra, 2009, Reduction of L-methionine selenoxide to seleno-L-methionine by endogenous thiols, ascorbic acid, or methimazole. *Biochem Pharmacol* **77**(1): p. 134-40.

129. Zhang, C., et al., 2001, L-arginine chlorination products inhibit endothelial nitric oxide production. *J Biol Chem* **276**(29): p. 27159-65.

130. Winterbourn, C.C., et al., 1992, Chlorohydrin formation from unsaturated fatty acids reacted with hypochlorous acid. *Arch Biochem Biophys* **296**(2): p. 547-55.

131. Carr, A.C., J.J.M. van den Berg, and C.C. Winterbourn, 1998, Differential reactivities of hypochlorous and hypobromous acids with purified *Escherichia coli* phospholipid: formation of haloamines and halohydrins. *Biochim Biophys Acta* **1392**(2-3): p. 254-64.

132. Carr, A.C., et al., 1997, Modification of red cell membrane lipids by hypochlorous acid and haemolysis by preformed lipid chlorohydrins. *Redox Rep* **3**(5-6): p. 263-71.

133. Vissers, M.C., A.C. Carr, and C.C. Winterbourn, 2001, Fatty acid chlorohydrins and bromohydrins are cytotoxic to human endothelial cells. *Redox Rep* **6**(1): p. 49-55.

134. Dever, G., et al., 2006, Fatty acid and phospholipid chlorohydrins cause cell stress and endothelial adhesion. *Acta Biochim Pol* **53**(4): p. 761-8.

135. Pattison, D.I., C.L. Hawkins, and M.J. Davies, 2003, Hypochlorous acid-mediated oxidation of lipid components and antioxidants present in low-density lipoproteins: Absolute rate constants, product analysis, and computational modeling. *Chem Res Toxicol* **16**(4): p. 439-49.

136. Skaff, O., D.I. Pattison, and M.J. Davies, 2007, Kinetics of hypobromous acid-mediated oxidation of lipid components and antioxidants. *Chem Res Toxicol* **20**(12): p. 1980-8.

137. Albert, C.J., et al., 2001, Reactive chlorinating species produced by myeloperoxidase target the vinyl ether bond of plasmalogens: identification of 2-chlorohexadecanal. *J Biol Chem* **276**(26): p. 23733-41.

138. Thukkani, A.K., et al., 2003, Myeloperoxidase-derived reactive chlorinating species from human monocytes target plasmalogens in low density lipoprotein. *J Biol Chem* **278**(38): p. 36365-72.

139. Anbukumar, D.S., et al., 2010, Chlorinated lipid species in activated human neutrophils: lipid metabolites of 2-chlorohexadecanal. *J Lipid Res* **51**(5): p. 1085-92.

140. Messner, M.C., et al., 2006, Selective plasmenylcholine oxidation by hypochlorous acid: formation of lysophosphatidylcholine chlorohydrins. *Chem Phys Lipids* **144**(1): p. 34-44.

141. Thukkani, A.K., et al., 2003, Identification of alpha-chloro fatty aldehydes and unsaturated lysophosphatidylcholine molecular species in human atherosclerotic lesions. *Circulation* **108**(25): p. 3128-33.

142. Ford, D.A., 2010, Lipid oxidation by hypochlorous acid: chlorinated lipids in atherosclerosis and myocardial ischemia. *Clin Lipidol* **5**(6): p. 835-52.

143. Zhang, R., et al., 2002, Defects in leukocyte-mediated initiation of lipid peroxidation in plasma as studied in myeloperoxidase-deficient subjects: systematic identification of multiple endogenous diffusible substrates for myeloperoxidase in plasma. *Blood* **99**(5): p. 1802-10.

144. Exner, M., et al., 2004, Thiocyanate catalyzes myeloperoxidase-initiated lipid oxidation in LDL. *Free Radic Biol Med* **37**(2): p. 146-55.

145. Lovaas, E., 1992, Free radical generation and coupled thiol oxidation by lactoperoxidase/SCN^-/H_2O_2. *Free Radic Biol Med* **13**(3): p. 187-95.

146. Ismael, F.O., et al., 2015, Comparative reactivity of the myeloperoxidase-derived oxidants HOCl and HOSCN with low-density lipoprotein (LDL): Implications for foam cell formation in atherosclerosis. *Arch Biochem Biophys* **573**: p. 40-51.

147. Spalteholz, H., K. Wenske, and J. Arnhold, 2005, Interaction of hypohalous acids and heme peroxidases with unsaturated phosphatidylcholines. *Biofactors* **24**(1-4): p. 67-76.

148. Hayatsu, H., S.K. Pan, and T. Ukita, 1971, Reaction of sodium hypochlorite with nucleic acids and their constituents. *Chem Pharm Bull* (10): p. 2189-92.

149. Whiteman, M., et al., 1999, Hypochlour acid-induced DNA base modification: Potentiation by nitrite: Biomarkers of DNA damage by reactive oxygen species. *Biochem Biophys Res Commun* **257**(2): p. 572-6.

150. Henderson, J.P., J. Byun, and J.W. Heinecke, 1999, Molecular Chlorine Generated by the Myeloperoxidase-Hydrogen Peroxide-Chloride System of Phagocytes Produces 5-Chlorocytosine in Bacterial RNA. *J Biol Chem* **274**(47): p. 33440-8.

151. Masuda, M., et al., 2001, Chlorination of guanosine and other nucleosides by hypochlorous acid and myeloperoxidase of activated human neutrophils. Catalysis by nicotine and trimethylamine. *J Biol Chem* **276**(44): p. 40486-96.

152. Badouard, C., et al., 2005, Detection of chlorinated DNA and RNA nucleosides by HPLC coupled to tandem mass spectrometry as potential biomarkers of inflammation. *J Chromatogr B Analyt Technol Biomed Life Sci* **827**(1): p. 26-31.

153. Henderson, J.P., et al., 2001, The eosinophil peroxidase-hydrogen peroxide-bromide system of human eosinophils generates 5-bromouracil, a mutagenic thymine analogue. *Biochemistry* **40**(7): p. 2052-9.

154. Henderson, J.P., et al., 2001, Bromination of deoxycytidine by eosinophil peroxidase: a mechanism for mutagenesis by oxidative damage of nucleotide precursors. *Proc Natl Acad Sci U S A* **98**(4): p. 1631-6.

155. Shen, Z.Z., et al., 2001, Eosinophil peroxidase catalyzes bromination of free nucleosides and double-stranded DNA. *Biochemistry* **40**(7): p. 2041-51.

156. Kawai, Y., et al., 2004, Endogenous formation of novel halogenated 2'-deoxycytidine. Hypohalous acid-mediated DNA modification at the site of inflammation. *J Biol Chem* **279**(49): p. 51241-9.

157. Wolthers, O.D., 2003, Eosinophile granule proteins in the assessment of airway inflammation in pediatric bronchial asthma. *Pediatr Allergy Immunol* **14**(4): p. 248-54.

158. Gaston, B., 2011, The biochemistry of asthma. *Biochim Biophys Acta* **1810**(11): p. 1017-24.

159. White Jr., W.E., K.M. Pruitt, and B. Mansson-Rahemtulla, 1983, Peroxidase-thiocyanate-peroxide antibacterial system does not damage DNA. *Antimicrob Agents Chemother* **23**(2): p. 267-72.

160. Suzuki, T. and H. Ohshima, 2003, Modification by fluoride, bromide, iodide, thiocyanate and nitrite anions of reaction of a myeloperoxidase-H_2O_2-Cl^- system with nucleosides. *Chem Pharm Bull* **51**(3): p. 301-4.

161. Rees, M.D., C.L. Hawkins, and M.J. Davies, 2003, Hypochlorite-mediated fragmentation of hyaluronan, chondroitin sulfates, and related N-acety glycosamines: Evidence for chloramide intermediates, free radical transfer reactions, and site-specific fragmentation. *JACS* **125**(45): p. 13719-33.

162. Jackson, R.L., S.J. Busch, and A.D. Cardin, 1991, Glycosaminoglycans: Molecular properties, protein interactions, and role in physiological processes. *Physiol Rev* **71**(2): p. 481-539.

163. Rees, M.D., D.I. Pattison, and M.J. Davies, 2005, Oxidation of heparan sulphate by hypochlorite: role of N-chloro derivatives and dichloramine-dependent fragmentation. *Biochem J* **391**(Pt 1): p. 125-34.

164. Rees, M.D., T.N. McNiven, and M.J. Davies, 2007, Degradation of extracellular matrix and its components by hypobromous acid. *Biochem J* **401**(2): p. 587-96.

165. Rees, M.D., et al., 2010, Myeloperoxidase-derived oxidants selectively disrupt the protein core of the heparan sulfate proteoglycan perlecan. *Matrix Biol* **29**(1): p. 63-73.

166. Winterbourn, C.C., 1985, Comparative reactivities of various biological compounds with myeloperoxidase-hydrogen peroxide-chloride, and similarity of the oxidant to hypochlorite. *Biochim Biophys Acta* **840**(2): p. 204-10.

167. Prutz, W.A., 1996, Hypochlorous acid interactions with thiols, nucleotides, DNA, and other biological substrates. *Arch Biochem Biophys* **332**(1): p. 110-20.

168. Hawkins, C.L., 2009, The role of hypothiocyanous acid (HOSCN) in biological systems. *Free Radic Res* **43**(12): p. 1147-58.

169. Vissers, M.C., et al., 1994, Membrane changes associated with lysis of red blood cells by hypochlorous acid. *Free Radic Biol Med* **16**(6): p. 703-12.

170. Vissers, M.C., A.C. Carr, and A.L.P. Chapman, 1998, Comparison of human red cell lysis by hypochlorous and hypobromous acids: insights into the mechanism of lysis. *Biochem J* **330**: p. 131-8.

171. De Sanctis, R., et al., 2004, *In vitro* protective effect of *Rhodiola rosea* extract against hypochlorous acid-induced oxidative damage in human erythrocytes. *Biofactors* **20**(3): p. 147-59.

172. Tedesco, I., et al., 2012, Protective Effect of gamma-Irradiation Against Hypochlorous Acid-Induced Haemolysis in Human Erythrocytes. *Dose Response* **11**(3): p. 401-12.

173. Hawkins, C.L., B.E. Brown, and M.J. Davies, 2001, Hypochlorite- and hypobromite-mediated radical formation and its role in cell lysis. *Arch Biochem Biophys* **395**(2): p. 137-45.

174. Roberts, R.L., B.J. Ank, and E.R. Steihm, 1991, Human eosinophils are more toxic than neutrophils in antibody-independent killing. *J Allergy Clin Immuno* **87**(6): p. 1105-15.

175. Grisham, M.B. and E.M. Ryan, 1990, Cytotoxic properties of salivary oxidants. *Am J Physiol* **258**(1): p. C115-21.

176. Lin, J., et al., 2013, Oxidized low density lipoprotein induced caspase-1 mediated pyroptotic cell death in macrophages: Implication in lesion instability? *PLOS One* **8**(4): p. e62148.

177. Vissers, M.C.M., J.M. Pullar, and M.B. Hampton, 1999, Hypochlorous acid causes caspase activation and apoptosis or growth arrest in human endothelial cells. *Biochem J* **344**(2): p. 443-9.

178. Schraufstatter, I.U., et al., 1990, Mechanisms of hypochlorite injury of target cells. *J Clin Invest* **85**(2): p. 554-62.

179. Yang, Y.T., M. Whiteman, and S.P. Gieseg, 2012, Intracellular glutathione protects human monocyte-derived macrophages from hypochlorite damage. *Life Sci* **90**(17-18): p. 682-8.

180. Jenner, A.M., et al., 2002, Vitamin C protects against hypochlorous acid-induced glutathione depletion and DNA base and protein damage in human vascular smooth muscle cells. *Arterioscler Thromb Vasc Biol* **22**(4): p. 574-80.

181. Slungaard, A. and J.R. Mahoney Jr, 1991, Bromide-dependent toxicity of eosinophil peroxidase for endothelium and isolated working rat hearts - A model for eosinophilic endocarditis. *J Exp Med* **173**(1): p. 117-26.

182. Wagner, B.A., et al., 2004, Role of Thiocyanate, Bromide and Hypobromous Acid in Hydrogen Peroxide-induced Apoptosis. *Free Rad Res* **38**(2): p. 167-75.

183. Cook, N.L., et al., 2012, Myeloperoxidase-derived oxidants inhibit sarco/endoplasmic reticulum Ca2+-ATPase activity and perturb Ca2+ homeostasis in human coronary artery endothelial cells. *Free Radic Biol Med* **52**(5): p. 951-61.

184. Bozonet, S.M., et al., 2010, Hypothiocyanous acid is a potent inhibitor of apoptosis and caspase 3 activation in endothelial cells. *Free Radic Biol Med* **49**(6): p. 1054-63.

185. Hauser, I.A., D.R. Johnson, and J.A. Madri, 1993, Differential induction of VCAM-1 on human iliac venous and arterial endothelial cells and its role in adhesion. *J Immunol* **151**(10): p. 5172-85.

186. Briones, M.A., et al., 2001, Expression of chemokine by human coronary-artery and umbilical-vein endothelial cells and its regulation by inflammatory cytokines. *Coron Artery Dis* **12**(3): p. 179-86.

187. Hawkins, C.L., D.I. Pattison, and M.J. Davies, 2002, Reaction of protein chloramines with DNA and nucleosides: evidence for the formation of radicals, protein-DNA cross-links and DNA fragmentation. *Biochem J* **365**: p. 605-15.

188. Pero, R.W., et al., 1996, Hypochlorous acid/N-chloramines are naturally produced DNA repair inhibitors. *Carcinogenesis* **17**(1): p. 13-8.

189. Summers, F.A., A. Forsman Quigley, and C.L. Hawkins, 2012, Identification of proteins susceptible to thiol oxidation in endothelial cells exposed to hypochlorous acid and N-chloramines. *Biochem Biophys Res Commun* **425**(2): p. 157-61.

190. Wagner, B.A., et al., 2002, Hydrogen peroxide-induced apoptosis of HL-60 human leukemia cells is mediated by the oxidants hypochlorous acid and chloramines. *Arch Biochem Biophys* **401**(2): p. 223-34.

191. Davis, R.J., 1993, The Mitogen-activated Protein Kinase Signal Transduction Pathway. *J Biol Chem* **268**(20): p. 14553-6.

192. Midwinter, R.G., M.C. Vissers, and C.C. Winterbourn, 2001, Hypochlorous acid stimulation of the mitogen-activated protein kinase pathway enhances cell survival. *Arch Biochem Biophys* **394**(1): p. 13-20.

193. Lane, A.E., et al., 2010, The myeloperoxidase-derived oxidant HOSCN inhibits protein tyrosine phosphatases and modulates cell signalling via the mitogen-activated protein kinase (MAPK) pathway in macrophages. *Biochem J* **430**(1): p. 161-9.

194. Wang, J.G., et al., 2006, The principal eosinophil peroxidase product, HOSCN, is a uniquely potent phagocyte oxidant inducer of endothelial cell tissue factor activity: a

potential mechanism for thrombosis in eosinophilic inflammatory states. *Blood* **107**(2): p. 558-65.

195. Wang, J.G., et al., 2006, Thiocyanate-dependent induction of endothelial cell adhesion molecule expression by phagocyte peroxidases: A novel HOSCN-specific oxidant mechanism to amplify inflammation. *J Immunol* **177**(12): p. 8714-22.

196. Carr, A.C. and C.C. Winterbourn, 1997, Oxidation of neutrophil glutathione and protein thiols by myeloperoxidase-derived hypochlorous acid. *Biochem J* **327**: p. 275-81.

197. Shelton, M.D., P.B. Chock, and J.J. Mieyal, 2005, Glutaredoxin: Role in reversible protein S-glutathionylation and regulation of redox signal transfuction and protein translocation. *Antioxid Redox Signal* **7**(3-4): p. 348-66.

198. Berndt, C., C.H. Lillig, and A. Holmgren, 2007, Thiol-based mechanisms of the thioredoxin and glutaredoxin systems: implications for diseases in the cardiovascular system. *Am J Physiol Heart Circ Physiol* **292**(3): p. H1227-36.

199. Lillig, C.H., C. Berndt, and A. Holmgren, 2008, Glutaredoxin systems. *Biochim Biophys Acta* **1780**(11): p. 1304-17.

200. Lu, J. and A. Holmgren, 2014, The thioredoxin antioxidant system. *Free Radic Biol Med* **66**: p. 75-87.

201. Meister, A., 1988, Glutathione metabolism and its selective modification. *J Biol Chem* **263**(33): p. 17205-8.

202. Chandler, J.D., et al., 2013, Selective metabolism of hypothiocyanous acid by mammalian thioredoxin reductase promotes lung innate immunity and antioxidant defense. *J Biol Chem* **288**(25): p. 18421-8.

203. Snider, G.W., et al., 2013, Selenocysteine confers resistance to inactivation by oxidation in thioredoxin reductase: comparison of selenium and sulfur enzymes. *Biochemistry* **52**(32): p. 5472-81.

204. Winterbourn, C.C. and A.J. Kettle, 2013, Redox reactions and microbial killing in the neutrophil phagosome. *Antioxid Redox Signal* **18**(6): p. 642-60.

205. Hampton, M.B., A.J. Kettle, and C.C. Winterbourn, 1998, Inside the neutrophil phagosome: Oxidants, myeloperoxidase, and bacterial killing. *Blood* **92**(9): p. 3007-17.

206. Klebanoff, S.J., 2005, Myeloperoxidase: friend and foe. *J Leukoc Biol* **77**(5): p. 598-625.

207. Klebanoff, S.J., 1967, Iodination of bacteria: A bactericidal mechanism. *J Exp Med* **126**(6): p. 1063-78.

208. Ihalin, R., et al., 1998, The effects of different (pseudo)halide substrates on peroxidase-mediated killing of Actinobacillus actinomycetemcomitans. *J Periodont Res* **33**(7): p. 421-7.

209. Shin, K., et al., 2002, Susceptibility of Helicobacter pylori and its urease activity to the peroxidase-hydrogen peroxide-thiocyanate antimicrobial system. *J Med Microbiol* **51**(3): p. 231-7.

210. Chapman, A.L., et al., 2002, Chlorination of bacterial and neutrophil proteins during phagocytosis and killing of Staphylococcus aureus. *J Biol Chem* **277**(12): p. 9757-62.

211. Schultz, C.P., et al., 1996, Thiocyanate levels in human saliva: Quantitation by Fourier transform infrared spectroscopy. *Anal Biochem* **240**(1): p. 7-12.

212. Reiter, B. and G. Harnulv, 1984, Lactoperoxidase antibacterial system - Natural occurence, functions and practical applications. *J Food Protect* **47**(9): p. 724-32.

213. Oram, J.D. and B. Reiter, 1966, The inhibition of Streptococci by lactoperoxidase, thiocyanate and hydrogen peroxide. *Biochem J* **100**(2): p. 373-81.

214. Clem, W.H. and S.J. Klebanoff, 1966, Inhibitory effect of saliva on glutamic acid accumulation by *Lactobacillus acidophilus* and the role of the lactoperoxidase-thiocyanate system. *J Bacteriol* **91**(5): p. 1848-53.

215. Wijkstrom-Frei, C., et al., 2003, Lactoperoxidase and human airway host defense. *American Journal of Respiratory Cell and Molecular Biology* **29**(2): p. 206-12.

216. Conner, G.E., M. Salathe, and R. Forteza, 2002, Lactoperoxidase and hydrogen peroxide metabolism in the airway. *Am J Respir Crit Care Med* **166**(12): p. S57-61.

217. El-Chemaly, S., et al., 2003, Hydrogen peroxide-scavenging properties of normal human airway secretions. *Am J Respir Crit Care Med* **167**(3): p. 425-30.

218. Conner, G.E., et al., 2007, The lactoperoxidase system links anion transport to host defense in cystic fibrosis. *FEBS Lett* **581**(2): p. 271-8.

219. Moskwa, P., et al., 2007, A novel host defense system of airways is defective in cystic fibrosis. *Am J Respir Crit Care Med* **175**(2): p. 174-83.

220. Aratani, Y., et al., 1999, Severe Impairment in Early Host Defense against Candida albicans in Mice Deficient in Myeloperoxidase. *Infect Immun* **67**(4): p. 1828-36.

221. Aratani, Y., et al., 2000, Differential host susceptibility to pulmonary infections in bacteria and fungi in mice deficient in myeloperoxidase. *J Infect Dis* **182**(4): p. 1276-9.

222. Hirche, T.O., et al., 2005, Myeloperoxidase plays critical roles in killing Klebsiella pneumoniae and inactivating neutrophil elastase: Effects on host defense. *J Immunol* **174**(3): p. 1557-65.

223. Homme, M., et al., 2013, Myeloperoxidase deficiency in mice exacerbates lung inflammation induced by nonviable Candida albicans. *Inflamm Res* **62**(11): p. 981-90.

224. Segal, A.W., 2005, How neutrophils kill microbes. *Annu Rev Immunol* **23**: p. 197-223.

225. Parry, M.F., et al., 1981, Myeloperoxidase deficiency - Prevalence and clinical significance. *Ann Intern Med* **95**(3): p. 293-301.

226. Nunoi, H., et al., 2003, Prevalence of inherited myeloperoxidase deficiency in Japan. *Microbiol Immunol* **47**(7): p. 527-31.

227. Kutter, D., et al., 2000, Consequences of total and subtotal myeloperoxidase deficiency: Risk or benefit? *Acta Haematologica* **104**(1): p. 10-5.

228. Stasia, M.J. and X.J. Li, 2008, Genetics and immunopathology of chronic granulomatous disease. *Semin Immunopathol* **30**(3): p. 209-35.

229. Nicholls, S.J. and S.L. Hazen, 2005, Myeloperoxidase and cardiovascular disease. *Arterioscler Thromb Vasc Biol* **25**(6): p. 1102-11.

230. Davies, M.J., et al., 2008, Mammalian heme peroxidases: from molecular mechanisms to health implications. *Antioxid Redox Signal* **10**(7): p. 1199-234.

231. Fu, X., et al., 2001, Hypochlorous acid oxygenates the cysteine switch domain of pro-matrilysin (MMP-7). A mechanism for matrix metalloproteinase activation and atherosclerotic plaque rupture by myeloperoxidase. *J Biol Chem* **276**(44): p. 41279-87.

232. Shabani, F., J. McNeil, and L. Tippett, 1998, The oxidative inactivation of tissue inhibitor of metalloproteinase-1 (TIMP-1) by hypochlorous acid (HOCl) is suppressed by anti-rheumatic drugs. *Free Radic Res* **28**(2): p. 115-23.

233. Hazen, S.L. and J.W. Heinecke, 1997, 3-Chlorotyrosine, a specific marker of myeloperoxidase-catalyzed oxidation, is markedly elevated in low density lipoprotein isolated from human atherosclerotic intima. *J Clin Invest* **99**(9): p. 2075-81.

234. Hazell, L.J., G. Baernthaler, and R. Stocker, 2001, Correlation between intima-to-media ratio, apolipoprotein B-100, myeloperoxidase, and hypochlorite-oxidized proteins in human atherosclerosis. *Free Radic Biol Med* **31**(10): p. 1254-62.

235. Zhang, R., et al., 2001, Association between myeloperoxidase levels and risk of coronary artery disease. *JAMA* **286**(17): p. 2136-42.

236. Meuwese, M.C., et al., 2007, Serum myeloperoxidase levels are associated with the future risk of coronary artery disease in apparently healthy individuals. The EPIC-Norfolk Prospective Population Study. *J Am Coll Cardiol* **50**(2): p. 159-65.

237. Stefanescu, A., et al., 2008, Prognostic value of plasma myeloperoxidase concentration in patients with stable coronary artery disease. *Am Heart J* **155**(2): p. 356-60.

238. Samsamshariat, S.Z., et al., 2011, Elevated plasma myeloperoxidase levels in relation to circulating inflammatory markers in coronary artery disease. *Biomark Med* **5**(3): p. 377-85.

239. Ndrepepa, G., et al., 2008, Myeloperoxidase level in patients with stable coronary artery disease and acute coronary syndromes. *Eur J Clin Invest* **38**(2): p. 90-6.

240. Tang, W.H.W., et al., 2011, Plasma myeloperoxidase predicts incident cardiovascular risks in stable patients undergoing medical management for coronary artery disease. *Clin Chem* **57**(1): p. 33-9.

241. Brennan, M.-L., et al., 2003, Prognostic value of myeloperoxidase in patients with chest pain. *N Engl J Med* **349**(17): p. 1595-604.

242. Haslacher, H., et al., 2012, Plasma myeloperoxidase level and peripheral arterial disease. *Eur J Clin Invest* **42**(5): p. 463-9.

243. Morrow, D.A., et al., 2007, National Academy of Clinical Biochemistry Laboratory Medicine Practice Guidelines: Clinical Characteristics and Utilization of Biochemical Markers in Acute Coronary Syndromes. *Circulation* **115**(13): p. e356-75.

244. Baldus, S., et al., 2003, Myeloperoxidase serum levels predict risk in patients with acute coronary syndromes. *Circulation* **108**(12): p. 1440-5.

245. Khan, S.Q., et al., 2007, Myeloperoxidase aids prognostication together with N-terminal pro-B-type natriuretic peptide in high-risk patients with acute ST elevation myocardial infarction. *Heart* **93**(7): p. 826-31.

246. Kaya, M.G., et al., 2012, Potential role of plasma myeloperoxidase level: In predicting long-term outcome of acute myocardial infarction. *Tex Heart I J* **39**(4): p. 500-6.

247. Naruko, T., 2002, Neutrophil infiltration of culprit lesions in acute coronary syndromes. *Circulation* **106**(23): p. 2894-900.

248. Apple, F.S., et al., 2009, Assessment of the multiple-biomarker approach for diagnosis of myocardial infarction in patients presenting with symptoms suggestive of acute coronary syndrome. *Clin Chem* **55**(1): p. 93-100.

249. Eggers, K.M., et al., 2010, Myeloperoxidase is not useful for the early assessment of patients with chest pain. *Clin Biochem* **43**(3): p. 240-5.

250. Baldus, S., et al., 2006, Heparins increase endothelial nitric oxide bioavailability by liberating vessel-immobilized myeloperoxidase. *Circulation* **113**(15): p. 1871-8.

251. Tang, W.H.W., et al., 2006, Plasma myeloperoxidase levels in patients with chronic heart failure. *Am J Cardiol* **98**(6): p. 796-9.

252. Doll, R., et al., 2004, Mortality in relation to smoking: 50 years' observations on male British doctors. *BMJ* **328**(7455): p. 1519-33.

253. Botti, T.P., et al., 1996, A comparison of the quantitation of macrophage foam cell populatons and the extent of apolipoprotein E deposition in developing atherosclerotic lesions in young people: High and low serum thiocyanate groups as an indication of smoking. *Atherosclerosis* **124**(2): p. 191-202.

254. Scanlon, C.E.O., et al., 1996, Evidence for more extensive deposits of epitopes of oxidized low density lipoprotein in aortas of young people with elevated serum thiocyanate levels. *Atherosclerosis* **121**(1): p. 23-33.

255. Wang, Z., et al., 2007, Protein carbamylation links inflammation, smoking, uremia and atherogenesis. *Nature Med* **13**(10): p. 1176-84.

256. Hawkins, C.L., 2014, Role of cyanate in the induction of vascular dysfunction during uremia: more than protein carbamylation? *Kidney Int* **86**(5): p. 875-7.

257. Verbrugge, F.H., W.H. Tang, and S.L. Hazen, 2015, Protein carbamylation and cardiovascular disease. *Kidney Int* **88**(3): p. 474-8.

258. Holzer, M., et al., 2012, Myeloperoxidase-derived chlorinating species induce protein carbamylation through decomposition of thiocyanate and urea: novel pathways generating dysfunctional high-density lipoprotein. *Antioxid Redox Signal* **17**(8): p. 1043-52.

259. Kitabayashi, C., et al., 2013, Positive association between plasma levels of oxidized low-density lipoprotein and myeloperoxidase after hemodialysis in patients with diabetic end-stage renal disease. *Hemodial Int* **17**(4): p. 557-67.

260. Nilsson, L., et al., 1996, Plasma cyanate concentrations in chronic renal failure. *Clin Chem* **42**(3): p. 482-3.

261. Morgan, P.E., et al., 2015, Thiocyanate supplementation decreases atherosclerotic plaque in mice expressing human myeloperoxidase. *Free Radic Res* **49**(6): p. 743-9.

262. Stary, H.C., et al., 1994, A definition of initial, fatty streak, and intermediate lesions of atherosclerosis. A report from the Committee on Vascular Lesions of the Council on Arteriosclerosis, American Heart Association. *Circulation* **89**(5): p. 2462-78.

263. Hamilton, C.A., 1997, Low-density lipoprotein and oxidised low-density lipoprotein: Their role in the development of atherosclerosis. *Pharmacol Ther* **74**(1): p. 55-72.

264. Maiolino, G., et al., 2013, The role of oxidized low-density lipoproteins in atherosclerosis: the myths and the facts. *Mediators Inflamm* **2013**: p. 714653.

265. Brown, M.S., P.T. Kovanen, and J.L. Goldstein, 1981, Regulation of plasma cholesterol by lipoprotein receptors. *Science* **212**(4495): p. 628-35.

266. Esterbauer, H., et al., 1992, The role of lipid peroxidation and antioxidants in oxidative modification of LDL. *Free Radic Biol Med* **13**: p. 341-90.

267. Yang, C.-Y., et al., 1986, Sequence, structure, receptor-binding domains and internal repeats of human apolipoprotein B-100. *Nature* **323**(6090): p. 738-42.

268. Brown, M.S. and J.L. Goldstein, 1976, Receptor mediated control of cholesterol metabolism. Study of human mutants has disclosed how cells regulate a substance that is both vital and lethal. *Science* **191**(4223): p. 150-4.

269. Hevonoja, T., et al., 2000, Structure of low density lipoprotein (LDL) particles: Basis for understanding molecular changes in modified LDL. *Biochem Biophys Acta Molec Cell Biol Lipids* **1488**(3): p. 189-210.

270. Proctor, S.D., D.F. Vine, and J.C.L. Mamo, 2002, Arterial retention of apolipoprotein B48- and B100-containing lipoproteins in atherogenesis. *Curr Opin Lipidol* **13**(5): p. 461-70.

271. Brown, M.S. and J.L. Goldstein, 1974, Suppression of 3-Hydroxy-3-methylglutaryl Coenzyme A Reductase Activity and Inhibition of Growth of Human Fibrpblasts by 7-Ketocholesterol. *J Biol Chem* **249**(22): p. 7306-14.

272. Chen, H.W., A.A. Kandutsch, and C. Waymouth, 1974, Inhibition of cell growth by oxygenated derivatives of cholesterol. *Nature* **251**(5474): p. 419-21.

273. Younis, N.N., et al., 2009, Lipoprotein glycation in atherogenesis. *Clin Lipidol* **4**(6): p. 781-90.

274. Apostolov, E.O., et al., 2009, Scavenger receptors of endothelial cells mediate the uptake and cellular proatherogenic effects of carbamylated LDL. *Arterioscler Thromb Vasc Biol* **29**(10): p. 1622-30.

275. Goldstein, J.L., et al., 1979, Binding site on macrophages that mediates uptake and degradation of acetylated low density lipoprotein, producing massive cholesterol deposition. *Proc Natl Acad Sci* **76**(1): p. 333-7.

276. Mitra, S., T. Goyal, and J.L. Mehta, 2011, Oxidized LDL, LOX-1 and atherosclerosis. *Cardiovasc Drugs Ther* **25**(5): p. 419-29.

277. Moore, K.J. and M.W. Freeman, 2006, Scavenger receptors in atherosclerosis: beyond lipid uptake. *Arterioscler Thromb Vasc Biol* **26**(8): p. 1702-11.

278. Heinecke, J.W., 1998, Oxidants and antioxidants in the pathogenesis of atherosclerosis: Implications for the oxidised low density lipoprotein hypothesis. *Atherosclerosis* **141**(1): p. 1-15.

279. Boudjeltia, K.Z., et al., 2004, Oxidation of low density lipoproteins by myeloperoxidase at the surface of endothelial cells: an additional mechanism to subendothelium oxidation. *Biochem Biophys Res Commun* **325**(2): p. 434-8.

280. Levitan, I., S. Volkov, and P.V. Subbaiah, 2010, Oxidized LDL: Diversity, patterns of recognition, and pathophysiology. *Antioxid Redox Signal* **13**(1): p. 39-75.

281. Hazell, L.J., et al., 1996, Presence of hypochlorite-modified proteins in human atherosclerotic lesions. *J Clin Invest* **97**(6): p. 1535-44.

282. Pirillo, A., G.D. Norata, and A.L. Catapano, 2013, LOX-1, oxLDL and atherosclerosis. *Mediat Inflamm* **2013**(Article ID 152786): p. 12.

283. Meisinger, C., et al., 2005, Plasma oxidized low-density lipoprotein, a strong predictor for acute coronary heart disease events in apparently healthy, middle-aged men from the general population. *Circulation* **112**(5): p. 651-7.

284. Malle, E., et al., 2000, Immunohistochemical evidence for the myeloperoxidase/H_2O_2/halide system in human atherosclerotic lesions - colocalization of myeloperoxidase and hypochlorite-modified proteins. *Eur J Biochem* **267**(14): p. 4495-503.

285. Koenig, W. and N. Khuseyinova, 2007, Biomarkers of atherosclerotic plaque instability and rupture. *Arterioscler Thromb Vasc Biol* **27**(1): p. 15-26.

286. Agner, K., Verdoperoxidase; a Ferment Isolated from Leucocytes. *Acta physiol Scand* Vol. 8. 1941: Norstedt.

287. Camejo, G., et al., 1989, Agarose isoelectric focusing of plasma low and very low density lipoproteins using the PhastSystem. *Anal Biochem* **182**(1): p. 94-7.

288. Delporte, C., et al., 2014, Impact of myeloperoxidase-LDL interactions on enzyme activity and subsequent posttranslational oxidative modifications of apoB-100. *J Lipid Res* **55**(4): p. 747-57.

289. Sokolov, A.V., et al., 2011, Revealing binding sites for myeloperoxidase on the surface of human low density lipoproteins. *Chem Phys Lipids* **164**(1): p. 49-53.

290. Sokolov, A.V., et al., 2014, Proatherogenic modification of LDL by surface-bound myeloperoxidase. *Chem Phys Lipids* **180**: p. 72-80.

291. Yang, C.Y., et al., 1999, Selective modification of apoB-100 in the oxidation of low density lipoproteins by myeloperoxidase in vitro. *J Lipid Res* **40**(4): p. 686-98.

292. Hazell, L.J. and R. Stocker, 1993, Oxidation of low-density lipoprotein with hypochlorite causes transformation of the lipoprotein into a high-uptake form for macrophages. *Biochem J* **290**(1): p. 165-72.

293. Hazell, L.J., J.J.M. van den Berg, and R. Stocker, 1994, Oxidation of low-density lipoprotein by hypochlorite causes aggregation that is mediated by modification of lysine residues rather than lipid oxidation. *Biochem J* **302**(1): p. 297-304.

294. Leeuwenburgh, C., et al., 1997, Mass spectrometric quantification of markers for protein oxidation by tyrosyl radical, copper, and hydroxyl radical in low density lipoprotein isolated from human atherosclerotic plaques. *J Biol Chem* **272**(6): p. 3520-6.

295. Clark, R.A., et al., 1986, Oxidation of lysine side-chains of elastin by the myeloperoxidase system and by stimulated human neutrophils. *Biochem Biophys Res Commun* **135**(2): p. 451-7.

296. Bridges, R.B., M.C. Fu, and S.R. Fehm, 1985, Increased neutrophil myeloperoxidase activity associated with cigarette smoking. *Eur J Respir Dis* **67**(2): p. 84-93.

297. Loke, W.M., et al., 2012, Products of 5-lipoxygenase and myeloperoxidase activities are increased in young male cigarette smokers. *Free Radic Res* **46**(10): p. 1230-7.

298. Spickett, C.M., et al., 2000, The reactions of hypochlorous acid, the reactive oxygen species produced by myeloperoxidase, with lipids. *Acta Biochim Pol* **47**(4): p. 889-99.

299. Jerlich, A., et al., 2000, Pathways of phospholipid oxidation by HOCl in human LDL detected by LC-MS. *Free Radic Biol Med* **28**(5): p. 673-82.

300. Carr, A.C., J.J.M. van den Berg, and C.C. Winterbourn, 1996, Chlorination of cholesterol in cell membranes by hypochlorous acid. *Arch Biochem Biophys* **332**(1): p. 63-9.

301. Kawai, Y., et al., 2006, Hypochlorous acid-derived modification of phospholipids: Characterization of aminophospholipids as regulatory molecules for lipid peroxidation. *Biochemistry* **45**(47): p. 14201-11.

302. Esterbauer, H., et al., 1989, Continuous monitoring of in vitro oxidation of human low density lipoprotein. *Free Radic Res Commun* **6**(1): p. 67-75.

303. Knott, H.M., et al., 2002, Comparative time-courses of copper-ion-mediated protein and lipid oxidation in low-density lipoprotein. *Arch Biochem Biophys* **400**(2): p. 223-32.

304. Burkitt, M.J., 2001, A critical overview of the chemistry of copper-dependent low density lipoprotein oxidation: roles of lipid hydroperoxides, alpha-tocopherol, thiols, and ceruloplasmin. *Arch Biochem Biophys* **394**(1): p. 117-35.

305. Vicca, S., et al., 2000, Caspase-dependent apoptosis in THP-1 cells exposed to oxidized low-density lipoproteins. *Biochem Biophys Res Commun* **273**(3): p. 948-54.

306. Sun, Y. and X. Chen, 2011, Ox-LDL-induced LOX-1 expression in vascular smooth muscle cells: role of reactive oxygen species. *Fundam Clin Pharmacol* **25**(5): p. 572-9.

307. Jeng, J.R., et al., 1993, Oxidized low-density lipoprotein enhances monocyte-endothelial cell binding against shear-stress-induced detachment. *Biochim Biophys Acta* **1178**(2): p. 221-7.

308. Stroka, K.M., I. Levitan, and H. Aranda-Espinoza, 2012, OxLDL and substrate stiffness promote neutrophil transmigration by enhanced endothelial cell contractility and ICAM-1. *J Biomech* **45**(10): p. 1828-34.

309. Liao, J.K., et al., 1995, Oxidized low-density lipoprotein decreases the expression of endothelial nitric oxide synthase. *J Biol Chem* **270**(1): p. 319 - 24.

310. Han, C.-Y., S.-Y. Park, and Y.K. Pak, 2000, Role of endocytosis in the transactivation of nuclear factor-κB by oxidized low-density lipoprotein. *Biochem J* **350**(829-37).

311. Maziere, C., et al., 1996, Oxidized low density lipoprotein induces activation of the transcription factor NF kappa B in Fibroblasts, endothelial and smooth muscle cells *Biochem Mol Biol Int* **39**(6): p. 1201-7.

312. Ares, M.P.S., et al., 1995, Oxidized LDL induces Transcription factor activator protein-1 but inhibits activation of nuclear factor-kappa-B in human vascular smooth muscle cells. *Arterioscler Thromb Vasc Biol* **15**(10): p. 1584-90.

313. Mazière, C., et al., 1997, Copper and cell-oxidized low-density lipoprotein induces activator protein 1 in fibroblasts, endothelial and smooth muscle cells. *FEBS Lett* **409**(3): p. 351-6.

314. Shatrov, V.A., et al., 2003, Oxidized low-density lipoprotein (oxLDL) triggers hypoxia-inducible factor-1alpha (HIF-1alpha) accumulation via redox-dependent mechanisms. *Blood* **101**(12): p. 4847-9.

315. Bochkov, V.N., 2002, Oxidized phospholipids stimulate tissue factor expression in human endothelial cells via activation of ERK/EGR-1 and Ca++/NFAT. *Blood* **99**(1): p. 199-206.

316. Maziere, C., et al., 2005, Oxidized low-density lipoprotein elicits an intracellular calcium rise and increases the binding activity of the transcription factor NFAT. *Free Radic Biol Med* **38**(4): p. 472-80.

317. Kuan, P., 1987, Cardiac Wilson's Disease. *Chest* **91**(4): p. 579-83.

318. Ehrenwald, E., G.M. Chisolm, and P.L. Fox, 1994, Intact Human Ceruloplasmin Oxidatively Modified Low Density Lipoprotein. *J Clin Invest* **93**(4): p. 1493-501.

319. Rodo, M., et al., 2000, The levels of serum lipids, vitamin E and low density lipoprotein oxidation in Wilson's disease patients. *Eur J Neurol* **7**(5): p. 491-4.

320. Fu, S., et al., 1998, Evidence for roles of radicals in protein oxidation in advanced human atherosclerotic plaque. *Biochem J* **333**: p. 519-25.

321. Yoshida, H. and R. Kisugi, 2010, Mechanisms of LDL oxidation. *Clin Chim Acta* **411**(23-24): p. 1875-82.

322. Stadler, N., R.A. Lindner, and M.J. Davies, 2004, Direct detection and quantification of transition metal ions in human atherosclerotic plaques: Evidence for the presence of elevated levels of iron and copper. *Arterioscler Thromb Vasc Biol* **24**(5): p. 949-54.

323. de Valk, B. and J.J.M. Marx, 1999, Iron, Atherosclerosis, and Ischemic Heart Disease. *Arch Intern Med* **159**(14): p. 1542-8.

324. Haidari, M., et al., 2001, Association of Increased Ferritin with Premature Coronary Stenosis in Men. *Clin Chem* **47**(9): p. 1666-72.

325. Brouwers, A., et al., 2004, Oxidized low-density lipoprotein, iron stores, and haptoglobin polymorphism. *Atherosclerosis* **176**(1): p. 189-95.

326. Niederau, C., 2000, Iron overload and atherosclerosis. *Hepatology* **32**(3): p. 672-4.

327. Kirk, E.A., J.W. Heinecke, and R.C. LeBoeuf, 2001, Iron overload diminishes atherosclerosis in apoE-deficient mice. *J Clin Invest* **107**(12): p. 1545-53.

328. Claeys, D., et al., 2002, Haemochromatosis mutations and ferritin in myocardial infarction: a case-control study. *Eur J Clin Invest* **32**: p. 3-8.

329. Koppel, H., et al., 2004, Hemochromatosis gene (HFE) polymorphisms are not associated with peripheral arterial disease. *Thromb Haemost* **91**(6): p. 1258-9.

330. Ellervik, C., et al., 2007, Hereditary hemochromatosis genotypes and risk of ischemic stroke. *Neurology* **68**(13): p. 1025-31.

331. Yunker, L.M., et al., 2006, The effect of iron status on vascular health. *Vasc Med* **11**(2): p. 85-91.

332. Bozzini, C., et al., 2002, Biochemical and Genetic Markers of Iron Status and the Risk of Coronary Artery Disease: An Angiography-based Study. *Clin Chem* **48**(4): p. 622-8.

333. Yamamoto, S., 1992, Mammalian lipoxygenases: molecular structures and functions. *Biochim Biophys Acta* **1128**(2-3): p. 117-31.

334. Kuhn, H., S. Banthiya, and K. van Leyen, 2015, Mammalian lipoxygenases and their biological relevance. *Biochim Biophys Acta* **1851**(4): p. 308-30.

335. Kuhn, H., et al., 1994, Oxidative modification of human lipoproteins by lipoxygenases of different positional specificities. *J Lipid Res* **35**(10): p. 1749-59.

336. Belkner, J., et al., 1993, Oxygenation of lipoproteins by mammalian lipoxygenases. *Eur J Biochem* **213**(1): p. 251-61.

337. Ylaherttuala, S., et al., 1990, Colocalisation of 15-lipoxygenase mRNA with epitopes of oxidzed low density lipoprotein in macrophage-rich areas of atherosclerotic lesions. *Proc Natl Acad Sci* **87**(18): p. 6959-63.

338. Sloane, D.L., et al., 1991, A primary determinant for lipoxygenase positional specificity. *Nature* **354**(6349): p. 149-52.

339. Ivanov, I., et al., 2010, Molecular enzymology of lipoxygenases. *Arch Biochem Biophys* **503**(2): p. 161-74.

340. Mathur, S.N., et al., 1985, Increased production of lipoxygenase products by cholesterol-rich mouse macrophages. *Biochim Biophys Acta* **837**(1): p. 13-9.

341. Parthasarathy, S., E. Wieland, and D. Steinberg, 1989, A role for endothelial cell lipoxygenase in the oxidative modification of low density lipoprotein. *Proc Natl Acad Sci* **86**(3): p. 1046-50.

342. Sparrow, C.P. and J. Olszewski, 1992, Cellular oxidative modification of low density lipoprotein does not require lipoxygenases. *Proc Natl Acad Sci* **89**(1): p. 128-31.

343. Firth, C.A. and S.P. Gieseg, 2007, Redistribution of metal ions to control low density lipoprotein oxidation in Ham's F10 medium. *Free Radic Res* **41**(10): p. 1109-15.

344. Baynes, J.W., 1991, Role of Oxidative Stress in Development of Complications in Diabetes. *Diabetes* **40**(4): p. 405-12.

345. Bucala, R., et al., 1993, Lipid advanced glycosylation: Pathway for lipid oxidation in vivo. *Proc Natl Acad Sci* **90**(14): p. 6434-8.

346. Brownlee, M., 1995, Advanced protein glycosylation in diabetes and aging. *Annu Rev Med* **46**: p. 223-34.

347. Baynes, J.W. and S.R. Thorpe, 1999, Role of Oxidative Stress in Diabetic Complications: A New Perspective on an Old Paradigm. *Diabetes* **48**(1): p. 1-9.

348. Babiy, A.V., et al., 1992, Increased oxidizability of plasma lipoproteins in diabetic patients can be decreased by probucol therapy and is not due to glycation. *Biochem Pharmacol* **43**(5): p. 995-1000.

349. Brown, B.E., R.T. Dean, and M.J. Davies, 2005, Glycation of low-density lipoproteins by methylglyoxal and glycolaldehyde gives rise to the in vitro formation of lipid-laden cells. *Diabetologia* **48**(2): p. 361-9.

350. Knott, H.M., et al., 2003, Glycation and glycoxidation of low-density lipoproteins by glucose and low-molecular mass aldehydes. Formation of modified and oxidized particles. *Eur J Biochem* **270**(17): p. 3572-82.

351. Beckman, J.S. and W.H. Koppenol, 1996, Nitric oxide, superoxide, and peroxynitrite: The good, the bad, and the ugly. *Am J Physiol* **271**(5): p. C1424-37.

352. Lancaster Jr., J.R., 2006, Nitroxidative, Nitrosative, and Nitrative Stress: Kinetic Predictions of Reactive Nitrogen Species Chemistry Under Biological Conditions. *Chem Res Toxicol* **19**(9): p. 1160-74.

353. Ischiropoulos, H., et al., 1992, Peroxynitrite-Mediated Nitration Catalyzed by Superoxide Dismutase. *Arch Biochem Biophys* **298**(2): p. 431-7.

354. Leeuwenburgh, C., et al., 1997, Reactive nitrogen intermediates promote low density lipoprotein oxidation in human atherosclerotic intima. *J Biol Chem* **272**(3): p. 1433-6.

355. Beckmann, J.S., et al., 1994, Extensive Nitration of Protein Tyrosines in Human Atherosclerosis Detected by Immunohistochemistry. *Biol Chem Hoppe Seyler* **375**(2): p. 81-8.

356. Graham, A., et al., 1993, Peroxynitrite modification of low-density lipoprotein leads to recognition by the macrophage scavenger receptor. *FEBS Lett* **330**(2): p. 181-5.

357. Darley-usmar, V.M., et al., 2009, The Simultaneous Generation of Superoxide and Nitric Oxide Can Initiate Lipid Peroxidation in Human Low Density Lipoprotein. *Free Radic Res Comm* **17**(1): p. 9-20.

358. Radi, R., et al., 1991, Peroxynitrite-Induced Membrane Lipid Peroxidation: The Cytotoxic Potential of Superoxide and Nitric Oxide. *Arch Biochem Biophys* **288**(2): p. 481-7.

359. Eiserich, J.P., et al., 1997, Formation of nitric oxide-derived inflammatory oxidants by myeloperoxidase in neutrophils. *Nature* **391**(6665): p. 393-7.

360. Byun, J., et al., 1999, Nitrogen dioxide radical generated by the myeloperoxidase-hydrogen peroxide-nitrite system promotes lipid peroxidation of low density lipoprotein. *FEBS Lett* **455**(3): p. 243-6.

361. Podrez, E.A., et al., 1999, Myeloperoxidase-generated reactive nitrogen species convert LDL into an atherogenic form in vitro. *J Clin Invest* **103**(11): p. 1547-60.

362. Steffen, Y., et al., 2006, Cytotoxicity of myeloperoxidase/nitrite-oxidized low-density lipoprotein toward endothelial cells is due to a high 7beta-hydroxycholesterol to 7-ketocholesterol ratio. *Free Radic Biol Med* **41**(7): p. 1139-50.

363. Sato, K., E. Niki, and H. Shimasaki, 1990, Free Radical-Mediated Chain Oxidation of Low Density Lipoprotein and its Synergistic Inhibition by Vitamin E and Vitamin C. *Arch Biochem Biophys* **279**(2): p. 402-5.

364. Hsuanyu, Y. and H.B. Dunford, 1999, Oxidation of clozapine and ascorbate by myeloperoxidase. *Arch Biochem Biophys* **368**(2): p. 413-20.

365. Rees, M.D., et al., 2014, Mechanism and regulation of peroxidase-catalyzed nitric oxide consumption in physiological fluids: critical protective actions of ascorbate and thiocyanate. *Free Radic Biol Med* **72**: p. 91-103.

366. Hazell, L.J. and R. Stocker, 1997, alpha-tocopherol does not inhibit hypochlorite-induced oxidation of apolipoprotein B-100 of low-density lipoprotein. *FEBS Lett* **414**(3): p. 541-4.

367. Podrez, E.A., et al., 2002, A novel family of atherogenic oxidized phospholipids promotes macrophage foam cell formation via the scavenger receptor CD36 and is enriched in atherosclerotic lesions. *J Biol Chem* **277**(41): p. 38517-23.

368. Glavind, J., et al., 1952, Studies on the role of lipoperoxides in human pathology II. The presence of peroxidized lipids in the atherosclerotic aorta. *Acta Pathol Microbiol Scand* **30**(1): p. 1-6.

369. Suarna, C., et al., 1995, Human Atherosclerotic Plaque Contains Both Oxidized Lipids and Relatively Large Amounts of α-Tocopherol and Ascorbate. *Arterioscler Thromb Vasc Biol* **15**(10): p. 1616-24.

370. Lee, S., et al., 2012, Role of phospholipid oxidation products in atherosclerosis. *Circ Res* **111**(6): p. 778-99.

371. Jha, P., et al., 1995, The Antioxidant Vitamins and Cardiovascular Disease - A Critical Review of Epidemiologic and Clinical Trial Data. *Ann Intern Med* **123**(11): p. 860-72.

372. Heinonen, O.P., et al., 1994, The Effect of Vitamin E and Beta Carotene on the Incidence of Lung Cancer and Other Cancers in Male Smokers. *N Engl J Med* **330**(15): p. 1029-35.

373. Tognoni, G., et al., 2001, Low-dose aspirin and vitamin E in people at cardiovascular risk: a randomised trial in general practice. *Lancet* **357**(9250): p. 89-95.

374. Hodis, H.N., et al., 2002, Alpha-tocopherol supplementation in healthy individuals reduces low-density lipoprotein oxidation but not atherosclerosis - The Vitamin E Atherosclerosis Prevention Study (VEAPS). *Circulation* **106**(12): p. 1453-9.

375. Lynch, S.M. and B. Frei, 1993, Mechanisms of copper- and iron-dependent oxidative modification of human low density lipoprotein. *J Lipid Res* **34**(10): p. 1745-53.

376. Frankel, E.N., et al., 1993, Inhibition of oxidation of human low-density lipoprotein by phenolic substances in red wine. *Lancet* **341**(8843): p. 454-7.

377. Miura, S., et al., 1994, The Inhibitory Effects of Tea Polyphenols (Flavan-3-ol Derivatives) on Cu2+ Mediated Oxidative Modification of Low Density Lipoprotein. *Biol Pharm Bull* **17**(12): p. 1567-72.

378. Pietta, P.G., 2000, Flavonoids as Antioxidants. *J Nat Prod* **63**(7): p. 1035-42.

379. Kerry, N. and C. Rice-Evans, 1999, Inhibition of peroxynitrite-mediated oxidation of dopamine by flavonoid and phenolic antioxidants and their structural relationships. *J Neurochem* **73**(1): p. 247-53.

380. Suzuki-Sugihara, N., et al., 2016, Green tea catechins prevent low-density lipoprotein oxidation via their accumulation in low-density lipoprotein particles in humans. *Nutr Res* **36**(1): p. 16-23.

381. Duthie, G.G., S.J. Duthie, and J.A.M. Kyle, 2000, Plant polyphenols in cancer and heart disease: implications as nutritional antioxidants. *Nutr Res Rev* **13**(1): p. 79-106.

382. Geleijnse, J.M., et al., 1999, Tea flavonoids may protect against atherosclerosis - The Rotterdam study. *Arch Intern Med* **159**(18): p. 2170-4.

383. Renaud, S. and M. Delorgeril, 1992, Wine, alcohol, platelets, and the French paradox for coronary heart disease. *Lancet* **339**(8808): p. 1523-6.

384. Eastmond, D.A., et al., 1986, Metabolic Activation of Phenol by Human Myeloperoxidase and Horseradish Peroxidase. *Molec Pharmacol* **30**(6): p. 674-9.

385. Goldman, R., et al., 1999, Myeloperoxidase-catalysed redox-cycling of phenol promotes lipid peroxidation and thiol oxidation in HL-60 cells. *Free Radic Biol Med* **29**(9-10): p. 1050-63.

386. Miyoshi, N., et al., 2007, Dietary flavonoid apigenin is a potential inducer of intracellular oxidative stress: The role in the interruptive apoptotic signal. *Arch Biochem Biophys* **466**(2): p. 274-82.

387. Blair-Johnson, M., T. Fiedler, and R. Fenna, 2001, Human Myeloperoxidase: Structure of a Cyanide Complex and Its Interaction with Bromide and Thiocyanate Substrates at 1.9 Å Resolution. *Biochemistry* **40**(46): p. 13990-7.

388. Westley, J., 1973, Rhodanese. *Adv Enzymol Relat Subj* **39**: p. 327-68.

389. Davies, B. and S.W. Edwards, 1989, Inhibition of myeloperoxidase by salicylhydroxamic acid. *Biochem J* **258**(3): p. 801-6.

390. Ikedasaito, M., et al., 1991, Salicylhydroxamic Acid Inhibits Myeloperoxidase Activity. *J Biol Chem* **266**(6): p. 3611-6.

391. Jerlich, A., et al., 2000, Comparison of HOCl traps with myeloperoxidase inhibitors in prevention of low density lipoprotein oxidation. *Biochim Biophys Acta* **1481**(1): p. 109-18.

392. Kettle, A.J., C.A. Gedye, and C.C. Winterbourn, 1997, Mechanism of inactivation of myeloperoxidase by 4-aminobenzoic acid hydrazide. *Biochem J* **321**: p. 503-8.

393. Graham, G.G., K.F. Scott, and R.O. Day, 2005, Tolerability of paracetamol. *Drug Saf* **28**(3): p. 227-40.

394. Marquez, L.A. and H.B. Dunford, 1993, Interaction of Acetaminophen with Myeloperoxidase Intermediates: Optimum Stimulation of Enzyme Activity. *Arch Biochem Biophys* **305**(2): p. 414-20.

395. Graham, G.G., et al., 1999, Current concepts of the actions of paracetamol (acetaminophen) and NSAIDs. *Inflammopharmacology* **7**(3): p. 255-63.

396. Vanzyl, J.M., K. Basson, and B.J. Vanderwalt, 1989, The inhibitory effect of acetaminophen on the myeloperoxidase-induced antimicrobial system of the polymorphonuclear leukocyte. *Biochem Pharmacol* **38**(1): p. 161-5.

397. Koelsch, M., et al., 2010, Acetaminophen (paracetamol) inhibits myeloperoxidase-catalyzed oxidant production and biological damage at therapeutically achievable concentrations. *Biochem Pharmacol* **79**(8): p. 1156-64.

398. Chou, T.M. and P. Greenspan, 2002, Effect of acetaminophen on the myeloperoxidase-hydrogen peroxide-nitrite mediated oxidation of LDL. *Biochim Biophys Acta Molec Cell Biol Lipids* **1581**(1-2): p. 57-63.

399. Ozsoy, M.B. and A. Pabuccuoglu, 2007, The effect of acetaminophen on oxidative modification of low-density lipoproteins in hypercholesterolemic rabbits. *J Clin Biochem Nutr* **41**(1): p. 27-31.

400. Kapiotis, S., et al., 1997, Paracetamol catalyzes myeloperoxidase-initiated lipid oxidation in LDL. *Arterioscler Thromb Vasc Biol* **17**(11): p. 2855-60.

401. Potter, D.W., D.W. Miller, and J.A. Hinson, 1985, Identification of Acetaminophen Polymerization Products Catalyzed by Horseradish Peroxidase. *J Biol Chem* **260**(22): p. 2174-80.

402. Larson, A.M., et al., 2005, Acetaminophen-induced acute liver failure: Results of a United States multicenter, prospective study. *Hepatology* **42**(6): p. 1364-72.

403. Soule, B.P., et al., 2007, Therapeutic and clinical applications of nitroxide compounds. *Antioxid Redox Signal* **9**(10): p. 1731-43.

404. Queiroz, R.F., S.M. Vaz, and O. Augusto, 2011, Inhibition of the chlorinating activity of myeloperoxidase by tempol: revisiting the kinetics and mechanisms. *Biochem J* **439**(3): p. 423-31.

405. Vaz, S.M. and O. Augusto, 2008, Inhibition of myeloperoxidase-mediated protein nitration by tempol: Kinetics, mechanism, and implications. *Proc Natl Acad Sci U S A* **105**(24): p. 8191-6.

406. Rees, M.D., et al., 2009, Inhibition of myeloperoxidase-mediated hypochlorous acid production by nitroxides. *Biochem J* **421**(1): p. 79-86.

407. Mudau, M., et al., 2012, Endothelial dysfunction: The early predictor of atherosclerosis. *Cardiovasc J Afr* **23**(4): p. 222-31.

408. Pennathur, S. and J.W. Heinecke, 2007, Oxidative stress and endothelial dysfunction in vascular disease. *Curr Diab Rep* **7**(4): p. 257-64.

409. Dzau, V.J., R.C. Braun-Dullaeus, and D.G. Sedding, 2002, Vascular proliferation and atherosclerosis: New perspectives and therapeutic strategies. *Nature Med* **8**(11): p. 1249-56.

410. Shroff, R.C. and C.M. Shanahan, 2007, The Vascular Biology of Calcification. *Semin Dial* **20**(2): p. 103-9.

411. Geer, J.C., 1965, Fine structure of human aortic intimal thickening and fatty streaks. *Lab Invest* **14**(10): p. 1764-83.

412. Plüddemann, A., C. Neyen, and S. Gordon, 2007, Macrophage scavenger receptors and host-derived ligands. *Methods* **43**(3): p. 207-17.

413. Yla-Herttuala, S., et al., 1991, Expression of monocyte chemoattractant protein 1 in macrophage-rich areas of human and rabbit atherosclerotic lesions. *P Natl Acad Sci USA* **88**(12): p. 5252-6.

414. Jovinge, S., et al., 1996, Human monocytes/macrophages release TNF-α in response to Ox-LDL. *Arterioscler Thromb Vasc Biol* **16**(12): p. 1573-9.

415. Baumann, H. and J. Gauldie, 1994, The acute phase response. *Immunol Today* **15**(2): p. 74-80.

416. Nagy, L., et al., 1998, Oxidized LDL regulates macrophage gene expression through ligand activation of PPAR gamme. *Cell* **93**(2): p. 229-40.

417. Westendorf, T., J. Graessler, and S. Kopprasch, 2005, Hypochlorite-oxidized low-density lipoprotein upregulates CD36 and PPARγ mRNA expression and modulates SR-BI gene expression in murine macrophages. *Mol Cell Biochem* **277**(1-2): p. 143-52.

418. Han, K.H., et al., 2000, Oxidized LDL reduces monocyte CCR2 expression through pathways involving peroxisome proliferator-activated receptor γ. *J Clin Invest* **106**(6): p. 793-802.

419. Syvaranta, S., et al., 2014, Potential pathological roles for oxidized low-density lipoprotein and scavenger receptors SR-AI, CD36, and LOX-1 in aortic valve stenosis. *Atherosclerosis* **235**(2): p. 398-407.

420. Mattaliano, M.D., et al., 2009, LOX-1-dependent transcriptional regulation in response to oxidized LDL treatment of human aortic endothelial cells. *Am J Physiol* **296**(6): p. C1329-37.

421. Adachi, H. and M. Tsujimoto, 2006, Endothelial scavenger receptors. *Prog Lipid Res* **45**(5): p. 379-404.

422. Price, D.T. and J. Loscalzo, 1999, Cellular adhesion molecules and atherogenesis. *Am J Med* **107**(1): p. 85-97.

423. Butcher, E.C., 1991, Leukocyte-endothelial cell recognition: Three (or more) steps to specificity and diversity. *Cell* **67**(6): p. 1033-6.

424. McEver, R.P. and R.D. Cummings, 1997, Role of PSGL-1 binding to selectins in leukocyte recruitment. *J Clin Invest* **100**(11 SUPPL.): p. S97-S103.

425. Kunkel, E.J. and K. Ley, 1996, Distinct phenotype of E-selectin-deficient mice: E-selectin is required for slow leukocyte rolling in vivo. *Circ Res* **79**(6): p. 1196-204.

426. Campbell, J.J., et al., 1996, Biology of chemokine and classical chemoattractant receptors: Differential requirements for adhesion-triggering versus chemotactic responses in lymphoid cells. *J Cell Biol* **134**(1): p. 255-66.

427. Berlin, C., et al., 1995, α4 Integrins mediate lymphocyte attachment and rolling under physiologic flow. *Cell* **80**(3): p. 413-22.

428. Marlin, S.D. and T.A. Springer, 1987, Purified intercellular adhesion molecule-1 (ICAM-1) is a ligand for lymphocyte function-associated antigen-1 (LFA-1). *Cell* **51**(4): p. 813-9.

429. Dustin, M.L. and T.A. Springer, 1988, Lymphocyte function-associated antigen-1 (LFA-1) interaction with intercellular adhesion molecule-1 (ICAM-1) is one of at least three mechanisms for lymphocyte adhesion to cultured endothelial cells. *J Cell Biol* **107**(1): p. 321-31.

430. Campbell, J.J., et al., 1998, Chemokines and the arrest of lumphocytes rolling under flow conditions. *Science* **279**(5349): p. 381-4.

431. Yang, L., et al., 2005, ICAM-1 regulates neutrophil adhesion and transcellular migration of TNF-alpha-activated vascular endothelium under flow. *Blood* **106**(2): p. 584-92.

432. Allen, S., et al., 1998, Native low density lipoprotein-induced calcium transients trigger VCAM-1 and E-selectin expression in cultured human vascular endothelial cells. *J Clin Invest* **101**(5): p. 1064-75.

433. Khan, B.V., et al., 1995, Modified low density lipoprotein and its consituents augment cytokine-activated vascular cell adhesion molecule-1 gene expression in human vascular endothelial cells. *J Clin Invest* **95**(3): p. 1262-70.

434. Cominacini, L., et al., 1997, Antioxidants inhibit the expression of intercellular cell adhesion molecule-1 and vascular cell adhesion molecule-1 induced by oxidized LDL on human umbilical vein endothelial cells. *Free Radic Biol Med* **22**(1-2): p. 117-27.

435. Takei, A., Y. Huang, and M.F. Lopes-Virella, 2001, Expression of adhesion molecules by human endothelial cells exposed to oxidized low density lipoprotein: Influences of degree of oxidation and location of oxidized LDL. *Atherosclerosis* **154**(1): p. 79-86.

436. Li, D. and J.L. Mehta, 2000, Antisense to LOX-1 inhibits oxidized LDL-mediated upregulation of monocyte chemoattractant protein-1 and monocyte adhesion to human coronary artery endothelial cells. *Circulation* **101**(25): p. 2889-95.

437. Porubsky, S., et al., 2004, Influence of native and hypochlorite-modified low-density lipoprotein on gene expression in human proximal tubular epithelium. *Am J Pathol* **164**(6): p. 2175-87.

438. Kopprasch, S., et al., 2004, The pivotal role of scavenger receptor CD36 and phagocyte-derived oxidants in oxidized low density lipoprotein-induced adhesion to endothelial cells. *Int J Biochem Cell B* **36**(3): p. 460-71.

439. Kopprasch, S., et al., 1998, Hypochlorite-modified low-density lipoprotein stimulates human polymorphonuclear leukocytes for enhanced production of reactive oxygen metabolites, enzyme secretion, and adhesion to endothelial cells. *Atheroscleosis* **136**(2): p. 315-24.

440. Matsuda, H. and T. Iyanagi, 1999, Calmodulin activates intramolecular electron transfer between the two flavins of neuronal nitric oxide synthase flavin domain. *Biochim Biophys Acta* **1473**(2-3): p. 345-55.

441. Vasquez-Vivar, J., et al., 1998, Superoxide generation by endothelial nitric oxide synthase: The influence of cafactors. *Proc Natl Acad Sci* **95**(16): p. 9220-5.

442. Kotsonis, P., et al., 2000, Allosteric regulation of neuronal nitric oxide synthase by tetrahydrobiopterin and suppression of auto-damaging superoxide. *Biochem J* **346**(3): p. 767-76.

443. Li, H., et al., 1999, Crystal structures of zinc-free and -bound heme domain of human inducible nitric-oxide synthase. Implications for dimer stability and comparison with endothelial nitric-oxide synthase. *J Biol Chem* **274**(30): p. 21276-84.

444. Vasquez-Vivar, J., et al., 2002, The ratio between tetrahydrobiopterin and oxidized tetrahydrobiopterin analogues controls superoxide release from endothelial nitric oxide synthase: an EPR spin trapping study. *Biochem J* **362**: p. 733-9.

445. Klatt, P., et al., 1996, Characterization of Heme-deficient Neuronal Nitric-oxide Synthase Reveals a Role for Heme in Subunit Dimerization and Binding of the Amino Acid Substrate and Tetrahydrobiopterin. *J Biol Chem* **271**(13): p. 7336-42.

446. Xu, J., et al., 2006, Uncoupling of endothelial nitric oxidase synthase by hypochlorous acid: role of NAD(P)H oxidase-derived superoxide and peroxynitrite. *Arterioscler Thromb Vasc Biol* **26**(12): p. 2688-95.

447. Talib, J., et al., 2014, The smoking-associated oxidant hypothiocyanous acid induces endothelial nitric oxide synthase dysfunction. *Biochem J* **457**(1): p. 89-97.

448. Nuszkowski, A., et al., 2001, Hypochlorite-modified low density lipoprotein inhibits nitric oxide synthesis in endothelial cells via an intracellular dislocalization of endothelial nitric-oxide synthase. *J Biol Chem* **276**(17): p. 14212-21.

449. Chen, C.A., et al., 2010, S-glutathionylation uncouples eNOS and regulates its cellular and vascular function. *Nature* **468**(7327): p. 1115-8.

450. Ohara, Y., T.E. Peterson, and D.G. Harrison, 1993, Hyperholesterolemia Increased Endothelial Superoxide Anion Production. *J Clin Invest* **91**(6): p. 2546-51.

451. Andrews, H.E., et al., 1987, Low-density lipoproteins inhibit endothelium-dependent relaxation in rabbit aorta. *Nature* **327**(6119): p. 237-9.

452. Kugiyama, K., et al., 1990, Impairment of endothelium-dependent arterial relaxation by lysolecithin in modified low-density lipoprotein. *Nature* **344**(6262): p. 160-2.

453. Galle, J., R. Busse, and E. Bassenge, 1991, Effects of Native and Oxidized Low Density Lipoproteins on Formation and Inactivation of Endothelium-Derived Relaxing Factor. *Arterioscler Thromb* **11**(1): p. 198-203.

454. Simon, B.C., L.D. Cunningham, and R.A. Cohen, 1990, Oxidized Low Density Lipoprotein Cause Contraction and Inhibit Endothelium-dependent Relaxation in the Pig Coronary Artery. *J Clin Invest* **86**(1): p. 75-9.

455. Hein, T.W., J.C. Liao, and L. Kuo, 2000, oxLDL specifically impairs endothelium-dependent, NO-mediated dilation of coronary arterioles. *Am J Physiol Heart Circ Physiol* **278**(1): p. H175-83.

456. Tanner, F.C. and G. Noll, 1991, Oxidized Low Density Lipoproteins Inhibit Relaxations of Porcine Coronary Arteries - Role of Scavenger Receptor and Endothelium-Derived Nitric Oxide. *Circulation* **83**(6): p. 2012-20.

457. Malhotra, J.D. and R.J. Kaufman, 2007, The endoplasmic reticulum and the unfolded protein response. *Semin Cell Dev Biol* **18**(6): p. 716-31.

458. Ma, Y., et al., 2002, Two Distinct Stress Signaling Pathways Converge Upon the CHOP Promoter During the Mammalian Unfolded Protein Response. *J Mol Biol* **318**(5): p. 1351-65.

459. Hou, N.S., et al., 2014, Activation of the endoplasmic reticulum unfolded protein response by lipid disequilibrium without disturbed proteostasis in vivo. *Proc Natl Acad Sci U S A* **111**(22): p. E2271-80.

460. Promlek, T., et al., 2011, Membrane aberrancy and unfolded proteins activate the endoplasmic reticulum stress sensor Ire1 in different ways. *Mol Biol Cell* **22**(18): p. 3520-32.

461. Rutkowski, D.T., et al., 2006, Adaptation to ER stress is mediated by differential stabilities of pro-survival and pro-apoptotic mRNAs and proteins. *PLoS Biol* **4**(11): p. e374.

462. Battson, M.L., D.M. Lee, and C.L. Gentile, 2017, Endoplasmic reticulum stress and the development of endothelial dysfunction. *Am J Physiol Heart Circ Physiol* **312**(3): p. H355-H67.

463. Muller, C., et al., 2013, Protein disulfide isomerase modification and inhibition contribute to ER stress and apoptosis induced by oxidized low density lipoproteins. *Antioxid Redox Signal* **18**(7): p. 731-42.

464. Sanson, M., et al., 2009, Oxidized low-density lipoproteins trigger endoplasmic reticulum stress in vascular cells: prevention by oxygen-regulated protein 150 expression. *Circ Res* **104**(3): p. 328-36.

465. Gargalovic, P.S., et al., 2006, The unfolded protein response is an important regulator of inflammatory genes in endothelial cells. *Arterioscler Thromb Vasc Biol* **26**(11): p. 2490-6.

466. Johnson, R.C., J.A. Leopold, and J. Loscalzo, 2006, Vascular calcification: pathobiological mechanisms and clinical implications. *Circ Res* **99**(10): p. 1044-59.

467. Auge, N., 2002, Oxidized LDL-Induced Smooth Muscle Cell Proliferation Involves the EGF Receptor/PI-3 Kinase/Akt and the Sphingolipid Signaling Pathways. *Arterioscler Thromb Vasc Biol* **22**(12): p. 1990-5.

468. Owens, C.G., M.S. Kumar, and B.R. Wamhoff, 2004, Molecular Regulation of Vascular Smooth Muscle Cell Differentiation in Development and Disease. *Physiol Rev* **84**(3): p. 767-801.

469. Hungerford, J.E. and C.D. Little, 1998, Developmental Biology of the Vascular Smooth Muscle Cell: Building a Multilayered Vessel Wall. *J Vasc Res* **36**(1): p. 2-27.

470. Looft-Wilson, R.C., et al., 2012, Interaction between nitric oxide signaling and gap junctions: effects on vascular function. *Biochim Biophys Acta* **1818**(8): p. 1895-902.

471. Orr, A.W., et al., 2010, Complex regulation and function of the inflammatory smooth muscle cell phenotype in atherosclerosis. *J Vasc Res* **47**(2): p. 168-80.

472. Argmann, C.A., et al., 2004, Human smooth muscle cell subpopulations differentially accumulate cholesteryl ester when exposed to native and oxidized lipoproteins. *Arterioscler Thromb Vasc Biol* **24**(7): p. 1290-6.

473. Liu, J., et al., 2014, Oxidized low-density lipoprotein increases the proliferation and migration of human coronary artery smooth muscle cells through the upregulation of osteopontin. *Int J Mol Med* **33**(5): p. 1341-7.

474. Chen, Y.J., et al., 2009, Osteopontin increases migration and MMP-9 up-regulation via alphavbeta3 integrin, FAK, ERK, and NF-kappaB-dependent pathway in human chondrosarcoma cells. *J Cell Physiol* **221**(1): p. 98-108.

475. Yu, J., et al., 2010, Oxidized low density lipoprotein-induced transdifferentiation of bone marrow-derived smooth muscle-like cells into foam-like cells in vitro. *Int J Exp Pathol* **91**(1): p. 24-33.

476. Delporte, C., et al., 2013, Low-density lipoprotein modified by myeloperoxidase in inflammatory pathways and clinical studies. *Mediat Inflamm* **2013**(Article ID 971579): p. 18.

477. Craig, W.Y., G.E. Palomaki, and J.E. Haddow, 1989, Cigarette smoking and serum lipid and lipoprotein concentrations: An analysis of published data. *BMJ* **298**(6676): p. 784-8.

478. Rudolph, T.K., V. Rudolph, and S. Baldus, 2008, Contribution of myeloperoxidase to smoking-dependent vascular inflammation. *Proc Am Thorac Soc* **5**(8): p. 820-23.

479. Carrell Morris, J., 1966, The acid ionization constant of HOCl from 5 to 35°. *J Phys Chem* **70**(12): p. 3798-805.

480. Hawkins, C.L., P.E. Morgan, and M.J. Davies, 2009, Quantification of protein modification by oxidants. *Free Radic Biol Med* **46**(8): p. 965-88.

481. Eyer, P., et al., 2003, Molar absorption coefficients for the reduced Ellman reagent: Reassessment. *Anal Biochem* **312**(2): p. 224-7.

482. Havel, R.J., H.A. Eder, and J.H. Bragdon, 1955, The distribution and chemical composition of ultracentrifugally separated lipoproteins in human serum. *J Clin Invest* **34**(9): p. 1345-53.

483. Kleifeld, O., et al., 2011, Identifying and quantifying proteolytic events and the natural N terminome by terminal amine isotopic labeling of substrates. *Nature Protoc* **6**(10): p. 1578-611.

484. Yehye, W.A., et al., 2015, Understanding the chemistry behind the antioxidant activities of butylated hydroxytoluene (BHT): a review. *Eur J Med Chem* **101**: p. 295-312.

485. Gutteridge, J.M.C., R. Richmond, and B. Halliwell, 1979, Inhibition of the Iron-Catalysed Formation of Hydroxyl Radicals from Superoxide and of Lipid Peroxidation by Desferrioxamine. *Biochem J* **184**(2): p. 469-72.

486. Maitra, D., et al., 2011, Mechanism of hypochlorous acid-mediated heme destruction and free iron release. *Free Radic Biol Med* **51**(2): p. 364-73.

487. Ekkati, A.R. and J.J. Kodanko, 2007, Targeting Peptides with an Iron-Based Oxidant: Cleavage of the Amino Acid Backbone and Oxidation of Side Chains. *JACS* **129**(41): p. 12390-1.

488. Smith, P.K., et al., 1985, Measurement of Protein Using Bicinchoninic Acid. *Anal Biochem* **150**(1): p. 76-85.

489. Dean, R.T., W. Hylton, and A.C. Allison, 1979, Induction of Macrophage Lysosomal Enzyme Secretion by Agents Acting at the Plasma Membrane. *Pathobiology* **47**(6): p. 454-62.

490. Kritharides, L., et al., 1993, A method for defining the stages of low-density lipoprotein oxidation by the separation of cholesterol- and cholesteryl ester-oxidation products using HPLC. *Anal Biochem* **213**(1): p. 79-89.

491. Headlam, H.A., et al., 2006, Inhibition of cathepsins and related proteases by amino acid, peptide, and protein hydroperoxides. *Free Radic Biol Med* **40**(9): p. 1539-48.

492. Hoppe, G., J. O'Neil, and H.F. Hoff, 1994, Inactivation of Lysosomal Proteases by Oxidized Low Density Lipoprotein is Partially Responsible for its Poor Degradation by Mouse Peritoneal Macrophages. *J Clin Invest* **94**(4): p. 1506-12.

493. Pfaffl, M.W., 2001, A new mathematical model for relative quantification in real-time RT-PCR. *Nucl Acids Res* **29**(9): p. e45.

494. Gopalakrishnan, B., et al., 2012, Detection of nitric oxide and superoxide radical anion by electron paramagnetic resonance spectroscopy from cells using spin traps. *J Vis Exp* (66): p. e2810.

495. Kojima, H., et al., 1998, Development of a fluorescent indicator for nitric oxide based on the fluorescein chromophore. *Chem Pharm Bull* **46**(2): p. 373-5.

496. Kojima, H., et al., 1998, Detection and Imaging of Nitric Oxide with Novel Fluorescent Indicators: Diaminofluoresceins. *Anal Chem* **70**(13): p. 2446-53.

497. Zielonka, J., et al., 2005, Mechanistic similarities between oxidation of hydroethidine by Fremy's salt and superoxide: Stopped-flow optical and EPR studies. *Free Radic Biol Med* **39**(7): p. 853-63.

498. Zielonka, J., J. Vasquez-Vivar, and B. Kalyanaraman, 2006, The confounding effects of light, sonication, and Mn(III)TBAP on quantitation of superoxide using hydroethidine. *Free Radic Biol Med* **41**(7): p. 1050-7.

499. Rosen, G.M. and B.A. Freeman, 1984, Detection of superoxide generated by endothelial cells. *Proc Natl Acad Sci USA* **81**(23): p. 7269-73.

500. Bradford, M.M., 1976, A Rapid and Sensitive Method for the Quantitation of Microgram Quantities of Protein Utilizing the Principle of Protein-Dye Binding. *Anal Biochem* **72**(1-2): p. 248-54.

501. Gee, K.R., et al., 2000, Chemical and physiological characterization of fluo-4 Ca(2+)-indicator dyes. *Cell Calcium* **27**(2): p. 97-106.

502. Moguilevsky, N., et al., 2004, Monoclonal antibodies against LDL progressively oxidized by myeloperoxidase react with ApoB-100 protein moiety and human atherosclerotic lesions. *Biochem Biophys Res Commun* **323**(4): p. 1223-8.

503. Jiang, X., et al., 2011, Oxidized low density lipoproteins--do we know enough about them? *Cardiovasc Drugs Ther* **25**(5): p. 367-77.

504. Tsimikas, S. and Y.I. Miller, 2011, Oxidative modification of lipoproteins: Mechanisms, role in inflammation and potential clinical applications in cardiovascular disease. *Curr Pharm Des* **17**(1): p. 27 - 37.

505. Balla, G., et al., 1991, Hemin: A Possible Physiological Mediator of Low Density Lipoprotein Oxidation and Endothelial Injury. *Arterioscler Thromb* **11**(6): p. 1700-11.

506. Breuer, O., et al., 1996, The oxysterols cholest-5-ene-3beta,4alpha-diol, cholest-5-ene-3beta,4beta-diol and cholestane-3beta,5alpha ,6alpha-triol are formed during in vitro oxidation of low density lipoprotein, and are present in human atherosclerotic plaques. *Biochim Biophys Acta* **1302**(2): p. 145-52.

507. Brown, A.J., et al., 1997, 7-Hydroperoxycholesterol and its products in oxidized low density lipoprotein and human atherosclerotic plaque. *J Lipid Res* **38**(9): p. 1730-45.

508. Kalyanaraman, B., W.E. Antholine, and S. Parthasarathy, 1990, Oxidation of low-density lipoprotein by Cu2+ and lipoxygenase: an electron spin resonance study. *Biochim Biophys Acta* **1035**(3): p. 286-92.

509. Dabbagh, A.J., et al., 1997, Effect of Iron Overload and Iron Deficiency on Atherosclerosis in the Hypercholesterolemic Rabbit. *Arterioscler Thromb Vasc Biol* **17**(11): p. 2638-45.

510. Lamb, D.J., et al., 1999, Dietary copper supplementation reduces atherosclerosis in the cholesterol-fed rabbit. *Atherosclerosis* **146**(1): p. 33-43.

511. Alissa, E.M., et al., 2004, The effects of coadministration of dietary copper and zinc supplements on atherosclerosis, antioxidant enzymes and indices of lipid peroxidation in the cholesterol-fed rabbit. *Int J Exp Path* **85**(6): p. 265-75.

512. Hamilton, I.M.J., W.S. Gilmore, and J.J. Strain, 2000, Marginal Copper Deficiency and Atherosclerosis. *Biol Trace Elem Res* **78**(1-3): p. 179-89.

513. Sempos, C.T., 2002, Do body iron stores increase the risk of developing coronary heart disease? *Am J Clin Nutr* **76**(3): p. 501-3.

514. Li, D., B. Yang, and J.L. Mehta, 1998, Ox-LDL induces apoptosis in human coronary artery endothelial cells: role of PKC, PTK, bcl-2, and Fas. *Am J Physiol Heart Circ Physiol* **275**(2): p. H568-76.

515. Xing, X., J. Baffic, and C.P. Sparrow, 1998, LDL oxidation by activated monocytes: Characterization of the oxidized LDL and requirement for transition metal ions. *J Lipid Res* **39**(11): p. 2201-8.

516. Blair, A., et al., 1999, Oxidized low density lipoprotein displaces endothelial nitric-oxide synthase (eNOS) from plasmalemmal caveolae and impairs eNOS activation. *J Biol Chem* **274**(45): p. 32512-9.

517. Cominacini, L., et al., 2000, Oxidized low density lipoprotein (ox-LDL) binding to ox-LDL receptor-1 in endothelial cells induces the activation of NF-κB through an increased production of intracellular reactive oxygen species. *J Biol Chem* **275**(17): p. 12633-8.

518. Li, D. and J.L. Mehta, 2000, Upregulation of Endothelial Receptor for Oxidized LDL (LOX-1) by Oxidized LDL and Implications in Apoptosis of Human Coronary Artery Endothelial Cells. *Arterioscler Thromb Vasc Biol* **20**(4): p. 1116-22.

519. Vergnani, L., et al., 2000, Effect of native and oxidized low-density lipoprotein on endothelial nitric oxide synthase and superoxide production. *Circulation* **101**(11): p. 1261-6.

520. Chavakis, E., et al., 2001, Oxidized LDL Inhibits Vascular Endothelial Growth Factor-Induced Endothelial Cell Migration by an Inhibitory Effect on the Akt/Endothelial Nitric Oxide Synthase Pathway. *Circulation* **103**(16): p. 2102-7.

521. Huang, Y., et al., 2001, Oxidized LDL differentially regulates MMP-1 and TIMP-1 expression in vascular endothelial cells. *Atheroscleosis* **156**(1): p. 119-25.

522. Virgili, F., et al., 2003, Effect of oxidized low-density lipoprotein on differential gene expression in primary human endothelial cells. *Antioxid Redox Signal* **5**(2): p. 237-47.

523. Chen, J., et al., 2004, Role of caspases in Ox-LDL-induced apoptotic cascade in human coronary artery endothelial cells. *Circ Res* **94**(3): p. 370-6.

524. Fleming, I., et al., 2005, Oxidized low-density lipoprotein increases superoxide production by endothelial nitric oxide synthase by inhibiting PKCalpha. *Cardiovasc Res* **65**(4): p. 897-906.

525. Ma, F.X., et al., 2006, Oxidized low density lipoprotein impairs endothelial progenitor cells by regulation of endothelial nitric oxide synthase. *J Lipid Res* **47**(6): p. 1227-37.

526. Cheng, J., et al., 2007, Oxidized low-density lipoprotein stimulates p53-dependent activation of proapoptotic Bax leading to apoptosis of differentiated endothelial progenitor cells. *Endocrinology* **148**(5): p. 2085-94.

527. Maziere, C., et al., 2010, Oxidized low density lipoprotein inhibits phosphate signaling and phosphate-induced mineralization in osteoblasts. Involvement of oxidative stress. *Biochim Biophys Acta* **1802**(11): p. 1013-9.

528. Yu, S., et al., 2011, Oxidized LDL at low concentration promotes in-vitro angiogenesis and activates nitric oxide synthase through PI3K/Akt/eNOS pathway in human coronary artery endothelial cells. *Biochem Biophys Res Commun* **407**(1): p. 44-8.

529. Kannan, Y., et al., 2012, Oxidatively modified low density lipoprotein (LDL) inhibits TLR2 and TLR4 cytokine responses in human monocytes but not in macrophages. *The J Biol Chem* **287**(28): p. 23479-88.

530. Makino, J., et al., 2015, Oxidized low-density lipoprotein accelerates the destabilization of extracellular-superoxide dismutase mRNA during foam cell formation. *Arch Biochem Biophys* **575**: p. 54-60.

531. Opper, C., et al., 1998, Effect of hypochlorite (HOCl)-modified low density lipoproteins and high density lipoproteins on platelet function. *Platelets* **9**(5): p. 339-41.

532. Dean, R.T. and K.H. Cheeseman, 1987, Vitamin E protects proteins against free radical damage in lipid environments. *Biochem Biophys Res Commun* **148**(3): p. 1277-82.

533. Chevallet, M., S. Luche, and T. Rabilloud, 2006, Silver staining of proteins in polyacrylamide gels. *Nat Protoc* **1**(4): p. 1852-8.

534. Neuhoff, V., et al., 1988, Improved staining of proteins in polyacrylamide gels including isoelectric focusing gels with clear background at nanogram sensitivity using Coomassie Brilliant Blue G-250 and R-250. *Electrophoresis* **9**(6): p. 255-62.

535. Zani, I.A., et al., 2015, Scavenger receptor structure and function in health and disease. *Cells* **4**(2): p. 178-201.

536. Sawamura, T., I. Wakabayashi, and T. Okamura, 2015, LOX-1 in atherosclerotic disease. *Clin Chim Acta* **440**: p. 157-63.

537. Stewart, C.R., et al., 2010, CD36 ligands promote sterile inflammation through assembly of a Toll-like receptor 4 and 6 heterodimer. *Nat Immunol* **11**(2): p. 155-61.

538. Inoue, K., et al., 2005, Overexpression of lectin-like oxidized low-density lipoprotein receptor-1 induces intramyocardial vasculopathy in apolipoprotein E-null mice. *Circ Res* **97**(2): p. 176-84.

539. Kettle, A.J. and C.C. Winterbourn, 1994, Assays for the chlorination activity of myeloperoxidase. *Oxygen Radicals in Biological Systems, Pt C* **233**: p. 502-12.

540. Vissers, M.C.M. and C.C. Winterbourn, 1991, Oxidative Damage to Fibronectin. 1. The Effects of the Neutrophil Myeloperoxidase System and HOCl. *Arch Biochem Biophys* **285**(1): p. 53-9.

541. Jürgens, G., et al., 1987, Modification of human serum low density lipoprotein by oxidation - Characterization and pathophysiological implications. *Chem Phys Lipids* **45**(2-4): p. 315-36.

542. Georgiou, C.D., et al., 2008, Mechanism of Coomassie brilliant blue G-250 binding to proteins: a hydrophobic assay for nanogram quantities of proteins. *Anal Bioanal Chem* **391**(1): p. 391-403.

543. Jentoft, N. and D.G. Dearborn, 1979, Labeling of Proteins by Reductive Methylation Using Sodium Cyanoborohydride. *J Biol Chem* **254**(11): p. 4359-65.

544. Kovanich, D., et al., 2012, Applications of stable isotope dimethyl labeling in quantitative proteomics. *Anal Bioanal Chem* **404**(4): p. 991-1009.

545. Scott, N.E., et al., 2017, Interactome disassembly during apoptosis occurs independent of caspase cleavage. *Mol Syst Biol* **13**(1): p. 906.

546. Prudova, A., et al., 2016, TAILS N-Terminomics and Proteomics Show Protein Degradation Dominates over Proteolytic Processing by Cathepsins in Pancreatic Tumors. *Cell Rep* **16**(6): p. 1762-73.

547. Schlage, P., et al., 2015, Matrix Metalloproteinase 10 Degradomics in Keratinocytes and Epidermal Tissue Identifies Bioactive Substrates with Pleiotropic Functions. *Mol Cell Proteomics* **14**(12): p. 3234-46.

548. Eckhard, U., et al., 2016, Active site specificity profiling of the matrix metalloproteinase family: Proteomic identification of 4300 cleavage sites by nine MMPs explored with structural and synthetic peptide cleavage analyses. *Matrix Biol* **49**: p. 37-60.

549. Ong, S.E., G. Mittler, and M. Mann, 2004, Identifying and quantifying in vivo methylation sites by heavy methyl SILAC. *Nat Methods* **1**(2): p. 119-26.

550. Zee, B.M. and B.A. Garcia, 2012, Discovery of lysine post-translational modifications through mass spectrometric detection. *Essays Biochem* **52**: p. 147-63.

551. Drapeau, G.R., Y. Boily, and J. Houmard, 1972, Purification and Properties of an Extracellular Protease of Staphylococcus aureus. *J Biol Chem* **247**(20): p. 6720-6.

552. Birktoft, J.J. and K. Breddam, *Proteolytic Enzymes: Serine and Cysteine Peptidases*, in *Methods Enzymol*. 1994, Academic Press. p. 114-26.

553. Prassl, R. and P. Laggner, 2009, Molecular structure of low density lipoprotein: current status and future challenges. *Eur Biophys J* **38**(2): p. 145-58.

554. Morel, I., et al., 1992, Antioxidant and free radical scavenging activities of the iron chelators pyoverdin and hydroxypyrid-4-ones in iron-loaded hepatocyte cultures: Comparison of their mechanism of protection with that of desferrioxamine. *Free Radic Biol Med* **13**(5): p. 499-508.

555. Zhu, B.-Z., et al., 1998, New modes of action of desferrioxamine: Scavenging of semiquinone radical and stimulation of hydrolysis of tetrachlorohydroquinone. *Free Radic Biol Med* **24**(2): p. 360-9.

556. Spalteholz, H., K. Wenske, and J. Arnhold, 2005, Interactions of hypohalous acids and heme peroxidases with unsaturated phosphatidylcholines. *BioFactors* **24**(1-4): p. 67-76.

557. Davies, M.J., et al., 1993, The expression of adhesion molecules ICAM-1, VCAM-1, PECAM, and E-selectin in human atherosclerosis. *J Pathol* **171**(3): p. 223-9.

558. Loppnow, H., et al., 2011, Contribution of vascular cell-derived cytokines to innate and inflammatory pathways in atherogenesis. *J Cell Mol Med* **15**(3): p. 484-500.

559. Ylä-Herttuala, S., et al., 1989, Evidence for the presence of oxidatively modified low density lipoprotein in atherosclerotic lesions of rabbit and man. *J Clin Invest* **84**(4): p. 1086-95.

560. Dwivedi, A., E.E. Anggard, and M.J. Carrier, 2001, Oxidized LDL-mediated monocyte adhesion to endothelial cells does not involve NFkappaB. *Biochem Biophys Res Commun* **284**(1): p. 239-44.

561. Sozzani, S., et al., 1991, The signal transduction pathway involved in the migration induced by a monocyte chemotactic cytokine. *J Immunol* **147**(7): p. 2215-21.

562. Cushing, S.D., et al., 1990, Minimally modified low density lipoprotein induces monocyte chemotactic protein 1 in human endothelial cells and smooth muscle cells. *Proc Natl Acad Sci U S A* **87**(13): p. 5134-8.

563. Scheller, J., et al., 2011, The pro- and anti-inflammatory properties of the cytokine interleukin-6. *Biochim Biophys Acta* **1813**(5): p. 878-88.

564. Hashizume, M. and M. Mihara, 2012, Blockade of IL-6 and TNF-alpha inhibited oxLDL-induced production of MCP-1 via scavenger receptor induction. *Eur J Pharmacol* **689**(1-3): p. 249-54.

565. Hong, D., et al., 2014, Ox-LDL induces endothelial cell apoptosis via the LOX-1-dependent endoplasmic reticulum stress pathway. *Atherosclerosis* **235**(2): p. 310-7.

566. Gargalovic, P.S., et al., 2006, Identification of inflammatory gene modules based on variations of human endothelial cell responses to oxidized lipids. *Proc Natl Acad Sci U S A* **103**(34): p. 12741-6.

567. Cullinan, S.B. and J.A. Diehl, 2006, Coordination of ER and oxidative stress signaling: the PERK/Nrf2 signaling pathway. *Int J Biochem Cell Biol* **38**(3): p. 317-32.

568. Cullinan, S.B. and J.A. Diehl, 2004, PERK-dependent activation of Nrf2 contributes to redox homeostasis and cell survival following endoplasmic reticulum stress. *J Biol Chem* **279**(19): p. 20108-17.

569. Jeyapaul, J. and A.K. Jaiswal, 2000, Nrf2 and c-Jun Regulation of Antioxidant Response Element (ARE)-Mediated Expression and Induction of γ-Glutamylcysteine Synthetase Heavy Subunit Gene. *Biochem Pharmacol* **59**(11): p. 1433-9.

570. Yang, Y.C., et al., 2011, Induction of glutathione synthesis and heme oxygenase 1 by the flavonoids butein and phloretin is mediated through the ERK/Nrf2 pathway and protects against oxidative stress. *Free Radic Biol Med* **51**(11): p. 2073-81.

571. Wild, A.C., H.R. Moinova, and R.T. Mulcahy, 1999, Regulation of γ-Glutamylcysteine Synthetase Subunit Gene Expression by the Transcription Factor Nrf2. *J Biol Chem* **274**(47): p. 33627-36.

572. Applegate, L.A., P. Luscher, and R.M. Tyrell, 1991, Induction of heme oxygenase: A general response to oxidant stress in cultured mammalian cells. *Cancer Res* **51**(3): p. 974-8.

573. Heiss, E.H., et al., 2009, Active NF-E2-related factor (Nrf2) contributes to keep endothelial NO synthase (eNOS) in the coupled state: role of reactive oxygen species (ROS), eNOS, and heme oxygenase (HO-1) levels. *J Biol Chem* **284**(46): p. 31579-86.

574. Thorup, C., et al., 1999, Carbon monoxide induces vasodilation and nitric oxide release but supresses endothelial NOS. *Am J Physiol* **277**(6): p. F882-9.

575. Ma, X., et al., 2007, NO and CO differentially activate soluble guanylyl cyclase via a heme pivot-bend mechanism. *EMBO J* **26**(2): p. 578-88.

576. Meister, A. and M.E. Andersen, 1983, Glutathione. *Ann Rev Biochem* **52**: p. 711-60.

577. Mosmann, T., 1983, Rapid Colorimetric Assay for Cellular Growth and Survival: Application to Proliferation and Cytotoxicity Assays. *J Immunol Methods* **65**(1-2): p. 55-63.

578. Haudenschild, C.C. and S.M. Schwartz, 1979, Endothelial regeneration. II. Restitution of endothelial continuity. *Lab Invest* **41**(5): p. 407-18.

579. Li, D.Y., et al., 1999, Upregulation of Endothelial Receptor for Oxidized Low-Density Lipoprotein (LOX-1) in Cultured Human Coronary Artery Endothelial Cells by Angiotensin II Type 1 Receptor Activation. *Circ Res* **84**(9): p. 1043-9.

580. Kume, N., et al., 1998, Inducible expression of lectin-like oxidized LDL receptor-1 in vascular endothelial cells. *Circ Res* **83**(3): p. 322-7.

581. Lutgens, S.P., et al., 2007, Cathepsin cysteine proteases in cardiovascular disease. *FASEB J* **21**(12): p. 3029-41.

582. Ismael, F.O., et al., 2016, Role of Myeloperoxidase Oxidants in the Modulation of Cellular Lysosomal Enzyme Function: A Contributing Factor to Macrophage Dysfunction in Atherosclerosis? *PLoS One* **11**(12): p. e0168844.

583. Lougheed, M., H. Zhang, and U.P. Steinbrecher, 1991, Oxidized Low Density Lipoprotein Is Resistant to Cathepsins and Accumulates within Macrophages. *J Biol Chem* **266**(22): p. 14519-25.

584. Urbich, C., et al., 2005, Cathepsin L is required for endothelial progenitor cell-induced neovascularization. *Nat Med* **11**(2): p. 206-13.

585. Premzl, A., V. Turk, and J. Kos, 2006, Intracellular proteolytic activity of cathepsin B is associated with capillary-like tube formation by endothelial cells in vitro. *J Cell Biochem* **97**(6): p. 1230-40.

586. Im, E., A. Venkatakrishnan, and A. Kazlauskas, 2005, Cathepsin B regulates the intrinsic angiogenic threshold of endothelial cells. *Mol Biol Cell* **16**(8): p. 3488-500.

587. Wei, D.H., et al., 2013, Cathepsin L stimulates autophagy and inhibits apoptosis of ox-LDL-induced endothelial cells: potential role in atherosclerosis. *Int J Mol Med* **31**(2): p. 400-6.

588. Li, D., et al., 2002, Statins modulate oxidized low-density lipoprotein-mediated adhesion molecule expression in human coronary artery endothelial cells: Role of LOX-1. *J Pharmacol Exp Ther* **302**(2): p. 601-5.

589. Apostolov, E.O., et al., 2007, Carbamylated low-density lipoprotein induces monocyte adhesion to endothelial cells through intercellular adhesion molecule-1 and vascular cell adhesion molecule-1. *Arterioscler Thromb Vasc Biol* **27**(4): p. 826-32.

590. Toma, L., et al., 2016, Glycated LDL increase VCAM-1 expression and secretion in endothelial cells and promote monocyte adhesion through mechanisms involving endoplasmic reticulum stress. *Mol Cell Biochem* **417**(1-2): p. 169-79.

591. Zhou, A.X. and I. Tabas, 2013, The UPR in atherosclerosis. *Semin Immunopathol* **35**(3): p. 321-32.

592. Galan, M., et al., 2014, Mechanism of endoplasmic reticulum stress-induced vascular endothelial dysfunction. *Biochim Biophys Acta* **1843**(6): p. 1063-75.

593. Schneider, E.G., H.T. Nguyen, and W.J. Lennarz, 1978, The effect of tunicamycin, an inhibitor of protein glycosylation, on embryonic development in the sea urchin. *J Biol Chem* **253**(7): p. 2348-55.

594. Yoshida, H., et al., 2001, Endoplasmic reticulum stress-induced formation of transcription factor complex ERSF including NF-Y (CBF) and activating transcription factors 6alpha and 6beta that activates the mammalian unfolded protein response. *Mol Cell Biol* **21**(4): p. 1239-48.

595. Afonyushkin, T., O.V. Oskolkova, and V.N. Bochkov, 2012, Permissive role of miR-663 in induction of VEGF and activation of the ATF4 branch of unfolded protein response in endothelial cells by oxidized phospholipids. *Atherosclerosis* **225**(1): p. 50-5.

596. Lee, S., et al., 2009, Ox-PAPC activation of PMET system increases expression of heme oxygenase-1 in human aortic endothelial cell. *J Lipid Res* **50**(2): p. 265-74.

597. Calay, D., et al., 2010, Copper and myeloperoxidase-modified LDLs activate Nrf2 through different pathways of ROS production in macrophages. *Antioxid Redox Signal* **13**(10): p. 1491-502.

598. Suh, J.H., et al., 2004, Decline in transcriptional activity of Nrf2 causes age-related loss of glutathione synthesis, which is reversible with lipoic acid. *Proc Natl Acad Sci U S A* **101**(10): p. 3381-6.

599. Thomas, J.P., P.G. Geiger, and A.W. Girotti, 1993, Lethal damage to endothelial cells by oxidized low density lipoprotein: role of selenoperoxidases in cytoprotection against lipid hydroperoxide- and iron-mediated reactions. *J Lipid Res* **34**(3): p. 479-90.

600. Walters-Laporte, E., et al., 1998, A High Concentration of Melatonin Inhibits In Vitro LDL Peroxidation But Not Oxidized LDL Toxicity Toward Cultured Endothelial Cells. *J Cardiovasc Pharmacol* **32**(4): p. 582-92.

601. Sata, M. and K. Walsh, 1998, Oxidized LDL activates fas-mediated endothelial cell apoptosis. *J Clin Invest* **102**(9): p. 1682-9.

602. Ermak, N., et al., 2008, Role of reactive oxygen species and Bax in oxidized low density lipoprotein-induced apoptosis of human monocytes. *Atherosclerosis* **200**(2): p. 247-56.

603. Ermak, N., et al., 2010, Differential apoptotic pathways activated in response to Cu-induced or HOCl-induced LDL oxidation in U937 monocytic cell line. *Biochem Biophys Res Commun* **393**(4): p. 783-7.

604. Marsche, G., et al., 2003, Class B scavenger receptors CD36 and SR-BI are receptors for hypochlorite-modified low density lipoprotein. *J Biol Chem* **278**(48): p. 47562-70.

605. Gent, J. and I. Braakman, 2004, Low-density lipoprotein receptor structure and folding. *Cell Mol Life Sci* **61**(19-20): p. 2461-70.

606. Brown, M.S. and J.L. Goldstein, 1975, Regulation of the activity of the low density lipoprotein receptor in human fibroblasts. *Cell* **6**(3): p. 307-16.

607. Armstrong, S.M., et al., 2015, A novel assay uncovers an unexpected role for SR-BI in LDL transcytosis. *Cardiovasc Res* **108**(2): p. 268-77.

608. Rosengren, B., O.A. Rayyes, and B. Rippe, 2002, Transendothelial Transport of Low-Density Lipoprotein and Albumin Across the Rat Peritoneum in vivo: Effects of the Transcytosis Inhibitors NEM and Filipin. *J Vasc Res* **39**(3): p. 230-7.

609. Bian, F., et al., 2014, C-reactive protein promotes atherosclerosis by increasing LDL transcytosis across endothelial cells. *Br J Pharmacol* **171**(10): p. 2671-84.

610. Bekkering, S., et al., 2014, Oxidized low-density lipoprotein induces long-term proinflammatory cytokine production and foam cell formation via epigenetic reprogramming of monocytes. *Arterioscler Thromb Vasc Biol* **34**(8): p. 1731-8.

611. Walpola, P.L., et al., 1995, Expression of ICAM-1 and VCAM-1 and Monocyte Adherence in Arteries Exposed to Altered Shear Stress. *Arterioscler Thromb Vasc Biol* **15**(1): p. 2-10.

612. Luu, N.T., et al., 2010, Responses of endothelial cells from different vessels to inflammatory cytokines and shear stress: evidence for the pliability of endothelial phenotype. *J Vasc Res* **47**(5): p. 451-61.

613. Erl, W., P.C. Weber, and C. Weber, 1998, Monocytic cell adhesion to endothelial cells stimulated by oxidized low density lipoprotein is mediated by distinct endothelial ligands. *Atheroscleosis* **136**(2): p. 297-303.

614. Frostegård, J., et al., 1991, Biologically modified LDL increases the adhesive properties of endothelial cells. *Atheroscleosis* **90**(2-3): p. 119-26.

615. Deshmane, S.L., et al., 2009, Monocyte chemoattractant protein-1 (MCP-1): an overview. *J Interferon Cytokine Res* **29**(6): p. 313-26.

616. Tabas, I., 2010, The role of endoplasmic reticulum stress in the progression of atherosclerosis. *Circ Res* **107**(7): p. 839-50.

617. Davies, P.F. and M. Civelek, 2011, Endoplasmic reticulum stress, redox, and a proinflammatory environment in athero-susceptible endothelium in vivo at sites of complex hemodynamic shear stress. *Antioxid Redox Signal* **15**(5): p. 1427-32.

618. Schneede, A., et al., 2011, Role for LAMP-2 in endosomal cholesterol transport. *J Cell Mol Med* **15**(2): p. 280-95.

619. Han, J. and R.J. Kaufman, 2016, The role of ER stress in lipid metabolism and lipotoxicity. *J Lipid Res* **57**(8): p. 1329-38.

620. Dong, Y., et al., 2010, Activation of AMP-activated protein kinase inhibits oxidized LDL-triggered endoplasmic reticulum stress in vivo. *Diabetes* **59**(6): p. 1386-96.

621. Oskolkova, O.V., et al., 2008, ATF4-dependent transcription is a key mechanism in VEGF up-regulation by oxidized phospholipids: critical role of oxidized sn-2 residues in activation of unfolded protein response. *Blood* **112**(2): p. 330-9.

622. Romanoski, C.E., et al., 2011, Network for activation of human endothelial cells by oxidized phospholipids: a critical role of heme oxygenase 1. *Circ Res* **109**(5): p. e27-41.

623. Daher, J., et al., 2014, Myeloperoxidase Oxidized LDL Interferes with Endothelial Cell Motility through miR-22 and Heme Oxygenase 1 Induction: Possible Involvement in Reendothelialization of Vascular Injuries. *Mediators Inflamm* **2014**: p. 1-14.

624. Wei, Y., et al., 2009, Hypochlorous acid-induced heme oxygenase-1 gene expression promotes human endothelial cell survival. *Am J Physiol Cell Physiol* **297**(4): p. C907-15.

625. Xiao, S., et al., 2016, MiR-22 promotes porcine reproductive and respiratory syndrome virus replication by targeting the host factor HO-1. *Vet Microbiol* **192**: p. 226-30.

626. Araujo, J.A., M. Zhang, and F. Yin, 2012, Heme oxygenase-1, oxidation, inflammation, and atherosclerosis. *Front Pharmacol* **3**: p. 119.

627. Agarwal, A., et al., 1998, Linoleyl Hydroperoxide Transcriptionally Upregulated Heme Oxygenase-1 Gene Expression in Human Renal Epithelial and Aortic Endothelial Cells. *J Am Soc Nephrol* **9**(11): p. 1990-7.

628. Ishikawa, K., et al., 1997, Induction of heme oxygenase-1 inhibits the monocyte transmigration induced by mildly oxidized LDL. *J Clin Invest* **100**(5): p. 1209-16.

629. Landmesser, U., B. Hornig, and H. Drexler, 2004, Endothelial function: a critical determinant in atherosclerosis? *Circulation* **109**(21 Suppl 1): p. II27-33.

630. Libby, P., 2002, Inflammation in atherosclerosis. *Nature* **420**(6917): p. 868-74.

631. Stocker, R. and J.F. Keaney, Jr., 2004, Role of oxidative modifications in atherosclerosis. *Physiol Rev* **84**(4): p. 1381-478.

632. Abu-Soud, H.M. and D.J. Stuehr, 1993, Nitric oxide synthases reveal a role for calmodulin in controlling electron transfer. *Proc Natl Acad Sci USA* **90**(22): p. 10779-72.

633. Forstermann, U. and W.C. Sessa, 2012, Nitric oxide synthases: regulation and function. *Eur Heart J* **33**(7): p. 829-37.

634. Kietadisorn, R., R.P. Juni, and A.L. Moens, 2012, Tackling endothelial dysfunction by modulating NOS uncoupling: new insights into its pathogenesis and therapeutic possibilities. *Am J Physiol Endocrinol Metab* **302**(5): p. E481-95.

635. Vergnani, L., et al., 2000, Effect of native and oxidized low-density lipoprotein on endothelial nitric oxide and superoxide production : key role of L-arginine availability. *Circulation* **101**(11): p. 1261-6.

636. Galle, J., et al., 1992, Inhibition of cyclic AMP- and cyclic GMP-mediated dilations in isolated arteries by oxidized low density lipoproteins. *Arterioscler Thromb* **12**(2): p. 180-6.

637. Kugiyama, K., et al., 1990, Impairment of endothelium-dependent arterial relaxation by lysolecithin in modified low-density lipoproteins. *Nature* **344**(6262): p. 160-2.

638. Shaul, P.W., et al., 1996, Acylation Targets Endothelial Nitric-oxide Synthase to Plasmalemmal Caveolae. *J Biol Chem* **271**(11): p. 6518-22.

639. Ju, H., et al., 1997, Direct interaction of endothelial nitric-oxide synthase and caveolin-1 inhibits synthetase activity. *J Biol Chem* **272**(30): p. 18522-5.

640. Drab, M., et al., 2001, Loss of caveolae, vascular dysfunction, and pulmonary defects in caveolin-1 gene-disrupted mice. *Science* **293**(5539): p. 2449-52.

641. Razani, B., et al., 2001, Caveolin-1 null mice are viable but show evidence of hyperproliferative and vascular abnormalities. *J Biol Chem* **276**(41): p. 38121-38.

642. Gratton, J.P., P. Bernatchez, and W.C. Sessa, 2004, Caveolae and caveolins in the cardiovascular system. *Circ Res* **94**(11): p. 1408-17.

643. Frank, P.G. and M.P. Lisanti, 2004, Caveolin-1 and caveolae in atherosclerosis: differential roles in fatty streak formation and neointimal hyperplasia. *Curr Opin Lipidol* **15**(5): p. 523-9.

644. Maniatis, N.A., et al., 2006, Novel mechanism of endothelial nitric oxide synthase activation mediated by caveolae internalization in endothelial cells. *Circ Res* **99**(8): p. 870-7.

645. Qian, J. and D. Fulton, 2013, Post-translational regulation of endothelial nitric oxide synthase in vascular endothelium. *Front Physiol* **4**: p. 347.

646. Dudzinski, D.M., et al., 2006, The regulation and pharmacology of endothelial nitric oxide synthase. *Annu Rev Pharmacol Toxicol* **46**: p. 235-76.

647. Nott, A., J.D. Robinson, and A. Riccio, 2008, DAF-FM detection of nitric oxide in embryonic cortical neurons. *Nat Protoc* **235**.

648. Duque, R.E., *Chapter 14: Interactive Data Analysis for Evaluation of B-Cell Neoplasia by Flow Cytometry*, in *Flow Cytometry, Part B*, D. Darzynkiewicz, J.P. Robinson, and H.A. Crissman, Editors. 1994, Elsevier. p. 231-42.

649. Xia, Y., et al., 2000, Electron paramagnetic resonance spectroscopy with N-methyl-D-glucamine dithiocarbamate iron complexes distinguishes nitric oxide and nitroxyl anion in a redox-dependent manner: Applications in identifying nitrogen monoxide products from nitric oxide synthase. *Free Radic Biol Med* **29**(8): p. 793-7.

650. Dimmeler, S., et al., 1999, Activation of nitric oxide synthase in endothelial cells by Akt-dependent phosphorylation. *Nature* **399**(6736): p. 601-5.

651. List, B.M., et al., 1997, Characterization of bovine endothelial nitric oxide synthase as a homodimer with down-regulated uncoupled NADPH oxidase activity: tetrahydrobiopterin binding kinetics and role of haem in dimerization. *Biochem J* **323**(1): p. 159-65.

652. Zhao, H., et al., 2005, Detection and characterization of the product of hydroethidine and intracellular superoxide by HPLC and limitations of fluorescence. *Proc Natl Acad Sci U S A* **102**(16): p. 5727-32.

653. Zielonka, J., J. Vasquez-Vivar, and B. Kalyanaraman, 2008, Detection of 2-hydroxyethidium in cellular systems: a unique marker product of superoxide and hydroethidine. *Nature Protoc* **3**(1): p. 8-21.

654. Maghzal, G.J. and R. Stocker, 2007, Improved analysis of hydroethidine and 2-hydroxyethidium by HPLC and electrochemical detection. *Free Radic Biol Med* **43**(7): p. 1095-6.

655. Goldberg, B. and A. Stern, 1976, Production of superoxide anion during the oxidation of hemoglobin by menadione. *Biochim Biophys Acta* **437**(2): p. 628-32.

656. Frank, P.G., et al., 2003, Caveolin, caveolae, and endothelial cell function. *Arterioscler Thromb Vasc Biol* **23**(7): p. 1161-8.

657. Abusoud, H.M. and D.J. Stuehr, 1993, Nitric oxide synthases reveal a role for calmodulin in controlling electron-transfer. *Proc Natl Acad Sci U S A* **90**(22): p. 10769-72.

658. Kawashima, S. and M. Yokoyama, 2004, Dysfunction of endothelial nitric oxide synthase and atherosclerosis. *Arterioscler Thromb Vasc Biol* **24**(6): p. 998-1005.

659. Arnold, W.P., et al., 1977, Nitric oxide activates guanylate cyclase and increases guanosine 3':5'-cyclic monophosphate levels in various tissue preparations. *Proc Natl Acad Sci U S A* **74**(8): p. 3203-7.

660. Bonetti, P.O., 2002, Endothelial dysfunction: A marker of atherosclerotic risk. *Arterioscler Thromb Vasc Biol* **23**(2): p. 168-75.

661. Boudjeltia, K.Z., et al., 2006, Triggering of inflammatory response by myeloperoxidase-oxidized LDL. *Biochem Cell Biol* **84**(5): p. 805-12.

662. Botti, T.P., et al., 1996, A comparison of the quantitation of macrophage foam cell populations and the extent of apolipoprotein E deposition in developing atherosclerotic lesions in young people: high and low serum thiocyanate groups as an indication of smoking. *Atherosclerosis* **124**(2): p. 191-202.

663. McCabe, T.J., et al., 2000, Enhanced electron flux and reduced calmodulin dissociation may explain "calcium-independent" eNOS activation by phosphorylation. *J Biol Chem* **275**(9): p. 6123-8.

664. Go, Y.M., et al., 2001, Endothelial NOS-dependent activation of c-Jun NH(2)- terminal kinase by oxidized low-density lipoprotein. *Am J Physiol Heart Circ Physiol* **281**(6): p. H2705-13.

665. Laude, A.J. and A.W. Simpson, 2009, Compartmentalized signalling: Ca2+ compartments, microdomains and the many facets of Ca2+ signalling. *FEBS J* **276**(7): p. 1800-16.

666. Ramasamy, S., S. Parthasarathy, and D.G. Harrison, 1998, Regulation of endothelial nitric oxide synthase gene expression by oxidized linoleic acid. *J Lipid Res* **39**(2): p. 268-76.

667. Robb, G.B., et al., 2004, Post-transcriptional regulation of endothelial nitric-oxide synthase by an overlapping antisense mRNA transcript. *J Biol Chem* **279**(36): p. 37982-96.

668. Zhang, W., et al., 2015, Roles of miRNA-24 in regulating endothelial nitric oxide synthase expression and vascular endothelial cell proliferation. *Mol Cell Biochem* **405**(1-2): p. 281-9.

669. Yan, L., et al., 2013, An intronic miRNA regulates expression of the human endothelial nitric oxide synthase gene and proliferation of endothelial cells by a mechanism related to the transcription factor SP-1. *PLoS One* **8**(8): p. e70658.

670. Yildiz, G. and A.T. Demiryurek, 1998, Ferrous iron-induced luminol chemiluminescence: A method for hydroxyl radical study. *J Pharmacol Toxicol Methods* **39**(3): p. 179-84.

671. Yamamoto, Y. and B.N. Ames, 1987, Detection of lipid hydroperoxides and hydrogen peroxide at picamole levels by an HPLC and isoluminol chemiluminescence assay. *Free Radic Biol Med* **3**(5): p. 359-61.

672. Negre-Salvayre, A., et al., 2017, Dual signaling evoked by oxidized LDLs in vascular cells. *Free Radic Biol Med* **106**: p. 118-33.

673. Cominacini, L., et al., 2001, The binding of oxidized low density lipoprotein (ox-LDL) to ox-LDL receptor-1 reduces the intracellular concentration of nitric oxide in endothelial cells through an increased production of superoxide. *J Biol Chem* **276**(17): p. 13750-5.

674. Steffen, Y., et al., 2007, Protein modification elicited by oxidized low-density lipoprotein (LDL) in endothelial cells: protection by (-)-epicatechin. *Free Radic Biol Med* **42**(7): p. 955-70.

675. Werner, E.R., et al., 2003, Tetrahydrobiopterin and Nitric Oxide: Mechanistic and Pharmacological Aspects. *Exp Biol Med* **228**(11): p. 1291-302.

676. Stroes, E., et al., 1997, Tetrahydrobiopterin Restores Endothelial Function in Hypercholesterolemia. *J Clin Invest* **99**(1): p. 41-6.

677. Fukuda, Y., et al., 2002, Tetrahydrobiopterin restores endothelial function of coronary arteries in patients with hypercholesterolaemia. *Heart* **87**(3): p. 264-9.

678. Ueda, S., et al., 2000, Tetrahydrobiopterin restores endothelial function in long-term smokers. *J Am Coll Cardiol* **35**(1): p. 71-5.

679. Cosentino, F., et al., 2008, Chronic treatment with tetrahydrobiopterin reverses endothelial dysfunction and oxidative stress in hypercholesterolaemia. *Heart* **94**(4): p. 487-92.

680. Kraehling, J.R., et al., 2016, Uncoupling Caveolae From Intracellular Signaling In Vivo. *Circ Res* **118**(1): p. 48-55.

681. Simionescu, M., A. Gafencu, and F. Antohe, 2002, Transcytosis of plasma macromolecules in endothelial cells: a cell biological survey. *Microsc Res Tech* **57**(5): p. 269-88.

682. Uittenbogaard, A., et al., 2000, High density lipoprotein prevents oxidized low density lipoprotein-induced inhibition of endothelial nitric-oxide synthase localization and activation in caveolae. *J Biol Chem* **275**(15): p. 11278-83.

683. Kumano-Kuramochi, M., et al., 2013, Lectin-like oxidized LDL receptor-1 is palmitoylated and internalizes ligands via caveolae/raft-dependent endocytosis. *Biochem Biophys Res Commun* **434**(3): p. 594-9.

684. Ghitescu, L., et al., 1986, Specific Binding Sites for Albumin Restricted to Plasmalemmal Vesicles of Continuous Capillary Endothelium: Receptor-mediated Transcytosis. *J Cell Biol* **102**(4): p. 1304-11.

685. Kim, M.J., J. Dawes, and W. Jessup, 1994, Transendothelial transport of modified low-density lipoproteins. *Atherosclerosis* **108**(1): p. 5-17.

686. Vasile, E., M. Simionescu, and N. Simionescu, 1983, Visualization of the Binding, Endocytosis, and Transcytosis of Low-density Lipoprotein in the Arterial Endothelium in Situ. *J Cell Biol* **96**(6): p. 1677-89.

687. Pritchard, K.A., et al., 2002, Native low-density lipoprotein induces endothelial nitric oxide synthase dysfunction: Role of heat shock protein 90 and caveolin-1. *Free Radic Biol Med* **33**(1): p. 52-62.

688. Uittenbogaard, A., et al., 2000, High-density lipoprotein prevents oxidized low density lipoprotein-induced inhibition of endothelial nitric-oxide synthase localization and activation in caveolae. *J Biol Chem* **275**(15): p. 11278-83.

689. Zhu, Y., et al., 2003, Low density lipoprotein induces eNOS translocation to membrane caveolae: the role of RhoA activation and stress fiber formation. *Biochim Biophys Acta Molec Cell Biol Lipids* **1635**(2-3): p. 117-26.

690. Zhao, Y.Y., et al., 2002, Defects in caveolin-1 cause dilated cardiomyopathy and pulmonary hypertension in knockout mice. *Proc Natl Acad Sci U S A* **99**(17): p. 11375-80.

691. Cohen, A.W., et al., 2003, Caveolin-1 null mice develop cardiac hypertrophy with hyperactivation of p42/44 MAP kinase in cardiac fibroblasts. *Am J Physiol Cell Physiol* **284**(2): p. C457-74.

692. Wunderlich, C., et al., 2006, Disruption of caveolin-1 leads to enhanced nitrosative stress and severe systolic and diastolic heart failure. *Biochem Biophys Res Commun* **340**(2): p. 702-8.

693. Wunderlich, C., et al., 2008, The adverse cardiopulmonary phenotype of caveolin-1 deficient mice is mediated by a dysfunctional endothelium. *J Mol Cell Cardiol* **44**(5): p. 938-47.

694. Luksha, L., S. Agewall, and K. Kublickiene, 2009, Endothelium-derived hyperpolarizing factor in vascular physiology and cardiovascular disease. *Atherosclerosis* **202**(2): p. 330-44.

695. Chen, G., H. Suzuki, and A.H. Weston, 1988, Acetylcholine releases endothelium-derived hyperpolarizing factor and EDRF from rat-blood vessels. *Brit J Pharmacol* **95**(4): p. 1165-74.

696. Frank, P.G., et al., 2008, Role of caveolin-1 in the regulation of lipoprotein metabolism. *Am J Physiol Cell Physiol* **295**(1): p. C242-8.

697. Chistiakov, D.A., A.N. Orekhov, and Y.V. Bobryshev, 2015, Vascular smooth muscle cell in atherosclerosis. *Acta Physiol (Oxf)* **214**(1): p. 33-50.

698. Klouche, M., et al., 2000, Enzymatically degraded, nonoxidized LDL induces human vascular smooth muscle cell activation, foam cell transformation, and proliferation. *Circulation* **101**(15): p. 1799-805.

699. Chaabane, C., M. Coen, and M.L. Bochaton-Piallat, 2014, Smooth muscle cell phenotypic switch: implications for foam cell formation. *Curr Opin Lipidol* **25**(5): p. 374-9.

700. Ye, Q., et al., 2014, Difference in LDL Receptor Feedback Regulation in Macrophages and Vascular Smooth Muscle Cells: Foam Cell Transformation Under Inflammatory Stress. *Inflammation* **37**(2): p. 555-65.

701. Rosenfeld, M.E. and R. Ross, 1990, Macrophage and Smooth Muscle Cell Proliferation in Atherosclerotic Lesions of WHHL and Comparably Hypercholesterolemic Fat-fed Rabbits. *Arteriosclerosis* **10**(5): p. 680-7.

702. Choi, H.Y., et al., 2009, ATP-binding cassette transporter A1 expression and apolipoprotein A-I binding are impaired in intima-type arterial smooth muscle cells. *Circulation* **119**(25): p. 3223-31.

703. Kiyan, Y., et al., 2014, oxLDL induces inflammatory responses in vascular smooth muscle cells via urokinase receptor association with CD36 and TLR4. *J Mol Cell Cardiol* **66**: p. 72-82.

704. Dejager, S., M. Mietussnyder, and R.E. Pitas, 1993, Oxidized Low Density Lipoproteins Bind to the Scavenger Receptor Expressed by Rabbit Smooth Muscle Cells and Macrophages. *Arterioscler Thromb* **13**(3): p. 371-8.

705. Ricciarelli, R., J.M. Zingg, and A. Azzi, 2000, Vitamin E reduces the uptake of oxidized LDL by inhibiting CD36 scavenger receptor expression in cultured aortic smooth muscle cells. *Circulation* **102**(1): p. 82-7.

706. Campbell, J.H. and G.R. Campbell, 2012, Smooth muscle phenotypic modulation--a personal experience. *Arterioscler Thromb Vasc Biol* **32**(8): p. 1784-9.

707. Campbell, G.R., et al., 1971, Degeneration and Regeneration of Smooth Muscle Transplants in Anterior Eye Chamber - An Ultrastructural Study. *Z Zellforsch Mikrosk Anat* **117**(2): p. 155-75.

708. Yoshida, T. and G.K. Owens, 2005, Molecular determinants of vascular smooth muscle cell diversity. *Circ Res* **96**(3): p. 280-91.

709. Duband, J.-L., et al., 1993, Calponin and SM22 as differentiation markers of smooth muscle: spatiotemporal distribution during avian embryonic development. *Differentiation* **55**(1): p. 1-11.

710. Gabbiani, G., et al., 1981, Vascular smooth muscle cells differ from other smooth muscle cells: Predominance of vimentin filaments and a specific a-type actin. *Proc Natl Acad Sci U S A* **78**(1): p. 298-302.

711. Matsushita, T., et al., 2007, Relationship of connexin43 expression to phenotypic modulation in cultured human aortic smooth muscle cells. *Eur J Cell Biol* **86**(10): p. 617-28.

712. Cai, W.J., et al., 2004, Presence of Cx37 and lack of desmin in smooth muscle cells are early markers for arteriogenesis. *Mol Cell Biochem* **262**(1-2): p. 17-23.

713. Shanahan, C.M., et al., 1994, High Expression of Genes for Calcification-regulating Proteins in Human Atherosclerotic Plaques. *J Clin Invest* **93**(6): p. 2393-402.

714. Giachelli, C.M., et al., *Osteopontin Expression in Cardiovascular Diseases*, in *Osteopontin: Role in Cell Signalling and Adhesion*, D.T. Denhardt, et al., Editors. 1995, New York Acad Sciences: New York. p. 109-26.

715. van Kempen, M.J.A. and H.J. Jongsma, 1999, Distribution of connexin37, connexin40 and connexin43 in the aorta and coronary artery of several mammals. *Histochem Cell Biol* **112**(6): p. 479-86.

716. Ko, Y.S., et al., 2001, Regional Differentiation of Desin, Connexin43, and Connexin45 Expression Patterns in Rat Aortic Smooth Muscle. *Arterioscler Thromb Vasc Biol* **21**(3): p. 455-64.

717. Han, X.J., et al., 2015, Knockdown of connexin 43 attenuates balloon injury-induced vascular restenosis through the inhibition of the proliferation and migration of vascular smooth muscle cells. *Int J Mol Med* **36**(5): p. 1361-8.

718. Scott, J.E., 1996, Proteodermatan and proteokeratan sulfate (decorin, lumican/fibromodulin) proteins are horseshoe shaped. Implications for their interactions with collagen. *Biochemistry* **35**(27): p. 8795-9.

719. Wong, A.P., N. Nili, and B.H. Strauss, 2005, In vitro differences between venous and arterial-derived smooth muscle cells: potential modulatory role of decorin. *Cardiovasc Res* **65**(3): p. 702-10.

720. Riessen, R., et al., 1994, Regional Differences in the Distribution of the Proteoglycans Biglycan and Decorin in the Extracellular Matrix of Atherosclerotic and Restenotic Human Coronary Arteries. *Am J Pathol* **144**(5): p. 962-74.

721. Evanko, S.P., et al., 1998, Proteoglycan distribution in lesions of atherosclerosis depends on lesion severity, structural characteristics, and the proximity of platelet-derived growth factor and transforming growth factor-beta. *Am J Pathol* **152**(2): p. 533-46.

722. Pentikainen, M.O., et al., 1997, The proteoglycan decorin links low density lipoproteins with collagen type I. *J Biol Chem* **272**(12): p. 7633-8.

723. Kovanen, P.T. and M.O. Pentikainen, 1999, Decorin links low-density lipoproteins (LDL) to collagen: A novel mechanism for retention of LDL in the atherosclerotic plaque. *Trends Cardiovasc Med* **9**(3-4): p. 86-91.

724. Adiguzel, E., et al., 2009, Collagens in the progression and complications of atherosclerosis. *Vasc Med* **14**(73-89).

725. Brisset, A.C., et al., 2007, Intimal smooth muscle cells of porcine and human coronary artery express S100A4, a marker of the rhomboid phenotype in vitro. *Circ Res* **100**(7): p. 1055-62.

726. Lawrie, A., et al., 2005, Interdependent serotonin transporter and receptor pathways regulate S100A4/Mts1, a gene associated with pulmonary vascular disease. *Circ Res* **97**(3): p. 227-35.

727. Spiekerkoetter, E., et al., 2009, S100A4 and bone morphogenetic protein-2 codependently induce vascular smooth muscle cell migration via phospho-extracellular signal-regulated kinase and chloride intracellular channel 4. *Circ Res* **105**(7): p. 639-47.

728. Tomarev, S.I. and N. Nakaya, 2009, Olfactomedin Domain-Containing Proteins: Possible Mechanisms of Action and Functions in Normal Development and Pathology. *Mol Neurobiol* **40**(2): p. 122-38.

729. Miljkovic-Licina, M., et al., 2012, Targeting olfactomedin-like 3 inhibits tumor growth by impairing angiogenesis and pericyte coverage. *Mol Cancer Ther* **11**(12): p. 2588-99.

730. Virmani, R., et al., 2000, Lessons From Sudden Coronary Death : A Comprehensive Morphological Classification Scheme for Atherosclerotic Lesions. *Arterioscler Thromb Vasc Biol* **20**(5): p. 1262-75.

731. Loecker, T.H., et al., 1992, Fluoroscopic coronary artery calcification and associated coronary disease in asymptomatic young men. *J Am Coll Cardiol* **19**(6): p. 1167-72.

732. Fitzgerald, P.J., T.A. Ports, and P.G. Yock, 1992, Contribution of Localized Calcium Deposits to Dissection After Angioplasty - An Observational Study Using Intravascular Ultrasound. *Circulation* **86**(1): p. 64-70.

733. Proudfoot, D., et al., 2002, Acetylated Low-Density Lipoprotein Stimulates Human Vascular Smooth Muscle Cell Calcification by Promoting Osteoblastic Differentiation and Inhibiting Phagocytosis. *Circulation* **106**(24): p. 3044-50.

734. Yan, J., et al., 2011, Decorin GAG synthesis and TGF-beta signaling mediate Ox-LDL-induced mineralization of human vascular smooth muscle cells. *Arterioscler Thromb Vasc Biol* **31**(3): p. 608-15.

735. Scatena, M., L. Liaw, and C.M. Giachelli, 2007, Osteopontin: a multifunctional molecule regulating chronic inflammation and vascular disease. *Arterioscler Thromb Vasc Biol* **27**(11): p. 2302-9.

736. Jono, S., et al., 2000, Phosphate regulation of vascular smooth muscle cell calcification. *Circ Res* **87**(7): p. E10-7.

737. Iyemere, V.P., et al., 2006, Vascular smooth muscle cell phenotypic plasticity and the regulation of vascular calcification. *J Intern Med* **260**(3): p. 192-210.

738. Giachelli, C.M., et al., 1993, Osteopontin is Elevated during Neointima Formation in Rat Arteries and is a Novel Component of Human Atherosclerotic Plaques. *J Clin Invest* **92**(4): p. 1686-96.

739. Giachelli, C.M. and S. Steitz, 2000, Osteopontin: a versatile regulator of inflammation and biomineralization. *Matrix Biol* **19**(7): p. 615-22.

740. Speer, M.Y., et al., 2010, Runx2/Cbfa1, but not loss of myocardin, is required for smooth muscle cell lineage reprogramming toward osteochondrogenesis. *J Cell Biochem* **110**(4): p. 935-47.

741. Severson, A.R., R.T. Ingram, and L.A. Fitzpatrick, 1995, Matrix proteins associated with bone calcification are present in human vascular smooth muscle cells grown *in vitro*. *In Vitro Cell Dev Biol Anim* **31**(11): p. 853-7.

742. Hoshi, K., et al., 1999, The primary calcification in bones follows removal of decorin and fusion of collagen fibrils. *J Bone Miner Res* **14**(2): p. 273-80.

743. Fischer, J.W., et al., 2004, Decorin promotes aortic smooth muscle cell calcification and colocalizes to calcified regions in human atherosclerotic lesions. *Arterioscler Thromb Vasc Biol* **24**(12): p. 2391-6.

744. Steitz, S.A., et al., 2001, Smooth Muscle Cell Phenotypic Transition Associated With Calcification: Upregulation of Cbfa1 and Downregulation of Smooth Muscle Lineage Markers. *Circulation Research* **89**(12): p. 1147-54.

745. Massaeli, H., et al., 1999, Oxidized low-density lipoprotein induces cytoskeletal disorganization in smooth muscle cells. *Am J Physiol Heart Circ Physiol* **277**(5): p. H2017-25.

746. He, C., et al., 2013, Mitofusin2 decreases intracellular cholesterol of oxidized LDL-induced foam cells from rat vascular smooth muscle cells. *J Huazhong Univ Sci Technolog Med Sci* **33**(2): p. 212-8.

747. Yin, Y.W., et al., 2014, TLR4-mediated inflammation promotes foam cell formation of vascular smooth muscle cell by upregulating ACAT1 expression. *Cell Death Dis* **5**(e1574).

748. Wada, T., et al., 1999, Calcification of Vascular Smooth Mucle Cell Cultures - Inhibition by Osteopontin. *Circ Res* **84**(2): p. 166-78.

749. Liu, T., et al., 2012, Regulation of S100A4 expression via the JAK2-STAT3 pathway in rhomboid-phenotype pulmonary arterial smooth muscle cells exposure to hypoxia. *Int J Biochem Cell Biol* **44**(8): p. 1337-45.

750. Frid, M.G., et al., 2009, Sustained hypoxia leads to the emergence of cells with enhanced growth, migratory, and promitogenic potentials within the distal pulmonary artery wall. *Am J Physiol Lung Cell Mol Physiol* **297**(6): p. L1059-72.

751. Goettsch, C., et al., 2011, Nuclear factor of activated T cells mediates oxidised LDL-induced calcification of vascular smooth muscle cells. *Diabetologia* **54**(10): p. 2690-701.

752. Sudo, R., et al., 2015, 7-Ketocholesterol-induced lysosomal dysfunction exacerbates vascular smooth muscle cell calcification via oxidative stress. *Genes Cells* **20**(12): p. 982-91.

753. Saito, E., et al., 2008, 7-ketocholesterol, a major oxysterol, promotes Pi-induced vascular calcification in cultured smooth muscle cells. *J Atheroscler Thromb* **15**(3): p. 130-7.

754. Hofbauer, L.C., et al., 2006, Interleukin-4 differentially regulates osteoprotegerin expression and induces calcification in vascular smooth muscle cells. *Thromb Haemost* **95**(4): p. 708-14.

755. Byon, C.H., et al., 2008, Oxidative stress induces vascular calcification through modulation of the osteogenic transcription factor Runx2 by AKT signaling. *J Biol Chem* **283**(22): p. 15319-27.

756. Chamley, J.H., et al., 1977, Comparison of Vascular Smooth Muscle Cells from Adult Human, Monkey and Rabbit in Primary Culture and in Subculture. *Cell Tissue Res* **177**(4): p. 503-22.

757. Chamley, J.H. and G.R. Campbell, 1974, Mitosis of Contractile Smooth-Muscle Cells in Tissue-culture. *Exp Cell Res* **84**(1-2): p. 105-10.

758. Chaabane, C., et al., 2013, Biological responses in stented arteries. *Cardiovasc Res* **99**(2): p. 353-63.

759. Stocker, R. and J.F. Keaney Jr, 2004, Role of oxidative modifications in atherosclerosis. *Physiol Rev* **84**(4): p. 1381-478.

760. Li, H. and U. Forstermann, 2013, Uncoupling of endothelial NO synthase in atherosclerosis and vascular disease. *Curr Opin Pharmacol* **13**(2): p. 161-7.

761. Vita, J.A., et al., 2004, Serum myeloperoxidase levels independently predict endothelial dysfunction in humans. *Circulation* **110**(9): p. 1134-9.

762. Hazen, S.L., et al., 1996, Molecular Chlorine Generated by the Myeloperoxidase-Hydrogen Peroxide-Chloride System of Phagocytes Converts Low Density Lipoprotein Cholesterol into a Family of Chlorinated Sterols. *J Biol Chem* **271**(38): p. 23080-8.

763. Hazen, S.L., et al., 1998, Human Neutrophils Employ the Myeloperoxidase Hydrogen Peroxide-Chloride System to Oxidize alpha-Amino Acids to a Family of Reactive Aldehydes - Mechanistic Studies Identifying Labile Intermediates Along the Reaction Pathway. *J Biol Chem* **273**(9): p. 4997-5005.

764. Vesey, C.J., et al., 1982, Blood carboxyhaemoglobin, plasma thiocyanate, and cigarette consumption: implications for epidemiological studies in smokers. *BMJ* **284**(6328): p. 1516-8.

765. Esterbauer, H., R.J. Schaur, and H. Zollner, 1991, Chemistry and Biochemistry of 4-Hydroxynonenal, Malondialdehyde and Related Aldehydes. *Free Radic Biol Med* **11**(1): p. 81-128.

766. Requena, J.R., et al., 1997, Quantification of malondialdehyde and 4-hydroxynonenal adducts to lysine residues in native and oxidized human low-density lipoprotein. *Biochem J* **322**: p. 317-25.

767. Spickett, C.M., 2013, The lipid peroxidation product 4-hydroxy-2-nonenal: Advances in chemistry and analysis. *Redox Biol* **1**: p. 145-52.

768. Chen, S.H., et al., 1986, The Complete cDNA and Amino Acid Sequence of Human Apolipoprotein B- 100. *J Biol Chem* **261**(28): p. 12918-21.

769. Weisgraber, K.H. and S.C. Rall Jr, 1987, Human Apolipoprotein B-100 Heparin-binding Sites. *J Biol Chem* **262**(23): p. 11097-103.

770. Knott, T.J., et al., 1986, Complete protein sequence and identification of structural domains of human apolipoprotein B. *Nature* **323**(6090): p. 734-8.

771. Boren, J., et al., 1998, Idenitification of the low density lipoprotein receptor-binding site in apolipoprotein B100 and the modulation of its binding activity by the carboxyl terminus in familial defective Apo-B100. *J Clin Invest* **101**(5): p. 1084-93.

772. Brown, M.S. and J.L. Goldstein, 1999, A proteolytic pathway that control the cholesterol content of membranes, cells, and blood. *Proc Natl Acad Sci U S A* **96**(20): p. 11041-8.

773. Ryoo, S., et al., 2006, Oxidized low-density lipoprotein-dependent endothelial arginase II activation contributes to impaired nitric oxide signaling. *Circ Res* **99**(9): p. 951-60.

774. Pandey, D., et al., 2014, OxLDL triggers retrograde translocation of arginase2 in aortic endothelial cells via ROCK and mitochondrial processing peptidase. *Circ Res* **115**(4): p. 450-9.

775. Ryoo, S., et al., 2011, OxLDL-dependent activation of arginase II is dependent on the LOX-1 receptor and downstream RhoA signaling. *Atherosclerosis* **214**(2): p. 279-87.

776. Hirata, K., et al., 1995, Low Concentration of Oxidized Low-Density Lipoprotein and Lysophosphatidylcholine Upregulate Constitutive Nitric Oxide Synthase mRNA Expression in Bovine Aortic Endothelial Cells. *Circ Res* **76**(6): p. 958-62.

777. Liao, J.K., et al., 1995, Oxidized Low-density Lipoprotein Decreases the Expression of Endothelial Nitrix Oxide Synthase. *J Biol Chem* **270**(1): p. 319-24.

778. Kawamura, K., et al., 2005, Bilirubin from heme oxygenase-1 attenuates vascular endothelial activation and dysfunction. *Arterioscler Thromb Vasc Biol* **25**(1): p. 155-60.

779. Jansen, T., et al., 2010, Conversion of biliverdin to bilirubin by biliverdin reductase contributes to endothelial cell protection by heme oxygenase-1-evidence for direct and indirect antioxidant actions of bilirubin. *J Mol Cell Cardiol* **49**(2): p. 186-95.

780. Datla, S.R., et al., 2007, Induction of heme oxygenase-1 in vivo suppresses NADPH oxidase derived oxidative stress. *Hypertension* **50**(4): p. 636-42.

781. Jiang, F., et al., 2006, NO modulates NADPH oxidase function via heme oxygenase-1 in human endothelial cells. *Hypertension* **48**(5): p. 950-7.

782. Wang, X., et al., 2007, Carbon monoxide protects against hyperoxia-induced endothelial cell apoptosis by inhibiting reactive oxygen species formation. *J Biol Chem* **282**(3): p. 1718-26.

783. Turkseven, S., et al., 2005, Antioxidant mechanism of heme oxygenase-1 involves an increase in superoxide dismutase and catalase in experimental diabetes. *Am J Physiol Heart Circ Physiol* **289**(2): p. H701-7.

784. Ahmad, M., et al., 2009, Heme oxygenase-1 induction modulates hypoxic pulmonary vasoconstriction through upregulation of ecSOD. *Am J Physiol Heart Circ Physiol* **297**(4): p. H1453-61.

785. Dulak, J., et al., 2008, Heme oxygenase-1 and carbon monoxide in vascular pathobiology: focus on angiogenesis. *Circulation* **117**(2): p. 231-41.

786. Ryter, S.W., J. Alam, and A.M.K. Choi, 2006, Heme oxygenase-1/carbon monoxide: From basic science to therapeutic applications. *Physiol Rev* **86**(2): p. 583-650.

787. Kim, H.P., et al., 2004, Caveolae compartmentalization of heme oxygenase-1 in endothelial cells. *FASEB J* **18**(10): p. 1080-9.

788. Penumathsa, S.V., et al., 2008, Strategic targets to induce neovascularization by resveratrol in hypercholesterolemic rat myocardium: role of caveolin-1, endothelial nitric oxide synthase, hemeoxygenase-1, and vascular endothelial growth factor. *Free Radic Biol Med* **45**(7): p. 1027-34.

789. Pae, H.O., et al., 2010, Role of heme oxygenase in preserving vascular bioactive NO. *Nitric Oxide* **23**(4): p. 251-7.

790. Pfenniger, A., et al., 2010, Gap junction protein Cx37 interacts with endothelial nitric oxide synthase in endothelial cells. *Arterioscler Thromb Vasc Biol* **30**(4): p. 827-34.

791. Nazarewicz, R.R., A. Bikineyeva, and S.I. Dikalov, 2013, Rapid and specific measurements of superoxide using fluorescence spectroscopy. *J Biomol Screen* **18**(4): p. 498-503.

792. Tang, J.L., et al., 1995, Role of SP1 in Transcriptional Activation of Human Nitric Oxide Synthase Type III Gene. *Biochem Biophys Res Commun* **213**(2): p. 673-80.

793. Wariishi, S., et al., 1995, A SP1 Binding Site in the GC-rich Region is Essential for a Core Promotor Activity of the Human Endothelial Nitric Oxide Synthase Gene. *Biochem Biophys Res Commun* **216**(2): p. 729-35.

794. Zhang, R., W. Min, and W.C. Sessa, 1995, Functional Analysis of the Human Endothelial Nitric Oxide Synthase Promotor - SP1 and GATA Factors are Necessary for Basal Transcription in Endothelial Cells. *J Biol Chem* **270**(25): p. 15320-6.

795. Karantzoulis-Fegaras, F., et al., 1999, Characterization of the human endothelial nitric-oxide synthase promoter. *J Biol Chem* **274**(5): p. 3076-93.

796. Navarro-Antolin, J., J. Rey-Campos, and S. Lamas, 2000, Transcriptional Induction of Endothelial Nitric Oxide Gene by Cyclosporine A - A Role for Activator Protein-1. *J Biol Chem* **275**(5): p. 2075-80.

797. Cieslik, K., et al., 1998, Transcriptional regulation of endothelial nitric-oxide synthase by lysophosphatidylcholine. *J Biol Chem* **273**(24): p. 14885-90.

798. Xing, F., et al., 2006, Role of AP1 element in the activation of human eNOS promoter by lysophosphatidylcholine. *J Cell Biochem* **98**(4): p. 872-84.

799. Kumar, S., et al., 2009, Hydrogen Peroxide Decreases Endothelial Nitric Oxide Synthase Promoter Activity through the Inhibition of Sp1 Activity. *DNA Cell Biol* **28**(3).

800. Ye, X., et al., 2015, LPS Down-Regulates Specificity Protein 1 Activity by Activating NF-kappaB Pathway in Endotoxemic Mice. *PLoS One* **10**(6): p. e0130317.

801. Santamarina-Fojo, S., et al., 2000, Complete genomic sequence of the human ABCA1 gene: Analysis of the human and mouse ATP-binding cassette A promoter. *Proc Natl Acad Sci U S A* **97**(14): p. 7987-92.

802. Lavrovsky, Y., et al., 1994, Identification of binding sites for transcription factors NF-kappaB and AP-2 in the promoter region of the human heme oxygenase 1 gene. *Proc Natl Acad Sci U S A* **91**(13): p. 2987-91.

803. Alam, J. and Z.N. Den, 1992, Distal AP-1 Binding Sites Mediate Basal Level Enhancement and TPA Induction of the Mouse Heme Oxygenase-1 Gene. *J Biol Chem* **267**(30): p. 21894-900.

804. Rojo, A.I., et al., 2006, Regulation of heme oxygenase-1 gene expression through the phosphatidylinositol 3-kinase/PKC-zeta pathway and Sp1. *Free Radic Biol Med* **41**(2): p. 247-61.

805. Traylor, A., T. Hock, and N. Hill-Kapturczak, 2007, Specificity protein 1 and Smad-dependent regulation of human heme oxygenase-1 gene by transforming growth factor-beta1 in renal epithelial cells. *Am J Physiol Renal Physiol* **293**(3): p. F885-94.

806. Alam, J. and J.L. Cook, 2007, How many transcription factors does it take to turn on the heme oxygenase-1 gene? *Am J Resp Cell Molec Biol* **36**(2): p. 166-74.

807. Ares, M.P.S., et al., 1995, Oxidized LDL Induces Transcription Factor Activator Protein–1 but Inhibits Activation of Nuclear Factor–κB in Human Vascular Smooth Muscle Cells. *Arterioscler Thromb Vasc Biol* **15**(10): p. 1584-90.

808. Rivard, A., N. Principe, and V. Andres, 2000, Age-dependent increase in c-fos activity and cyclin A expression in vascular smooth muscle cells - A potential link between aging, smooth muscle cell proliferation and atherosclerosis. *Cardiovasc Res* **45**(4): p. 1026-34.

809. Bidder, M., et al., 2002, Osteopontin Transcription in Aortic Vascular Smooth Muscle Cells Is Controlled by Glucose-regulated Upstream Stimulatory Factor and Activator Protein-1 Activities. *J Biol Chem* **277**(46): p. 44485-96.

810. Stary, H.C., 1989, Evolution and progression of atherosclerotic lesions in coronary arteries of children and young adults. *Arteriosclerosis* **9**(1 SUPPL.): p. I19-I32.

811. Hao, H., G. Gabbiani, and M.L. Bochaton-Piallat, 2003, Arterial smooth muscle cell heterogeneity: implications for atherosclerosis and restenosis development. *Arterioscler Thromb Vasc Biol* **23**(9): p. 1510-20.

812. Triggle, C.R., et al., 2012, The endothelium: influencing vascular smooth muscle in many ways. *Can J Physiol Pharmacol* **90**(6): p. 713-38.

813. Takano, H., K.A. Dora, and C.J. Garland, 2005, Spreading vasodilation in resistance arteries. *J Smooth Muscle Res* **41**(6): p. 303-11.

814. Figueroa, X.F. and B.R. Duling, 2009, Gap junctions in the control of vascular function. *Antioxid Redox Signal* **11**(2): p. 251-66.

815. Powell, R.J., et al., 1996, Endothelial cell modulation of smooth muscle cell morphology and organizational growth pattern. *Ann Vasc Surg* **10**(1): p. 4-10.

816. Nakaki, T., M. Nakayama, and R. Kato, 1990, Inhibition by nitric oxide and nitric oxide-producing vasodilators of DNA synthesis in vascular smooth muscle cells. *Eur J Pharmacol* **189**(6): p. 347-53.

817. Guo, K., V. Andres, and K. Walsh, 1998, Nitric Oxide–Induced Downregulation of Cdk2 Activity and Cyclin A Gene Transcription in Vascular Smooth Muscle Cells. *Circulation* **97**(20): p. 2066-72.

818. Ishida, A., et al., 1997, Induction of the cyclin-dependent kinase inhibitor p21(Sdi1/Cip1/Waf1) by nitric oxide-generating vasodilator in vascular smooth muscle cells. *J Biol Chem* **272**(15): p. 10050-7.

819. Kader, K.N., et al., 2000, eNOS-overexpressing endothelial cells inhibit platelet aggregation and smooth muscle cell proliferation in vitro. *Tissue Eng* **6**(3): p. 241-51.

820. Lincoln, T.M., et al., 1998, Nitric oxide - cyclic GMP pathway regulates vascular smooth muscle cell phenotypic modulation: implications in vascular diseases. *Acta Physiol Scand* **164**(4): p. 507-15.

821. Sarkar, R., et al., 1997, Dual cell cycle-specific mechanisms mediate the antimitogenic effects of nitric oxide in vascular smooth muscle cells. *J Hypertens* **15**(3): p. 275-83.

822. Brown, D.J., et al., 2005, Endothelial cell activation of the smooth muscle cell phosphoinositide 3-kinase/Akt pathway promotes differentiation. *J Vasc Surg* **41**(3): p. 509-16.

823. Chandler, J.D. and B.J. Day, 2012, Thiocyanate: a potentially useful therapeutic agent with host defense and antioxidant properties. *Biochem Pharmacol* **84**(11): p. 1381-7.